UNIVERSITY OF CALIFORNIA
RIVERSIDE

AND

SAN DIEGO STATE UNIVERSITY

Phylogenomics, Integrative Taxonomy, and Population Genomics in the Travunioidea (Arachnida, Opiliones, Laniatores)

A Dissertation submitted in partial satisfaction
of the requirements for the degree of

Doctor of Philosophy

in

Evolutionary Biology

by

Shahan Derkarabetian

December 2017

Dissertation Committee:
Dr. Marshal Hedin, Co-Chairperson
Dr. Cheryl Hayashi, Co-Chairperson
Dr. Tod Reeder
Dr. David Reznick

Copyright by
Shahan Derkarabetian
2017

The Dissertation of Shahan Derkarabetian is approved:

Committee Co-Chairperson

Committee Co-Chairperson

University of California, Riverside
San Diego State University

ACKNOWLEDGEMENTS

I have an immense number of people and institutions to thank for assistance in various ways throughout my dissertation.

Chapter 1: I thank the following people and institutions for loans of specimens used in genetic analyses: southern hemisphere Triaenonychidae, Synthetonychiidae, and *Hinzuania* were made available by Charles Griswold and Darrell Ubick (California Academy of Sciences); *Holoscotolemon* samples were provided by Axel Shonhöfer; and a specimen of *Trojanella serbica* was provided by Ivo Karaman. I sincerely thank Nobuo Tsurusaki for his hospitality, knowledge, and assistance during fielwork in Japan. For assistance in collecting North American travunioids, I thank Marshal Hedin, Casey Richart, Allan Cabrero, James Starrett, and Erik Ciaccio. I am indebted to Brant Faircloth for initial training in UCE laboratory procedures at Louisiana State University, and for answering the plethora of follow up questions I had regarding laboratory work and bioinformatic processing. I thank Darrell Ubick for providing morphological training at the California Academy of Sciences. Funding for this project was provided by an NSF grant (DEB #1354558) to Marshal Hedin. Additional funding was provided by an NSF Doctoral Dissertation Improvement Grant (DEB #1601208) and the American Arachnology Society Vincent Roth Fund for Systematics.

Chapter 2: For specimen loans I thank Lorenzo Prendini (American Museum of Natural History), Darrell Ubick (California Academy of Sciences), and Paula Cushing and Heather Thorwald (Denver Museum of Nature and Science). I also thank Casey

Richart for use of his personal collection. For assistance with fieldwork I thank Joe Deas, Damian Elias, Ryan Fawcett, Lars Hedin, Marshal Hedin, William Leonard, Maureen McCormack, Casey Richart, Andrew Smith, Steven Thomas, Jeffrey Underwood and, especially, David Steinmann for his invaluable and continuing collecting efforts. For assistance with permits, permissions, and collecting of cave species I thank Gretchen Baker and Ben Roberts (Great Basin National Park), Lynette Kemp and Rhea Armstrong (Lewis and Clark Caverns), and Jeremy Stiles and James Reiter (Cave of the Winds). For SEM imaging I thank Joel Ledford. For digital imaging I thank Casey Richart and Alexa Feist. Technical training for RNA extractions was provided by Amy Hubert and James Starrett. Discussions with Sean Harrington improved phylogenetic methodology. Two anonymous reviewers significantly improved the content of the published manuscript. This chapter was published in *PLoS One* (https://doi.org/10.1371/journal.pone.0104982).

Chapter 3**:** I sincerely thank James Starrett and Mercedes Burns for significant assistance with ddRAD-seq laboratory work, and Andrew Gottscho for initial training in ddRAD-seq library preparation methods and discussions regarding analyses. For assistance with fieldwork I thank Joe Deas, Angela DiDomenico, Damian Elias, Kristen Emata, Ryan Fawcett, Erika Garcia, Marshal Hedin, Maureen McCormack, Casey Richart, Axel Schönhofer, Dan Sitzmann, Eric Stiner, and Steven Thomas. I thank Jordan Satler for providing custom scripts for creating input files for fastsimcoal2 as well as helpful discussions. Conversations with Paul Maier provided some useful insight. This research was funded by an NSF grant awarded to MH (DEB 1354558). Comments from

Bryan Carstens and four anonymous reviewers helped to improve the manuscript. This chapter was published in *Molecular Ecology* (10.1111/mec.13789).

There are several individuals who deserve particularly special thanks. First is my advisor Marshal Hedin. Through the 12 years I have known him, he has been my advisor and friend, giving me the advice and opportunities needed that set me on my path as a scientist. While an undergraduate, he gave me an opportunity to conduct independent research in his lab. After my M.S., when I struggled to stay in academia, a phone call from him asking me to join him as a doctoral student, gave me a reason to stay. He gave me the freedom to explore and find myself as a researcher, while always keeping me on solid ground. We have been working together 12 years, but it feels like we are just getting started, and I look forward to many more years of friendship and collaboration.

I would also like to thank the rest of my doctoral committee for their guidance and advice in figuring out my next step. Tod Reeder has always been an excellent source for research and academic advice. Cheryl Hayashi's vast knowledge has been an inspiration. The Hedin lab throught the years has always been an important source of support, not just as labmates, but also as friends. Three people in particular have supported me as close friends through the many ups and downs of my time as a doctoral student: Casey Richart, Ketan Patel, and Sean Harrington. The Garden will never die. Finally, I thank my family for giving me the freedom and support to pursue my passions. As a child, my parents taught me what hard work looks and how to take pride in what I do, and my brother taught me what critical thinking is. This dissertation would not have been possible without them.

DEDICATION

I dedicate this dissertation to my neice and nephew, Emme and Roman.

Never stop exploring.

ABSTRACT OF THE DISSERTATION

Phylogenomics, Integrative Taxonomy, and Population Genomics in the Travunioidea (Arachnida, Opiliones, Laniatores)

by

Shahan Derkarabetian

Doctor of Philosophy, Graduate Program in Evolutionary Biology
University of California, Riverside and San Diego State University, December 2017
Dr. Marshal Hedin and Dr. Cheryl Hayashi, Co-Chairpersons

My dissertation research utilizes next-generation sequencing (NGS) technology and associated bioinformatics processing to answer systematic and evolutionary questions in Opiliones (harvestmen) at different taxonomic scales, focusing on the Laniatores superfamily Travunioidea and particularly the travunioid genus *Sclerobunus*. Opiliones are a diverse group of arachnids with over 6500 described species distributed on every continent except Antarctica. Despite relatively high diversity (e.g., more described species than mammals), harvestmen are poorly studied.

This dissertation research has three main projects. The first chapter is a higher-level phylogenetics and taxonomic study of the Travunioidea, a clade of ~80 species of harvestmen distributed throughout the Holarctic. Here I utilized ultraconserved elements (UCE) for phylogenomic reconstruction using multiple types of phylogenetic reconstruction methods. Based on results, a new taxonomic classification is proposed for the Travunioidea, including the identification and diagnosis of a new family, and I reassess the phylogenetic utility of morphological characters used to differentiate and

diagnose travunioid taxa. The second chapter focuses on species delimitation of the western North American travunioid genus *Sclerobunus*. I utilized modern integrative taxonomic methods, using both discovery-based and validation-based approaches by combining morphometrics, mitochondrial genetic data, genitalic morphology, and nuclear genetic data derived from newly developed genes based on a comparative transcriptomics approach. This research resulted in a revision of the genus including synonymy of the genus *Cyptobunus*, elevation of four subspecies, and the description of five new species. The third chapter is a phylogeographic analysis of *Sclerobunus robustus*, a species distributed throughout the southwestern United States. A hypothesis-based framework was adopted, where stable habitats (i.e., potential refugia) were identified through ecological niche modeling, and hypotheses regarding genetic patterns associated with these refugia were developed. Hypotheses were tested by using genetic data in the form of loci and SNPs derived from double-digest RAD sequencing methods. Two large refugial regions were identified and population genomic analyses supported the presence of both.

TABLE OF CONTENTS

LIST OF FIGURES

Chapter 1

Chapter 2

Chapter 3

LIST OF TABLES

INTRODUCTION

While the topics of my three dissertation chapters are diverse and not directly related to each other, they share two things in common: 1) incorporating recent advances in evolutionary biology, whether theoretical, analytical, and/or methodological; and 2) harvestmen as the focal taxon. The chapters are organized in a trend of decreasing taxonomic hierarchy of nested taxa, beginning with higher-level phylogenomics of the superfamily Travunioidea in Chapter 1, a revision of the travunioid genus *Sclerobunus* in Chapter 2, and population genomics of *S. robustus* in Chapter 3.

The field of molecular systematics has transitioned from phylogenetic studies using single- or multi-locus datasets to phylogenomic studies with 100s - 1000s of informative loci. Associated with this transition is a concomitant increase in the resolution and support of phylogenies, helping to resolve relationships and taxonomic issues. New genome-level resources and protocols have been incorporated into vertebrate systematics, while invertebrate systematics has lagged behind despite their vastly higher species diversity. This has been particularly evident in the arachnids. Chapter 1 uses a new developed arachnid-specific ultraconserved element probe set to acquire 100s of loci for phylogenomic analyses, which are then used for a taxonomic reclassification and reassessment of morphological characters traditionally used in travunioid classification.

The importance of a species as a unit in biology is well known. However, the definition of a species has been surrounded by much debate. As such, it is important to operationally delimit species in an objective and repeatable manner. In harvestmen, and

many other invertebrate lineages, the vast majority of species are still described using traditional morphological methods, which can be subjective. Chapter 2 (doi: 10.1371/journal.pone.0104982) utilizes relatively recent developments in integrative taxonomy and species delimitation coupled with analytical methods designed to increase objectivety in species delimitation. I use morphology and newly developed nuclear markers derived from transcriptome sequencing to conduct phylogenetic and species delimitation analyses under an integrative framework, which resulted in a taxonomic revision of the genus *Sclerobunus*.

With the relative ease of collecting vast amounts of genome-scale data, it becomes easier to test specific phylogeographic hypotheses and demographic scenarios in a model-based framework. I use this approach to explore the phylogeographic history of *Sclerobunus robustus*, a species restricted to moist high elevation forests throughout southwestern North America. In Chapter 3 (doi: 10.1111/mec.13789), I use bioclimatic data analysis to develop demographic and phylogeographic hypotheses regarding refugia, which are then tested using ddRAD-Seq data. Ecological niche modeling across multple time frames identify two regions of persistent habitat, which are treated as potential refugia. Phylogenomic and population genomic analyses date these refugia to the Pliocene and confirm genetic and demographic patterns expected based on the location of refugia.

Through this work and the resuting publications, it has been my goal to bring these recent advancements into an organismal group where the vast majority of taxonomic work is still conducted using traditional morphological approaches and/or

standard Sanger sequencing. Similarly, by focusing on Opiliones, I hope to expose this relatively poorly studied group to a broader evolutionary biology audience.

CHAPTER 1

Phylogenomic revision of Travunioidea (Arachnida, Opiliones, Laniatores) using sequence capture of ultraconserved elements

Molecular phylogenetics has been transitioning into the phylogenomics era, utilizing next generation sequencing technologies that allow unprecedented levels of resolution in animal systematics, particularly in understudied taxa like invertebrates. Within the most diverse harvestmen (Opiliones) suborder Laniatores the vast majority of relationships at all taxonomic levels have yet to be explored fro a modern molecular systematic perspective. Travunioidea is an early-diverging lineage of laniatorean harvestmen with a Laurasian distribution having species distributed in eastern Asia, eastern and western North America, and central Europe. This clade has had a challenging taxonomic history, but the current classification consists of ~77 species in three families – the Travuniidae, Paranonychidae, and Nippononychidae. The classification of the Travunioidea has traditionally been based on structure of the tarsal claws of the hind legs. However, it is becoming increasingly clear that tarsal claw structure is not an ideal character for use in defining taxonomic groupings due to homoplasy at all taxonomic levels. Here, we utilize an arachnid-specific probeset targeting over 1000 ultraconserved elements (UCEs) to reconstruct the phylogenetic relationships of the Travunioidea. Data matrices consisting of 100s of loci were used in maximum likelihood, Bayesian and species tree analyses. Resulting phylogenies recover three consistent and highly supported clades. The phylogenetic position and taxonomic status of the enigmatic genera

Trojanella and *Yuria* are less certain. Based on the resulting phylogenies a revision of Travunioidea is proposed, now consisting of the Travuniidae, Paranonychidae (Nippononychidae is synonymized), and the new family Cryptomastridae, diagnosed here. In addition, we reassess the phylogenetic utility of morphological characters used to differentiate and diagnose travunioid taxa. The inappropriateness of the tarsal claw in diagnosing higher-level taxa is further corroborated. The phylogenetic utility and diagnostic features of the intestinal complex and male genitalia are discussed in light the phylogenomic results.

I. INTRODUCTION

Most biologists and laypersons living in northern climates are familiar with the "daddy longlegs" or "harvestmen" – relatively large-bodied, abundant, conspicuous members of forest arthropod communities. Fewer appreciate the more "cryptic" Opiliones, which in fact represent the bulk of species diversity in this arachnid lineage. Opiliones are taxonomically rich, comprising 46 families, over 1,640 genera, and more than 6,600 described species (summarized in Kury 2000; Machado et al. 2007; Kury 2013). Within Opiliones, considerable phylogenetic progress has been made recently, summarized by Pinto-da-Rocha et al. (2007) and reviewed/updated in Giribet et al. (2010), and Giribet and Sharma (2015), including transcriptome-based phylogenomic approaches used in Sharma and Giribet (2014) and Fernandez et al (2017). Opiliones diversity falls into four primary clades, including the "mite harvestmen"

(Cyphophthalmi), typical "daddy longlegs" (Eupnoi and Dyspnoi), and the "short-legged" or "armored" harvestmen (Laniatores). Laniatores is strongly supported as monophyletic, is the most species-rich group of harvestmen (with over 4100 described species), and can be found on all continents except for Antarctica. Many laniatoreans are tropical, where these animals are conspicuous and occupy a wide variety of habitats. Temperate laniatoreans are less noticeable, and in the Holarctic, are mostly small-bodied (~1.5 - 4 mm) predators restricted to cryophilic habitats (e.g., under decaying logs or rocks, in leaf litter, in caves, etc.).

The substantial taxonomic diversity of Laniatores is relatively under-studied from a formal phylogenetic perspective. The molecular phylogenetic research of Giribet et al. (2010), which focused on relationships within Laniatores, changed this situation and formed the framework for further systematic investigation in this arachnid group. Following this study, Sharma and Giribet (2011) conducted a phylogenetic analysis representing the most inclusive study of Laniatores to date. In these studies, they recovered four primary Laniatorean lineages, including the Synthetonychiidae Forster, 1954 (New Zealand), Triaenonychidae Sørensen, 1886 (mostly south temperate), Travunioidea Absolon & Kratochvíl, 1932 (north temperate), and Grassatores Kury, 2002 (broadly distributed, most diversity in the tropics). Although the sampling of travunioid taxa in these studies was incomplete (only 6-7 of 24 travunioid genera sampled), these preliminary results and morphology (reviewed in Giribet & Kury 2007) support the monophyly of a north temperate group of taxa that comprise the focal group of this study – the Travunioidea (Figures 1.1 and 1.2).

Classification within the Travunioidea has traditionally been based on structure of the tarsal claws of the hind legs. As others have noted, it has become increasingly clear that tarsal claw structure is not an ideal character for use in defining taxonomic groupings in this clade, as claw structure is highly homoplastic and variable at all taxonomic levels (e.g. Shear 1977; Maury 1988; Hunt and Hickman 1993; Karaman 2005; Shear and Derkarabetian 2008). For example, many travunioids were formerly grouped with the Triaenonychidae, sharing trident-shaped tarsal claw morphology. The transfer of all "north temperate triaenonychids" to the Travunioidea was first hinted at by Staręga (1971), proposed based on intestinal morphology by Dumitrescu (1975, 1976), and has since been supported with additional morphological (Giribet and Kury 2007; Mendes 2009) and genetic data from multiple studies (e.g., Derkarabetian et al. 2010; Giribet et al. 2010; Sharma and Giribet 2011). Other somatic morphological characters have been used to diagnose travunioid taxa (e.g., free lateral sclerites), but these characters may be retained plesiomorphic states (Pinto-da-Rocha and Giribet 2007) and/or potentially neotonic (Rambla 1980; Hunt and Hickman 1993). To illustrate the complication in the use of these characters specifically in travunioids, Karaman (2005) described the monotypic genus *Trojanella*, yet left it unplaced within Travunioidea due to the uncertainty and homoplasy surrounding the diagnostic characters typically used to assign travunioid taxa.

Travunioidea has had a long and complicated taxonomic history, dating to 1861 with the description of the first species. Many European species were described by multiple authors throughout the late 1800s and early 1900s, resulting in many

nomenclatural errors, which are thoroughly discussed in Kury and Mendes (2007). The vast majority of travunioid diversity was described during the mid-1960s to mid-1970s by Briggs (1969, 1971a, 1971b, 1974) in North America and Suzuki (1964, 1972, 1975a, 1975b, 1976) in Japan. Following this burst of taxonomic research very few studies focused on travunioids with the exception of two describing new European species (Tedeschi and Sciaky 1991; Karaman 2005), until sustained research began in the mid 2010s. During the mid-late 2010s, continued morphological work and the incorporation of genetic data confirmed the unsuitability of tarsal-claw taxonomy and resulted in several nomenclatural changes including new familial names (Giribet et al. 2010) and synonymies at the subfamilial, generic, and species levels (Shear and Derkarabetian 2008; Derkarabetian & Hedin 2014). Recent studies incorporating genetic and morphological analyses have led to the discovery, delimitation, and description of new travunioid species from North America (Derkarabetian & Hedin 2014; Starrett et al. 2016).

More recently, Kury et al. (2014) provided a checklist of Travunioidea, make some taxonomic revisions, and provide a new taxonomy, which serves as the starting point for this study. In this classification, Travunioidea includes 77 species/subspecies in 24 genera classified into three families – the Travuniidae Absolon & Kratochvíl, 1932 (including the historical Travuniidae, Cladonychiidae Hadži, 1935, and Briggsidae Özdikmen & Demir, 2008 as subfamilies), Paranonychidae Briggs, 1971, and Nippononychidae Suzuki, 1975. A summary of the historical classifications is presented in Table 1.1. While the monophyly of Travunioidea is certain, internal phylogenetic

relationships are largely unresolved. The most comprehensive phylogenetic analyses of Travunioidea were conducted by Derkarabetian et al. (2010) and included samples from 10 genera. Although this study was not focused on relationships among Travunioidea and only included samples from North America, the resulting phylogeny indicated a need for a taxonomic revision with multiple families and subfamilies recovered as non-monophyletic. It is premature to discuss definitive morphological synapomorphies for all travunioids, as all hypothesized members have never been surveyed for all relevant morphological characters. However, likely morphological synapomorphies include the presence of a four-lobed ovipositor and a bipartite intestinal *diverticulum tertium* (Dumitrescu 1975, 1976; reviewed in Giribet & Kury 2007).

A genus-level phylogeny of Travunioidea and a stable classification would serve as the phylogenetic context for future taxonomic and evolutionary studies in this group. The stability of any phylogenetic-based classification is reliant on high confidence and support for internal relationships. Genome-wide approaches have produced phylogenies with generally higher nodal support and have resolved difficult relationships (e.g., Crawford et al. 2012; McCormack et al. 2012; Blaimer et al. 2015; Garrison et al. 2016; Hamilton et al. 2016). In this paper we utilize an arachnid-specific probeset targeting over 1000 UCEs (Faircloth 2017) to reconstruct the phylogenetic relationships of the Travunioidea. The phylogenetic utility of this probeset at multiple evolutionary scales was demonstrated previously (Starrett et al. 2017). The taxon sample includes representatives of 20 described genera and all currently and historically recognized families and subfamilies, plus outgroups. Although previous papers have examined

relationships among Laniatores using a wider range of taxa (Giribet et al 2010; Sharma and Giribet 2011), this study includes the most complete taxon set to date for Travunioidea allowing a proper re-evaluation of the taxonomic classification and morphology.

II. MATERIALS AND METHODS

(1) Taxon sampling

In total 56 samples were included in this study (Appendix A.1), including 39 Travunioidea, 14 non-travunioid Laniatores (8 Triaenonychidae, 2 Synthetonychiidae, and 4 Grassatores), and 3 outgroup taxa (one from each of the other three harvestmen suborders). Forty-eight samples were newly sequenced for this study. Two samples from every travunioid genus were included (in most cases from two different species), with the following exceptions: *Trojanella serbica* Karaman, 2005 is represented by a single specimen; and the European travuniids, which contains five currently recognized genera (Kury and Mendes 2007), are only represented by two specimens of the genus *Peltonychia* (=*Hadziani)*, as many European travuniids are rare and difficult to obtain.

(2) Molecular data collection

Genomic DNA was extracted from whole bodies using the Qiagen DNeasy Blood and Tissue Kit (Qiagen, Valencia, CA). For several larger specimens (body size greater than 3-4 mm) only legs, pedipalps, chelicerae were used in extractions. Extractions were

quantified using a Qubit Fluorometer (Life Technologies, Inc.) Broad Range kit and quality was assessed via gel electrophoresis on a 0.8% agarose gel. Up to 500 ng were used in sonication procedures, using a Bioruptor for 7 cycles at 30 sec on and 90 sec off. Samples were run out on a gel to verify sonication success.

Library preparation followed the general protocol of Starrett et al. (2017), with some modifications. Briefly, libraries were prepared using the KAPA Hyper Prep Kit (Kapa Biosystems), using up to 250 ng DNA (i.e., half reaction of manufacturer's protocol) as starting material. Ampure XP beads (Beckman Coulter) were used for all cleanup steps. For samples containing <250 ng total, all DNA was used in library preparation. After end-repair and A-tailing, 5 μM universal adapter stubs (University of Georgia, EHS DNA Lab) were ligated onto libraries. Libraries were then amplified in a 25 μl reaction, which consisted of 15 μl adapter-ligated DNA, 25 μl 1X HiFi HotStart ReadyMix, and 2.5 μl of each Illumina TruSeq dual-indexed primer at 10 μM (i5 and i7) with modified 8-bp indexes (Glenn et al. 2016). Amplification conditions were 98 °C for 45 s, then 16 cycles of 98 °C for 15 s, 60 °C for 30 s, and 72 °C for 60 s, followed by a final extension of 72 °C for 60 s. Samples were quantified to ensure amplification success. Equimolar amounts of libraries were combined into 1000 ng pools consisting of eight samples each (125 ng per sample).

Target enrichment was performed on pooled libraries using the MYbaits Arachnida 1.1K version 1 kit (MYcroarray, Inc.) following the Target Enrichment of Illumina Libraries v. 1.5 protocol (http://ultraconserved.org/#protocols). Hybridization was conducted at 65 °C for 24 hours, then libraries were bound to streptavidin beads

(Dynabeads MyOne C1, Invitrogen) and washed. Following hybridization, pools were amplified in a 50 µl reaction consisting of 15 µl of hybridized pools, 25 µl Kapa HiFi HotStart ReadyMix, 5 µl dH20, and 5 µM (2.5 µl) of each of TruSeq forward and reverse primers. Amplification conditions consisted of 98 °C for 45 s, then 16 cycles of 98 °C for 15 s, 60 °C for 30 s, and 72 °C for 60 s, followed by a final extension of 72 °C for 5 minutes. Following an additional cleanup, libraries were quantified using a Qubit fluorometer. Molarity was determined with an Agilent 2100 Bioanalyzer and equimolar mixes were prepared for sequencing on an Illumina NextSeq (University of California, Riverside Institute for Integrative Genome Biology) with 150 bp PE reads.

(3) Bioinformatic and phylogenomic analyses

Raw demultiplexed reads were processed entirely in the PHYLUCE pipeline (Faircloth 2015). Quality control and adapter removal were conducted with the ILLUMIPROCESSOR wrapper (Faircloth 2013). Assemblies were created with TRINITY r2013-02-25 (Grabherr et al. 2011) at default settings. Contigs were matched to probes using minimum coverage and minimum identity values of 65. UCE loci were aligned with MAFFT (Katoh and Standley 2013) and trimmed with GBLOCKS (Castresana 2000; Talavera & Castresana 2007) implemented in the PHYLUCE pipeline. Individual UCE alignments were imported into Geneious 10.1 (Biomatters Ltd.) and manually inspected for obvious alignment errors and to remove any obvious non-homologous sequences (e.g. any ingroup sequences that were more divergent than outgroup taxa). Two datasets were produced including loci at two different taxon coverage thresholds (50% and 70%). All bioinformatic analyses were performed on a late 2015 iMac, except for contig assembly,

which was run on the University of California, Riverside Institute for Integrative Genome Biology Linux cluster.

Concatenated and partitioned analyses were run on both datasets including maximum likelihood, Bayesian, and coalescent-based analyses. Maximum likelihood trees were estimated with RAxML v8.2 (Stamatakis 2014) using rapid bootstrap algorithm, 500 bootstrap replicates, and the GTRGAMMA model. Bayesian analyses were conducted using the BEAST v2.4 package (Bouckaert et al. 2014) with partitions and models determined by PartitionFinder v1.1.1 (Lanfear et al. 2012). Analyses were run for 50 million generations, logging every 1000 generations, with 10% burnin. To assess convergence, Tracer (Rambaut et al. 2014) was used to check for ESS values >200 and examine stationarity of parameters. Two separate analyses were run to check for convergence between runs. To incorporate a coalescent approach, ASTRAL-II (Mirarab et al. 2014; Mirarab and Warnow 2015) was used with individual gene trees estimated in RAxML with 500 bootstrap replicates.

III. RESULTS

(1) Sequencing results

Sequencing results and data matrix statistics are presented in Appendix A.1 and Table 1.2. The average number of UCE loci sequenced was 535 across all travunioid samples and 483 across all samples included in this study. The 70% taxon coverage

matrix included 164 loci (length of 36,131 bp, 220.31 bp average locus length) and the 50% taxon coverage matrix included 437 loci (85,883 bp, 196.53 average locus length).

(2) Phylogenomic analyses

All analyses, with the exception of the partitioned BEAST analysis, recover Travunioidea as the earliest diverging Laniatores lineage (Figure 1.3). However, the partitioned BEAST analysis recovers Travunioidea + Triaenonychoidea Sørensen, 1886 (Synthetonychiidae + Travunioidea), previously called Insidiatores Loman, 1900, sister to the Grassatores. Synthetonychiidae is recovered as sister to Triaenonychidae with full support in the BEAST analyses, but is recovered as sister to all non-travunioid Laniatores (Triaenonychidae + Grassatores) in the RAxML and ASTRAL analyses, with weaker support. The enigmatic *Fumontana* is fully supported as sister to all remaining Triaenonychidae across all analyses, with long branches indicating it's unique biogeographic placement as the only northern hemisphere triaenonychid (Figure 1.4).

Travunioidea is monophyletic and fully supported across all phylogenies and all analyses (Figure 1.4). Within Travunioidea, no families (and all but one subfamily) as currently defined in Kury et al. (2014) are monophyletic in any analyses (Figure 1.5). The monotypic *Trojanella* is recovered sister to all remaining travunioids in all analyses. However, in the ASTRAL analyses it is sister to the Travuniidae (except *Cryptomaster*, *Speleomaster*) (Figure 1.5B). The western North American genera *Cryptomaster* and *Speleomaster* are recovered as monophyletic, and although the placement of *Cryptomaster* + *Speleomaster* is not consistent across analyses, they are never sister to or

included within the Travuniidae or Cladonychiinae *sensu* Kury et al (2014). In all analyses, the Briggsinae (*Briggsus* + *Isolachus*) are recovered within a largely travuniid clade, and always sister to *Speleonychia*. Eastern North American Cladonychiinae (*Erebomaster* + *Theromaster*) are sometimes recovered sister to the European Cladonychiinae (*Holoscotolemon*) + *Peltonychia*, or sister to the Briggsinae, both cases with low support. The two samples of the European travuniid genus *Peltonychia* included in this study are not monophyletic, *P. lepreuri* is found sister to *Holoscotolemon* while *P. clavigera* is found sister to either Briggsinae + *Speleonychia* or *Erebomaster* + *Theromaster*. The relationships among these lineages are generally weakly supported. All analyses recover a clade comprised of the former northern "triaenonychids", now in two families Paranonychidae and Nippononychidae, although neither are monophyletic. The Californian endemic genus *Zuma* is recovered within a clade comprised of Japanese taxa (except *Yuria* and *Paranonychus fuscus*). The placement of the Japanese genus *Yuria* differs considerably across analyses, and is recovered as sister to each of the other major lineages. Most importantly, *Yuria* is never recovered with the other nippononychids.

(3) Phylogenomic revision

The approach to establish a stable classification involved identifying the largest group of terminal taxa that are always monophyletic and always highly supported across all phylogenetic analyses. These consistently highly supported clades are here treated as equivalent to families. Three clades are consistent across all analyses (Figure 1.5). First, a clade containing the majority of travuniid genera *sensu* Kury et al. (2014): *Peltonychia*,

Holoscotolemon, *Erebomaster*, *Theromaster*, *Speleonychia*, *Briggsus*, and *Isolachus*. This clade retains the familial name Travuniidae Absolon & Kratochvíl 1932, under the assumption that the unsampled European Travuniinae are most related to *Peltonychia* and *Holoscotolemon* given some morphological similarity (see Discussion). Second, a clade containing all genera currently included in the Paranonychidae and Nippononychidae of Kury et al (2014). This clade will retain the familial name Paranonychidae Briggs 1971. Third, a clade consisting of the two former Cladonychiinae genera *Cryptomaster* and *Speleomaster* endemic to the Pacific Northwest of North America, which is described below as the new family **Cryptomastridae n. fam.** (Figure 1.6). Both *Trojanella* and *Yuria* are considered *incertae sedis* given their uncertain phylogenetic placement (see Discussion). From the Kury et al. (2014) classification, the composition of all travunioid subfamilies has changed with the following transfers formally made here: *Holoscotolemon* from Cladonychiinae to Travuniinae; *Speleonychia* from Travuniinae to Briggsinae; *Kaolinonychus* and *Kainonychus* from Paranonychinae to Nippononychinae; *Zuma* from Sclerobuninae to Nippononychinae; *Metanonychus* from Paranonychinae to Sclerobuninae. The familial name Sclerobunidae was previously elevated by Giribet et al. (2010) to include *Zuma* and other the "northern triaenonychids". However, since the name Paranonychidae, and the subfamily Paranonychinae Briggs 1971, was used first, the name Sclerobunidae, derived from Sclerobuninae Dumitrescu, 1976, is now considered a junior synonym of Paranonychidae. Kury et al. (2014) includes *Paranonychus fuscus* (formerly *Mutsunonychus fuscus*) as a synonym of *Paranonychus brunneus* based on Shear's (1986) statement "*Paranonychus brunneus* (=*Mutsunonychus fuscus* Suzuki;

Paranonychidae)". Later in Shear and Derkarabetian (2008), the genus *Mutsunonychus* was formally synonymized under *Paranonychus*, and although a potential species level synonymy was noted, it was not formally established. The levels of UCE divergence between *P. brunneus* and *P. fuscus* are consistent with species level divergences (Figure 1.5), and as such, *P. fuscus* (Suzuki 1976) is treated as a distinct species here. The new phylogenomics-based classification, used hereafter, is summarized in Table 1.3.

(4) Taxonomy

Suborder **LANIATORES** Thorell, 1876

Family **CRYPTOMASTRIDAE n. fam.** Derkarabetian and Hedin

Type genus: *Cryptomaster* Briggs 1969, by present designation

Type species: *Cryptomaster leviathan*, Briggs 1969

Diagnosis. The Cryptomastridae can be diagnosed from all other travunioids by the presence of a distal swelling on tibia II that bears enlarged setae (Figure 1.6A,C), a sexually dimorphic structure found only in males. Both genera are fairly distinctive. *Cryptomaster* is easily identified as the largest (>2.5 mm body length) laniatorean in the Pacific Northwest of North America and largest member of Travunioidea, although two size forms exist (Starrett et al. 2016). *Speleomaster* is a troglobitic taxon restricted to lava tubes showing extreme levels of troglomorphy with complete absence of eyes, extremely reduced pigmentation, and leg elongation. Although unrelated, *Speleomaster* and

Speleonychia are both highly troglomorphic obligates of lava tubes in the Pacific Northwest, found in Idaho and Washington, respectively. Aside from their disjunct geographic distribution, *Speleomaster* can be differentiated from *Speleonychia* by the absence of a free ninth tergite and lateral sclerites, and by the presence of bifurcating tarsal claws of the hind legs (*Speleonychia* with a peltonychium). The cryptomastrid genera can be distinguished from the eastern North American Cladonychiinae (*Erebomaster* + *Theromaster*) by the spination of the pedipalpal tarsus, previously noted by Briggs (1969, 1974). Cryptomastrids possess five prominent spines on the lateral margins of the pedipalpal tarsus, three on the prolateral margin and two on the retrolateral margin. *Erebomaster* and *Theromaster* possess three pairs of prominent lateral spines (in some *Theromaster*, the two apical retrolateral spines are fused at the base).

Included genera and species

Cryptomaster Briggs 1969. Described by Briggs (1969) and originally included only *Cryptomaster leviathan* Briggs 1969 from the Coastal Range of southwestern Oregon. A second species, *Cryptomaster behemoth* Starrett and Derkarabetian 2016, was described from the southern portion of the Cascade Range in Oregon (Starrett et al. 2016).

Speleomaster Briggs 1974. Briggs (1974) described the genus and both species, *Speleomaster lexi* Briggs 1974 and *Speleomaster pecki* Briggs 1974, from lava tubes of the Snake River Plain in southern Idaho.

IV. DISCUSSION

(1) Laniatores relationships

All but one of the phylogenomic analyses conducted here recovers Travunioidea as the earliest diverging Laniatores lineage, a relationship that has not been recovered in any previously conducted genetic analyses. However, in an unpublished dissertation Mendes (2009) conducted morphological analyses that recovered a paraphyletic grade of travunioid lineages as the earliest diverging Laniatores. Additionally, Travunioidea is shown as the earliest diverging Laniatores in a phylogeny based on multiple studies and unpublished morphological data (Giribet and Kury 2007). Intestinal morphology also supports Travunioidea as the most-early diverging Laniatores (see below). The multilocus phylogenetic analyses of Giribet et al. (2010) and Sharma and Giribet (2011) recover Synthetonychiidae as earliest diverging. The partitioned BEAST analysis conducted here (Figure 1.3) recovered a split between the Grassatores and a clade containing the Travunioidea + Triaenonychoidea (Insidiatores). The only other phylogenetic analysis to recover an Insidiatores versus Grassatores topology was that of Fernandez et al (2016) in which a transcriptomic-based phylogenomic approach was used. The placement of Synthetonychiidae has varied across molecular studies, recovered as the earliest diverging Laniatores (Giribet et al. 2010; Sharma and Giribet 2011), sister to Travunioidea (Fernandez et al. 2016), or sister to Triaenonychidae + Grassatores or to Triaenonychidae in analyses here (Figure 1.3). Synthetonychiidae have traditionally been

placed with Triaenonychidae in the superfamily Triaenonychoidea, but kept as a distinct family due to its very unique morphology.

(2) Travunioidea classification and relationships

Travunioidea includes 80 nominal taxa (species/subspecies), six subfamilies, three families, and two unplaced genera. The composition of each subfamily has changed throughout each historical classification scheme (Table 1.1). Here, the composition of all subfamilies is changed again (Table 1.3). Within Travuniidae, the relationships are still uncertain, and the stability of the subfamilial limits will be dependent upon future incorporation of unsampled European travuniids, particularly *Travunia*. All genera in the Paranonychidae have been sampled and the generic relationships are consistent and highly supported across all analyses (Figure 1.5).

It is not surprising that *Trojanella* is the sole representative of the most early-diverging travunioid lineage given Karaman's (2005) statement that this species is a "unique and isolated phylogenetic line in the superfamily". Karaman's decision to leave *Trojanella* unplaced in Travunioidea was made to highlight, and as a consequence of, the commonly used morphological characters that hinder a reliable taxonomy within this group. The traditional Travuniidae are clearly polyphyletic; every species included in these analyses is recovered in a different place in the phylogeny. Although unsampled for this study, we retain all traditional European travuniids (*Arbasus*, *Buemarinoa*, *Dinaria*, *Travunia*) in the family Travuniidae. The morphological distinction between *Arbasus* and *Buemarinoa* is minimal and entirely based on tarsal segmentation, which is typical of the

"Roewerian classification" system that resulted in taxa being over split based on irrelevant characters (e.g., Kury et al. 2015). As such, for the purposes of this taxonomic revision these two genera can be considered a single lineage. Aside from the original descriptions with basic drawings (Roewer 1935; 1956), virtually no taxonomic work has been done on *Arbasus* and *Buemarinoa*. However, Kury and Mendes (2007) note that they "both look superficially like *Hadziani* [=*Peltonychia*], but with clear troglomorphic traits…", and their inclusion in Travuniidae here seems justified. Similarly, the status of *Travunia* and *Dinaria* as distinct genera has been questioned (Novak 2004), and here considered one lineage. The exact placement of these taxa is less clear morphologically, although penis musculature suggest that they should be placed within Travuniidae (see below).

In the analyses here, *Peltonychia* is recovered as paraphyletic, in some cases with strong support. These species are from two separate geographic regions: *P. clavigera* from the Pyrenees of northern Spain and southern France, and *P. lepreuri* from the Alps of northern Italy. Penis morphology across all *Peltonychia* is very similar, and this genus is likely monophyletic. More focused, European-centric species level analyses are needed to resolve this issue, and it is very likely that *Peltonychia* is sister to *Holoscotolemon*, a relationship suggested based on penis morphology (Martens 1986). The Cladonychiinae are recovered as polyphyletic. The divergence seen here between *Erebomaster* + *Theromaster* and other former Cladonychiinae is also reflected in the chemical composition of defensive secretions (Shear et al. 2014). The sister relationship of *Speleonychia* to the Briggsinae (*Briggsus* + *Isolachus*) is not surprising given the close

geographic proximity of these genera and the unique shared morphological characters. *Briggsus* and *Isolachus* are limited to the moist coastal ranges of Oregon and Washington (>50 inches yearly rainfall), while *Speleonychia* is troglobitic and restricted to lava flows surrounding Mt. Adams, in western Washington.

Although the study of Derkarabetian et al. (2010) only included North American travunioids, the relationships of paranonychids recovered here are the same, notably *Paranonychus* as the earliest diverging genus, and a sister relationship between *Sclerobunus* and *Metanonychus*. The Japanese genera *Metanipponony chus* and *Nipponony chus* show levels of UCE divergence consistent with congeners (Figure 1.5). Intermediate morphological forms between *Nipponony chus japonicus* and *Metanipponony chus daisensis* can be found where the two species come into contact (Tsurusaki pers. comm.). These genera are differentiated only by tarsal claw structure: *Metanipponony chus* possessing a ventral tooth on the median prong of the hind claws. The original drawings of male genitalia show that *M. daisensis* and *N. japonicus* differ in the width of the stylus (Suzuki 1975b). However, the penis of *N. japonicus* is highly similar to that of the geographically proximate *M. tomishimai tomishimai*.

(3) The trouble with travuniids

Two taxa are left *incertae sedis*: the monotypic genera *Trojanella* and *Yuria*, both included in Travuniidae by Kury et al. (2014). The reasons for these taxa being left unplaced relate to the lack of samples for four genera of "true travuniids" from Europe, and the incredibly long and complex taxonomic history of this group dating back to 1860.

The lack of samples and the resulting uncertainty with this group is expected given the immense number of issues surrounding the European travuniids, nomenclatural and otherwise. Kury and Mendes (2007) focus entirely on nomenclatural issues, resolving them at the familial and generic level, and in doing so note that "the [traditional] family Travuniidae constitutes one of the worst problems of the laniatorid taxonomy of the 20th century". In addition to Kury and Mendes (2007), several others have discussed the diverse array of problems plaguing travunioid taxonomy (Novak 2005; Novak and Gruber 2000; Karaman 2005). The issues include, but are not limited to, description of two species in two different genera based on the same material, autosynonymy of a genus name, proposal of unavailable family and genus names, genus description without designation of type species, species descriptions based on juveniles, mistranslation of foreign languages, disregard for correct taxonomic changes, mismatched type localities, type localities accidentally and intentionally incorrectly named, inability to find further specimens from type localities despite much effort, and destruction of type localities.

In this study we were unable to include samples from four European genera that are all troglobitic: *Arbasus*, *Buemarinoa*, *Dinaria*, and *Travunia*. Three of these genera are monotypic, single-site endemics: *Arbasus caecus* (Simon 1911) from France, *Buemarinoa patrizii* Roewer, 1956 from Sardinia, and *Dinaria vjetrenicae* (Hadži 1932) from Bosnia and Herzegovina. The genus *Travunia* includes four species *T. borisi*, *T. hofferi*, *T. jandai*, and *T. troglodytes*, all restricted to caves in the Southern Dinarid karst. It is unclear how many actual species exist. Novak (2004) questioned the validity of *Travunia*, *Dinaria*, and *Abasola* at the generic level, and *Abasola* was later synonymized

with *Travunia* (Kury and Mendes 2007). *Travunia* may be oversplit and has 2-3 species of questionable status (Novak 2004, 2005). The distinct generic status of *Arbasus* and *Buemarinoa* has also been doubted (Kury and Mendes 2007). Despite being unsampled, these taxa are retained in the family Travuniidae. Given uncertainty in taxonomic status of unsampled species and genera, we refrain from placing *Trojanella* into a distinct taxonomic category. The classification presented here assumes that the unsampled genera are related to *Peltonychia*, as all previous authors and classifications have done. However, there is a possibility that some may be related to *Trojanella* given close geographic proximity (i.e., *Travunia*). Even though the European Travuniidae have received much attention from a taxonomic standpoint, a great deal of focused and devoted research including fieldwork, morphological, and phylogenetic analyses would be needed to fully resolve the issues of this notoriously difficult clade.

The second taxon left unplaced is the monotypic genus *Yuria*. When *Yuria pulchra* was first described it was placed in Travuniidae because the tarsal claw is a peltonychium (Suzuki 1964, 1975a). Based on morphological analyses, Mendes (2009) recovered *Yuria* sister to *Nipponony chus* (Paranonychidae) with two shared characters. Kury et al. (2014) later transferred this genus to the Nipponony chidae, which contained most of the other Japanese travunioids. In analyses here, placement and support for *Yuria* varies highly depending on analysis type, being alternately placed sister to each one of the three recognized families (Figure 1.5). The weakly supported nodes and alternative placements are likely due to the short branches of the early diverging nodes within Travunioidea, potentially indicating rapid divergence among these major lineages.

Morphology complicates matters further, as *Yuria* possess a free ninth tergite and lateral sclerites, plesiomorphic characters that are potentially neotonic and shared with the Briggsinae. The penis morphology of *Yuria* is also relatively unique (see below).

(4) Morphological reevaluation

The tarsal claw - Prior to the utilization of genetic data, classification of travunioids and diagnostic differences were largely based on morphological characters that are now known to either be plesiomorphic or highly homoplastic and variable. In particular, the structure of the tarsal claw of legs III and IV, and number of side branches on the median prong, were used heavily to diagnose genera and propose taxonomic and phylogenetic hypotheses. Both Briggs (1971a) and Suzuki (1975b) assumed that relatively complex claws (higher number of side branches) were primitive in Travunioidea, while the simpler claws (single side branch) were derived. However, they disagreed as to which taxon was the earliest diverging. Briggs proposed *Briggsus*/*Isolachus* as the earliest diverging, largely due to the presence of a free ninth tergite and lateral sclerites (discussed below), while Suzuki proposed the nippononychines (then with three genera) with higher number of side branches. The results here further corroborate the inappropriateness of this character, as no clear evolutionary patterns exist for tarsal claw structure.

A type of modified tarsal claw termed a peltonychium united the "traditional Travuniidae", a structure now known to be convergent in several unrelated troglobitic species (e.g., *Peltonychia*, *Speleonychia*, *Trojanella*). The morphological distinction

between the typical trident-shaped tarsal claw (with variable number of side-branches) and a peltonychium is not entirely clear in some travunioids (e.g. *Izunonychus*, *Metanippononychus*), and the transition between forms is best documented in the triaenonychid genus *Lomanella* (Hunt and Hickman 1993). However, *all* of the 18 travunioid species (not including subspecies) with a clear peltonychium are found in caves, 10 of which are either described to be troglobitic (cave-obligate) and/or show high levels of troglomorphy. An additional six species are described to have reduced pigmentation (relative to surface-only species), five of which are only reported from caves. Two remaining species are inconsistent with this pattern. First, *Peltonychia lepreuri*, from the Alps of northern Italy and Switzerland is recorded from both cave and surface habitats (considered a troglophile) and retains black pigment. Second, *Yuria* from southern Japan, which has two subspecies: *Y. pulchra pulchra* and *Y. p. briggsi*. The subspecies differ in their pigmentation and habitat: *Y. p. pulchra* is only known from surface habitats under woody debris, while *Y. p. briggsi*, shows some reduced pigmentation, and is recorded from both cave and surface habitats. It has been suggested that the peltonychium, and other plesiomorphic characters, are convergent through neoteny (Rambla 1980; Hunt and Hickman 1993; Karaman 2005). The hind tarsal claws of juvenile triaenonychids and travunioids have more side branches than adults (e.g., Hunt and Hickman 1993; Suzuki 1975b), and some juveniles additionally possess a fleshy projection termed an arolium (e.g., *Briggsus*), and a pseudonychium (median tarsal claw) (Shultz and Pinto-da-Rocha 2007; Gnaspini 2007). As such, the peltonychium may a retained adult form of these juvenile structures (Hunt and Hickman 1993).

The ninth tergite and lateral sclerites - The traditional Briggsinae (*Briggsus* + *Isolachus*) were hypothesized to be a relatively early diverging lineage within Travunioidea (Briggs 1971, Giribet and Kury 2007). This was due to the presence of a free ninth tergite, and lateral sclerites, a plesiomorphic condition found in the other suborders of harvestmen. Conversely, penis morphology suggested this group is derived given the relatively simple penis structure (Martens 1986). *Speleonychia* also possess a distinct ninth tergite and lateral sclerites, now shown to be a shared condition with *Briggsus* + *Isolachus* (Figure 1.5). Rambla (1980) argued that these characters are neotonic, retained in adult from nymphal stages, and as such are derived. All phylogenomic analyses here support the derived nature of these characters in Briggsinae, as they are recovered well within the Travuniidae in all analyses. However, not all travunioid taxa with a free ninth tergite and free lateral sclerites are restricted to this clade, as *Yuria* also possess both characters (Suzuki 1964, 1975a). While the placement of *Yuria* is uncertain, it is never recovered with the Briggsinae. Outside of Travunioidea, the only other laniatorean taxa to possess free lateral sclerites are in the genus *Hickmanoxyomma* Hunt 1990, a largely cave-dwelling triaenonychid genus endemic to Tasmania (Hunt 1990). In this genus the presence of five pairs of free lateral sclerites (2-3 in travunioids) are a diagnostic character for the *H. cavaticum* species group containing four species, all only recorded only from caves, and some showing troglomorphy. All other species in this genus lack lateral sclerites. Hunt (1990) suggested it might be correlated with reduced sclerotization associated with troglomorphy, but also reiterated Rambla's (1980) view of neoteny. No clear phylogenetic, evolutionary, or ecological

pattern exists for these characters and their presence in multiple unrelated lineages suggests their plesiomorphic nature.

The midgut - Studies focusing on the digestive tract started in the 1920s, but the work of Dumitrescu (e.g., 1974, 1975, 1976) contributed significantly, particularly to the phylogenetic utility of midgut morphology in Opiliones. The Laniatores midgut can be divided into three pairs of diverticula: diverticulum 1 (DI) and opisthosomal diverticula 2 and 3 (OD2 and OD3), each with variable branching patterns. These structures were more recently renamed to better reflect homology with the other harvestmen suborders (Shultz and Pinto-da-Rocha 2007): D1, OD2, and OD3 were previously called DI, DII, and DIII, respectively, in the work of Dumitrescu and other earlier researchers. Based on branching patterns Dumitrescu noted issues with the "traditional taxonomy" of Laniatores and Travunioidea. By examining taxa representing "northern triaenonychids", traditional travuniids, Synthetonychiidae, and Triaenonychidae, Dumitrescu (1975, 1976) noticed the similarity of the "northern triaenonychids" to that of the Travuniidae, instead of the southern hemisphere triaenonychids. All Triaenonychoidea and Grassatores possess an OD3 with three branches while the northern triaenonychids and Travuniidae possess an OD3 with two branches. As such, he placed the "northern triaenonychids" taxa into the family Paranonychidae, an elevation of the subfamily Paranonychinae established by Briggs (1971). The name Paranonychidae was used by a few subsequent authors (e.g., Shear 1982, 1986; Ubick and Dunlop 2005), but from a classification standpoint it was not incorporated into the taxonomy as the four "northern triaenonychid" subfamilies were left in the Triaenonychidae (e.g., Kury 2003; Pinto-da-Rocha and Giribet 2007). Later,

several molecular phylogenetic studies supported the relationship of "northern triaenonychids" to the other travunioid families (Giribet et al., 2010; Hedin and Thomas 2010; Derkarabetian et al. 2010; Sharma and Giribet 2011), and the familial name Paranonychidae was finally correctly included in Opiliones taxonomy by Kury (2013).

The phylogenomic analyses presented here allow for a reexamination of the intestinal morphology research of Dumitrescu (1975, 1976). First, the recovery here of Travunioidea as the earliest diverging Laniatores lineage is reflected in the branching pattern of OD3. All Travunioidea possess an OD3 with two branches, a characteristic shared with the other harvestmen suborders, while the Synthetonychiidae, Triaenonychidae, and Grassatores possess three branches. This phylogenetic utility of OD3 was also shown in the morphological analyses of Mendes (2009), which recovered Travunioidea as the earliest diverging lineage of Laniatores. The variation in the structure of D1 may have some phylogenetic value within Travunioidea and the three major lineages recovered here. While the intestines of Cryptomastridae have yet to be examined, there is a distinction between the Paranonychidae and Travuniidae. Of the taxa examined by Dumitrescu (1975, 1976), the paranonychids possess a simple D1 with no branches, while all taxa corresponding to Travuniidae possess a relatively complex D1 with 2-3 branches or is distinctly triangular in shape. Samples of *Briggsus* and *Speleonychia* were included and look very similar to each other, particularly the D1, which is recorded to be 3-branched in *Briggsus* and triangular in *Speleonychia* (Dumitrescu 1976). Dumitrescu did not note the similarity, instead stating *Speleonychia* was most similar to *Nippononychus japonicus* (then *Peltonychia japonica*, placed in

Travuniidae), perhaps subjectively limited by the classification system of the time. It is clear that there is phylogenetic utility in midgut morphology at higher taxonomic levels, and with a more stable classification of Travunioidea, more thoroughly sampled analyses of intestinal morphology can be conducted.

The penis - The Laniatores penis can be divided into two main parts, the truncus (shaft), and the relatively complex and taxon-specific apical glans, which contains the stylus, sperm duct, and various combinations of plates, spines, setae, etc. In Travunioidea, Triaenonychidae, and Synthetonychiidae the glans is expanded via muscles while in the Grassatores expansion relies on hydraulic pressure. Based on descriptions and drawings, the musculature and glans complexity can be used to diagnose and differentiate travunioid lineages as defined here (Briggs 1971b; Suzuki 1975a, 1975b; Martens 1986; Karaman 2005; Pinto-da-Rocha and Giribet 2007; Derkarabetian and Hedin 2014; Starrett et al. 2016). In all taxa except the European Travuniidae, the musculature fills the entire length of the truncus up to the glans. The muscle is restricted to only the basal portion of the truncus in the European travuniids. In *Trojanella serbica* the muscle is limited to distal part of truncus and glans. The complexity of the glans makes it a highly variable and informative morphological character across Laniatores. In Travunioidea, the glans is relatively simple and plate-like without dorsal, dorsolateral, or ventral plates in *Trojanella*, Cryptomastridae, and Travuniidae, while in *Yuria* and Paranonychidae the glans is relatively complex. The dorsal plate is absent from all travunioids, except *Yuria,* which possesses a dorsal plate that is fused to the stylus.

Although relationships within the Travuniidae are still uncertain and the genitalia of some taxa have never been examined, some patterns are evident. The Travuniinae differ from all other Travuniidae in that the musculature does not fill the entirety of the truncus, being limited to the basal portion only (Martens 1986; Pinto-da-Rocha and Giribet 2007). Although placed in different traditional families, the genera *Holoscotolemon* and *Peltonychia* share very similar glans morphology (Martens, 1986). Based on the glans structure, the traditional travuniids can be split into two groups, those from the Pyrenees and Alps (*Peltonychia*) with musculature restricted to the extreme basal portion of the truncus and clear articulation between truncus and glans, and those from the Dinarid Karst (*Dinaria* and *Travunia*) with the musculature filling the basal 2/3 of the truncus and an undefined division between the truncus and glans (Kury and Mendes 2007). *Dinaria* and *Travunia* may represent a "transitional form" between *Peltonychia* + *Holoscotolemon* and the North American travuniids that have musculature filling the entire truncus. The genitalia of *Buemarinoa* and *Arbasus* have never been examined. Given the consistent and highly supported relationships within Paranonychidae, diagnostic differences of paranonychid lineages can be seen in penis morphology. Dorsolateral plates are present but reduced in two pairs of sister genera *Sclerobunus* + *Metanonychus* and *Metanippononychus* + *Nippononychus* (Briggs 1971b; Suzuki 1975b; Derkarabetian and Hedin 2014). Additionally, *Sclerobunus* + *Metanonychus* (Sclerobuninae) show a distinct setae bearing process similar to a ventral plate ("sensillenträger" of Martens), that is fused to the base of the stylus in nippononychines. The clade consisting of *Zuma* + *Izunonychus* + *Kainonychus* possess a

modified sperm duct that is expanded distally (Briggs 1971b; Suzuki 1975b). Additionally, as opposed to other Japanese paranonychids which have a stylus that is fused to the ventral plate, the stylus of both *Izunonychus* + *Kainonychus* is separated from the ventral plate (Suzuki 1975b).

The overall trend across Opiliones suborders is one of increasing complexity. The earliest-diverging suborder Cyphophthalmi has a spermatopositor, the Dyspnoi and Eupnoi have a simple penis with little modifications, and the derived Laniatores possess the most complex penes (Macías-Ordóñez 2010). Within Laniatores the trend of increasing complexity is maintained, as Travunioidea with relatively simple glans is the most early-diverging Laniatores. The Travunioidea and Triaenonychoidea use muscles for glans expansion, a condition shared with Eupnoi and Dyspnoi. Relative to travunioids, the synthetonychiids and triaenonychids have slightly more complex glans structures with dorsolateral plates. Finally, in the most derived laniatorean lineage Grassatores, muscles are absent and the glans requires hydraulic pressure to expand. In Travunioidea, Martens (1986) noted a tendency towards simplification of the glans, and Karaman (2005) additionally noted a correlation where simplification of the glans structure is associated with reduction of penis musculature to basal portion of the truncus. Both Martens and Karaman argued that the simple glans of travunioids ("traditional travuniids") is a derived condition, as all Triaenonychoidea have relatively complex glans with dorsolateral plates and a distinct process bearing setae, two characters lost in many travunioids. Most phylogenomic analyses conducted here recover Travunioidea as the most early-diverging Laniatores lineage suggesting a trend of simple to complex penis

structure. Within Travunioidea, *Trojanella* with a simple plate-like penis is ancestral, while the relatively complex glans of sclerobunines is derived. Within Paranonychidae, the earliest-diverging *Paranonychus* possess the simplest glans. However, the reduction of musculature to the basal portion of the truncus in Travuniinae may be considered derived, as all other travunioids (except *Trojanella*) have musculature filling the entire truncus.

Potentially confounding any obvious evolutionary trend in Travunioidea is that fact that the simplest glans and reduced musculature are found in cave-inhabiting taxa (e.g., *Trojanella*, *Dinaria, Travunia*). These taxa are cave obligates, and often called "living fossils" as they are thought to be remnants of long-extinct surface taxa. Their surface ancestors may potentially have had more complex penes, similar to that of most paranonychids or triaenonychoids. As discussed previously, there is a strong correlation between the presence of a peltonychium and cave habitation in Travunioidea. Similarly, Hunt and Hickman (1993) note a correlation between claw structure and penis - the presence of a peltonychium is typically associated with plate reduction of the glans. The non-troglomorphic morphological changes (i.e., peltonychium, simplification of glans) seen in obligate-cave dwelling travunioid harvestmen may be developmentally and/or genetically linked with the typical suite of adaptive morphological changes that are associated with cave habitation. The dorsal, dorsolateral, and lateral plates of the glans typical of the more complex penes, do not form until the end of the nymphal development cycle (Hunt and Hickman 1993), and the simple juvenile penis may be retained in adulthood through neoteny perhaps mediated by linkage with troglomorphic characters.

Given an underlying developmental/genetic linkage, significant morphological changes may indirectly occur in the penis due to the extreme selective pressure of cave habitats acting on "typical" troglomorphic characters. For example, the genus *Sclerobunus* contains 12 species in three species groups (Derkarabetian and Hedin 2014). Each species group has distinctive penis morphology, but within each species group, penis morphology is highly conserved across species (Derkarabetian et al. 2011). Within the *S. robustus* group, penis morphology cannot be used to diagnose and differentiate the seven species, with the exception of *S. speoventus* and *S. steinmanni*, both of which are highly troglomorphic and only recorded from caves.

(5) Context for future research

This phylogenomic study provides a more stable taxonomy for Travunioidea, which serves as a starting point for species-level phylogenomics and provides the phylogenetic context to explore interesting evolutionary questions relating to character evolution, alpha taxonomy, and biogeography.

Morphological and chemical evolution - Many Travunioidea are cave-obligate taxa with species from 14 genera showing some degree of troglomorphy, possessing homoplastic morphological adaptations that develop as a response to the absence of light. Travunioidea can be an excellent system to study the repeated evolution of troglomorphy, as it has evolved at multiple taxonomic levels (e.g., within families, genera, species) with multiple independently derived taxa showing varying degrees of troglomorphy. For example, within the genus *Sclerobunus*, troglomorphy has evolved *at least* five times

independently across multiple species and within single species and is time-correlated (Derkarabetian et al. 2010; Derkarabetian and Hedin 2016). A species-level phylogeny would allow for an accurate estimate of the number of independent evolutions of troglomorphy and allow for in-depth morphological analyses exploring the rate and timing of this adaptive morphology, as well as providing the phylogenetic framework for comparative studies (e.g., gene expression).

Similarly, chemical evolution can be explored in this phylogenomic context. Harvestmen possess repugnatorial glands, which are used to store chemical cocktails that are secreted in defensive behavior. Chemical composition across lineages has been shown to have some phylogenetic value, particularly in Laniatores (Raspotnig 2012; Raspotnig et al. 2014). Similarly a study focusing on Travunioidea and Triaenonychoidea has shown high levels of divergence in chemical composition between taxa formerly united under the traditional taxonomy (i.e. Cladonychiidae) (Shear et al 2014). Given phylogenetic context, detailed chemical analyses can be used to discover novel chemicals, identify biochemical pathways, compare pathways of identical chemicals found in independent lineages, and explore the evolution of biochemical pathways across taxa. Species in the genus *Sclerobunus* and *Holoscotolemon* are known to produce nicotine as part of the chemical cocktail (Ekpa et al. 1984; Raspotnig et al. 2011; Shear et al. 2014). It is unknown whether this is sequestered from the environment (i.e., prey items) or if the harvestmen produces nicotine *de novo*. However, acquisition from prey items seems unlikely, as other travunioids syntopic with *Sclerobunus* do not produce nicotine (Shear et al. 2014). The lack of evidence for *de novo* nicotine production in animals, its presence

in multiple species of two unrelated travunioid genera, and the production of compounds chemically related to nicotine (alkaloids) in other travunioids suggests a common underlying biochemical pathway that may be slightly modified in different travunioid taxa.

Biogeography and alpha taxonomy - Cryophilic harvestmen are useful in biogeographic analyses because of restricted ecological constraints and extremely low vagility. Previous molecular phylogenetic studies on harvestmen with these biological characteristics have shown compelling biogeographic patterns (e.g., Boyer et al. 2007; Thomas and Hedin 2008; Giribet et al. 2011; Schönhofer et al. 2015; Boyer et al. 2015). The Travunioidea have a temperate Laurasian distribution with species found in eastern Asia, eastern and western North America, and central Europe, with notable absences from central Asia (Figure 1.2). Recent divergence dating analyses show an ancient origin of Travunioidea dating to >200 million years (Giribet et al. 2010; Sharma and Giribet 2011). Several travunioid lineages show trans-continental distributions. For example, members of the Travuniidae are distributed in Europe and eastern and western North America, while the Paranonychidae show a trans-Pacific distribution with genera in western North America, Japan and Korea. Many other harvestmen show similar broad distributions within the Holarctic including the Sironidae, *Caddo*, *Leiobunum*, and many Dyspnoi (Suzuki 1972; Suzuki et al. 1977; Shultz and Regier 2009; Hedin et al. 2012; Schönhofer et al. 2013). With a well-resolved phylogeny explicit hypotheses can be tested (Sanmartin et al. 2001; Wen et al. 2016).

The biological characteristics of essentially all travunioids are quite similar (e.g., dispersal-limited, restricted to cryophilic microhabitats in north temperate latitudes). Regional clades are relatively ancient, allowing ample time for the accumulation of species diversity. In addition, the presence of rare, completely blind, troglobitic species in several different geographic areas speaks to the ancient origin of the Travunioidea. It is likely that troglobitic species, especially those in central Europe, have an unknown diversity concealed by adaptive troglomorphy. Similarly, many ancient lineages can be found in the moist, coastal forests of the Pacific Northwest (Briggsidae, *Metanonychus*) that have likely persisted in refugia through climatic cycles. Additionally, all of these taxa consist of species and subspecies that are short-range endemics. Congeneric species syntopy is rare, probably because of ecological niche conservatism that prevents resource partitioning. This ecological niche conservatism likely plays an important role in speciation (see model of Wiens 2004). As such, there is a high potential for species discovery and recent species-level studies focusing on the travunioid genera *Sclerobunus* and *Cryptomaster* have resulted in the description of new species (Derkarabetian and Hedin 2014; Starrett et al. 2016), while ongoing studies in other travunioid genera are identifying further undescribed species (Hedin lab unpublished).

V. REFERENCES

Absolon K, Kratochvíl J (1932) Peltaeonychidae, nova čeled slepých opilionidu z jeskýn jihoillyrské oblasti. *Prírода*, **25**, 153–156.

Blaimer BB, Brady SG, Schultz TR, Lloyd MW, Fisher BL, Ward PS (2015) Phylogenomic methods outperform traditional multi-locus approaches in resolving deep evolutionary history: a case study of formicine ants. *BMC Evolutionary Biology*, **15**, 271.

Bouckaert R, Heled J, Kühnert D, Vaughan T, Wu CH, Xie, D, Suchard MA, Rambaut A, Drummond AJ (2014) BEAST 2: a software platform for Bayesian evolutionary analysis. *PLoS Computational Biology*, **10**, e1003537.

Boyer SL, Clouse RM, Benavides LR, Sharma P, Schwendinger PJ, Karunarathna I, Giribet G (2007) Biogeography of the world: a case study from cyphophthalmid Opiliones, a globally distributed group of arachnids. *Journal of Biogeography*, **34**, 2070-2085.

Boyer SL, Baker CM, Popkin-Hall ZR, Laukó DI, Wiesner HA, Quay RH (2015) Phylogeny and biogeography of the mite harvestmen (Arachnida: Opiliones: Cyphophthalmi) of Queensland, Australia, with a description of six new species from the rainforests of the Wet Tropics. *Invertebrate Systematics*, **29**, 37-70.

Briggs TS (1969) A new holarctic family of laniatorid phalangids (opiliones). *Pan-Pacific Entomologist*, **45**, 35.

Briggs TS (1971a) Relict harvestmen from the Pacific northwest (Opiliones). *Pan Pacific Entomologist*, **47**, 165-178.

Briggs TS (1971b) The harvestmen of family Triaenonychidae in North America (Opiliones). Occasional Papers of the California Academy of Sciences, **90**, 1-43.

Briggs TS (1974) Troglobitic harvestmen recently discovered in North American lava tubes (Travuniidae, Erebomastridae, Triaenonychidae: Opiliones). *Journal of Arachnology*, **1**, 205-214.

Castresana J (2000) Selection of conserved blocks from multiple alignments for their use in phylogenetic analysis. *Molecular Biology and Evolution*, **17**, 540-552.

Crawford NG, Faircloth BC, McCormack JE, Brumfield RT, Winker K, Glenn TC (2012) More than 1000 ultraconserved elements provide evidence that turtles are the sister group of archosaurs. *Biology Letters*, **8**, 783–786.

Derkarabetian S, Steinmann DB, Hedin M (2010) Repeated and time-correlated morphological convergence in cave-dwelling harvestmen (Opiliones, Laniatores) from montane western North America. *PLoS One*, **5(5)**, e10388.

Derkarabetian S, Ledford J, Hedin M (2011) Genetic diversification without obvious genitalic morphological divergence in harvestmen (Opiliones, Laniatores, *Sclerobunus robustus*) from montane sky islands of western North America. *Molecular Phylogenetics and Evolution*, **61**, 844-853.

Derkarabetian S, Hedin M (2014) Integrative taxonomy and species delimitation in harvestmen: a revision of the western North American genus *Sclerobunus* (Opiliones: Laniatores: Travunioidea). *PLoS One*, **9(8)**, e104982.

Dumitrescu DO (1974a) Contribution à l'étude de l'appareil digestif (intestin moyen) des Opilions (Arachnida). *Travaux du Muséum d'Histoire naturelle (Grigore Antipa)*, **14**, 95–107.

Dumitrescu DO (1975) Contribution a l'étude morphologique de l'appareil digestif (intestin moyen) des opilions. *Proceedings of the 6th International Arachnology Congress, Amsterdam IV*, 150-155.

Dumitrescu DO (1976) Recherches morphologiques sur l'appareil digestif (intestin moyen) des Gonyleptomorphi (Arachnida, Opilionida). *Travaux du Muséum d'Histoire naturelle (Grigore Antipa)*, **17**, 17–30.

Ekpa O, Wheeler JW, Cokendolpher JC, Duffield RM (1984) N, N-Dimethyl-β-phenylethylamine and bornyl esters from the harvestman *Sclerobunus robustus* (Arachnida: Opiliones). *Tetrahedron Letters*, **25**, 1315-1318.

Faircloth BC (2013) Illumiprocessor: a Trimmomatic wrapper for parallel adapter and quality trimming. dx. doi. org/10.6079/J9ILL.

Faircloth BC (2015) PHYLUCE is a software package for the analysis of conserved genomic loci. *Bioinformatics*, **32**, 786-788.

Faircloth BC (2017) Identifying conserved genomic elements and designing universal bait sets to enrich them. *Methods in Ecology and Evolution*, **8**, 1103-1112.

Fernández R, Sharma PP, Tourinho AL, Giribet G (2017) The Opiliones tree of life: shedding light on harvestmen relationships through transcriptomics. *Proceedings of the Royal Society B*, **284**, 20162340.

Garrison NL, Rodriguez J, Agnarsson I, Coddington JA, Griswold CE, Hamilton CA, Hedin M, Kocot KM, Ledford JM, Bond JE (2016) Spider phylogenomics: untangling the Spider Tree of Life. *PeerJ*, **4**, e1719.

Giribet G, Vogt L, González AP, Sharma P, Kury AB (2010) A multilocus approach to harvestman (Arachnida: Opiliones) phylogeny with emphasis on biogeography and the systematics of Laniatores. *Cladistics*, **26**, 408-437.

Giribet G, Kury AB (2007) Phylogeny and Biogeography. In: *Harvestmen: The Biology of Opiliones*. Eds. Pinto-da-Rocha R, Machado G, Giribet G. Harvard University Press, Cambridge, Massachusetts, and London, England. Pp. 62-87.

Giribet G, Sharma PP, Benavides LR, Boyer SL, Clouse RM, De Bivort BL, Dimitrov D, Kawauchi GY, Murriene J, Schwendinger PJ (2011) Evolutionary and biogeographical history of an ancient and global group of arachnids (Arachnida: Opiliones: Cyphophthalmi) with a new taxonomic arrangement. *Biological Journal of the Linnean Society*, **105**, 92-130.

Giribet G, Sharma PP (2015) Evolutionary biology of harvestmen (Arachnida, Opiliones). *Annual Review of Entomology*, **60**, 157-175.

Gnaspini P (2007) Development. In: *Harvestmen: The Biology of Opiliones*. Eds. Pinto-da-Rocha R, Machado G, Giribet G. Harvard University Press, Cambridge, Massachusetts, and London, England. Pp. 455-472.

Grabherr MG, Haas BJ, Yassour M, Levin JZ, Thompson DA, Amit I, et al. (2011) Full-length transcriptome assembly from RNA-Seq data without a reference genome. *Nature Biotechnology*, **29**, 644-652.

Hadži J (1932) Prilog poznavanju pećinske faune Vjetrenice.(Pseudoscorpionidea: *Neobisium* (*Blothus*) *vjetrenicae* sp. n., Opilionidea: *Travunia vjetrenicae* sp. n., *Nelima troglodytes* Roewer). *Glas Srpske Kraljevske Akademije*, **151**, 103–157.

Hadži J (1935) Ein eigentumlicher neuer Hölen-Opilionid aus Nord-Amerika, *Cladonychium corii* g.n. sp. n. *Biologia Generalis*, **11**, 49–72.

Hamilton CA, Lemmon AR, Lemmon EM, Bond JE (2016) Expanding anchored hybrid enrichment to resolve both deep and shallow relationships within the spider tree of life. *BMC Evolutionary Biology*, **16**, 212.

Hedin M, Thomas SM (2010) Molecular systematics of eastern North American Phalangodidae (Arachnida: Opiliones: Laniatores), demonstrating convergent morphological evolution in caves. *Molecular Phylogenetics and Evolution*, **54**, 107-121.

Hedin M, Tsurusaki N, Macías-Ordóñez R, Shultz JW (2012) Molecular systematics of sclerosomatid harvestmen (Opiliones, Phalangioidea, Sclerosomatidae): geography is better than taxonomy in predicting phylogeny. *Molecular Phylogenetics and Evolution*, **62**, 224-236.

Hunt GS (1990) *Hickmanoxyomma*, a new genus of cavernicolous harvestmen from Tasmania (Opiliones: Triaenonychidae). *Records of the Australian Museum*, 42, 45-68.

Hunt GS, Hickman JL (1993) A revision of the genus *Lomanella* Pocock and its implications for family level classification in the Travunioidea (Arachnida: Opiliones: Triaenonychidae). *Records of the Australian Museum*, **45**, 81-119.

Karaman IM (2005) *Trojanella serbica* gen. n., sp. n., a remarkable new troglobitic travunioid (Opiliones, Laniatores, Travunioidea). *Revue Suisse de Zoologie*, **112**, 439-456.

Katoh K, Standley DM (2013) MAFFT multiple sequence alignment software version 7: improvements in performance and usability. *Molecular Biology and Evolution*, **30**, 772-780.

Kury AB (2000 onwards) Classification of Opiliones. Museu Nacional/UFRJ website. Online at: http://www.museunacional.ufrj.br/mndi/Aracnologia/opiliones.html.

Kury AB (2003) Annotated catalogue of the Laniatores of the new World (Arachnida, opiliones). *Revista Ibérica de Aracnología*, **1**, 5-337.

Kury AB (2013) Order Opiliones Sundevall, 1833. Animal Biodiversity: An outline of higher–level classification and survey of taxonomic richness (Addenda 2013). *Zootaxa*, **3703**, 27-33.

Kury AB, Mendes AC (2007) Taxonomic status of the European genera of Travuniidae (Arachnida, Opiliones, Laniatores). *Munis Entomology & Zoology*, **2**, 1-14.

Kury AB, Mendes AC, Souza DR (2014) World Checklist of Opiliones species (Arachnida). Part 1: Laniatores–Travunioidea and Triaenonychoidea. *Biodiversity Data Journal*, **2**, e4094.

Kury AB, Pérez-González A (2015) A companion to Part 2 of the World Checklist of Opiliones species (Arachnida): Laniatores–Samooidea, Zalmoxoidea and Grassatores *incertae sedis*. *Biodiversity Data Journal*, **3**, e6663.

Lanfear R, Calcott B, Ho SY, Guindon S (2012) PartitionFinder: combined selection of partitioning schemes and substitution models for phylogenetic analyses. *Molecular Biology and Evolution*, **29**, 1695-1701.

Machado G, Pinto-da-Rocha R, Giribet G (2007) What are harvestmen? In: *Harvestmen: The Biology of Opiliones*. Eds. Pinto-da-Rocha R, Machado G, Giribet G. Harvard University Press, Cambridge, Massachusetts, and London, England. Pp. 1-13.

Macías-Ordóñez R, Machado G, Pérez-González A, Shultz JW (2010) Genitalic evolution in Opiliones. In: *The Evolution of Primary Sexual Characters in Animals*. Eds. Leonard JL, Córdoba-Aguilar A. Oxford University Press, New York. Pp. 285-306.

Martens J (1986) Die grossgliederung der Opiliones und die evolution der ordnung (Arachnida). In: *Actas 10 Congreso Internacional de Aracnologia, Jaca/Espana*. Ed. Barrienos JA. Instituto Pirenaico de Ecologia & Grupo de Aracnologia, Barcelona. Pp. 289-310.

Maury EA (1988) Triaenonychidae sudamericanos V. Un nuevo genero de opiliones cavernicolas de la Patagonia (Opiliones, Laniatores). *Mémoires de Biospéologie*, **15**, 117-131.

Mendes AC (2009) *Avaliação do status sistemático dos táxons supragenéricos de Insidiatores Loman, 1902 (Arachnida, Opiliones, Laniatores)*. Unpublished Ph.D. Thesis, Ciências Biológicas (Zoologia) – Museu Nacional, Universidade Federal do Rio de Janeiro.

McCormack JE, Faircloth BC, Crawford NG, Gowaty PA, Brumfield RT, Glenn TC (2012) Ultraconserved elements are novel phylogenomic markers that resolve placental mammal phylogeny when combined with species-tree analysis. *Genome Research*, **22**, 746–754.

Mirarab S, Reaz R, Bayzid MS, Zimmermann T, Swenson MS, Warnow T (2014) ASTRAL: genome-scale coalescent-based species tree estimation. *Bioinformatics*, **30**, i541-i548.

Mirarab S, Warnow T (2015) ASTRAL-II: coalescent-based species tree estimation with many hundreds of taxa and thousands of genes. *Bioinformatics*, **31**, i44-i52.

Novak T (2004) An overview of harvestmen (Arachnida: Opiliones) in Croatia. *Natura Croatica*, **13**, 231-296.

Novak T (2005) An overview of harvestmen (Arachnida: Opiliones) in Bosnia and Herzegovina. *Natura Croatica*, **14**, 301-350.

Novak T, Gruber J (2000) Remarks on published data on harvestmen (Arachnida: Opiliones) from Slovenia. In *Annales, (Koper) Series Historia Naturalis*, **10**, 281-308.

Özdikmen H, Demir H (2008) New family and genus names, Briggsidae nom. Nov. and *Briggsus* nom nov., for the harvestmen (Opiliones: Laniatores). *Munis Entomology and Zoology*, **3**, 174-176.

Pinto-da-Rocha R, Machado G, Giribet G (2007) Harvestmen: The Biology of Opiliones. Harvard University Press, Cambridge, Massachusetts, and London, England. 608 pp.

Pinto-da-Rocha R, Giribet G (2007) Taxonomy. In: *Harvestmen: The Biology of Opiliones*. Eds. Pinto-da-Rocha R, Machado G, Giribet G. Harvard University Press, Cambridge, Massachusetts, and London, England. Pp. 88-246.

Rambaut A, Drummond AJ (2012) Tracer v1. 4. 2007.

Rambla, M. (1980). *Neoteny in Opiliones*. In: *Verhandlungen 8. Internationaler Arachnologen Kongress*. Ed. Gruber J. Abgehalten an der Universität für Bodenkultur, Wien. Pp. 489-492.

Raspotnig G (2012) Scent gland chemistry and chemosystematics in harvestmen. *Biologia Serbica*, **34**, 5-18.

Raspotnig G, Schaider M, Föttinger P, Komposch C, Karaman I (2011) Nitrogen-containing compounds in the scent gland secretions of European cladonychiid harvestmen (Opiliones, Laniatores, Travunioidea). *Journal of Chemical Ecology*, **37**, 912.

Raspotnig G, Bodner M, Schäffer S, Koblmüller S, Schönhofer A, Karaman I (2015) Chemosystematics in the Opiliones (Arachnida): a comment on the evolutionary history of alkylphenols and benzoquinones in the scent gland secretions of Laniatores. *Cladistics*, **31**, 202-209.

Roewer CF (1935) Opiliones. Fünfte Serie, zugleich eine Revision aller bisher bekannten Europäischen Laniatores. Biospeologica. LXII. *Archives de Zoologie Expérimentale et Générale*, Paris, **78**, 1–96.

Roewer CF (1956) Cavernicole Arachniden aus Sardinien II. *Fragmenta Entomologica*, Roma, **2**, 97–104.

Sanmartin I, Enghoff H, Ronquist F (2001) Patterns of animal dispersal, vicariance and diversification in the Holarctic. *Biological Journal of the Linnean Society*, **73**, 345-390.

Schönhofer AL, McCormack M, Tsurusaki N, Martens J, Hedin M (2013) Molecular phylogeny of the harvestmen genus *Sabacon* (Arachnida: Opiliones: Dyspnoi) reveals multiple Eocene–Oligocene intercontinental dispersal events in the Holarctic. *Molecular Phylogenetics and Evolution*, **66**, 303-315.

Schönhofer AL, Vernesi C, Martens J, Hedin M (2015) Molecular phylogeny, biogeographic history, and evolution of cave-dwelling taxa in the European harvestman genus *Ischyropsalis* (Opiliones: Dyspnoi). *Journal of Arachnology*, **43**, 40-53.

Sharma PP, Giribet G (2011) The evolutionary and biogeographic history of the armoured harvestmen–Laniatores phylogeny based on ten molecular markers, with the description of two new families of Opiliones (Arachnida). *Invertebrate Systematics*, **25**, 106-142.

Sharma PP, Giribet G (2014) A revised dated phylogeny of the arachnid order Opiliones. *Frontiers in Genetics*, **5**, 255.

Shear WA (1977) *Fumontana deprehendor*, n. gen., n. sp., the first triaenonychid opilionid from eastern North America (Opiliones: Laniatores: Triaenonychidae). *Journal of Arachnology*, **3**, 177-183.

Shear WA (1982) Opiliones. In: *Synopsis and classification of living organisms*. Vol 2. Ed. Parker SP. McGraw Hill Book Co, New York. Pp. 104-110.

Shear WA (1986) A cladistic analysis of the opilionid superfamily Ischyropsalidoidea, with descriptions of the new family Ceratolasmatidae, the new genus *Acuclavella*, and four new species. *American Museum Novitates*, **2844**, 1-29.

Shear WA, Derkarabetian S (2008) Nomenclatorial changes in Triaenonychidae: *Sclerobunus parvus* Roewer is a junior synonym of *Paranonychus brunneus* (Banks), *Mutsunonychus* Suzuki is a junior synonym of *Paranonychus* Briggs, and Kaolinonychinae Suzuki is a junior synonym of Paranonychinae Briggs (Opiliones: Triaenonychidae). *Zootaxa*, **1809**, 67-68.

Shear WA, Jones TH, Guidry HM, Derkarabetian S, Richart CH, Minor M, Lewis JJ (2014) Chemical defenses in the opilionid infraorder Insidiatores: divergence in

chemical defenses between Triaenonychidae and Travunioidea and within travunioid harvestmen (Opiliones) from eastern and western North America. *Journal of Arachnology*, **42**, 248-256.

Shultz JW, Pinto-da-Rocha, R (2007). Morphology and Functional Anatomy. In: *Harvestmen: The Biology of Opiliones*. Eds. Pinto-da-Rocha R, Machado G, Giribet G. Harvard University Press, Cambridge, Massachusetts, and London, England. Pp. 14-61.

Shultz JW, Regier JC (2009) *Caddo agilis* and *C. pepperella* (Opiliones, Caddidae) diverged phylogenetically before acquiring their disjunct, sympatric distributions in Japan and North America. *Journal of Arachnology*, **37**, 238-240.

Sørensen WE (1886) Opiliones. In: *Die Arachniden Australiens nach der Natur beschrieben und abgebildet*, volume 2. Eds. Koch L, von Keyserling E. Bauer & Raspe, Nürnberg, pp. 53–86.

Stamatakis A (2014) RAxML version 8: a tool for phylogenetic analysis and post-analysis of large phylogenies. *Bioinformatics*, **30**, 1312-1313.

Staręga W (1971) Bemerkungen uber die verbreitung einger familien der weberknechte (Opiliones). *Proceedings Arachnologorum Congressus Internationalis V Brno*, 59–63.

Starrett J, Derkarabetian S, Richart CH, Cabrero A, Hedin M (2016) A new monster from southwest Oregon forests: *Cryptomaster behemoth* sp. n. (Opiliones, Laniatores, Travunioidea). *ZooKeys*, **555**, 11-35.

Starrett J, Derkarabetian S, Hedin M, Bryson RW, McCormack JE, Faircloth BC (2017) High phylogenetic utility of an ultraconserved element probe set designed for Arachnida. *Molecular Ecology Resources*, **17**, 812-823.

Suzuki S (1964) A remarkable new genus of Travuniidae (Phalangida) from Japan. *Annotationes Zoologicae Japonenses*, **37**, 168-173.

Suzuki S (1972) Report on a collection of Opiliones from Poroshiridake, Hokkaido. *Memoires of the National Science Museum Tokyo*, **5**, 37-44.

Suzuki S (1972) On the discontinuous distribution in some Opiliones. *Acta Arachnologica*, **24**, 1-8.

Suzuki S (1975a) The harvestmen of Family Travuniidae from Japan (Travunoidea, Opiliones, Arachnida). *Journal of Science of Hiroshima University (Series B, Division 1)*, **26**, 53-63.

Suzuki S (1975b) The harvestmen of family Triaenonychidae in Japan and Korea (Travunoidea, Opiliones, Arachnida). *Journal of Science of Hiroshima University (Series B, Division 1)*, **26**, 65-101.

Suzuki S (1976) Two triaenonychid harvestmen from the northeast, Japan (Triaenonychidae, Opiliones, Arachnida). *Journal of Science of the Hiroshima University (Series B, Division 1)*, **26**, 177-185.

Suzuki S, Tomishima K, Yano S, Tsurusaki N (1977) Discontinuous distributions in relict harvestmen (Opiliones, Arachnida). *Acta Arachnologica*, **27**, 121-138.

Talavera G, Castresana J (2007) Improvement of phylogenies after removing divergent and ambiguously aligned blocks from protein sequence alignments. *Systematic Biology*, **56**, 564-577.

Tedeschi M, Sciaky R (1994) Three new Italian species of the genus *Holoscotolemon* (Arachnida Opiliones Erebomastridae). *Bollettino del Museo Civico di Storia Naturale di Verona*, **18**, 1–10.

Thomas SM, Hedin M (2008) Multigenic phylogeographic divergence in the paleoendemic southern Appalachian opilionid *Fumontana deprehendor* Shear (Opiliones, Laniatores, Triaenonychidae). *Molecular Phylogenetics and Evolution*, **46**, 645-658.

Thorell TTT (1876) Descrizione di alcune specie di Opilioni dell' Arcipelago Malese appartenenti al Museo Civico di Genova. *Annali del Museo Civico di Storia Naturale di Genova*, **9**, 111–138.

Ubick D, Dunlop JA (2005) On the placement of the Baltic amber harvestman *Gonyleptes nemastomoides* Koch & Berendt, 1854, with notes on the phylogeny of Cladonychiidae (Opiliones, Laniatores, Travunioidea). *Fossil Record*, **8**, 75-82.

Wen J, Nie ZL, Ickert-Bond SM (2016) Intercontinental disjunctions between eastern Asia and western North America in vascular plants highlight the biogeographic importance of the Bering land bridge from late Cretaceous to Neogene. *Journal of Systematics and Evolution*. **54**, 469-490.

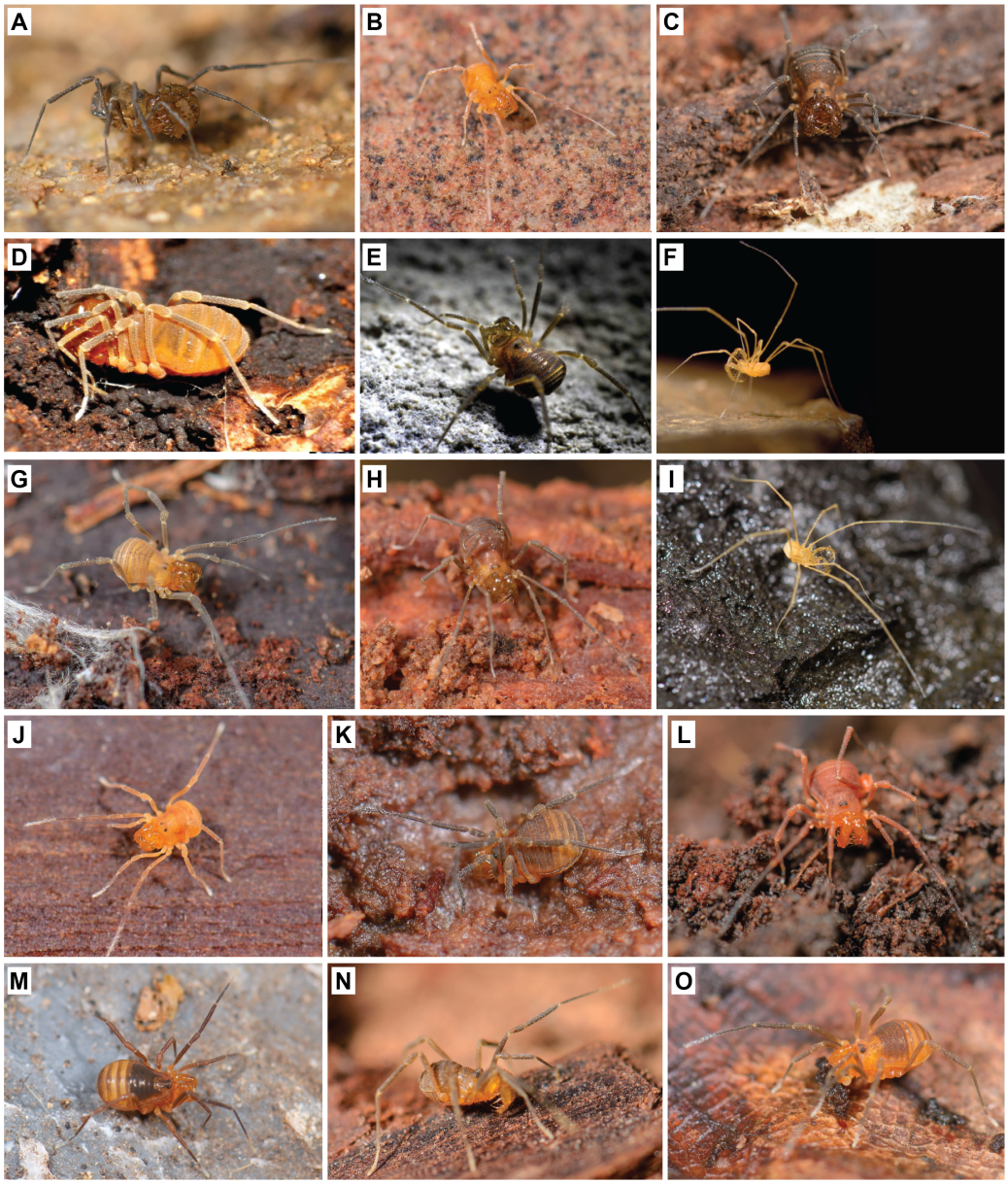

Figure 1.1. Live photos of travunioid harvestmen. A) *Theromaster brunneus*; B) *Erebomaster* sp.; C) *Cryptomaster leviathan*; D) *Holoscotolemon lessiniense*; E) *Peltonychia lepreuri*; F) *Trojanella serbica*; G) *Briggsus* sp.; H) *Isolachus spinosus*; I) *Speleonychia sengeri*; J) *Yuria pulchra*; K) *Paranonychus brunneus*; L) *Sclerobunus nondimorphicus*; M) *Metanippononychus* sp.; N) *Zuma acuta*; O) *Kainonychus akamai*. All photos by M. Hedin, except D, E (A. Schönhofer), and F (I. Karaman).

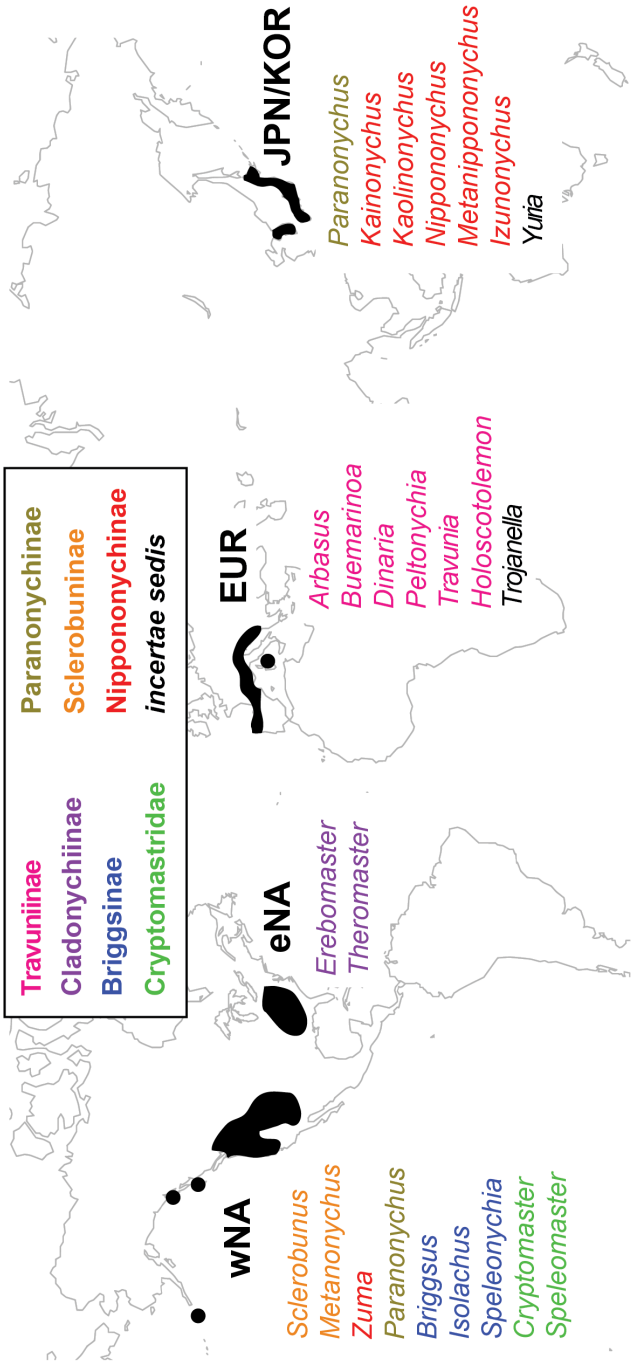

Figure 1.2. Geographic distribution of travunioid genera. Colors correspond to classification proposed in this study. wNA = western North America, eNA = eastern North America, EUR = central and southern Europe, JPN/KOR = Japan and South Korea.

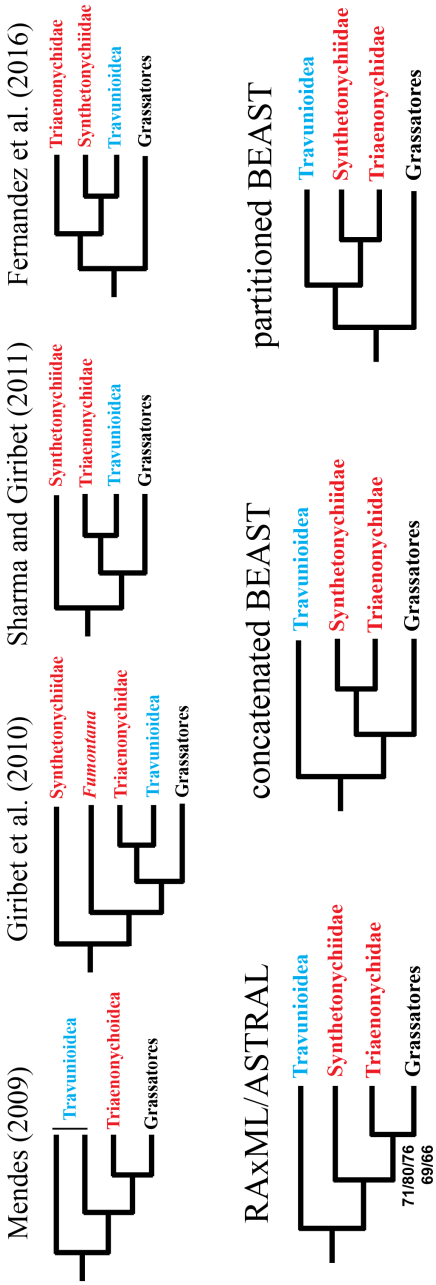

Figure 1.3. Phylogenetic relationships among major laniatorean lineages. Lower phylogenies correspond to results presented in this study. Nodes are fully supported (100% bootstrap or 1.0 posterior probability), unless indicated. Numbers in RAxML /ASTRAL phylogeny correspond to support values: top row are bootstrap support values for the 50% RAxML concatenated / 70% RAxML concatenated / 70% RAxML partitioned analyses; bottom row are 50% ASTRAL / 70% ASTRAL concatenated analyses.

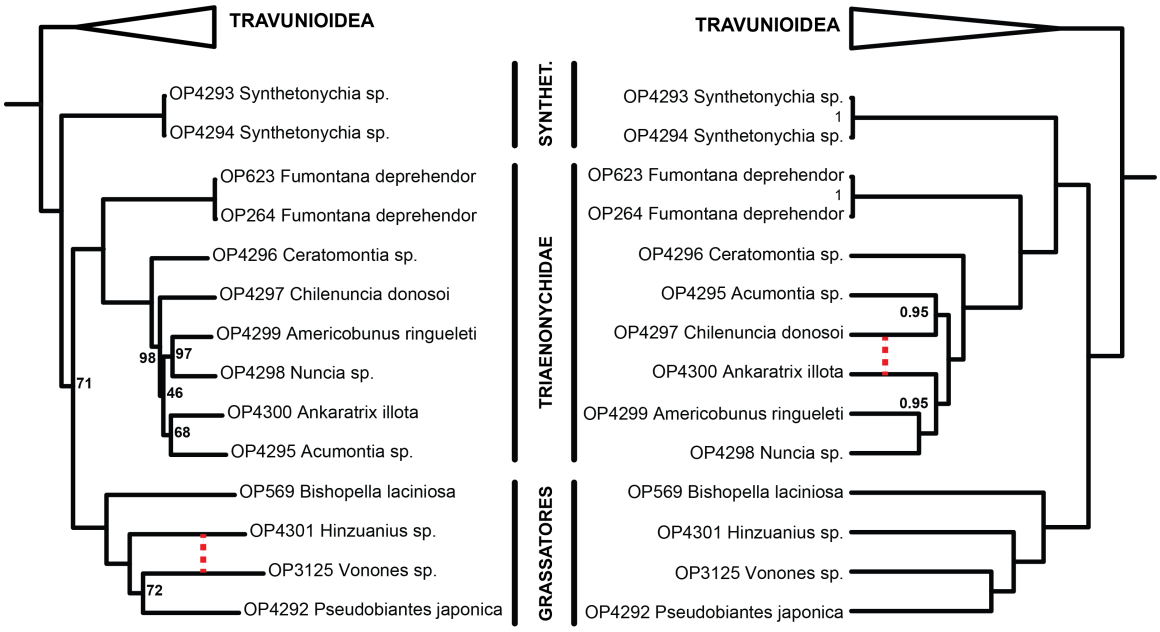

Figure 1.4. Phylogenetic relationships of non-travunioid lineages. Left: topology of all RAxML and ASTRAL analyses. Red dotted line indicates alternative placement of *Vonones* in ASTRAL 50% topology. Bootstrap support values are for RAxML 50% analysis, and are 100 unless indicated. Right: topology for BEAST concatenated analyses, red line indicates alternative placement for *Chilenuncia* and *Ankaratrix* in the BEAST 70% analysis. Posterior probabilities are 1.0 unless indicated.

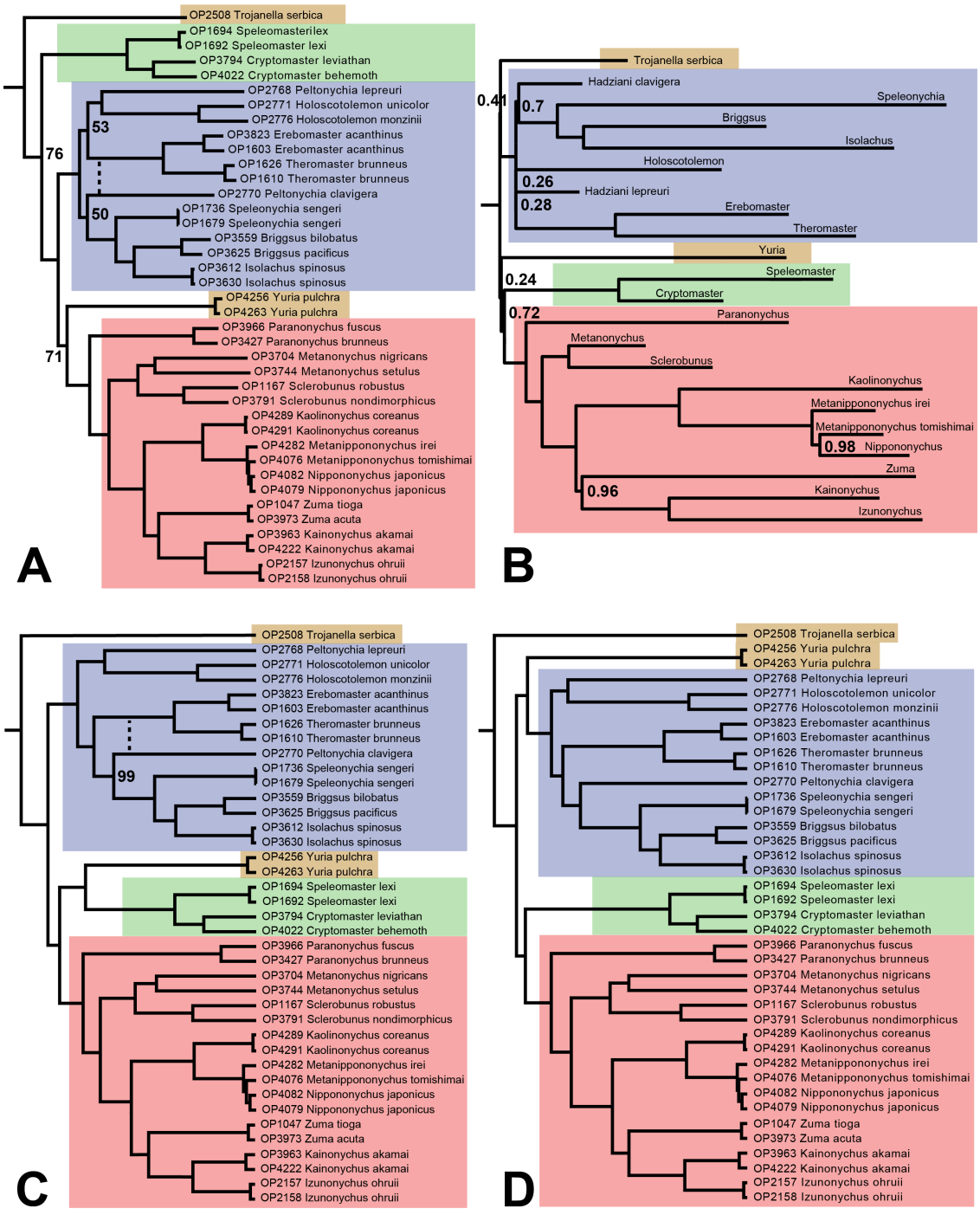
OP2508 Trojanella serbica
OP1694 Speleomasterilex
OP1692 Speleomaster lexi
OP3794 Cryptomaster leviathan
OP4022 Cryptomaster behemoth
OP2768 Peltonychia lepreuri
OP2771 Holoscotolemon unicolor
OP2776 Holoscotolemon monzinii
OP3823 Erebomaster acanthinus
OP1603 Erebomaster acanthinus
OP1626 Theromaster brunneus
OP1610 Theromaster brunneus
OP2770 Peltonychia clavigera
OP1736 Speleonychia sengeri
OP1679 Speleonychia sengeri
OP3559 Briggsus bilobatus
OP3625 Briggsus pacificus
OP3612 Isolachus spinosus
OP3630 Isolachus spinosus
OP4256 Yuria pulchra
OP4263 Yuria pulchra
OP3966 Paranonychus fuscus
OP3427 Paranonychus brunneus
OP3704 Metanonychus nigricans
OP3744 Metanonychus setulus
OP1167 Sclerobunus robustus
OP3791 Sclerobunus nondimorphicus
OP4289 Kaolinonychus coreanus
OP4291 Kaolinonychus coreanus
OP4282 Metanippononychus irei
OP4076 Metanippononychus tomishimai
OP4082 Nippononychus japonicus
OP4079 Nippononychus japonicus
OP1047 Zuma tioga
OP3973 Zuma acuta
OP3963 Kainonychus akamai
OP4222 Kainonychus akamai
OP2157 Izunonychus ohruii
OP2158 Izunonychus ohruii
53
76
50
71
A
Trojanella serbica
Hadziani clavigera
Speleonychia
Briggsus
Isolachus
Holoscotolemon
Hadziani lepreuri
Erebomaster
Theromaster
Yuria
Speleomaster
Cryptomaster
Paranonychus
Metanonychus
Sclerobunus
Kaolinonychus
Metanippononychus irei
Metanippononychus tomishimai
Nippononychus
Zuma
Kainonychus
Izunonychus
0.41
0.7
0.26
0.28
0.24
0.72
0.98
0.96
B
99
C
D

Figure 1.5 (previous page). Phylogenetic relationships among travunioid genera from analyses in this study. A) 50% RAxML concatenated; B) 50% ASTRAL concatenated; C) 50% BEAST concatenated; D) 70% BEAST partitioned. Dotted lines in A and C correspond to alternative placements of *Peltonychia clavigera* in the 70% analyses. Nodes are fully supported (100% bootstrap or 1.0 posterior probability), unless indicated.

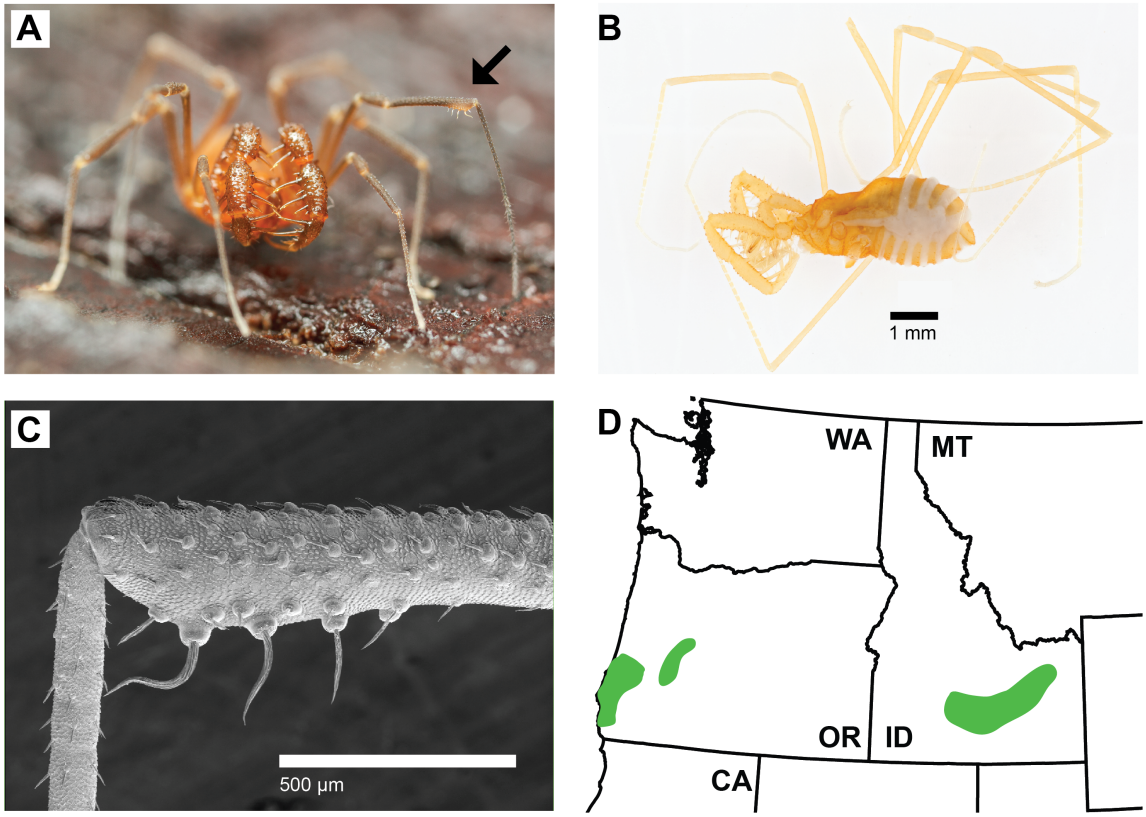

Figure 1.6. Cryptomastridae n. fam. A) *Cryptomaster*, arrow denotes sexually dimorphic swelling diagnostic of Cryptomastridae; B) *Speleomaster*, habitus; C) Scanning electron micrograph of tibial swelling, from Starrett et al. (2016); D) geographic distribution of Cryptomastridae in the Pacific Northwest of North America.

Table 1.1. Historical classification of the Travunioidea. Traditional classification refers to the taxonomy in place after the mid-1970s.

Traditional	**Kury et al. (2014)**
Travunioidea	**Travunioidea**
Travuniidae	**Travuniidae**
Abasola	**Travuniinae**
Arbasus	*Arbasus*
Buemarinoa	*Buemarinoa*
Dinaria	*Dinaria*
Kratochviliola	*Peltonychia*
Peltonychia	*Speleonychia*
Travunia	*Travunia*
Speleonychia	*Trojanella*
Yuria	**Cladonychiinae**
Cladonychiidae	*Cryptomaster*
Cryptomaster	*Erebomaster*
Erebomaster	*Holoscotolemon*
Holoscotolemon	*Speleomaster*
Speleomaster	*Theromaster*
Theromaster	**Briggsinae**
Pentanychidae	*Briggsus*
Pentanychus	*Isolachus*
Isolachus	
Triaenonychoidea (in part)	**Paranonychidae**
"northern" Triaenonychidae	**Sclerobuninae**
Sclerobuninae	*Sclerobunus*
Sclerobunus	*Zuma*
Cyptobunus	**Paranonychinae**
Zuma	*Paranonychus*
Paranonychinae	*Metanonychus*
Paranonychus	*Kaolinonychus*
Metanonychus	*Kainonychus*
Kainonychus	**Nippononychidae**
Kaolinonychinae	*Nippononychus*
Kaolinonychus	*Metanippononychus*
Mutsunonychus	*Izunonychus*
Nippononychinae	*Yuria*
Nippononychus	
Metanippononychus	
Izunonychus	

Table 1.2. UCE matrix statistics. PIC = parsimony-informative characters.

Taxon coverage %	# loci	Length	Mean locus length	# PIC	% PIC	Variable sites	Constant sites
50	437	85883	196.53	32175	0.375	6620	47088
70	164	36131	220.31	13999	0.387	3116	19016

Table 1.3. Proposed revised classification. The number of species/subspecies at each taxonomic level is in parentheses.

Travunioidea (67/17)	
Travuniidae (39/2)	**Paranonychidae (28/15)**
Travuniinae (23)	**Paranonychinae (3)**
Arbasus (1)	*Paranonychus* (3)
Buemarinoa (1)	**Sclerobuninae (15/7)**
Dinaria (1)	*Metanonychus* (3/7)
Peltonychia (8)	*Sclerobunus* (12)
Travunia (4)	**Nippononychinae (10/8)**
Holoscotolemon (8)	*Kaolinonychus* (1/2)
Cladonychiinae (5/2)	*Metanippononychus* (4/4)
Erebomaster (3/2)	*Nippononychus* (1)
Theromaster (2)	*Zuma* (2)
Briggsinae (7)	*Kainonychus* (1/2)
Briggsus (5)	*Izunonychus* (1)
Isolachus (1)	
Speleonychia (1)	
Cryptomastridae (4)	***incertae sedis* (2/1)**
Cryptomaster (2)	*Trojanella* (1)
Speleomaster (2)	*Yuria* (1/2)

CHAPTER 2

Integrative taxonomy and species delimitation in harvestmen: A revision of the western North American genus *Sclerobunus* (Opiliones: Laniatores: Travunioidea)

Alpha taxonomy, and specifically the delimitation of species, is becoming increasingly objective and integrative. The use of coalescent-based methods applied to genetic data is providing new tools for the discovery and delimitation of species. Here, we use an integrative approach via a combination of discovery-based multivariate morphological analyses to detect potential new species. These potential species are then used as *a priori* species in hypothesis-driven validation analyses with genetic data. This research focuses on the harvestmen genus *Sclerobunus* found throughout the mountainous regions of western North America. Based on our analyses, we conduct a revision of *Sclerobunus* resulting in synonymy of *Cyptobunus* with *Sclerobunus* including transfer of *S. cavicolens* **comb. nov.** and elevation of both subspecies of *S. ungulatus*: *S. ungulatus* **comb. nov.** and *S. madhousensis* **comb. nov., stat. nov.** The three subspecies of *S. robustus* are elevated, *S. robustus, S. glorietus* **stat. nov.**, and *S. idahoensis* **stat. nov**. Additionally, five new species of *Sclerobunus* are described from New Mexico and Colorado, including *S. jemez* **sp. nov.**, *S. klomax* **sp. nov.**, *S. skywalkeri* **sp. nov.**, *S. speoventus* **sp. nov.**, and *S. steinmanni* **sp. nov.** Several of the newly described species are single-cave endemics, and our findings suggest that further

exploration of western North American cave habitats will likely yield additional new species.

I. INTRODUCTION

In order to accurately identify and describe the diversity of life, species must be delimited operationally (Sites and Marshall 2004). With increasing stability of the conceptual definition of a species (de Queiroz 2007), the operational delimitation of species becomes an easier task (Schlick-Steiner et al. 2010; Camargo and Sites 2013). It is becoming increasingly clear that taxonomy, and species delimitation in particular, must become an integrative field utilizing multiple independent lines of evidence (Schlick-Steiner et al. 2010; Padial et al. 2010) as any single dataset may not accurately reflect species limits and relationships (e.g., due to morphological convergence, gene tree/species tree discordance, etc.). Proper integrative species delimitation should incorporate a combination of discovery-based approaches without *a priori* species hypotheses and, following this, hypothesis-driven approaches, which test those groups that are delimited based on discovery methods (Schlick-Steiner et al. 2010; Camargo and Sites 2013; Carstens et al. 2013). Additionally, in order to decrease the degree of subjectivity that is common in traditional alpha-taxonomic practices, species delimitation methods are moving towards increasing objectivity (Camargo and Sites 2013). For example, recently developed methods accomplish this by relying on statistical thresholds to delimit species in multivariate morphological space (Ezard et al. 2010), or posterior

probability distributions to determine support for the presence of a species tree node (Yang and Rannala 2010).

The discovery and documentation of biodiversity at the species level is especially important for conservation biology (Agapow et al. 2004), particularly in taxa that are relatively poorly studied (either due to sheer diversity of species and/or proportionally few taxonomists). With the almost ubiquitous incorporation of genetic data in systematics, the discovery and documentation of new and cryptic species is increasing (Bickford et al. 2007), seemingly correlated with the use of coalescent-based species delimitation methods (Camargo and Sites 2013; Fujita et al. 2012). Recent studies have shown the potential for these methods in the discovery of new and cryptic species in taxa that are either poorly known, morphologically conserved, show low vagility, and/or have narrow ecological limits (Niemiller et al. 2012; Barley et al. 2013; Giarla et al. 2014; Parmakelis et al. 2013; Satler et al. 2013). The order Opiliones (commonly called harvestmen) is a diverse group of arachnids with over 6500 described species (Kury 2013), distributed on every continent except Antarctica. Despite being a fairly diverse group (i.e., more described species than mammals), harvestmen are relatively poorly studied. The vast majority of harvestmen species show low vagility with high ecological constraints; attributes that have resulted in the discovery of many new, and sometimes cryptic, species when studied using modern molecular approaches (Boyer et al. 2007; Hedin and Thomas 2010; Giribet and Shear 2010; Derkarabetian et al. 2010; Derkarabetian et al. 2011; Arthofer et al. 2013; Richart and Hedin 2013).

In this study we focus on the harvestmen genera *Sclerobunus* and *Cyptobunus*, which are broadly distributed throughout the mountainous regions of western North America. These genera are ecologically limited to moist, dark microhabitats, typically found under logs and rocks in high-elevation forests or in caves. The first species of *Sclerobunus* was described from Colorado by A. S. Packard in 1877 as *Scotolemon robustum* (Packard 1877). Later, Banks (1893) described the new genus *Sclerobunus*, and included two species: Packards' *Scotolemon robustum*, renamed *Sclerobunus robustus* (Packard, 1877), and *Sclerobunus brunneus*. This second species was later transferred to the genus *Paranonychus* Briggs, 1971. Banks' (1893) description of *Sclerobunus robustus* was based on specimens from Colorado, Utah (originally described by Packard), and Washington. Roewer (1931) then described a new species, *Sclerobunus parvus*, from Vancouver Island, British Columbia. Many years later in a revision of the North American "Triaenonychidae", Briggs (1971) included two species of *Sclerobunus*. The first species, *Sclerobunus nondimorphicus* was described as new from Oregon, Washington, and southern British Columbia (this species includes Banks' (1893) specimen of *S. robustus* from Washington). The second species, *S. robustus*, was redescribed and recorded with a very broad distribution throughout the American southwest and Rocky Mountains. Within this species, Briggs described three subspecies: *S. robustus robustus* from Arizona and New Mexico, *S. r. glorietus* from a single locality in northern New Mexico, and *S. r. idahoensis* from Idaho. More recently, Shear and Derkarabetian (2008), upon examination of the type specimens of *S. parvus*, synonymized this taxon with *Paranonychus brunneus* (Banks, 1893). Currently,

Sclerobunus includes two species: *Sclerobunus nondimorphicus* and *Sclerobunus robustus*, itself including three subspecies.

The taxonomic and phylogenetic relationship between *Sclerobunus* and its sister genus *Cyptobunus* remains uncertain. All *Cyptobunus* are known only from cave habitats and are highly troglomorphic. Banks (1905) described the new genus and species, *Cyptobunus cavicolus*, from Lewis and Clark Caverns, Montana based on a juvenile specimen (as mentioned by Roewer 1915) and remarked that this taxon "is but a cavernicolous adaptation of *Sclerobunus*" (Banks 1905). With adult specimens, Crosby and Bishop (1924) synonymized *Cyptobunus* with *Sclerobunus* and this synonymy was acknowledged by Goodnight and Goodnight (1943). Later, Briggs (1971) described the new species *C. ungulatus*, with two subspecies: *C. u. ungulatus* from Model Cave in Great Basin National Park, Nevada and *C. u. madhousensis* from North Madhouse Cave near Provo, Utah. Briggs retained separate genera noting differences in several somatic characters, but also remarked on the general similarity in male genitalia. Historically, *Sclerobunus* are only known from epigean habitats. However, recent fieldwork has uncovered many new populations of troglomorphic *Sclerobunus* from cave and talus habitats, extending the known habitat preference for this taxon (Derkarabetian et al. 2010). *Sclerobunus* populations found in caves show varying degrees of troglomorphy including decreased pigmentation, elongation of appendages, and attenuation of spines. Based on this, it is possible that *Cyptobunus* taxa merely represent highly derived *Sclerobunus*. A recent genetic analysis by Derkarabetian et al. (2010) recovered *Cyptobunus* phylogenetically nested within *Sclerobunus* and showed that troglomorphy

evolved independently at least three times; however, this was only a two-gene study. Although there remains uncertainty in the relationship between *Sclerobunus* and *Cyptobunus*, their monophyly relative to other closely related genera is certain and reflected in penis morphology (Briggs 1971) and genetic data (Derkarabetian et al. 2010).

The morphological and genetic analyses of Derkarabetian et al. (2010) suggested that there are several new morphologically distinct, genetically divergent species within *Sclerobunus*. Here, we use discovery-based methods to identify multivariate clusters using morphometric data, which are then treated as putative species in species tree analyses using eight newly developed nuclear loci. Following this, we use a hypothesis-driven approach to test alternative species delimitation hypotheses using the multigenic nuclear dataset. Based on results of our species delimitation analyses, we conduct a revision of *Sclerobunus*, including *Cyptobunus*.

II. MATERIALS AND METHODS

(1) Taxon sampling

Fieldwork was conducted in the summer months of 2006, 2007, and 2008 throughout the mountainous regions of western North America. Samples representing all species and subspecies of *Sclerobunus* and *Cyptobunus* were collected for analyses (Appendices B.1 and B.2). Fresh specimens were collected from type localities for all species and subspecies, except *S. nondimorphicus*, *S. r. robustus*, and *S. r. idahoensis*. For these taxa, type localities could not be accessed either due to vague locality records

or unsuitable habitat, and fresh samples were collected from as near the type locality as possible. All specimens were collected by hand; those destined for molecular analyses were placed in 100% EtOH and stored at -80° C, while specimens to be used in morphological analyses were stored in 80% EtOH.

Samples from caves in Great Basin National Park, Nevada were collected under a Scientific Research Collecting Permit from the U.S. National Park Service permit granted to the authors (GRBA-2007-SCI-0008). Permission to collect in Lewis and Clark Caverns, Montana was given by the Montana State Park staff and samples from Cave of the Winds, Colorado were collected with permission from the management staff. In general, sample sizes from cave populations were limited either purposefully due to conservation concerns, or due to rarity of individuals. To increase the sample size for some cave populations, recently collected specimens from Cave of the Winds and newly discovered Mallory Cave, Colorado specimens from the Denver Museum of Nature and Science were included. In addition, specimens collected from Terrero Cave, New Mexico held in the California Academy of Sciences collection were included in morphological analyses.

(2) Morphometric analyses

The morphometric dataset included 18 linear measurements taken using an Olympus SZX12 microscope equipped with an ocular micrometer (Appendices B.3 and B.4). The characters chosen included the length and width of the scute, chelicerae, and genital operculum, height and width of the ocularium, height of the pedipalpal femur, and

length of the second leg. For some specimens, certain characters could not be measured, for example, missing genital opercula or legs (total of 2.4% missing data). In these cases, missing values were estimated with SPSS v. 20 (IBM Corp.) using the Multiple Imputation function with default settings and 10 iterations. The average of 10 iterations was used as the missing value in the final analyses. Because of sexual dimorphism, analyses were conducted on separate male and female datasets.

We utilize an algorithmic approach described by Ezard et al. (2010) that relies on statistical thresholds at multiple steps to objectively define species clusters in multivariate morphospace. This method is used as a discovery-based approach to identify putative species, which we then further tested with genetic data. The Ezard et al. method has several advantages over traditional PCA (Ezard et al. 2010). First, traditional PCA using a covariance matrix assume normally distributed data, which is usually not met in biological datasets that contain multiple species. Our data do not meet this assumption as multiple species are included and 7 of 18 characters are not normally distributed (Shapiro-Wilks test; results not shown). Second, analyses computed via correlation matrices can be negatively influenced by outliers, which can skew orientation of the axes. To circumvent these issues, this method uses robust scale estimators that perform better with non-normal data. Use of the median to scale the data de-emphasizes the effects of any outliers, and is more useful in discriminating incipient species. The Bayesian Information Criteria (BIC) is used to choose the optimal model among possible models that vary in the size, orientation, and number of clusters. Importantly, this method can be used as a null model of morphological homogeneity. Finally, the automation and use of

multiple thresholds increases reproducibility and similarity in interpretations across datasets and taxa. We implemented the Ezard et al. method using the default protocol with the k-value set to 18 (total number of characters measured in this study) using R 3.0.2 (R Core Team, 2013).

We did not include holotype specimens in morphometric analyses for two main reasons: First, all species of *Sclerobunus* are allopatric in distribution, with one exception at Taos Ski Valley, New Mexico, which is discussed below and at length in Derkarabetian et al. (2010). As such, we argue that inclusion of fresh specimens from the type locality is just as valuable as including holotypes. The allopatric distribution of *Sclerobunus* species eliminates the possibility that type series specimens are heterospecific or that specimens collected from type localities represent multiple species. Second, holotype specimens range from 40-100+ years old and may not be in suitable condition for morphometric analyses, particularly the more fragile cave species.

(3) Molecular data collection

Recent studies have shown the potential for high throughput data in shallow level phylogenetics (McCormack et al. 2011; McCormack et al 2012; Lemmon and Lemmon 2012) and the utility of transcriptomic data in phylogenetics (e.g., Kocot et al. 2011; Hartmann et al. 2012) including studies in harvestmen [6]. Illumina transcriptome data were already available for *Sclerobunus nondimorphicus* and the outgroup genus *Theromaster* (Hedin et al. 2012). To supplement these data, total RNA was extracted from a population of *S. robustus* from the Huachuca Mountains, Arizona. Prior to RNA

extraction, the midgut was dissected out while immersed in RNAlater to reduce potential microbial contamination. Total RNA was extracted from whole specimens (midgut removed) using TRIzol (Invitrogen, Carlsbad, CA) and the RNeasy MiniElute Cleanup Kit (Qiagen, Valencia, CA). RNA samples were sent to the HudsonAlpha Institute for Biotechnology (www.hudsonalpha.org) where normalized libraries were prepared and 50 base pair paired-end reads were sequenced using Illumina HiSeq technology. The raw read data were quality filtered using Trim Galore! (http://www.bioinformatics.babraham.ac.uk/projects/trim_galore/) and Prinseq (Schmeider and Edwards 2011) and assembled using default parameters in Trinity (Grabherr er al. 2011) on an Intel XEON server with 100 GB of SDRAM. Raw reads have been deposited in the Sequence Read Archive [BioProject ID PRJNA254507: accessions SRS654678, SRS654733, SRS654734]. Assembled transcriptomes were searched locally against known single copy, single exon *Ixodes* proteins (http://www.vectorbase.org) to identify orthologous genes shared in all three harvestmen transcriptomes in Geneious Pro 6 (http://www.geneious.com). Via comparison of these orthologs, specifically between the two congeneric *Sclerobunus* transcriptomes, hundreds of rapidly evolving exon and UTR gene regions were identified, and PCR primers were designed targeting 8 of these gene regions for analyses (Appendix B.5).

Genomic DNA was extracted from specimens (2-3 legs) using the Qiagen Dneasy Kit (Qiagen, Valencia, CA), per manufacturer's protocol. All PCR reactions contained 0.8 µl of genomic DNA mixed into a cocktail containing 2.5 µl of each primer (10.0 µl), 2.5 µl 10X PCR buffer, 0.5 µl 10mM dNTP mixture (0.2 mM of each dNTP), 0.75 µl 50

mM Magnesium Chloride, 0.1 µl of Platinum *Taq* DNA polymerase (Invitrogen), and 15.3 µl of tissue culture water bringing the total reaction to 25 µl. All 8 nuclear gene regions were amplified using a *single* set of PCR cycle conditions: 94ºC for 3 min, (94ºC for 60 sec, 62ºC for 75 sec, 72ºC for 90 sec) repeated 10 times, followed by (94ºC for 15 sec, 57ºC for 75 sec, 72ºC for 90 sec) repeated 30 times, then 72ºC for 5 min. PCR products from successful experiments were plate purified (Millipore) and sent to Macrogen USA for direct Sanger sequencing.

Based on a comparison of transcriptomic data, we developed primers for 61 exon and untranslated (UTR) nuclear gene regions, 23 of which successfully amplified for a small panel of 4 *Sclerobunus* taxa (2 *S. robustus*, 1 *S. glorietus*, and 1 *S. nondimorphicus*). Of these, 8 gene regions were pursued further based on informativeness and minimal levels of heterozygosity. It has been shown that species limits can be successfully determined with ≥5 loci and moderate sample sizes (5 specimens per species), even with short node depths and gene flow (Ence and Carstens 2011; Zhang et al. 2011). The 8 nuclear loci included six exonic regions and two 3'UTR regions, and were sequenced for 43 total samples of *Sclerobunus* and *Cyptobunus* (Appendix B.6) using the primers and PCR conditions detailed in Appendix B.5. Bi-directional Sanger reads were assembled into contigs, edited, and unambiguously aligned using Geneious Pro 6 (http://www.geneious.com). Diversity statistics and tests for recombination and neutrality for each locus were calculated using DnaSP v 5 (Librado and Rozas 2009). Haplotypes were determined using Phase 2.1.1 (Stephens et al. 2001). Both of the 3' UTR loci contained some sequences that could not be resolved to

haplotypes. For these two loci, unresolved sequences were removed prior to tests of recombination and neutrality. GenBank accession numbers are provided in Appendix B.7. Matrices with phased sequences are available from the Dryad Digital Repository: doi:10.5061/dryad.hj6r1.

(4) Species tree analyses

The clusters recovered from morphological, discovery-based analyses were used in conjunction with clades recovered in the COI mtDNA analyses of Derkarabetian et al. (2011) to define *a priori* species hypotheses for species trees analyses. In previous analyses, three well-supported, deeply divergent species groups are recovered: a clade from the Pacific Northwest including *S. nondimorphicus* and *S. r. idahoensis*, a clade including all *Cyptobunus*, and a clade including all southwestern *Sclerobunus*. The monophyly and distinctiveness of these three species groups is also reflected in genitalic morphology (Derkarabetian et al. 2010; Briggs 1971). Morphometric clusters may include multiple species; in these clusters, species group assignments can help resolve cases of clustering due to broad "morphospace convergence" between taxa from different species groups, or cases of potential conspecificity of putatively different species within the same species groups (FIGURE 2.1). In instances where clusters contain specimens from two different species groups, those divergent taxa will be considered separate putative species. Clusters with potentially different taxa from the same species group will rely on validation analyses.

All genetic analyses conducted use only the 8 nuclear genes sequenced here; we do not reanalyze or include previously collected nuclear (Derkarabetian et al. 2010) or mitochondrial data (Derkarabetian et al. 2011) (see Discussion). Different populations of the geographically widespread subspecies *S. robustus robustus* represent potential cryptic species (Derkarabetian et al. 2011), but because our current nuclear genetic sampling for this taxon is limited, this subspecies was treated as a single taxon in this paper.

To determine rooting and ingroup polarity, we conducted preliminary analyses including only the six exons with *Theromaster* as the outgroup. The 3' UTR gene regions were either not present in the sequenced *Theromaster* transcriptome, or could not be unambiguously aligned to the ingroup. Following this, all subsequent species tree analyses were conducted on the complete 8-gene set with *Theromaster* sequences removed. Models of evolution and optimal partitioning strategy were determined with PartitionFinder (Lanfear et al. 2012) using the BIC to choose optimal models. The species tree was reconstructed using the *BEAST algorithm (Heled and Drummond 2010). Analyses were run for 200 million generations logging every 1000 generations, implemented in BEAST 1.8 (Drummond et al. 2012) using the CIPRES portal (http://www.phylo.org/sub_sections/portal/). Each resulting run was checked for stationarity and for ESS values above 200 with Tracer 1.5 (Drummond and Rambaut 2007). Species trees were reconstructed with TreeAnnotator (http://beast.bio.ed.ac.uk/TreeAnnotator) from 180,000 trees (10% burnin removal). Individual gene trees were reconstructed using RAxML version 8 (Stamatakis 2014) with

the GTRGAMMA model and 1000 rapid bootstrap replicates. All gene and species trees are available from the Dryad Digital Repository: doi:10.5061/dryad.hj6r1.

(5) Species delimitation analyses

We use the general lineage concept (as defined in de Queiroz 2007) as our theoretical concept of a species and utilize multiple analyses to provide supporting criteria with which we can operationally delimit general lineage species. Groups of samples showing concordance across different data sets and analyses (identified as different morphometric clusters, highly supported mtDNA clades, validated nuclear clades, and distinguishable via general morphology) are considered species (Carstens et al. 2013). A general workflow for the species delimitation decision-making process is provided in FIGURE 2.1.

The Bayesian program BPP (Yang and Rannala 2010; Rannala and Yang 2013) was used to test specific species delimitation hypotheses. This program conducts multilocus, coalescent-based analyses requiring a guide tree and specification of two priors controlling population size and divergence time. The program incorporates a reversible-jump Markov chain Monte Carlo algorithm (rjMCMC) that explores all possible species delimitation models, ultimately providing an assessment of the probability of a node being present. Although BPP is known to recover a higher number of partitions relative to other programs, particularly for micro-allopatric taxa with deep genetic divergences, we believe that BPP used in conjunction with discovery-based analyses can lead to informed, conservative decisions about species delimitations Satler

et al. 2013). Specific hypotheses tested included the following: *S. nondimorphicus* + *S. robustus idahoensis*, *C. ungulatus ungulatus* + *C. u. madhousensis*, Cave of the Winds + Mallory Cave, and within the *S. r. glorietus* complex: *S. r. glorietus* (Glorieta Canyon, New Mexico) + *S. r. glorietus* (Taos Ski Valley), southern *S. r. glorietus* + *S. r. glorietus* (Glorieta Canyon), and the syntopic surface and troglomorphic populations of *S. r. glorietus* from Taos Ski Valley. The species tree recovered from *BEAST analyses based on morphological clusters was used as the input guide tree. In BPP, the rjMCMC species delimitation method (Rannala and Yang 2013) was used with algorithm 0 (ε=10), rates were allowed to vary among loci (locusrate =1), gaps and ambiguous columns were removed (cleandata =1), and the analysis was set for automatic fine-tune adjustments. Four different combinations of theta (θ) and tau (τ) priors were used to span a diversity of possible population sizes and divergence times. Each prior combination was run twice to check convergence of runs and proper mixing. Analyses were run for 200,000 generations, sampling every 5 generations with 20,000 burnin. Posterior probabilities greater than 95 for the presence of a node are considered supported species delimitations.

Using the gene trees estimated with RAxML, we calculated the genealogical sorting index (*gsi*) for each gene and the ensemble genealogical sorting index (gsi_T) (Cummings et al. 2008) using the *gsi* website (http://www.genealogicalsorting.org) with 10,000 replicates. The *gsi* statistic assesses the level of genealogical exclusivity of a group where values range from 0 (a random distribution of haplotypes) to 1 (exclusive ancestry, monophyly), and the ensemble analysis (gsi_T) incorporates uncertainty of

relationships and integrates across all gene trees. The groups assessed consisted of the putative species identified via discovery-based analyses (FIGURE 2.1).

(6) Taxonomy

Digital images were taken using a Visionary Digital system (http://www.visionarydigital.com). Several images were taken at different focal planes and combined using Zerene Stacker (Zerene Systems LLC). Scanning electron microscopy was conducted using methods outlined in Derkarabetian et al. (2011). Leg and pedipalp illustrations were done using a drawing tube attached to an Olympus SZX12 microscope with subsequent tracing in Adobe Illustrator CS5. Penis illustrations were traced from digital images. Digital images have been deposited to Morphbank; image ID numbers are included in the figure legends. A Google Earth kmz file with all known localities including sites from this study, previous studies, and geo-referenced museum records for each species is available online at (https://doi.org/10.1371/journal.pone.0104982.s007). All relevant information will be integrated into Encyclopedia of Life webpages (http://www.eol.org) for each species.

(7) Nomenclatural acts

The electronic edition of this article conforms to the requirements of the amended International Code of Zoological Nomenclature, and hence the new names contained herein are available under that Code from the electronic edition of this article. This published work and the nomenclatural acts it contains have been registered in ZooBank,

the online registration system for the ICZN. The ZooBank LSIDs (Life Science Identifiers) can be resolved and the associated information viewed through any standard web browser by appending the LSID to the prefix "http://zoobank.org/". The LSID for this publication is: urn:lsid:zoobank.org:pub:46DB0A1A-E317-4CD3-A124-53E97418C4B0. The electronic edition of this work was published in a journal with an ISSN, and has been archived and is available from the following digital repositories: PubMed Central, LOCKSS.

III. RESULTS

(1) Taxon sampling

All collecting localities from recent fieldwork for this study, including specimens used in morphological and/or genetic analyses, are shown in FIGURES 2.2 and 2.3.

(2) Morphometric analyses

Here, we present the results of the multivariate clustering method of Ezard et al. (2010). The analysis of male specimens retained 3 components (FIGURE 2.4) and selected the EEE model (ellipsoidal, equal volume, shape and orientation) with 9 clusters as optimal. Clusters correspond to *ungulatus*, Mallory Cave, Cave of the Winds + *madhousensis*, *cavicolens* + Terrero Cave, northern *glorietus* (Taos Ski Valley and Glorieta Canyon), southern *glorietus* + *robustus* from Bradford Canyon, New Mexico, and three separate clusters largely corresponding to *nondimorphicus*, *idahoensis*, and *robustus*. The recovery of the Bradford Canyon *robustus* specimens with the generally

smaller-bodied *glorietus* subspecies is not surprising considering Bradford Canyon specimens have the smallest body size of any *robustus* population known. The *nondimorphicus* cluster included 2 specimens of *idahoensis*, one of which is the largest *idahoensis* sampled (Goose Creek, Montana). Two specimens of *ungulatus* were considered significant outliers but were not removed from analyses.

Analysis of female specimens retained 2 components (Appendix B.8) and the optimal model chosen was the EEE model with 4 clusters corresponding to *glorietus* (northern and southern), *robustus* + *idahoensis* + *nondimorphicus*, Cave of the Winds + Mallory Cave, and *cavicolens* + Terrero Cave + Taos Ski Valley troglomorph. Although we include female morphometric analyses, we mainly rely on results of the male analyses for downstream decisions, as males are more variable and easily distinguished.

(3) Molecular data collection

GenBank accession numbers and the final genetic dataset are shown in Appendices B.5, B.6, and B.7 and alignment statistics are provided in TABLE 2.1. In total, original data for 8 nuclear gene regions were gathered from 36 *Sclerobunus* and 7 *Cyptobunus* samples. For each locus, no more than 5 samples were missing data (average of 2 sequences missing per gene), and no single specimen had more than one missing gene region (in total, 4.3% missing data).

(4) Species tree analyses

Model and partition selection via BIC resulted in single partitions for each gene region (TABLE 2.1). Individual RAxML gene trees are included in Appendix B.9. Preliminary rooting analyses recovered northwestern *Sclerobunus* (*nondimorphicus* and *idahoensis*) as sister to all remaining lineages. Nodes were considered highly supported if the posterior probability values exceeded 95. In the species tree (FIGURE 2.5), all nodes were resolved with 100% posterior probability, with the exception of the node containing the southwestern *Sclerobunus* and the node between *glorietus* and *klomax*. The genus *Cyptobunus* is phylogenetically nested within *Sclerobunus* with 100% posterior probability. Therefore, as the generic name *Sclerobunus* has precedence (Banks 1893), we synonymize *Cyptobunus* with *Sclerobunus*, and all species of *Cyptobunus* are transferred to *Sclerobunus* (see below).

The fact that the species tree is well resolved, with the exception of two nodes, confirms the presence of three species groups recovered in previous analyses (Derkarabetian et al. 2010; Derkarabetian et al. 2011) and helps resolve those morphological clusters containing more than one putative species. In this regard, morphometric clusters containing species from different species groups are easily separated. In the male analysis (FIGURE 2.4) a single specimen of *idahoensis* was recovered within a cluster comprised of mostly *robustus* specimens, a cluster included all *cavicolens* and Terrero Cave specimens, and another cluster included all Cave of the Winds and *madhousensis* specimens. Similarly in the female analysis, a single cluster included the Taos Ski Valley troglomorph, Terrero Cave, and *cavicolens* specimens

(Appendix B.8). As these clusters contain taxa from different species groups, they do not represent potential conspecific taxa clusters, but instead represent cases of morphological convergence across distantly related taxa. The two clusters including multiple taxa from the same species group (*nondimorphicus*/*idahoensis* and *robustus*/southern *glorietus*) were not delimited at this step and relied upon validation methods. Taken together, the morphometric and species trees analyses, coupled with previous genetic analyses, conservatively support *at least* eight putative species corresponding to *nondimorphicus*/*idahoensis*, *cavicolens*, *ungulatus* (two subspecies), Cave of the Winds/Mallory Cave, *robustus*, southern *glorietus,* northern *glorietus*, and Terrero Cave/Taos Ski Valley troglomorph.

(5) Species delimitation

Results of the BPP species delimitation analyses are shown in FIGURE 2.5. All species, including all putative new species and morphometric clusters containing multiple putative species from the same species group, were delimited with 100% posterior probability in all runs under all prior combinations. The two subspecies of *ungulatus* are an exception. Morphological clustering methods showed a clear distinction between the two subspecies of *ungulatus*. However, in the delimitation analyses with higher values of theta, $\theta \sim \Gamma(2, 10)$, indicative of large effective population sizes, the presence of the node was not supported. For cave species, which generally have small populations sizes, the analyses with low values of theta, $\theta \sim \Gamma(2, 1000)$, may be more appropriate priors for delimitation. Additionally, these isolated cave populations are separated by over 240

kilometers of arid, uninhabitable terrain where dispersal and gene flow is impossible. This extreme isolation clearly supports these two subspecies as separately evolving lineages. As such, we elevate both subspecies to full species: *S. ungulatus* **comb. nov.** and *S. madhousensis* **comb. nov., stat. nov.** Morphometric clustering methods (FIGURE 2.4) and genetic delimitation analyses (FIGURE 2.5) distinguished the new species *S. speoventus* **stat. nov.** (Cave of the Winds) from *S. steinmanni* **stat. nov.** (Mallory Cave). Although the *S. madhousensis* specimens clustered with *S. speoventus*, these two taxa are from different species groups (FIGURE 2.4) and are qualitatively morphologically different. Results of *gsi* analyses show exclusive ancestry for all species in at least 5 of 8 loci, with the exception of *S. robustus*, which was exclusive for only 3 of 8 loci and S. *nondimorphicus*, *S. idahoensis,* and *S. glorietus*, which were non-exclusive for all loci (TABLE 2.2). The gsi_T is greater than 0.5 for all species and greater than 0.8 for 8 of 11 species, demonstrating that a high degree of genealogical sorting has occurred in these species and they are progressing towards exclusive ancestry.

A summary of all species delimitation analyses in the context of an integrative taxonomic framework is shown in FIGURE 2.6. Results presented here support the presence of five new species and the elevation of all three subspecies of *S. robustus: S. robustus*, *S. glorietus* **stat. nov.,** and *S. idahoensis* **stat. nov.** The species *S. idahoensis*, a former subspecies of *S. robustus*, is not sister to other *S. robustus* subspecies, and was successfully delimited from *S. nondimorphicus* (see Taxonomy for details). Within the *S. glorietus* complex three species were delimited based on morphology (FIGURE 2.4): a

northern clade (*S. glorietus* **stat. nov.**), a southern clade (*S. skywalkeri* **sp. nov.**), and the highly troglomorphic population from Taos Ski Valley (*S. klomax* **sp. nov.**).

Based on multivariate morphological clustering, there is evidence that the *S. r. glorietus* subspecies comprises more than one species; however, species limits are uncertain due to sparse geographic sampling. It is important to note that the subspecies *S. r. glorietus* was described from only a single locality, Glorieta Canyon, New Mexico. As such, and because one of the highly troglomorphic populations is recovered *within* the *S. r. glorietus* complex, we simultaneously estimated species limits and species trees for this complex using the Bayes factor delimitation (BFD) method of Grummer et al. (2014), testing several different species limit combinations (FIGURE 2.7). This method, based on Bayes factors, is beneficial in cases where species limits are uncertain as topological uncertainty is accounted for, and *a priori* species relationships are not required (Grummer et al. 2014). Additionally, we ran a *BEAST analysis in which each individual *S. r. glorietus* population was considered a separate species, then tested each species (population) using BPP (FIGURE 2.7). Although BFD analyses slightly favor including the Glorieta Canyon population with the southern *S. glorietus* clade, the support is not strong (both BF and posterior probability). Species tree analyses in which each population of *S. glorietus* are considered putative species resulted in little support for relationships within the complex, except for *S. skywalkeri*.

We also describe a new troglomorphic species from Terrero Cave, *S. jemez* **sp. nov.** Genetic data for this cave population were not available for this study and access to the cave to collect fresh specimens could not be granted, as the cave is culturally

significant to the Jemez Pueblo. Although the *S. jemez* specimens clustered with the *S. cavicolens* specimens in male and female morphometric analyses (FIGURE 2.4, Appendix B.8), these taxa are from different species groups and easily distinguished morphologically. In the female morphometric analyses (Appendix B.8), the *S. jemez* specimens additionally clustered with the *S. klomax* specimens. These two species can be differentiated based on several characters (see below). Geographic evidence also supports this distinction as these caves are separated by over 90 km.

(6) Taxonomy

Here, we synonymize, redescribe, and elevate all *Cyptobunus* under *Sclerobunus* (*S. cavicolens* **comb. nov.**, *S. ungulatus* **comb. nov.**, and *S. madhousensis* **comb. nov., stat. nov.**), redescribe and elevate all three *S. robustus* subspecies to full species (*S. robustus*, *S. glorietus* **stat. nov.**, and *S. idahoensis* **stat. nov.**), and describe five new *Sclerobunus* species (*S. jemez* **sp. nov.**, *S. klomax* **sp. nov.**, *S. skywalkeri* **sp. nov.**, *S. speoventus* **sp. nov.**, and *S. steinmanni* **sp. nov.)**. Additionally, the previously unknown males of *S. madhousensis* are described. Penis morphology in *Sclerobunus* is relatively conserved within species groups; detailed examination within and between the *S. robustus* and *S. glorietus* species show very little variation (Derkarabetian et al. 2011). However, diagnostic differences in penis morphology can be seen between the three species groups recovered in all phylogenetic analyses (FIGURE 2.8), hereafter referred to as the *cavicolens*, *nondimorphicus*, and *robustus* species groups. At the species level, only *S. speoventus* and *S. steinmanni* show diagnostic differences in penis morphology

(FIGURE 2.9). Despite little genitalic divergence within species groups, conspicuous variation can be seen in somatic morphology (FIGURES 2.10, 2.11, 2.12, 2.13, 2.14).

Abbreviations for museums and collections: AMNH = American Museum of Natural History, CAS = California Academy of Sciences, CHR = personal collection of Casey H. Richart, DMNS = Denver Museum of Nature and Science, SDSU = San Diego State University Terrestrial Arthropod Collection. DNA vouchers held in the SDSU collection are indicated by "OP" numbers. With the exception of commercial caves, GPS coordinates for cave localities, including type localities, are purposefully withheld for the protection of those cave habitats.

Morphological abbreviations: CI = coxae I, CII = coxae II, DCS = distal cheliceral segment, GO = genital operculum, LI = leg I, LII = leg II, LII/SL = leg II total length to scute length ratio, OC = ocularium, PCS = proximal cheliceral segment, PF = pedipalpal femur, PT = pedipalpal tibia, SBT = spine-bearing tubercle. All measurements are in millimeters.

Sclerobunus Banks, 1893

Scotolemon [part] Packard, 1877: 164

Phalangodes [part] Packard, 1888: 48

Sclerobunus Banks, 1893: 152; Banks, 1901: 672; Banks, 1911: 415; Roewer, 1915: 87; Roewer, 1923: 596-597; Crosby and Bishop, 1924: 104; Goodnight and Goodnight, 1943: 645-646; Dumitrescu, 1976: 20; Briggs, 1971: 8; Shear, 1977: 178; Edgar, 1990: 540; Kury, 2003: 18; Derkarabetian et al., 2010; Derkarabetian et al., 2011

Cyptobunus, Banks, 1905: 251-252; Roewer, 1915: 62; Roewer, 1923: 631; Roewer, 1931: 152-154; Briggs 1971: 8-9; Shear, 1977: 178; Edgar, 1990; 540

Cryptobunus [misspelling], Rambla and Juberthie, 1994: 222

Type Species: *Sclerobunus robustus* (Packard, 1977)

Diagnosis. *Sclerobunus* can be differentiated from other travunioid genera by the combination of a penis having: lateral plates extending dorsally; lingulate ventral plate extending perpendicular to dorsal plate, with acute apex (lateral view); dorsal plate rounded distally, slightly curved, with a single pair of subapical lateral spines.

Description. Body length 1.68-3.68, length of scute 1.58-2.69. Body surface structure microgranulate-rivulose, integument color reddish/brown, yellow/orange to yellow in troglomorphic species, with or without black pigment. Anterior margin of scute with 1-4 tubercles on each shoulder; highly troglomorphic species without tubercles. OC recessed from anterior margin. Pedipalps strongly armed with many spine-like tubercles each bearing elongate setae subapically; first 3 proximal ventral spines of femur larger followed by 3 or more smaller spines; patella with 2 medial SBTs at distal margin; tibia with row of 4-6 medial spines and row of 4-7 lateral spines; tarsus with 4 large lateral and medial spines. LI femur with ventral row of 3 or more SBTs.

Sexual Dimorphism. As noted by Briggs (1971), the PF is noticeably thicker in males of all *Sclerobunus* (except *S. nondimorphicus*). We note two additional sexually dimorphic characters. First, in males the CII lobes found along the ventral midline possess 2-3 pairs of apophyses (Figure 2.12d), while female CII lobes do not possess apophyses. Second, males possess a small distal process on the ventral surface of the

pedipalpal tarsus (Figure 2.12e). Males of the *S. nondimorphicus* group may additionally possess many smaller asetose tubercles in 2 rows extending proximally.

Distribution. Mountainous regions of western North America (Arizona, New Mexico, Colorado, Utah, Nevada, Montana, Idaho, Oregon, Washington, and British Columbia).

Key to species groups of *Sclerobunus*

1. Penis with lateral plates extending dorsally into fan-shaped projections, ventral plate compressed dorsoventrally (FIGURE 2.8a); anterior margin of scute without tubercles on shoulders; isolated caves in Montana, Nevada, and Utah (= *Cyptobunus*)… ***S. cavicolens* group**

   Penis with lateral plates extending dorsally to an elongate process with acute apex, ventral plate more elongate (FIGURE 2.8b,c); anterior margin of scute with at least one tubercle on shoulders (Figure 2.12f) … **2**

2. Penis with dorsal surface of ventral plate smooth (FIGURE 2.8b); Pacific Northwest (WA, OR, BC, ID, MT)… ***S. nondimorphicus* group**

   Penis with dorsal surface of ventral plate with many folds (FIGURES 2.8c and 2.9); southwestern North America (AZ, NM, UT, CO)… ***S. robustus* group**

***Sclerobunus cavicolens* group**

Diagnosis. Penis with lateral plates extending dorsally into fan-shaped projections and extending ventrally into bifurcate plate, ventral plate compressed dorsoventrally and reduced in size (FIGURE 2.8a). No tubercles on the anterior margin of the scute.

Included species. *S. cavicolens* (Banks), *S. ungulatus* (Briggs), *S. madhousensis* (Briggs).

Distribution. Isolated caves and cave systems in Montana, Nevada, and Utah.

Key to adults of *S. cavicolens* group

1. Scute length under 1.7 mm; PF with 6 ventral SBTs, pedipalpal tibia with 4 large retrolateral spines (Figure 2.13a); LII length less than 9 mm; Lewis and Clark Caverns, MT… ***S. cavicolens* comb. nov.**

   Scute length over 1.7 mm; PF with 7 or more ventral SBTs, pedipalpal tibia with 5 or more retrolateral spines (Figure 2.13b,c); LII length over 9 mm… **2**

2 Scute length 1.7-2 mm; LII length under 12 mm; caves near Provo, UT… ***S. madhousensis* comb. nov., stat. nov.**

   Scute length over 2 mm; LII length over 13 mm; caves in Great Basin National Park, NV… ***S. ungulatus* comb. nov.**

Sclerobunus cavicolens (Banks, 1905)

Figures: **map** 2.3a; **habitus** 2.10a; **pedipalp** 2.13a; **leg I** 2.14a

Cyptobunus cavicolus, Banks 1905: 252, fig 1; Roewer, 1915: 62, 167; Roewer, 1923: 631; Roewer, 1931: 152

Sclerobunus cavicolens, Crosby and Bishop 1924: 104; Goodnight and Goodnight 1943: 646-647, fig 8-9; Goodnight and Goodnight, 1960; 37

Sclerobunus robustus [part], Roewer, 1931: 153

Cytobunus cavicolens [misspelling], Goodnight and Goodnight, 1943: 646

Cyptobunus cavicolens, Briggs 1971: 4-5, figs 1-9, map 1; Edgar, 1990: 540; Kury, 2003: 18

Type Material. Holotype male collected from a cave near Limespur, Montana (Lewis and Clark Caverns, formerly Morrison Cave: N45.8386, W111.8668), depth of 190 feet, juvenile, 1905 (MCZ, not examined). For descriptions, Briggs (1971) and Goodnight and Goodnight (1943) used additional specimens collected from the type locality: Big Spring Room and Cathedral Room of Morrison Cave (Lewis and Clark Caverns), 60 miles west of Bozeman, Montana, February 22, 1941 collected by H. B. Mills and A. L. Jellison (AMNH, not examined).

Diagnosis. Compared to other species in the *S. cavicolens* group, *S. cavicolen*s is less troglomorphic, with present but highly reduced lateral prongs on the hind claws. Diagnosed based on small body size (scute length <1.7 mm), shorter legs (LII <9 mm), and only 4 spines on pedipalpal tibia.

Description. MALE: (N=3). Body length 1.8-2.4, scute length 1.58-1.68, greatest width of anterior scute 1.06-1.09, greatest width of opisthosoma 1.65-1.73. Integument yellow, with very faint black pigment. OC height 0.08, width 0.22-0.23. OC low, rounded. Pedipalpal coxae with 1 SBT at distal margin (lateral edge). CI with 7 spines, some on tubercles. CII lobes with 2 apophyses. GO length 0.3-0.32, width 0.37-0.38. PCS greatest width 0.21, single dorsal SBT at distal edge, 1-2 small ventrolateral SBTs at distal margin. DCS length 0.67-0.71, greatest width 0.15-0.21. PF height 0.3-0.31, with row of 5 small dorsal SBTs, 1-3 mesodorsal SBTs, 3 medial spines, row of 6 ventral spines; PT with 4 medial spines, 5 lateral spines. LI femur with row of 3-4 SBTs; tibia

usually with 1 small tubercle, but can be without. LII total length 8.87-8.95: trochanter 0.34-0.35, femur 2.1, patella 0.63-0.64, tibia 1.79-1.82, metatarsus 1.88-1.94, tarsus 2.11-2.15. LII/SL 5.3-5.68.

FEMALE: (N=1). Body length 2.23, scute length 1.67, greatest width of anterior scute 1.01, greatest width of opisthosoma 1.78. OC height 0.09, width 0.23. GO length 0.29, width 0.39. PCS width 0.21. DCS length 0.64, width 0.22. PF height 0.26. LII total length 8.38: trochanter 0.41, femur 1.94, patella 0.68, tibia 1.66, metatarsus 1.76, tarsus 1.93. LII/SL 5.02.

Material Examined. MONTANA: **Jefferson Co.:** Morrison Cave (Lewis and Clark Caverns), Big Spring Room, 60 miles west of Bozeman (N45.8386, W111.8668), 22 February 1941, H.B. Mills, 1 male, 2 adults (AMNH); Lewis and Clark Caverns, on walls in Paradise Room (N45.8386, W111.8668), 4 July 2008, S. Derkarabetian, C. Richart, J. Underwood, 2 males, 1 female, 1 juvenile (SDSU: OP2143-OP2145).

Distribution. Only known from the type locality.

Genetic Data. GenBank accession numbers: KJ585335-KJ585337, KJ585089-KJ585091, KJ585129- KJ585131, KJ585212- KJ585214, KJ585170- KJ585172, KJ585292- KJ585294, KJ585046- KJ585048, KJ585253- KJ585255.

Sclerobunus madhousensis (Briggs, 1971), comb. nov., stat. nov.

Figures: **map** 2.3a; **habitus** 2.10c; **pedipalp** 2.13c; **leg I** 2.14c

Cyptobunus ungulatus madhousensis, Briggs 1971: 6, figs 19-25, map 1; Kury, 2003: 18

Cytobunus ungulatus madhousensis [misspelling], Edgar, 1990: 541, fig 19.18

Cryptobunus ungulatus madhousensis [misspelling], Rambla and Juberthie, 1994: 222

Type Material. Holotype female, North Madhouse Cave, near Provo, Utah (GPS withheld), 27 May 1965, Stan Moulton (AMNH, not examined).

Diagnosis. *S. madhousensis* can be differentiated from *S. cavicolens* by a complete lack of pigment, lack of prongs on hind claws, pedipalpal tibia with 5 or more medial spines. Diagnosed from *S. ungulatus* by the shorter length of LII (10-12 mm).

Description. MALE: (N=2). Body length 2.16-2.46, length of scute 1.91-1.94, greatest width of anterior scute 1.29-1.32, greatest width of opisthosoma 1.92-1.98. Integument of body yellow-yellow/orange in color, faint to no pigment on anterior scute. OC height 0.08-0.12, width 0.22. OC low and rounded, wider than long in dorsal view. Pedipalpal coxae with 1 SBT at distal margin (lateral edge). CI with 7-8 spines. CII lobes with 1-2 apophyses. Both missing genital opercula. Chelicerae elongate. PCS greatest width 0.23-0.24, single dorsal SBT at distal edge, 2 small ventrolateral SBTs at distal margin. DCS length 0.75-0.82, greatest width 0.24-0.25. Pedipalps elongate. PF height 0.37-0.38, with dorsal row of 6-8 SBTs, 3-4 mesodorsal SBTs, 4-5 elongate medial spines, ventral row of 7-8 elongate spines; PT with 5 large medial spines, 5 large lateral spines. Legs extremely elongate. LI femur with ventral row of 4-5 SBTs, the third being smallest; tibia usually without ventral tubercles, but may have a single very small tubercle. LII total length 10.87-11.65: trochanter 0.42-0.43, femur 2.66-2.8, patella 0.77-0.79, tibia 2.37-2.44, metatarsus 2.2-2.56, tarsus 2.45-2.63. LII/SL 5.61-6.09.

Material Examined. UTAH: **Utah Co.:** North Madhouse Cave (GPS withheld), 27 April 2003, M. Porter, 1 male (SDSU: OP240); Professor Buss Cave (GPS withheld), 27 April 2003, M. Porter, 1 male (SDSU: OP239).

Distribution. Known only from North Madhouse and Professor Buss Caves near Provo, Utah.

Genetic Data. GenBank accession numbers: KJ585339, KJ585340, KJ585094, KJ585095, KJ585134, KJ585135, KJ585217, KJ585218, KJ585175, KJ585176, KJ585297, KJ585298, KJ585051, KJ585052, KJ585258, KJ585259.

Sclerobunus ungulatus (Briggs, 1971), comb. nov.

Figures: **map** 2.3a; **penis** 2.8a; **habitus** 2.10b; **pedipalp** 2.13b; **leg I** 2.14b

Cyptobunus ungulatus ungulatus, Briggs 1971: 5, figs 10-18, map 1; Taylor et al. 2008: 314; Kury, 2003: 18

Cyptobunus ungulatus, Edgar, 1990: 540

Type Material. Holotype male, allotype female from Model Cave, near Baker, White Pine County, Nevada (GPS withheld), 24 August 1952, R. de Saussure (AMNH, not examined).

Diagnosis. *S. ungulatus* differentiated from *S. cavicolens* by a complete lack of pigment, lack of prongs on hind claws, pedipalpal tibia with 5 or more medial spines. Diagnosed from *S. madhousensis* by the longer length of LII (>13 mm).

Description. MALE: (N=3). Body length 2.75-3.17, length of scute 2.15-2.17, greatest width of anterior scute 1.41-1.54, greatest width of opisthosoma 2.15-2.27. Integument of body yellow-yellow/orange in color, no pigment. OC height 0.08-0.09, width 0.27-0.29. OC low, rounded, wider than long in dorsal view. Pedipalpal coxae with 1 SBT at distal margin (lateral edge). CI with 8-9 spines. CII lobes with 1-2 apophyses. GO length 0.361, width 0.444 (most missing opercula). Chelicerae elongate. PCS greatest width 0.28, single dorsal SBT at distal edge, 2 small ventrolateral SBTs at distal margin. DCS length 0.91-0.94, greatest width 0.23-0.3. Pedipalps elongate. PF height 0.41-0.43, with dorsal row of 6 SBTs, 1-3 mesodorsal spines, 4-5 elongate medial spines, ventral row of 7-9 elongate spines; PT with 5-6 large medial spines, 5-6 large lateral spines. Legs extremely elongate. LI femur with ventral row of 3 SBTs, the third being smallest; tibia usually without ventral tubercles, but may have a single very small tubercle. LII total length 13.6-14.5: trochanter 0.52-0.54, femur 3.3-3.5, patella 0.91-0.94, tibia 2.9-3.1, metatarsus 3.0-3.3, tarsus 3.0-3.1. LII/SL 6.33-6.67.

Material Examined. NEVADA: **White Pine Co.:** Model Cave (GPS withheld), near Baker, 24 August 1952, R. de Saussure, 1 female, 1 adult (AMNH: A146, A147); Model Cave (GPS withheld), near Baker, total darkness, walls, 24 August 1952, R. de Saussure, 1 female, 1 adult (AMNH: A142); Model Cave (GPS withheld), near Baker, total darkness, wall and floor, 27 August 1952, R. de Saussure, 1 adult (AMNH: A133); Model Cave (GPS withheld), el. 2070 m, Great Basin National Park, on walls of cave, 25 June 2007, S. Derkarabetian, D. Elias, M. Hedin, L. Hedin, 3 males, 2 females (SDSU; GBPA:427 #8394-8398); Ice Cave (GPS withheld), el. 2070 m, Great Basin National

Park, on walls of cave, 25 June 2007, S. Derkarabetian, D. Elias, M. Hedin, L. Hedin, 1 female, 2 juveniles (SDSU; GBPA:427 #8391-8393).

Distribution. Known from multiple caves in Great Basin National Park (Taylor et al. 2008, pg. 314).

Genetic Data. GenBank accession numbers: KJ585338, KJ585092, KJ585093, KJ585132, KJ585133, KJ585215, KJ585216, KJ585173, KJ585174, KJ585295, KJ585296, KJ585049, KJ585050, KJ585256, KJ585257.

Sclerobunus nondimorphicus group

Diagnosis. The dorsal surface of the ventral plate of the penis is smooth, without pair of small ventral spines on lateral plates (FIGURE 2.8b).

Included species. *S. nondimorphicus* Briggs, *S. idahoensis* (Briggs).

Distribution. Pacific Northwest North America: Coast and Cascade ranges of northern Oregon, Washington, and southwestern British Columbia and the northern Rocky Mountains of Idaho and western Montana.

Key to adults of *S. nondimorphicus* group

1. Body with little to no black pigment (FIGURE 2.10d); OR, WA, BC… ***S. nondimorphicus***

   Body with much black pigment (FIGURE 2.10e); ID, MT… ***S. idahoensis* stat. nov.**

Sclerobunus nondimorphicus Briggs, 1971

Figures: **map** 2.2; **habitus** 2.10d; **pedipalp** 2.13d; **leg I** 2.14d

Sclerobunus robusta [part], Banks, 1893: 152

Sclerobunus robustus [part], Banks 1901, 672; Banks, 1902: 593; Banks, 1911: 416; Roewer, 1923: 597, fig 746

Sclerobunus nondimorphicus, Briggs, 1971: 9, figs 42-53; Bragg and Leech, 1972: 70; Dumitrescu, 1976: 18, fig 14; Edgar, 1990: 540, fig 19.22; Kury, 2003: 18-19; Bragg and Holmberg, 2009: 30

Type Material. Holotype male and allotype female from 8.6 miles northwest of Easton on U.S. Highway 90, Kittitas County, Washington (N47.3101, W121.3148), collected on 23 June 1966 by T. Briggs, V. F. Lee, A. Jung, and K. Hom (CAS, not examined). **Paratypes:** 3 miles southeast of Rhododendron, near Mt. Hood, Clackamas County, Oregon (N45.3052, W121.87), 5 September 1976, T. Briggs, K. Hom, R. Lem, W. Lum, J. Nishio, 1 male (CAS, examined); 1 mile south Saddle Mountain State Park, Clatsop County, Oregon (N45.9639, W123.6885), under logs on ground, Sitka spruce forest biome, 7 August 1967, T. Briggs, A. Jung, 1 male (CAS, examined); 5.5 miles south Clatskanie, Columbia County, Oregon (46.0985, W123.2052), Sitka spruce log, 8 August 1967, K. Hom, 1 female, 1 juvenile (CAS, examined); 5.5 miles South Clatskanie, Columbia County, Oregon (46.0985, W123.2052), under surface of bark, Sitka spruce, 8 August 1967, K. Hom, 1 male, 2 females (CAS, examined); 5.5 miles south Clatskanie, Columbia County, Oregon (46.0985, W123.2052), bark and cut wood on ground, Sitka spruce forest, 8 August 1967, T. Briggs, 1 male (CAS, examined); 20.8 miles east of Queets on US 101, Grays harbor County, Washington (N47.4788, W123.9867), 22 June 1966, T. Briggs, V. Lee, A. Jung, 5 males, 2 females (CAS,

examined); 6.8 miles south Neilton, Grays Harbor County, Washington (N47.3203, W123.9094), 22 June 1966, T. Briggs, V. Lee, A. Jung, K. Hom, 1 male (CAS, examined); 4.5 miles southwest Hoh Rainforest Road on US 101, Kings County, Washington, 22 June 1968, A. Jung, 1 male (CAS, examined); 16.4 miles northwest Hyak on US 90, Kings County, Washington (N47.4439, W121.6751), 23 June 1966, T. Briggs, V. Lee, A. Jung, K. Hom, 1 juvenile (CAS, examined); Ohanapecosh Campground, Mt. Rainier National Park, Lewis County, Washington (N46.7344, W121.5703), under surface of log, Douglas fir and cedar forest, 8 August 1967, T. Briggs, 1 male, 1 female (CAS, examined); 17.8 miles east of Hope, Manning Park, British Columbia (N49.2403, W121.1489), dense forest, 23 August 1969, T. Briggs, 3 males, 4 juveniles (CAS, examined).

Diagnosis. Compared to *S. idahoensis*, with much less black pigmentation on the scute and males do not have obvious swelling of the pedipalpal femur.

Description. MALES: (N=7). Body length 2.84-3.16, length of scute 2.28-2.5, greatest width of anterior scute 1.58-1.68, greatest width of opisthosoma 2.31-2.59. Integument of body orange, with some black pigment, anterior scute with some pigment, lighter color directly behind OC. Anterior margin with 3-4 small tubercles (sometimes 1-2). OC height 0.17-0.19, width 0.38-0.41. OC variable, angled slightly forward, typically equal length and width in dorsal view, but can be wider, eyes connected with lighter black pigment. Pedipalpal coxae with a single SBT at distal margin. CI with 10 or more spines, some on tubercles. CII lobes generally with 3 apophyses, sometimes 2 or 4. GO length 0.41-0.47, width 0.47-0.52. Chelicerae lighter in color, without pigment. PCS

greatest width 0.28-0.31, 1-2 small dorsal SBTs at distal edge, 1-2 small ventrolateral SBTs at distal edge. DCS length 0.87-0.91, greatest width 0.31-0.34. Pedipalps lighter in color, without pigment. PF height 0.52-0.6, with dorsal row of 5-7 SBTs, 2-3 mesodorsal spines, row of 3-4 medial spines, row of 6-7 ventral spines (rarely 5); PT with row of 4-5 medial spines, 5 lateral spines. Legs with black pigment on tibia, metatarsus, and tarsus. LI femur with row of 3-4 ventral SBTs; tibia with 1-2 ventral SBTs. LII total length 9.14-9.56: trochanter 0.47-0.54, femur 2.24-2.53, patella 0.76-0.83, tibia 1.93-2.03, metatarsus 2.14-2.38, tarsus 1.45-1.6. LII/SL 3.75-4.16.

FEMALES: (N=4). Body length 2.92-3.66, scute length 2.36-2.53, greatest width of anterior scute 1.54-1.62, greatest width of opisthosoma 2.66-2.75. OC height 0.17-0.22, width 0.37-0.4. CII with 0-2 tubercles at posterior margin. GO length 0.42-0.47, width 0.55-0.56. PCS width 0.28-0.3. DCS length 0.85-0.88, greatest width 0.3-0.31. PF height 0.4-0.44. LII total length 8.25-9.16: trochanter 0.48-0.57, femur 2.03-2.2, patella 0.7-0.79, tibia 1.64-1.97, metatarsus 1.92-2.3, tarsus 1.33-1.4. LII/SL 3.41-3.66.

Other Material Examined. OREGON: **Benton Co.**: Mary's Peak Road, Mary's Peak, 0.1 miles west of FR 30 (N44.4964, W123.5457), el. 790 m, *Picea* forest, bark piles, 1 October 2010, S. Derkarabetian, M. McCormack, 2 females (SDSU); Mary's Peak Campground, Mary's Peak (N44.5087, W123.5582), el. 1070 m, *Picea* forest, bark piles, 1 October 2010, S. Derkarabetian, M. McCormack, 4 males, 1 female, 1 juvenile (SDSU). **Clackamas Co.**: 2.3 miles southeast of Rhododendron on FR 12 (N45.301, W121.8959), under bark and logs, 11 May 2011, S. Derkarabetian, A. Smith, 1 female (SDSU); Mermaloose Trail, 12 miles south of SR 224 along FR 45 (Mermaloose Creek

Road) (N45.0986, W122.2219), el. 1100 m, mixed forest, woody debris, 16 August 2011, S. Derkarabetian, 1 male, 2 females (SDSU). **Clatsop Co.**: Lee Wooden Park, SR 202 4.3 miles north of SR 103 (N45.9576, W123.5815), el. 219 m, 16 June 2007, mixed forest, C. Richart, A. Fusek, 1 male (CHR1695), 1 female (CHR1696) (CHR). **Tillamook Co.**: Munson Creek Falls State Natural Area, 1.5 miles east of US 101 on Munson Creek Road (N45.3650, W123.7730), el. 100 m, mixed forest woody debris, 1 August 2011, S. Derkarabetian, 2 males, 1 juvenile (SDSU).

WASHINGTON: **Jefferson Co.**: Ruby Beach, Olympic National Park (N47.7098, W124.4137), el. 24 m, mixed forest, 2 July 2007, C. Richart, D. Richart, 2 males, 2 females, 1 juvenile (CHR). **King Co.**: Rattlesnake Lake, along Rattlesnake Ledge Trail, south of North Bend at US 90 (N47.4346, W 121.7722), el. 300 m, 30 December 2002, M. Hedin, C. Talbot, 1 female (SDSU). **Lewis Co.**: Rainbow Falls State Park, SR 6 16.1 miles west of US 15 (N46.6301, W123.233), streamside woody debris, C. Richart, 1 male (CHR); tributary of Iron Creek, FR 25 4.6 miles south of FR 300 (N46.4033, W121.9902), el. 6676 m, streamside woody debris, mixed forest, 6 August 2008, C. Richart, 1 male (CHR2483), 1 female (CHR). **Pacific Co.**: Ellsworth Creek Preserve TNC, along Ellsworth Creek (N46.4139, W123.8922), el. 69 m litter and woody debris, 2 April 2008, S. Derkarabetian, C. Richart, W. Leonard, 1 male (SDSU); along tributary of North Nemah River (N46.4916, W123.8242), el. 25 m, Berlese extraction of moss and woody debris, 20 September 2008, C. Richart 1 female (CHR).

Distribution. Coast and Cascade ranges of Oregon, Washington, and southern British Columbia.

Genetic Data. GenBank accession numbers: KJ585327- KJ585330, KJ585081- KJ585084, KJ585122- KJ585124, KJ585205- KJ585208, KJ585162- KJ585165, KJ585284- KJ585287, KJ585038- KJ585041, KJ585246- KJ585249, KJ585386, KJ585372, KJ585375, KJ585388, KJ585378, KJ585383, KJ585369, KJ585380.

Sclerobunus idahoensis (Briggs, 1971), stat. nov.

Figures: **map** 2.2; **penis** 2.8b; **habitus** 2.10e; **pedipalp** 2.13e; **leg I** 2.14e

Sclerobunus robustus idahoensis Briggs, 1971: 11-12, figs. 61-66, map 1; Kury, 2003: 19

Type Material. Holotype male and allotype female from 2.8 miles northwest of Clarkia on State Highway 3, Shoshone County, Idaho (N47.0316, W116.2205), 11 August 1967, T. Briggs, K. Hom, A. Jung (CAS, not examined). **Paratypes:** 6.3 miles north of Headquarters, Clearwater County, Idaho (N46.7019, W115.8031), under surface of log, cedar, fir and spruce, 12 August 1967, T. Briggs, 1 male, 1 juvenile (CAS, examined); opposite Apgar Campground, Clearwater National Forest, Idaho County, Idaho (N46.214, W115.5374), under surface of log, cedar, fir and spruce, 12 August 1967, T. Briggs, 1 male, 1 female (CAS, examined); 17.25 miles southwest of Little North Fork of Clearwater River on Clearwater Road, Shoshone County, Idaho, 11 August 1967, T. Briggs, K. Hom, A. Jung, 1 male, 2 female, 4 juveniles (CAS, examined).

Diagnosis. Distinguished from *S. nondimorphicus* by the presence of more black pigment.

Description. MALE: (N=15). Body length 2.69-3.24, scute length 2.16-2.55, greatest width of anterior scute 1.44-1.73, greatest width of opisthosoma 2.24-2.73. Integument of body deep orange in color, scute with heavy black pigment, sometimes solid, extremities lighter in color. Anterior margin of scute with 3-5 tubercles. OC height 0.14-0.26, width 0.34-0.43. OC rounded to somewhat pointed, angled forward slightly, equal length and width in dorsal view, eyes connected with black pigment, anterior scute with patterned pigment. Pedipalpal coxae with single large SBT at distal margin (lateral edge). CI with 10 or more spines (up to 18), some on tubercles. CII lobes with either 2 or 3 apophyses, the third being smallest, if present. GO length 0.41-0.48, width 0.44-0.58. PCS greatest width 0.22-0.32, 2 (rarely a single) small dorsal SBTs at distal edge, 2 (rarely a single) small ventrolateral SBTs at distal edge. DCS length 0.79-0.93, greatest width 0.29-0.34. Pedipalps typically without black pigment. PF height 0.47-0.58, with dorsal row of 5-7 SBTs (sometimes 4), 2-4 mesodorsal spines, 3-4 medially, ventral row of 7-8 spines (sometimes 5 or 9); PT with row of 4-5 medial spines (sometimes 6), 5 lateral spines (rarely 6). Legs with black pigment on the tibia, metatarsus, and tarsus. LI femur with row of 3-5 ventral SBTs; tibia with 1-2 ventral SBTs. LII total length 7.82-9.58: trochanter 0.45-0.52, femur 1.91-2.35, patella 0.71-0.87, tibia 1.6-2.04, metatarsus 1.8-2.4, tarsus 1.26-1.5. LII/SL 3.23-4.17.

FEMALES: (N=11). Body length 2.8-3.68, scute length 2.3-2.69, greatest width of anterior scute 1.41-1.69, greatest width of opisthosoma 2.4-2.83. OC height 0.16-0.23, width 0.36-0.41. CII and CIII can have fewer tubercles. GO length 0.37-0.46, width 0.46-0.53. PCS greatest width 0.26-0.32. DCS length 0.8-0.91, greatest width 0.28-0.32. PF

height 0.39-0.45. LII total length 7.09-9.0: trochanter 0.44-0.52, femur 1.71-2.2, patella 0.66-0.82, tibia 1.48-1.9, metatarsus 1.64-2.2, tarsus 1.12-1.42. LII/SL 2.86-3.74.

Other Material Examined. IDAHO: **Clearwater Co.**: Rhodes Creek, 2.0 miles southeast of SR 11 on FSR 250 (N46.4767, W115.7809), el. 960 m, *Abies grandis* forest litter, 19 July 2008, C. Richart, 10 males, 2 females (CHR). **Idaho Co.**: tributary of Crooked Creek, 14.1 miles south of Red River Road on FSR 222 (N45.5791, W115.4431), el. 1870 m, *Abies* forest, leaf litter, 7 July 2008, S. Derkarabetian, C. Richart, J. Underwood, 3 males, 3 females (CHR); Grouse Creek, 1.9 miles southwest of Hungary Ridge Road on FSR 1299 (N45.812, W115.953), el. 1005 m, *Abies* forest, leaf litter, 6 July 2008, S. Derkarabetian, C. Richart, J. Underwood, 7 males, 3 females (CHR); 0.8 miles south of Selway River Road on FSR 443 (N46.0385, W115.2943), el. 535 m, conifer forest, forest litter and streamside woody debris, 6 July 2008, S. Derkarabetian, C. Richart, J. Underwood, 4 males, 2 females, 2 juveniles (CHR); DeVoto Memorial Cedar Grove (N46.4293, W115.1335), el. 1100 m, old growth *Thuja plicata* forest, leaf litter, 5 July 2008, S. Derkarabetian, C. Richart, J. Underwood, 9 males, 3 females, 2 juveniles (CHR). **Kootenai Co.**: Rose Lake, 1.5 miles north of US 23 on South Rose Creek Road (N47.5531, W116.4967), el. 660 m, *Tsuga heterophylla* and *Abies grandis* forest, woody debris, 23 July 2011, S. Derkarabetian, C. Richart, 8 males, 5 females, 1 juvenile (SDSU). **Shoshone Co.**: Hobo Cedar Grove Botanical Area, St. Joe National Forest (N47.0860, W116.1129), el. 1250 m, old growth *Thuja plicata*, *Taxus brevifolia*, along creeks/seeps, 25 July 2011, S. Derkarabetian, C. Richart, 2 male, 3 female, 1 juvenile (SDSU); Placer Creek Road, 4.6 miles southeast of High Street

(N47.4303, W115.8913), el. 1110 m, *Tsuga heterophylla*, *Thuja plicata*, *Abies grandis* forest litter, 29 July 2008, C. Richart, 3 males, 2 females (CHR).

MONTANA: **Mineral Co.**: 9.3 miles south of Frontage Road of I-90 on FSR 320 (N47.1102, W115.0095), el. 1156 m, *Pseudotsuga menziesii*, *Thuja plicata* forest, streamside woody debris, 10 July 2012, C. Richart, 2 males (SDSU); Goose Creek, 9.7 miles south of Mullan Gulch Road on FSR 282 (N47.2279, W115.2464), el. 1305 m, *Thuja plicata*, *Abies grandis*, *Picea* forest litter, 30 July 2008, C. Richart, 1 male, 3 females, 1 juvenile (CHR); Deep Creek, 9.7 miles southwest of Diamond Match Road on Trout Creek Road (N47.0464, W114.9503), el. 1106 m, *Pseudotsuga menziesii*, *Thuja plicata* forest, streamside woody debris, 30 July 2008, C. Richart, 1 female (SDSU); 9 miles west of St. Regis (N47.332, W115.2625), 10 August 1929, 1 male (AMNH). **Missoula Co.**: Spring Gulch, 0.3 kilometers northwest of US 12 (N46.7378, W114.5351), el. 1279 m, decomposing log, 18 June 2009, P. Marek, 2 males, 1 female (SDSU).

Distribution. Mountainous regions of northern Idaho (northern Rocky Mountains north of the Salmon River) and extreme western Montana (Bitterroot Range).

Genetic Data. GenBank accession numbers: KJ585331- KJ585334, KJ585085- KJ585088, KJ585125- KJ585128, KJ585209- KJ585211, KJ585166- KJ585169, KJ585288- KJ585291, KJ585042- KJ585045, KJ585250- KJ585252.

Comments. Both *S. nondimorphicus* and *S. idahoensis* were delimited as separate species. Differences exist in somatic morphology, morphometric analyses largely supports two distinct clusters corresponding to the two species (FIGURE 2.4), and

coalescent-based analyses support the presence of a species tree node (FIGURE 2.5). Despite this, these two species are non-monophyletic in all gene trees (FILE S6) and *gsi* statistics do not support monophyly for any genes (TABLE 2.2). Multispecies coalescent models, like that implemented in BPP, may still support species status despite the non-monophyly of gene trees, as incongruence among gene trees is attributed to deep coalescence (Knowles and Carstens 2007; Degnan and Rosenberg 2009). Previous analyses based on mitochondrial COI support the reciprocal monophyly of these two species (Derkarabetian et al. 2011) providing additional evidence for distinct species and the deep coalescence of nuclear genes. Biogeography also supports species status as these species occupy regions separated by a well-known biogeographical break seen in numerous species (Brunsfeld et al 2001). This situation requires further study with denser geographic and genetic sampling, especially to determine if more fine-scale geographical patterns exist within either *S. nondimorphicus* or *S. idahoensis*.

Sclerobunus robustus group

Diagnosis. The dorsal surface of the ventral plate of the penis has many folds, with a pair of small ventral spines on lateral plates (FIGURES 2.8c and 2.9).

Included species. *S. robustus* Briggs, *S. glorietus* (Briggs), *S. jemez* sp. nov., *S. klomax* sp. nov., *S. skywalkeri* sp. nov., *S. speoventus* sp. nov., and *S. steinmanni* sp. nov.

Distribution. Mountainous regions of Arizona, New Mexico, Colorado, and southeastern Utah, including caves.

Key to adults of *S. robustus* species group

1. OC not angled forward (Figure 2.12a)… **2**

   OC angled forward to some degree (Figure 2.12b,c)… **3**

2. Body with very little, if any, black pigment (FIGURE 2.11a); LI tibia with one or two ventral SBTs (Figure 2.14f); subapical spines of penis strongly curved, ventral plate normal (FIGURE 2.9a); Cave of the Winds, CO… ***S. speoventus* sp. nov.**

   Body and legs with considerable faint black pigment (FIGURE 2.11b); LI tibia with three or more ventral SBTs (Figure 2.14g); subapical spines of penis normal, ventral plate dorsoventrally compressed (FIGURE 2.9b); Mallory Cave, CO… ***S. steinmanni* sp. nov.**

3. LII length over 8 mm… **4**

   LII length under 8 mm… **5**

4. Pedipalpal tibia with 4 prolateral and 5 retrolateral SBTs (Figure 2.13j); 6-7 SBTs on CI; LI femur with 3 ventral SBTs (Figure 2.14j); northern NM… ***S. klomax* sp. nov.**

   Pedipalpal tibia with 5 prolateral and 5-7 retrolateral SBTs (Figure 2.13k); 10 or more SBTs on CI; LI femur with 4-6 ventral SBTs (Figure 2.14k); Terrero Cave, NM… **S. *jemez* sp. nov.**

5. Scute length usually under 1.8 mm; male PF height under 0.5 mm; northern NM… ***S. glorietus* stat. nov.**

   Scute length usually over 1.8 mm; male PF height over 0.5 mm… **6**

6. Male LII length generally over 7 mm; scute length generally over 2.2 mm; OC apex rounded in profile (Figure 2.12b); AZ, NM, CO, UT… ***S. robustus***

Male LII length generally under 6.2 mm; scute length generally under 2.2 mm; some populations with OC apex pointed in profile (Figure 2.12c); central NM… ***S. skywalkeri* sp. nov.**

Sclerobunus robustus (Packard, 1877)

Figures: **map** 2.3b; **penis** 2.8c; **habitus** 2.11c, 2.12b,e,f; **pedipalp** 2.13h; **leg I** 2.14h

Scotolemon robustum, Packard, 1877: 164, fig 8

Phalangodes robusta, Simon, 1879a: 185; Simon, 1879b: 156

Phalangodes robustus, Packard, 1888: 48, fig 13

Sclerobunus robusta [part], Banks, 1893: 152

Sclerobunus robustus, [part] Banks, 1894: 431; Banks, 1901, 672; Banks, 1902: 593; Banks, 1911: 416; Roewer, 1915: 87, fig 13; Roewer, 1923: 597, fig 746; Ekpa et al., 1984

Sclerobunus robustus robustus, Briggs, 1971: 10-11, figs 54-60, map 1; Cokendolpher et al., 1993; Kury, 2003: 19

Type Material. Paratypes: 1 specimen, West Cliff, Colorado (MCZ: Cat # 39045, not examined); 4 specimens, West Cliff, Colorado (MCZ: Cat # 39048, not examined). **Syntypes:** 2 specimens, Colorado (MCZ: Cat # 39044, not examined).

Diagnosis. Diagnosed from all other surface species in the *S. robustus* group by its larger body size (scute length generally >2.2 mm) and longer legs (LII generally >7 mm). Some populations of *S. robustus* are very similar to *S. skywalkeri* in morphological characteristics (i.e., Bradford Canyon), but can be distinguished based on geographical

distribution. Differentiated from cave-adapted species of the *S. robustus* group by its lack of troglomorphic features. Several populations of cave-inhabiting *S. robustus* are known, however they can be diagnosed from all troglomorphic species of the *S. robustus* group based on LII length (<8 mm in *S. robustus*, >8 mm in troglomorphic species).

Description. MALE: (N=13). Body length 2.44-3.18, length of scute 1.91-2.63, greatest width of anterior scute 1.28-1.66, greatest width of opisthosoma 1.89-2.72. Integument of body orange in color, lighter in cave populations, presence of black pigment ranges from faint (Northeast clade) to much (Southeast clade), anterior scute may have pigment (Southeast and Southwest clades). Anterior margin with 2-4 tubercles. OC height 0.12-0.18, width 0.25-0.37. OC rounded, angled forward. Pedipalpal coxae usually with two SBTs at distal margin, one larger, some with only a single larger tubercle (Haviland clade). CI with 10 or more spines, some on tubercles. CII with 1-4 distal posterior tubercles, 5-6 in some (Northeast clade). CII lobes with 2-3 apophyses. GO length 0.31-0.39, width 0.37-0.43. Chelicerae lighter in color, usually without black pigment, some with pigment (Southeast and Southwest clades). PCS greatest width 0.22-0.32, a single small dorsal SBT at distal edge, 1-2 small ventrolateral SBTs at distal edge, some with 3-4 (Southwest clade). DCS length 0.7-0.98, width 0.36-0.35. Pedipalps lighter in color, some with pigment (Central eastern, Southeastern, and Southwestern clades). PF height 0.53-0.82, with dorsal row of 6-8 SBTs, 9-11 in some (Southwest clade), 3-4 medial spines, row of 6-8 ventrally, most with small spine inserted within the first 3 larger spines; PT with row of 4-5 large medial spines, 5-6 lateral spines, some with 3-4 (Southeast clade). Legs lighter in color, generally with black pigment on femur,

patella, tibia, metatarsus, tarsus. LI femur generally with row of 3 ventral SBTs; tibia with 1 or 2 ventral SBTs. LII total length 5.63-7.87: trochanter 0.37-0.52, femur 1.31-2.14, patella 0.56-0.75, tibia 1.18-1.79, metatarsus 1.28-2.09, tarsus 0.93-1.33. LII/SL 2.86-3.9.

Variation. Considerable variation exists within this species. Clades noted in parentheses above are those named in Derkarabetian et al. (2011).

Material Examined. ARIZONA: **Pima Co.**: Santa Catalina Mountains, vic. Sunset Trailhead (N32.4265, W110.7424), el. 2377 m, mixed conifer forest, north-facing slope, 15 July 2006, J. Deas, S. Derkarabetian, M. Hedin, S. Thomas, 4 males, 8 females, 3 juveniles (SDSU).

COLORADO: **Custer Co.**: HWY 165, south of McKenzie junction, Wet Mountains (N38.1336, W105.1791), el. 2710 m, mixed aspen/conifer forest, above small stream, 2 July 2007, S. Derkarabetian, D. Elias, M. Hedin, 7 males, 6 females (SDSU). **Garfield Co.**: Hanging Lake Park, Hanging Lake Trail, along Dead Horse Creek (N39.5985, W107.191), el. 2118 m, under woody debris, mixed forest, 1 August 2009, S. Derkarabetian, M. McCormack, 2 males (SDSU). **Gilpin Co.**: Apex Valley Road, junction with HWY 119, 1.7 miles north of Black Hawk on 119 (N39.8192, W105.5132), el. 2580 m, north-facing slope, pine forest, 31 July 2009, S. Derkarabetian, M. McCormack, 2 males (SDSU). **La Plata Co.**: vic. Haviland Lake Campground, off HWY 550, north of Durango (N37.5329, W107.807), el. ~2440 m, north-facing hillside, mixed conifer, 28 June 2007, S. Derkarabetian, D. Elias, M. Hedin, 11 males, 5 females, 12 juveniles (SDSU). **Rio Grande Co.**: Church Creek Trailhead, southwest of South Fork,

off HWY 160 (N37.6481, W106.652), el. 2530 m, mixed aspen/conifer ravine, 28 June 2007, S. Derkarabetian, D. Elias, M. Hedin, 27 males, 9 females (SDSU).

NEW MEXICO: **Otero Co.**: HWY 244, southwest of Silver Springs in Bradford Canyon, northeast of Cloudcroft (N32.978, W105.7087), el. ~2650 m, Douglas fir/aspen forest on shallow north-facing slope, 19 July 2006, J. Deas, S. Derkarabetian, M. Hedin, S. Thomas, 1 male, 3 females (SDSU). **Sandoval Co.**: Jemez Mountains, HWY 4, 3.9 miles west of junction with HWY 501 at Los Alamos (N35.8384, W106.4044), el. ~2743 m, mixed aspen/spruce/pine flats, J. Deas, S. Derkarabetian, M. Hedin, S. Thomas, 14 males, 7 females.

UTAH: **San Juan Co.**: La Sal Mountains, La Sal Pass Road (N38.4155, W109.2242), el. ~2900 m, aspen grove, 27 June 2007, S. Derkarabetian, D. Elias, M. Hedin, 9 males, 8 females (SDSU).

Distribution. Known from Arizona, Colorado, New Mexico, and southeastern Utah.

Genetic Data. GenBank accession numbers: KJ585356- KJ585367, KJ585112- KJ585121, KJ585150- KJ585161, KJ585235- KJ585245, KJ585193- KJ585204, KJ585315- KJ585326, KJ585069- KJ585080, KJ585274- KJ585283, KJ585387, KJ585373, KJ585376, KJ585389, KJ585379, KJ585384, KJ585370, KJ585381.

Sclerobunus glorietus (Briggs, 1971), stat. nov.

Figures: **map** 2.3b; **habitus** 2.11d, 2.12d; **pedipalp** 2.13i; **leg I** 2.14i

Sclerobunus robustus glorietus, Briggs, 1971: 12, figs 67-72, map 1; Kury, 2003: 19

Type Material. Holotype male and allotype female from 4 miles southeast of Glorieta Baldy Lookout, Santa Fe County, New Mexico (N35.608, W105.769), collected on 14 August 1968 by T. Briggs, K. Hom, and D. Owyang (CAS, not examined). **Topotypes** (10 males, 1 female) with same locality information as holotype (CAS, examined).

Diagnosis. This is the smallest species of *Sclerobunus* and is diagnosed from other *S. robustus* group members based on body size (male scute length <1.8 mm). The lesser degree of black pigmentation on the body can help diagnose this taxon from smaller specimens of *S. skywalkeri*.

Description. MALE: (N=5). Body length 1.91-2.17, length of scute 1.69-1.83, greatest width of anterior scute 1.06-1.15, greatest width of opisthosoma 1.69-1.82. Integument of body orange, with some black pigment, anterior scute with lighter, patterned pigment, without pigment behind OC. Anterior margin with 3-4 tubercles. OC height 0.09-0.13, width 0.22-0.27. OC tall, rounded, angled forward. Pedipalpal coxae with 2 SBTs at distal margin. CI with 8 spines, some on tubercles. CII with 7 posterior distal tubercles. CII lobes with 2 apophyses. GO length 0.27, width 0.33. Chelicerae lighter in color. PCS width 0.21-0.22, 1 small dorsal SBT at distal edge, 1-2 small ventrolateral SBTs at distal edge. DCS length 0.6-0.65, greatest width 0.23-0.24. PF height 0.37-0.43, with dorsal row of 6-8 tubercles, row of 6-7 ventral spines; PT with row of 4 medial spines, row of 4-5 lateral spines. Legs with light black pigment on femur,

patella, tibia, metatarsus, tarsus. LI femur with row of 3 ventral SBTs; tibia with 1-2 ventral SBTs. LII total length 4.7-5.1: trochanter 0.31-0.34, femur 1.08-1.13, patella 0.47-0.5, tibia 0.96-1.06, metatarsus 0.99-1.12, tarsus 0.78-0.93. LII/SL 2.71-2.83.

FEMALE: (N=3). Body length 2.13-2.36, scute length 1.74-1.8, greatest width of anterior scute 1.01-1.03, greatest width of opisthosoma 1.72-1.88. OC height 0.09-0.12, width 0.22-0.24. GO 0.23-0.27, width 0.33-0.37. PCS width 0.2-0.21. DCS length 0.58-0.59, greatest width 0.22-0.23. PF height 0.28-0.29. LII total length 4.45-4.78: trochanter 0.3-0.33, femur 1.04-1.16, patella 0.44-0.46, tibia 0.9-0.98, metatarsus 0.94-0.96, tarsus 0.81-0.9. LII/SL 2.56-2.66.

Material Examined. NEW MEXICO: **Santa Fe Co.**: north of Glorieta Baptist Camp, Glorieta Canyon (N35.6118, W105.7703), in north-facing Douglas fir thicket, el. 2347 m, 20 July 2006, S. Derkarabetian, J. Deas, M. Hedin, S. Thomas, 2 males, 2 females (SDSU: OP890-892); north of Aspen Ranch on Rio Nambe (N35.8281, W105.8251), el. 2500 m, 30 April 1978, D.C. Lowrie (AMNH); near ski area northeast of Santa Fe (N35.7883, W105.7959), C.C. Hoff, 3 females (AMNH); Santa Fe Baldy near Santa Fe (N35.8329, W105.7586), C.C. Hoff, 1 male (AMNH). **Taos Co**.: Taos Ski Valley road (HWY 150, northeast of Arroyo Seco), 7.7 miles from junction of SR 150 and SR 230, forested talus slope, along SR 150 (N35.6118, W105.7703), 20 July 2006 by J. Deas, S. Derkarabetian, M. Hedin, S. Thomas, 2 males, 2 females (SDSU: OP881-883); same collecting locality as previous, 3 July 2007, S. Derkarabetian, D. Elias, M. Hedin, L. Hedin, 1 male, 3 females (SDSU: OP1169-1171); same collecting locality as previous, 4 June 2008, S. Derkarabetian, R. Fawcett, 1 male, 1 female, I juvenile (SDSU:

OP2119); same collecting locality as previous, 30 July 2009, S. Derkarabetian, M. McCormack, 1 female (SDSU).

Distribution. Known from the southern Sangre de Cristo Mountain Range in New Mexico.

Genetic Data. GenBank accession numbers: KJ585351- KJ585353, KJ585107- KJ585109, KJ585146- KJ585147, KJ585230- KJ585232, KJ585188- KJ585190, KJ585310- KJ585312, KJ585064- KJ585066, KJ585269- KJ585271.

Comments. In prior analyses (Derkarabetian et al. 2010) the *S. glorietus* complex only included 4 samples with only one highly supported branch, a sister relationship between *S. klomax* and the *S. glorietus* population from Taos Ski Valley. In previous COI-only analyses (Derkarabetian et al. 2011), *S. skywalkeri* is monophyletic and highly supported, *S. klomax* and the *S. glorietus* from Taos Ski Valley were reciprocally monophyletic with low support, and *S. glorietus* from Glorieta Canyon was recovered sister to the entire *S. robustus* species group. Similar difficulties occurred in the present study in which morphological clusters were not supported by gene trees. In most gene trees, the Glorieta Canyon population of *S. glorietus* was recovered either within or sister to *S. skywalkeri* populations, however, support for these relationships was low (FILE S6). Despite this uncertainty, and given that BPP analyses are sensitive to guide tree topology (Yang and Rannala 2010), we argue that defining three species within the *S. glorietus* complex based on the morphometric clustering and qualitative morphological similarity is the most conservative and intuitive choice and unlikely to result in future synonymy with increased sampling. Further sampling focused on the geographic gap between the

two populations of *S. glorietus* may eliminate the discrepancy between the morphological and genetic data seen here.

Sclerobunus jemez sp. nov.

urn:lsid:zoobank.org:act:748E456F-F63E-47E5-889C-5E2331557EA2

Figures: **map** 2.3b; **habitus** 2.11f; **pedipalp** 2.13k; **leg I** 2.14k

Type Material. Holotype male from Terrero Cave, Santa Fe County, New Mexico (GPS withheld), collected on 18 June 1975 by W. C. Welbourn (CAS, examined). **Paratypes:** 1 male, 2 females same collecting data as holotype (CAS, examined). Holotype and paratypes deposited at CAS.

Etymology. The specific epithet is a noun in apposition named in honor of the Jemez Pueblo for whom Terrero Cave is culturally and spiritually significant.

Diagnosis. Diagnosed from all other species in the *S. robustus* group by a combination of scute length of 1.9-2.0 mm and LII length between 8.0-9.0 mm. *S. jemez* is generally less troglomorphic than *S. steinmanni*, *S. speoventus* and *S. klomax*. The first three proximal ventral spines of the PF are stouter and shorter than other troglomorphic species. *S. jemez* has more spines on CI (8-12) compared to *S. klomax* (6-7).

Description. MALE: Holotype (1 paratype). Body length 2.11 (2.18), length of scute 2.0 (1.93), greatest width of anterior scute 1.25 (1.23), greatest width of opisthosoma 1.88 (1.96). Integument of body yellowish in color, anterior scute slightly darker, no pigment present. Anterior margin of scute with 2-3 tubercles. OC height

0.94(1.0), width 0.23 (0.23). OC tall, rounded, anteriorly directed, as wide as long. Pedipalpal coxae with a single SBT at distal margin (lateral edge). CI with 10 spines, some on large tubercles. CII with 4-5 distal posterior tubercles. CII with 2 small, thin apophyses (left apophysis damaged on holotype, paratype with 3). GO length 0.29 (0.3), width 0.32 (0.33). Chelicerae elongate. PCS greatest width 0.21 (0.23), single small spine at anterior dorsal margin, 2 small ventrolateral SBTs at distal margin. DCS length 0.75 (0.74), width 0.24 (0.25). Pedipalps elongate. PF height 0.42 (0.41), with dorsal row of 7-8 small SBTs, 4 small mesodorsal SBTs, 3 elongate medial spines, row of 8 elongate ventral spines; PT with row of 5 large medial spines, 6-7 large lateral spines. Legs elongate. LI trochanter with several ventral setae, one on small tubercle; femur with ventral row of 5-6 SBTs, the second being smallest; tibia with ventral row of larger 2-3 SBTs. LII total length 9.09 (8.78): trochanter 0.4 (0.41), femur 2.04 (2.08), patella 0.71 (0.69), tibia 1.87 (1.72), metatarsus 1.96 (1.86), tarsus 2.11 (2.02). LII/SL 4.55 (4.55).

FEMALE: 2 paratypes. Body length 2.16-2.3, scute length 1.94-1.97, greatest width of anterior scute 1.23, greatest width of opisthosoma 1.94. OC height 0.09-0.11, width 0.21-0.22. GO length 0.31, width 0.36-0.38. PCS width 0.22-0.23. DCS length 0.71-0.88, width 0.24. PF height 0.32-0.33. LII total length 8.08-8.34: trochanter 0.4-0.42, femur 1.96-2.04, patella 0.62-0.64, tibia 1.62-1.64, metatarsus 1.67-1.73, tarsus 1.79-1.93. LII/SL 4.1-4.32.

Distribution. Known only from type locality.

Sclerobunus klomax **sp. nov.**

urn:lsid:zoobank.org:act:2156504D-0E52-4AD5-8DDD-56A45CB1ED24

Figures: **map** 2.3b; **habitus** 2.11e; **pedipalp** 2.13j; **leg I** 2.14j

Type Material. Holotype female, from rock pile on forested talus slope, el. 2865 m, along SR 150, 7.7 miles from junction of SR 150 and SR 230, vic. Taos Ski Valley, Taos County, New Mexico (N35.6118, W105.7703), collected on 3 July 2007 by S. Derkarabetian, D. Elias, M. Hedin, L. Hedin, (deposited at CAS; SDSU: OP1171). GenBank accession numbers: KJ585355, KJ585111, KJ585149, KJ585234, KJ585192, KJ585314, KJ585068, KJ585273. **Paratypes:** 1 female, same collecting data as holotype, collected on 20 July 2006 by J. Deas, S. Derkarabetian, M. Hedin, S. Thomas (SDSU DNA voucher OP972). GenBank accession numbers: KJ585354, KJ585110, KJ585148, KJ585233, KJ585191, KJ585313, KJ585067, KJ585272; 1 female, same collecting data as holotype, collected on 30 July 2009 by S. Derkarabetian, M. McCormack (SDSU).

Etymology. The specific epithet is a noun in apposition from the Greek word *klomax*, meaning "heap of stones, stony place". This refers to the known habitat of this species, from montane rock piles.

Diagnosis. Differentiated from all surface *Sclerobunus* species and its nearest relative, (syntopic) *S. glorietus*, by its troglomorphic features. Differs from all currently known troglomorphic *Sclerobunus* by a combination of a low, anteriorly directed OC, near absence of black pigmentation, smaller body size, and fewer setae on CI.

Description. FEMALE: Holotype (2 paratypes). Body length 2.12 (1.95-2.18), length of scute 1.85 (1.63-1.82), greatest width of anterior scute, 1.17 (1.08-1.16),

greatest width of opisthosoma 1.94 (1.72-1.95). Integument of body uniformly orange/yellow in color, anterior scute with very little faint pigment, scute margins slightly darker. Anterior margin of scute with 3 tubercles. OC height 0.08 (0.09-0.1), width 0.19 (0.2). OC low, anteriorly directed, triangular in profile, roughly as long as wide, black pigment connecting eyes. Pedipalpal coxae with 1 SBT at distal margin. CI with 6-7 setae, some on tubercles. GO length 0.29 (0.21), width 0.36 (0.32-0.34). Chelicerae elongate. PCS greatest width 0.22 (0.2-0.21), with a single distal mesodorsal seta, single distolateral seta. DCS length 0.72 (0.67-0.7), width 0.23 (0.22). Pedipalps elongate. PF height 0.33 (0.29-0.32), with dorsal row of 5-6 small SBTs, 2-3 small mesodorsal spines, a row of 3 elongate medial spines, ventral row of 8-9 elongate spines; patella with a single distolateral tubercle with seta at anterior margin; PT with row of 4 large medial spines, 5 lateral spines. Legs elongate. LI femur with ventral row of three SBTs, the third being smallest; tibia with ventral row of larger setae, two arising from tubercles. Holotype female missing both LII past femur. LII total length ? (8.03-8.63): trochanter 0.41 (0.38-0.41), femur 2.09 (1.93-2.06), patella ? (0.57-0.63), tibia ? (1.55-1.77), metatarsus ? (1.57-1.67), tarsus ? (2.04-2.09). LII/SL ? (4.74-4.93). Lateral prongs of hind tarsal claws somewhat reduced.

MALE: Unknown.

Variation. There is some variation in the spination counts on the PF.

Natural History. All specimens of this species were collected from beneath rock piles in a small area of forested, south-facing talus slope. Only three specimens have been found, despite four separate visits over four years to the type locality. It is possible that

specimens inhabit deeper layers of the talus slope (superficial subterranean habitats) and might have a broader regional distribution in similar microhabitats.

Distribution. Known only from the type locality.

Remarks. In *Sclerobunus*, there is only a single case of sympatry: at Taos Ski Valley where the highly troglomorphic *S. klomax* can be found syntopic with a population of *S. glorietus*. This location has been discussed in detail elsewhere (Derkarabetian et al. 2010), however we reiterate that the troglomorphic *S. klomax* has only been collected from beneath rock piles, while *S. glorietus* are found underneath logs and rocks resting on the surface. This sympatry with an absence of known hybrids additionally supports the status of two separate species.

Sclerobunus skywalkeri sp. nov.

urn:lsid:zoobank.org:act:28C72714-D99A-44FD-9F1D-5EE3FBBB7113

Figures: **map** 2.3b; **habitus** 2.11g, 2.12c; **pedipalp** 2.13l; **leg I** 2.14l

Type Material. Holotype male, road to Capilla Peak in Canon Huevo, Manzano Mountains, Cibola NF, Torrance County, New Mexico (N34.6658, W106.3907), 19 July 2006, J. Deas, S. Derkarabetian, M. Hedin, S. Thomas (deposited at CAS). **Paratypes:** 1 male, 1 female, same collecting locality information as holotype (deposited at CAS); 4 males, 1 female, same locality information as holotype (SDSU: OP907-911). OP908 GenBank accession numbers: KJ585348, KJ585104, KJ585143, KJ585227, KJ585185, KJ585307, KJ585061, KJ585267; 1 male, 5 females, FR 193, 4 miles east of HWY 547

in Lobo Canyon, northeast of Grants, Mt. Taylor, Cibola Co., New Mexico (N35.2318, W107.6388), 21 July 2006, J. Deas, S. Derkarabetian, M. Hedin, S. Thomas (deposited at CAS); 1 male, 1 female, 2 juveniles, FR 193, 4 miles east of HWY 547 in Lobo Canyon, northeast of Grants, Mt. Taylor, Cibola Co., New Mexico (N35.2318, W107.6388), 21 July 2006, J. Deas, S. Derkarabetian, M. Hedin, S. Thomas (SDSU: OP901-904). OP903 GenBank accession numbers: KJ585350, KJ585106, KJ585145, KJ585229, KJ585187, KJ585309, KJ585063; 3 males, 10.2 miles from SR 14 along Sandi Crest Road, north-facing mixed forest, Sandia Mountains, Bernalillo County, New Mexico (N35.2099, W106.4308), 3 June 2008, S. Derkarabetian, R. Fawcett (SDSU: OP2101-2103). OP2101 GenBank accession numbers: KJ585349, KJ585105, KJ585144, KJ585228, KJ585186, KJ585308, KJ585062, KJ585268.

Etymology. The specific epithet is in reference to the character Luke Skywalker and is used to recognize the multi-generational influence and significance of the original Star Wars trilogy. This name also reflects the fact that this species is found only at high elevations in "sky island" montane habitats, and thus appears to "walk the sky".

Diagnosis. Differentiated from *S. glorietus* by greater PF height (>0.5 mm) and larger body size (scute length >1.8 mm) and differentiated from *S. robustus* by generally smaller body size (scute length <2.2 mm) and shorter legs (<7 mm). Some populations of *S. robustus* (i.e., Bradford Canyon) are very similar to *S. skywalkeri* in morphological characteristics, but can be differentiated based on geographical distribution. Differentiated from the cave-dwelling species of *S. robustus* group based on lack of troglomorphic characters.

Description. MALE: Holotype (5 paratypes). Body length 2.4 (2.28-2.51), scute length 2.05 (1.91 2.19), greatest width of anterior scute 1.27 (1.23-1.32), greatest width of opisthosoma 1.98 (1.92-2.1). Integument of body deep orange-orange/red, with much black pigment, anterior scute with patterned black pigment. Anterior margin of scute with 3 tubercles. OC height 0.16 (0.1-0.2), width 0.28 (0.26-0.29). OC tall, rounded, angled forward, eyes connected with black pigment. Pedipalpal coxae with 2 SBTs at distal margin. CI with 8 spines, some on tubercles. CII with 5 distal posterior tubercles. With 3 apophyses at CII complex. GO length 0.29 (0.29-0.31), width 0.35 (0.36-0.39). Cheliceral integument lighter, with some black pigment. PCS width 0.23 (0.23-0.27), single dorsal SBT at distal edge, single ventrolateral seta at distal margin. DCS length 0.74 (0.63-0.73), greatest width 0.26 (0.24-0.27). Pedipalpal integument lighter, with some black pigment. PF height 0.54 (0.5-0.59), with dorsal row of 6 small SBTs, 5 small mesodorsal tubercles, row of 3 medial spines, ventral row of 7 spines, with small spines between second and third spines; PT with row of 4 large medial spines, row of 5 lateral spines. All leg segments with black pigment. LI femur with row of 3 ventral SBTs; tibia with ventral row of 2 SBTs. LII total length 6.13 (5.49-6.07): trochanter 0.4 (0.38-0.41), femur 1.48 (1.33-1.44), patella 0.54 (0.5-0.57), tibia 1.25 (1.15-1.28), metatarsus 1.46 (1.18-1.42), tarsus 0.99 (0.91-1.02). LII/SL 2.99 (2.68-3.03).

FEMALES: 3 paratypes. Body length 2.06-2.56, scute length 1.81-2.0, greatest width of anterior scute 1.08-1.22, greatest width of opisthosoma 1.84-1.93. OC height 0.13-0.17, width 0.22-0.24. GO length 0.27-0.3, width 0.36-0.38. PCS greatest width 0.21-0.23. DCS length 0.6-0.66, greatest width 0.22-0.24. PF height 0.29-0.32. LII total

length 4.4-5.19: trochanter 0.29-0.36, patella 0.47-0.51, tibia 0.91-1.05, metatarsus 0.94-1.11, tarsus 0.75-0.89. LII/SL 2.46-2.59.

Variation. Variation exists in the shape of the OC: individuals from Sandia Mountains have an acute pointed OC, those from Mt. Taylor are rounded, while Manzano Mountain individuals are intermediate.

Other Material Examined. NEW MEXICO: **Bernalillo Co.**: Sandia Mountains, C.C. Hoff, 1 female (AMNH: S354); Tejano Canyon, Sandia Mountains, 1 female (AMNH: S-275). **Cibola Co.**: Mt. Taylor (N35.2412, W107.6082), el. 3307 m, under rocks, 10 August 2013, Garrett B. Hughes, 1 male, 2 females (SDSU); near and at top of Mt. Taylor, C.C. Hoff, 1 female (AMNH); near the Lillies, Mt. Taylor (N35.2694, W107.6315), CC. Hoff, 1 male (AMNH: S-1543). **Sandoval Co.**: Sandia Mountains, C.C. Hoff, 4 males, 1 female (AMNH: S-310). **Torrance Co.**: 1 mile south Capillo Peak, NW of Manzano (N34.6883, W106.3999), C.C. Hoff, 1 female (AMNH).

Distribution. Known from three isolated mountain ranges in central New Mexico (Manzano Mountains, Sandia Mountains, and San Mateo Mountains).

Sclerobunus speoventus sp. nov.

urn:lsid:zoobank.org:act:750E9704-830D-4623-AE11-FD612A200C61

Figures: **map** 2.3b; **penis** 2.9a; **habitus** 2.11a, 2.12a; **pedipalp** 2.13f; **leg I** 2.14f

Type Material. Holotype male from Thieves Canyon, Cave of the Winds, on moist ground and rocks, el. 2135 m, El Paso County, Colorado (N38.8728, W104.9203),

collected on 12 March 2009 by D. Steinmann (DMNS 2009-44). **Paratypes:** 4 males, 1 female, 1 juvenile, same collecting data as holotype (DNMS 2009-44). Holotype male and 6 paratypes deposited at DMNS.

Etymology. The specific epithet is masculine and is a combination of the Latin words for cave (*speo-*) and wind (*vent-*), and refers to the type locality of Cave of the Winds.

Diagnosis. Differentiated from all surface *Sclerobunus* by a highly troglomorphic appearance. Distinguished from *S. steinmanni* by a relative lack of black pigment on the dorsum, slightly smaller size, the presence of a single ventral tubercle bearing spine on LI tibia and strongly curved subapical spines on the penis.

Description. MALE: Holotype (6 paratypes). Body length 2.34 (2.11-2.63), length of scute 1.94 (1.93-2.2), greatest width of anterior scute 1.35 (1.38-1.45), greatest width of opisthosoma 2.1 (2.1-2.3). Integument of body uniformly yellow/orange in color, anterior scute with very little, extremely faint, black pigment. Anterior margin of scute with 3-4 tubercles. OC height 0.09 (0.07-0.12), width 0.24 (0.25-0.28). OC tall, rounded, slightly wider than long, eyes connected with black pigment. Pedipalpal coxae with 2 SBTs at distal margin (lateral edge), posterior spine larger than anterior. CI with 11 spines, several large tubercles. With 2 apophyses at CII complex. GO length 0.32 (0.33-0.36), width 0.37 (0.36-0.39). Chelicerae elongate. PCS greatest width 0.25 (0.25-0.28), single dorsal SBT at distal edge, single small ventrolateral SBT at distal margin. DCS length 0.83 (0.87-0.93), width 0.28 (0.29-0.32). Pedipalps elongate. PF height 0.53 (0.49-0.61), with dorsal row of 7 small SBTs, 4 small mesodorsal spines, a row of 3

elongate medial spines, ventral row of 8 elongate spines; PT with row of 5 large medial spines, 6 lateral spines. Legs elongate. LI femur with ventral row of five SBTs, the second and third being smallest; tibia with ventral row of larger setae, one arising from a small tubercle. LII total length 10.82 (10.33-11.33): trochanter 0.42 (0.43-0.47), femur 2.5 (2.4-2.66), patella 0.8 (0.83-0.89), tibia 2.26 (2.11-2.34), metatarsus 2.59 (2.45-2.74), tarsus 2.25 (2.0-2.3). LII/SL 5.58 (4.74-5.77).

FEMALE: (N=5; 1 paratype). Body length 2.14-2.63, scute length 1.96-2.1, greatest width of anterior scute 1.27-1.4, greatest width of opisthosoma 1.88-2.38. OC height 0.08-0.13, width 0.21-0.26. GO length 0.3-0.33, width 0.34-0.39. PCS width 0.24-0.27. DCS length 0.82-0.89, width 0.27-0.29. PF height 0.38-0.43. LII total length 9.65-10.11: trochanter 0.38-0.46, femur 2.24-2.33, patella 0.74-0.82, tibia 1.96-2.15, metatarsus 2.2-2.39, tarsus 1.93-2.08. LII/SL 4.65-5.04.

Variation. Variation exists in the spination of the pedipalp. The CII lobes show variation in the number of apophyses (2-3), even within an individual.

Other Material Examined. COLORADO: **El Paso Co.**: Cave of the Winds (N38.8728, W104.9203), Grand Concert Hall, on moist walls, 2 July 2007, S. Derkarabetian, M. Hedin, J. Reiter, 3 males (SDSU: OP1128; one used for SEM; one dissected for genitalia), 3 females (SDSU: OP1127, OP1129; one dissected for genitalia); Manitou Springs, Cave of the Winds, Manitou Grand Caverns Section, Old Water Barrel (N38.8728, W104.9203), 2 February 1984, J. W. Meacham, 1 female, 1 juvenile (CAS).

Distribution. Known only from type locality.

Genetic Data. GenBank accession numbers: KJ585343-: KJ585346, KJ585099-KJ585102, KJ585138- KJ585141, KJ585222- KJ585225, KJ585180- KJ585183, KJ585302- KJ585305, KJ585056- KJ585059, KJ585262- KJ585265.

Sclerobunus steinmanni sp. nov.

urn:lsid:zoobank.org:act:008ED6F7-05A9-49AF-9F49-CF96B8F6E8CC

Figures: **map** 2.3b; **penis** 2.9b; **habitus** 2.11b; **pedipalp** 2.13g; **leg I** 2.14g

Type Material. Holotype male from twilight zone on wall in Mallory Cave, el. 2135 m, Boulder County, Colorado (GPS withheld), collected on 29 November 2008 by D. Steinmann (DMNS; SDSU: OP2568). OP2568 GenBank accession numbers: KJ585341, KJ585096, KJ585136, KJ585219, KJ585177, KJ585299, KJ585053. **Paratypes:** 1 male paratype, 3 female paratypes from dark zone on wall in Mallory Cave, Boulder County, Colorado, collected on 15 November 2012 by D. Steinmann (DMNS; SDSU: OP3108-OP3109). OP3108 and OP3109 GenBank accession numbers: KJ585342, KJ585097- KJ585098, KJ585137, KJ585220- KJ585221, KJ585178-KJ585179, KJ585300- KJ585301, KJ585054- KJ585055, KJ585260- KJ585261. Holotype male and paratypes deposited at DMNS.

Etymology. This species is named in honor of David B. Steinmann who collected all known individuals of this species as well as discovered and collected many other new populations of cave-dwelling *Sclerobunus* throughout Colorado.

Diagnosis. Differentiated from all surface *Sclerobunus* by a highly troglomorphic appearance. Distinguished from *S. speoventus* by the presence of some black pigment on the dorsum and legs, slightly larger size, the presence of a more than one ventral tubercle bearing setae on LI tibia, penis with normal subapical spines and dorsoventrally compressed ventral plate.

Description. MALE: Holotype (male paratype). Body length 2.63 (2.74), length of scute 2.38 (2.38), greatest width of anterior scute 1.74 (1.63), greatest width of opisthosoma 2.64 (2.48). Integument of body uniformly yellow/orange in color, anterior scute with faint patterned black pigment, patch of lighter pigment posterior to OC, opisthosoma with faint black pigment evenly spread. Anterior margin with 4-5 tubercles. OC height 0.09 (0.1), width 0.24 (0.26). OC tall, roughly as long as wide, with black pigment connecting eyes. Pedipalpal coxae with 1 SBT at distal margin. CI with 14 setae, some large and on tubercles. With 2 apophyses at CII complex. GO length (0.38), width (0.41). Chelicerae elongate. PCS greatest width 0.3 (0.29), 2 small dorsal STs at distal edge, 2 small ventrolateral SBTs at distal edge. DCS length 0.97 (0.93), width 0.32 (0.32). Pedipalps elongate. PF height 0.68 (0.61), with dorsal row of 6-7 small SBTs, 4 small mesodorsal spines, a row of 3-4 elongate medial spines, ventral row of 8 elongate spines; PT with row of 5 large medial spines, 5-6 lateral spines, 2 dorsal rows of small spines, several small ventral spines. Legs elongate, with faint black pigment. LI femur with ventral row of 6 SBTs, alternating between larger and smaller tubercles, the larger being more developed than in other *Sclerobunus*; tibia with ventral row of larger setae, 3 arising from tubercles, the middle being largest. LII total length 12.43 (11.84): trochanter

0.53 (0.55), femur 2.94 (2.77), patella 1.03 (0.96), tibia 2.64 (2.45), metatarsus 3.0 (2.81), tarsus 2.3 (2.3). LII/SL 5.22 (4.96). Lateral prongs of hind tarsal claw slightly reduced.

FEMALE: 3 paratypes. Body length 2.63-3.02, scute length 2.33-2.46, greatest width of anterior scute 1.58-1.59, greatest width of opisthosoma 2.58-2.69. OC height 0.12-0.13, width 0.3-0.31. GO length 0.34-0.38, width 0.42-0.44. PCS width 0.26-0.28. DCS length 0.93-0.97, width 0.29-0.31. Pedipalpal coxae with 2 distal tubercles bearing setae. PF height 0.49-0.52. LII total length 10.41-10.89: trochanter 0.54-0.55, femur 2.45-2.61, patella 0.88-0.93, tibia 2.18-2.33, metatarsus 2.4-2.5, tarsus 1.94-1.99. LII/SL 4.42-4.48.

Distribution. Known only from the type locality.

IV. DISCUSSION

(1) Species delimitation

Species delimitation is becoming increasingly objective and taxonomy more integrative, utilizing both discovery and validation approaches employing multiple lines of evidence (Schlick-Steiner et al. 2010). Here, multiple lines of evidence are used to support all species of *Sclerobunus*: morphometric clustering, genetic analyses utilizing multiple nuclear loci, previously conducted mitochondrial analyses (Derkarabetian et al. 2010; Derkarabetian et al. 2011), and general morphology. To date, only two studies have used the method of Ezard et al. (2010), the original study and a second by Pearson and Ezard (2013), both examining morphological differentiation in fossil foraminifera. We

implemented this method on extant taxa as a means to develop *a priori* species hypotheses to be tested using hypothesis-based genetic analyses. Here, the method was used on a dataset consisting of multiple species where it successfully delimited clusters representing multiple putative species. Any clusters containing more than one species were easily differentiated using phylogenetic analyses, as either the species were not sister taxa or validation analyses confirmed genetic distinctiveness. This dataset represents a relatively simple situation in which to apply this method considering that most species of *Sclerobunus* can be distinguished by eye. However, we believe this method has great utility in modern species delimitation studies and testing its efficacy is essential, especially with regards to species complexes with little obvious morphological differentiation.

Other protocols have been developed that rely on morphological data to identify morphometric clusters that are later used as *a priori* species hypotheses. For example, Seifert et al. (2014) developed a hypothesis-free protocol that uses several morphometric clustering methods, which may be used in combination with other lines of evidence, to develop species hypotheses. The "nest-centroid" clustering method was specifically developed for and demonstrated with eusocial organisms where, in the case of ants, nest samples are treated as distinct classes in multivariate statistical analyses. The application and utility of this protocol using only morphometric data was shown by the identification and description of a new cryptic ant species (Seifert et al. 2014). Given the increasing number of cryptic species being described (Camargo and Sites 2013), using the recently developed morphological-based methods (Ezard et al. 2010; Seifert et al. 2014) as a tool

for identifying putative species, particularly when used in conjunction with genetic data, is promising.

The integrative nature of this study provides support for the utility of coalescent-based methods in species delimitation, which are becoming increasingly relevant given the common discovery of cryptic species complexes (Camargo and Sites 2013). Although mitochondrial genes have been used with great utility in animal systematics, many concerns have been raised about relying on mtDNA as the sole marker in phylogenetic and species delimitation analyses (Galtier et al. 2009). Similarly, some studies have demonstrated that species trees derived from multilocus nuclear datasets can provide higher levels of resolution and support relative to analyses based solely on mitochondrial genes (e.g., Near and Keck 2013), empirically demonstrating the need for less reliance on mitochondrial data. Under an integrative taxonomic framework, mitochondrial and nuclear datasets represent independent lines of evidence (Schlick-Steiner et al. 2010) and should be analyzed separately. We did not reanalyze or include previously published COI data for *Sclerobunus* for several reasons. Thorough phylogenetic analyses of COI have already been conducted, including divergence dating and *gsi* analyses, documenting deep genetic divergences between species and populations (Derkarabetian et al. 2011). On average, animal mitochondrial genes sort four times faster than nuclear genes and tend to show more extreme levels of genetic divergence, particularly in low vagility, microhabitat specialist taxa. As such, nuclear genes provide a more conservative estimate for species delimitation decisions. We believe that for our system and dataset, including mitochondrial genes in multilocus nuclear validation analyses (BPP) would inflate

genetic divergences between putative species and potentially result in a more liberal number of species delimited. For example, 37 of 41 *populations* sampled showed COI *gsi* values of 1 (monophyly), indicative of the extreme levels of mitochondrial genetic divergence seen in this genus (Derkarabetian et al. 2011); however, at the species level, most nuclear genes still show some degree of non-monophyly (TABLE 2.2).

(2) Delimiting cave-obligate species

The importance of genetic data in the systematics of cave-adapted species is well documented (Wiens et al. 2003; Paquin and Hedin 2004); however, studies using explicit species delimitation methodology in cave taxa are scarce (e.g., Niemiller et al. 2012). All cave species in this study do not experience gene flow with other cave species given the vast distances between caves. The cave species that are recovered as sister taxa in these analyses (the *S. cavicolens* group and *S. steinmanni*/*S. speoventus*) are not likely the result of speciation after an initial cave-invasion by an ancestral species. These cave species are from distinct, unconnected cave systems and suitable habitat is not present in the intervening regions between caves. Similarly, and in addition to morphological differences, we believe this same reasoning allows us to elevate the two subspecies of *S. ungulatus* to separate species. It is probable that these cave populations are each independently derived from different, now-extinct surface populations. Even with the discovery and increasing recognition of the importance of non-cave subterranean habitats (superficial subterranean habitats) (Culver and Pipan 2009), post-invasion speciation is still unlikely given the vast distances between caves and likely impossible as the desert

basin habitats involved do not possess superficial subterranean habitats. Gene flow with surface forms is possible in some cases, but most focal caves are surrounded by unsuitable surface habitats.

(3) Cave conservation and exploration

This study highlights the need for further conservation efforts and exploration in western North American caves. For example, *S. klomax* and *S. steinmanni* are only known from a few specimens despite multiple collecting attempts. Most other cave species of *Sclerobunus*, and many North American arachnids in general, are rare in collections. However, despite the general rarity and numerous destructive threats facing caves and the organisms inhabiting them, only a handful of taxa are listed as endangered (Elliot 2000). Notably, all but one of the 12 arachnid species listed as endangered in the United States is a cave-obligate species (http://ecos.fws.gov/tess_public/SpeciesReport.do?groups=J&listingType=L&mapstatus=1).

Given the large number of caves in western North America not yet explored from a biological perspective, the potential for discovery of new cave populations of *Sclerobunus* is high. Records exist of cave-dwelling *Sclerobunus robustus* from several caves in isolated mountain ranges in Arizona (Welbourn 1999), but these likely represent recent, local cave invasions within *S. robustus*. More importantly, several unsampled records represent potentially new species, in particular, a juvenile *Sclerobunus* collected from Crystal Falls Cave, Idaho (Briggs 1974). Additional research would help clarify the

interesting situation uncovered at Taos Ski Valley. To date, only 3 female specimens of *S. klomax* have been found from rock piles within a very small area (~100m^2) of south-facing forested-talus slope. Further fieldwork is needed to determine if this species has a broader geographic distribution and whether it only exists in superficial subterranean habitats or can be found in any nearby caves. Taken together, the description of four new, highly troglomorphic *Sclerobunus* from Colorado and northern New Mexico, and the possibility of other new cave-adapted species and populations, portray a picture of active troglomorphic evolution in a region that is not typically considered a hotspot for cave biodiversity.

V. REFERENCES

Agapow PM, Bininda-Emonds ORP, Crandall KA, Gittleman JL, Mace GM, et al. (2004) The impact of species concept on biodiversity studies. *Quarterly Review of Biology*, **79**, 161-179.

Arthofer W, Rauch H, Thaler-Knoflach B, Moder K, Muster C, Schlick-Steiner BC, Steiner FM (2013) How diverse is *Mitopus morio*? Integrative taxonomy detects cryptic species in a small-scale sample of a widespread harvestman. *Molecular Ecology*, **22**, 3850-3863.

Banks N (1893) The Phalangida Mecostethi of the United States. *Transactions of the American Entomological Society*, **20**, 149-152.

Banks N (1905) A new genus and species of Phalangida. *Entomological News*, **1**, 251-253.

Barley AJ, White J, Diesmos AC, Brown RM (2013). The challenge of species delimitation at the extremes: diversification without morphological change in Philippine sun skinks. *Evolution*, **67**, 3556-3572.

Bickford D, Lohman DJ, Sodhi NS, Ng PK, Meier R, et al. (2007) Cryptic species as a window on diversity and conservation. *Trends in Ecology and Evolution*, **22**, 148-155.

Boyer L, Baker JM, Giribet G (2007) Deep genetic divergences in *Aoraki denticulata* (Arachnida, Opiliones, Cyphophthalmi): a widespread 'mite harvestman'defies DNA taxonomy. *Molecular Ecology*, **16**, 4999-5016.

Briggs T (1971) The harvestmen of the family Triaenonychidae in North America. *Occasioanl Papers of the California Academy of Sciences*, **90**, 1-43.

Briggs T (1974) Troglobitic harvestmen recently discovered in North American lava tubes (Travuniidae, Erebomastridae, Triaenonychidae: Opiliones). *Journal of Arachnology*, **1**, 205-214.

Camargo A, Sites J (2013) Species delimitation: a decade after the renaissance. In: Pavlinov I, editor. The Species Problem - Ongoing Issues. InTech.

Carstens BC, Pelletier TA, Reid NM, Satler JD (2013) How to fail at species delimitation. *Molecular Ecology*, **22**, 4369-4383.

Crosby CR, Bishop SC (1924) The genus *Cyptobunus* Banks (Phalangida). *Entomological News*, **35**, 104.

Culver DC, Pipan T (2009) The biology of caves and other subterranean habitats. Oxford University Press. 256 p.

Cummings MP, Neel MC, Shaw KL (2008) A genealogical approach to quantifying lineage divergence. *Evolution*, **62**, 2411-2422.

De Queiroz K (2007) Species concepts and species delimitation. *Systematic Biology*, **56**, 879-886.

Degnan JH, Rosenberg NA (2009) Gene tree discordance, phylogenetic inference and the multispecies coalescent. *Trends in Ecology and Evolution*, **24**, 332-340.

Derkarabetian S, Steinmann DB, Hedin M (2010) Repeated and time-correlated morphological convergence in cave-dwelling harvestmen (Opiliones, Laniatores) from montane western North America. *PLOS One*, **5(5)**, e10388.

Derkarabetian S, Ledford J, Hedin M (2011) Genetic diversification without obvious genitalic morphological divergence in harvestmen (Opiliones, Laniatores, *Sclerobunus robustus*) from montane sky islands of western North America. *Molecular Phylogenetics and Evolution*, **61**, 844-853.

Drummond AJ, Rambaut A (2007) BEAST: Bayesian evolutionary analysis by sampling trees. *BMC Evolutionary Biology*, **7**, 214.

Drummond AJ, Suchard MA, Xie D, Rambaut A (2012) Bayesian phylogenetics with BEAUti and the BEAST 1.7. *Molecular Biology and Evolution*, **29**, 1969-1973.

Elliot WR (2000) Conservation of the North American cave and karst biota. In: Wilkens H, Culver DC, Humphreys WF, editors. Ecosystems of the World 30: Subterranean Ecosystems. Amsterdam: Elsevier. pp. 665-689.

Ence DD, Carstens BC (2011) SpedeSTEM: a rapid and accurate method for species delimitation. *Molecular Ecology Resources*, **11**, 473-480.

Ezard T, Pearson P, Purvis A (2010) Algorithmic approaches to aid species' delimitation in multidimensional morphospace. *BMC Evolutionary Biology*, **10**, 175.

Fujita MK, Leache AD, Burbrink FT, McGuire JA, Moritz C (2012) Coalescent-based species delimitation in an integrative taxonomy. *Trends in Ecology and Evolution*, **27**, 480-488.

Giarla TC, Voss RS, Jansa SA (2014) Hidden diversity in the Andes: Comparison of species delimitation methods in montane marsupials. *Molecular Phylogenetics and Evolution*, **70**, 137-151.

Giribet G, Shear WA (2010) The Genus *Siro* Latreille, 1796 (Opiliones, Cyphophthalmi, Sironidae), in North America with a phylogenetic analysis based on molecular data and the description of four new species. *Bulletin of the Museum of Comparative Zoology*, **160**, 1-33.

Grabherr MG, Haas BJ, Yassour M, Levin JZ, Thompson DA, et al. (2011) Full-length transcriptome assembly from RNA-Seq data without a reference genome. *Nature Biotechnology*, **29**, 644-652.

Grummer JA, Bryson RW, Reeder TW (2013) Species delimitation using Bayes factors: simulations and application to the *Sceloporus scalaris* species group (Squamata: Phrynosomatidae). Systematic Biology, **63**, 119-133.

Goodnight CJ, Goodnight ML (1943) New and little known Phalangids from the United States. *Americn Midland Naturalist*, **29**, 643-656.

Hartmann S, Helm C, Nickel B, Meyer M, Struck TH, et al. (2012). Exploiting gene families for phylogenomic analysis of myzostomid transcriptome data. *PLOS One*, **7(1)**, e29843.

Hedin M, Thomas SM (2010) Molecular systematics of eastern North American Phalangodidae (Arachnida: Opiliones: Laniatores), demonstrating convergent morphological evolution in caves. *Molecular Phylogenetics and Evolution*, **54**, 107-121.

Hedin M, Starrett J, Akhter S, Schönhofer AL, Shultz, JW (2012) Phylogenomic resolution of Paleozoic divergences in harvestmen (Arachnida, Opiliones) via analysis of next-generation transcriptome data. *PLOS One*, **7(8)**, e42888.

Heled J, Drummond AJ (2010) Bayesian inference of species trees from multilocus data. *Molecular Biology and Evolution*, **27**, 570-580.

Knowles LL, Carstens BC (2007) Delimiting species without monophyletic gene trees. *Systematic Biology*, **56**, 887-895.

Kocot KM, Cannon JT, Todt C, Citarella MR, Kohn AB, et al. (2011) Phylogenomics reveals deep molluscan relationships. *Nature*, **477**, 452-456.

Kury AB (2013) Order Opiliones Sundevall, 1833. Animal Biodiversity: An outline of higher–level classification and survey of taxonomic richness (Addenda 2013). *Zootaxa*, **3703**, 27-33.

Lanfear R, Calcott B, Ho SY, Guindon S (2012) PartitionFinder: combined selection of partitioning schemes and substitution models for phylogenetic analyses. *Molecular Biology and Evolution*, **29**, 1695-1701.

Lemmon AR, Lemmon EM (2012) High-throughput identification of informative nuclear loci for shallow-scale phylogenetics and phylogeography. *Systematic Biology*, **61**, 745-761.

Librado P, Rozas J (2009) DnaSP v5: a software for comprehensive analysis of DNA polymorphism data. *Bioinformatics*, **25**, 1451-1452.

McCormack JE, Hird SM, Zellmer AJ, Carstens BC, Brumfield RT (2011) Applications of next-generation sequencing to phylogeography and phylogenetics. *Molecular Phylogenetics and Evolution*, **66**, 526-538.

McCormack JE, Maley JM, Hird SM, Derryberry EP, Graves GR, Brumfield RT (2012) Next-generation sequencing reveals phylogeographic structure and a species tree for recent bird divergences. *Molecular Phylogenetics and Evolution*, **62**, 397-406.

Niemiller ML, Near TJ, Fitzpatrick BM (2012) Delimiting species using multilocus data: diagnosing cryptic diversity in the southern cavefish, *Typhlichthys subterraneus* (Teleostei: Amblyopsidae). *Evolution*, **66**, 846-866.

Packard AS (1877) On a new cave fauna in Utah. *Bulletin of the United States Geological and Geographical Survey of the Territories*, **3**, 157–169.

Padial JM, Miralles A, De la Riva I, Vences M (2010) The integrative future of taxonomy. *Frontiers in Zoology*, **7**, 16.

Parmakelis A, Kotsakiozi P, Stathi I, Poulikarakou S, Fet V (2013) Hidden diversity of *Euscorpius* (Scorpiones: Euscorpiidae) in Greece revealed by multilocus species-delimitation approaches. *Biological Journal of the Linnean Society*, **110**, 728-748.

Paquin P, Hedin M (2004) The power and perils of 'molecular taxonomy': a case study of eyeless and endangered *Cicurina* (Araneae: Dictynidae) from Texas caves. *Molecular Ecology*, **13**, 3239-3255.

Pearson PN, Ezard TH (2013) Evolution and speciation in the Eocene planktonic foraminifer *Turborotalia*. *Paleobiology*, **40**, 130-143.

Richart C, Hedin M (2013) Three new species in the harvestmen genus *Acuclavella* (Opiliones, Dyspnoi, Ischyropsalidoidea), including description of male *Acuclavella quattuor* Shear, 1986. *ZooKeys*, **311**, 19-68.

Roewer CF (1915) Die Familie der Triaenonychidae der Opiliones - Laniatores. *Archiv für Naturgeschichte*, **80**, 61–168.

Roewer CF (1931) Über Triaenonychiden. *Zeitschrift für wissenschaftliche Zoologie*, **138**, 137-185.

Satler JD, Carstens BC, Hedin M (2013) Multilocus species delimitation in a complex of morphologically conserved trapdoor spiders (Mygalomorphae, Antrodiaetidae, *Aliatypus*). *Systematic Biology*, **62**, 805-823.

Schlick-Steiner BC, Steiner FM, Seifert B, Stauffer C, Christian E, Crozier RH (2010) Integrative taxonomy: a multisource approach to exploring biodiversity. *Annual Reviews in Entomology*, **55**, 421-438.

Schmieder R, Edwards R (2011) Quality control and preprocessing of metagenomic datasets. *Bioinformatics*, **27**, 863-864.

Shear WA, Derkarabetian S (2008) Nomenclatorial changes in Triaenonychidae: *Sclerobunus parvus* Roewer is a junior synonym of *Paranonychus brunneus* (Banks), *Mutsunonychus* Suzuki is a junior synonym of *Paranonychus* Briggs, and Kaolinonychinae Suzuki is a junior synonym of Paranonychinae Briggs (Opiliones: Triaenonychidae). *Zootaxa*, **67**, 1809.

Sites Jr, JW, Marshall JC (2004) Operational criteria for delimiting species. *Annual Reviews in Ecology, Evolution, and Systematics*, **35**, 199-227.

Stephens M, Donnelly P (2003) A comparison of bayesian methods for haplotype reconstruction from population genotype data. *The American Journal of Human Genetics*, **73**, 1162-1169.

Welbourn WC (1999) Invertebrate cave fauna of Kartchner caverns, Kartchner caverns, Arizona. *Journal of Cave and Karst Studies*, **61**, 93-101.

Wiens JJ, Chippindale PT, Hillis DM (2003) When are phylogenetic analyses misled by convergence? A case study in Texas cave salamanders. *Systematic Biology*, **52**, 501-514.

Yang Z, Rannala B (2010) Bayesian species delimitation using multilocus sequence data. *Proceedings of the National Academy of Sciences USA*, **107**, 9264-9269.

Zhang C, Zhang DX, Zhu T, Yang Z (2011) Evaluation of a Bayesian coalescent method of species delimitation. *Systematic Biology*, **60**, 747-761.

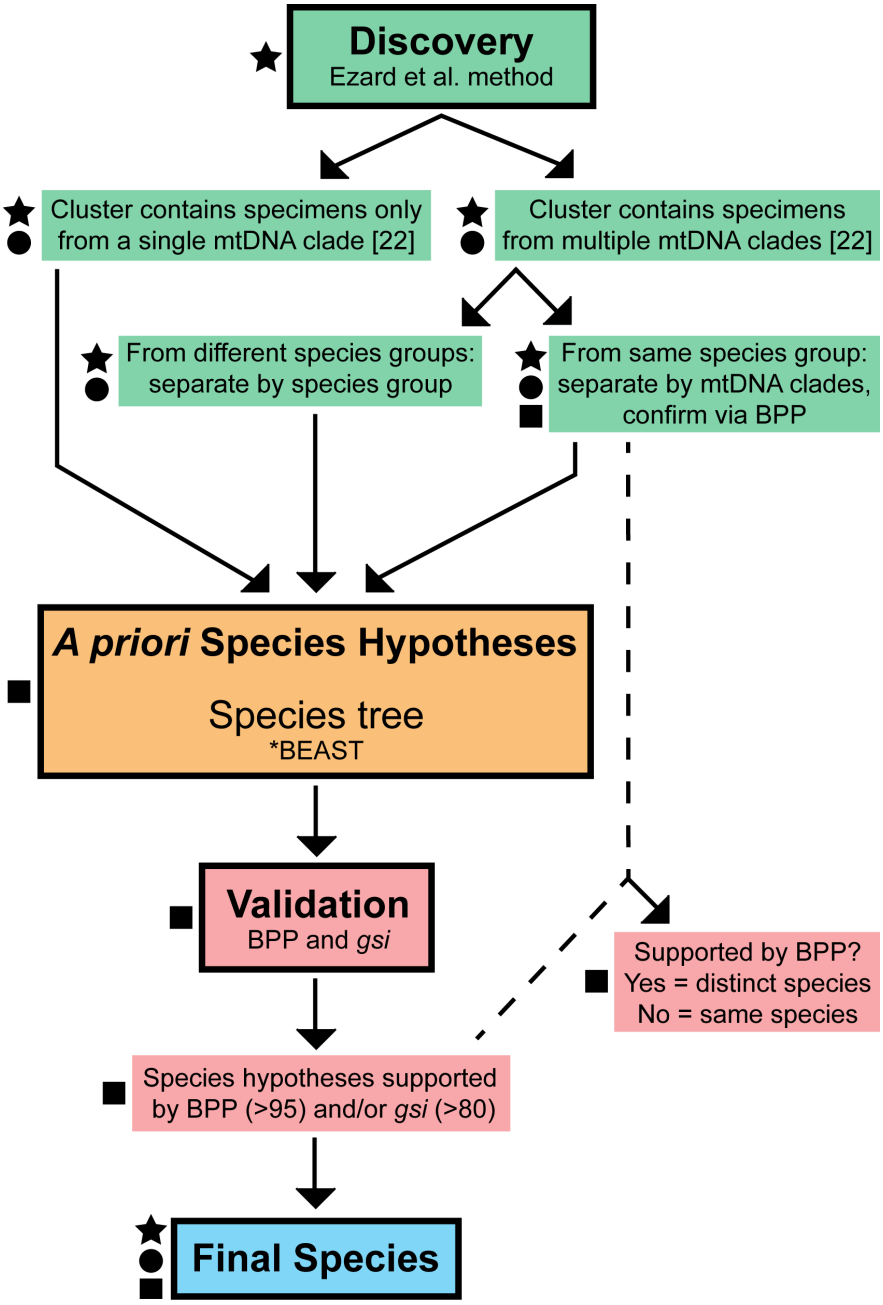

Figure 2.1. Species delimitation decision-making workflow. Symbols to the left of each step represent the different classes of data used at that particular step: star = morphological data; circle = mitochondrial data (COI); square = nuclear data.

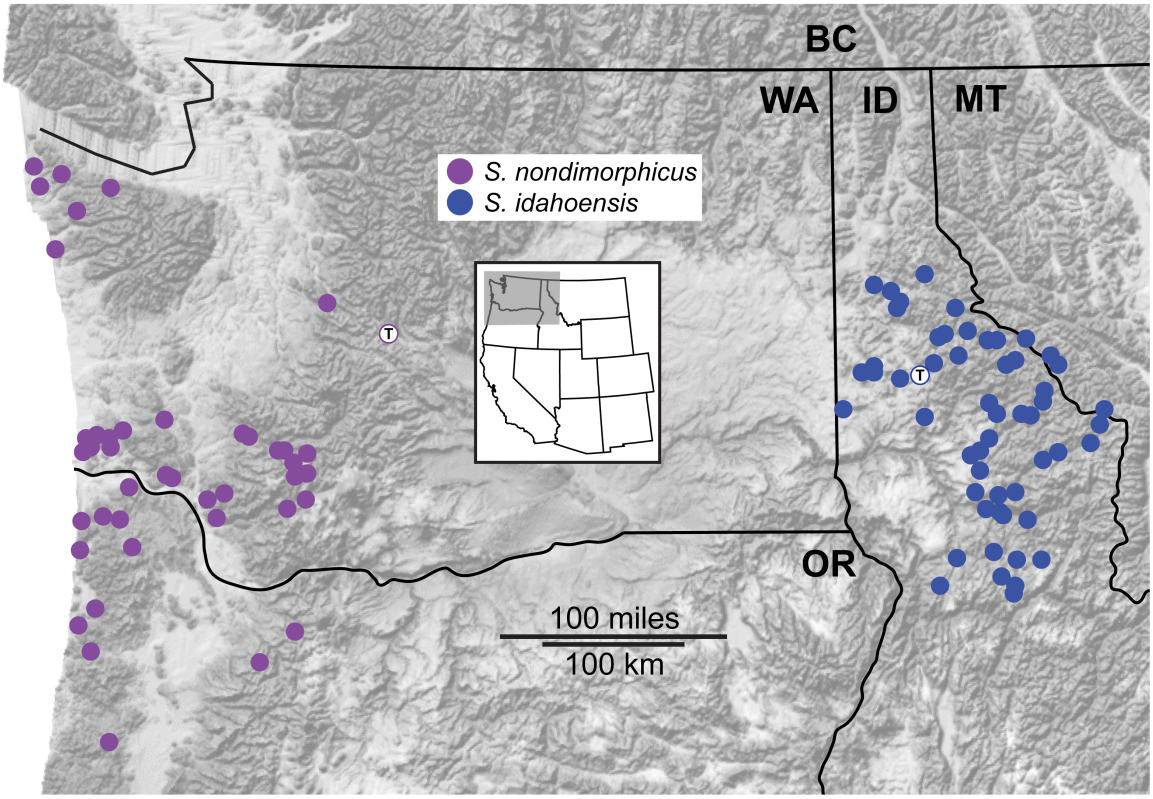

Figure 2.2. Geographic sampling of the *nondimorphicus* group. Localities are those from recent fieldwork. Localities with "T" correspond to type localities.

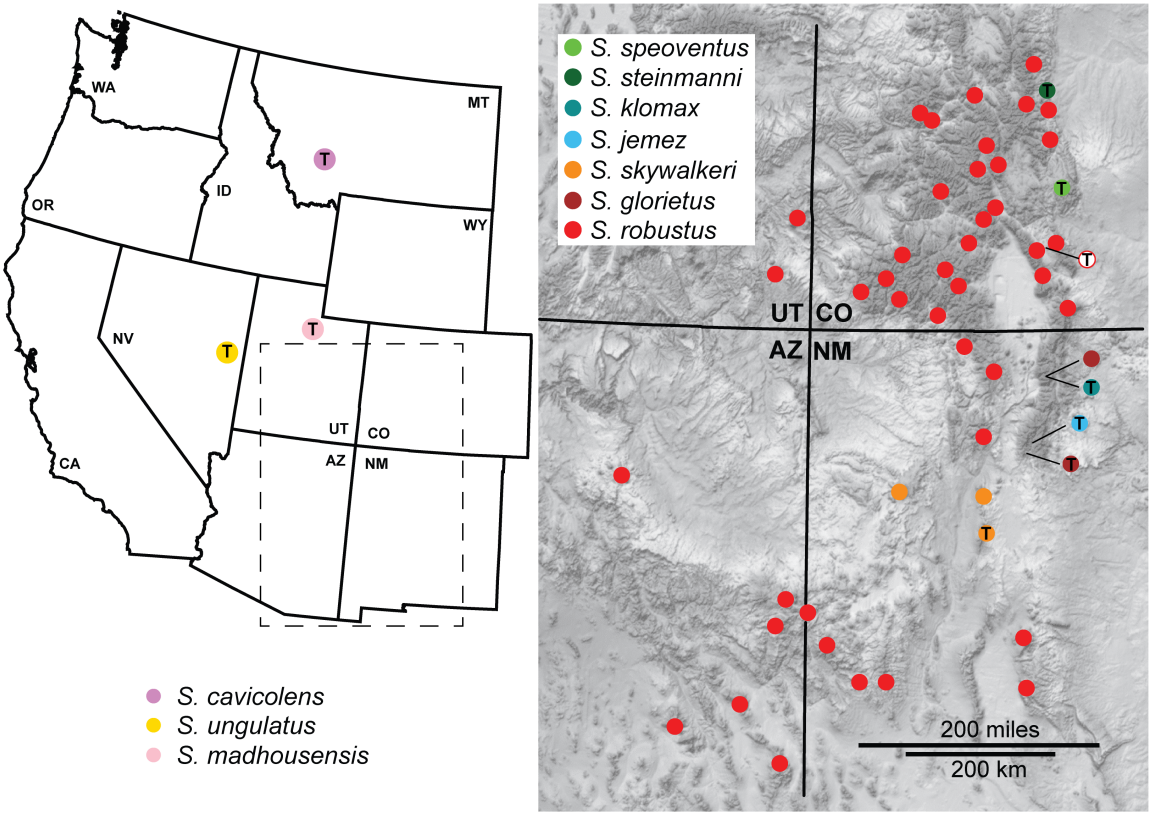

Figure 2.3. Geographic sampling of the *cavicolens* and *robustus* groups. Localities are those from recent fieldwork. Localities with "T" correspond to type localities. Type localities with solid circles correspond to localities sampled during this study.

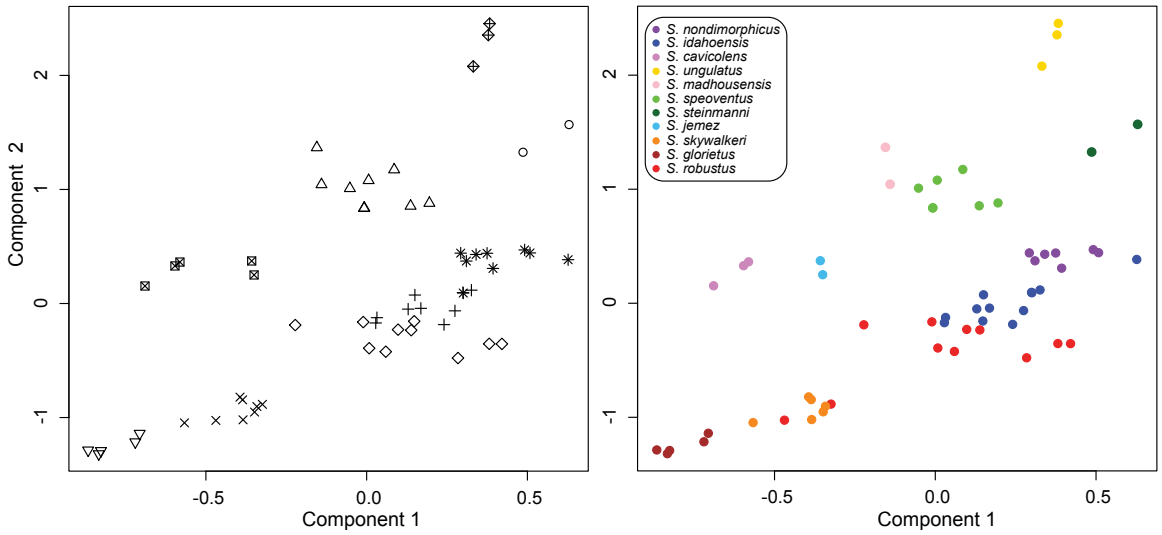

Figure 2.4. Multivariate clustering results. Left panel: specimens grouped by delimited clusters. Right panel: specimens colored by species (both previously and newly described).

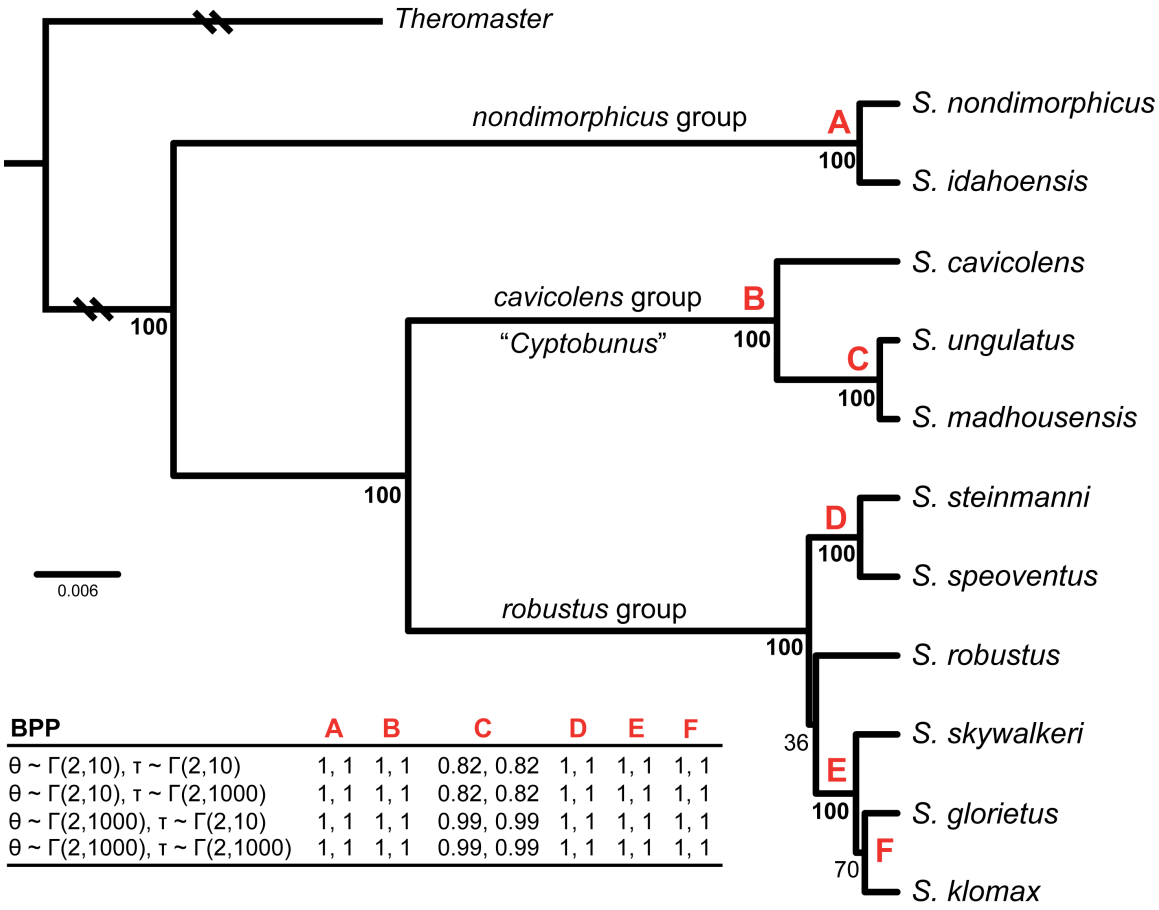

BPP	A	B	C	D	E	F
θ ~ Γ(2,10), τ ~ Γ(2,10)	1, 1	1, 1	0.82, 0.82	1, 1	1, 1	1, 1
θ ~ Γ(2,10), τ ~ Γ(2,1000)	1, 1	1, 1	0.82, 0.82	1, 1	1, 1	1, 1
θ ~ Γ(2,1000), τ ~ Γ(2,10)	1, 1	1, 1	0.99, 0.99	1, 1	1, 1	1, 1
θ ~ Γ(2,1000), τ ~ Γ(2,1000)	1, 1	1, 1	0.99, 0.99	1, 1	1, 1	1, 1

Figure 2.5. *BEAST species tree with BPP species delimitations. Numbers below nodes on species tree correspond to posterior probability support. Earliest diverging braches shortened for graphical purposes. At bottom left, BPP results with 4 different prior combinations. Numbers correspond to results of the two separate BPP runs. Red letters correspond to those nodes on the species tree.

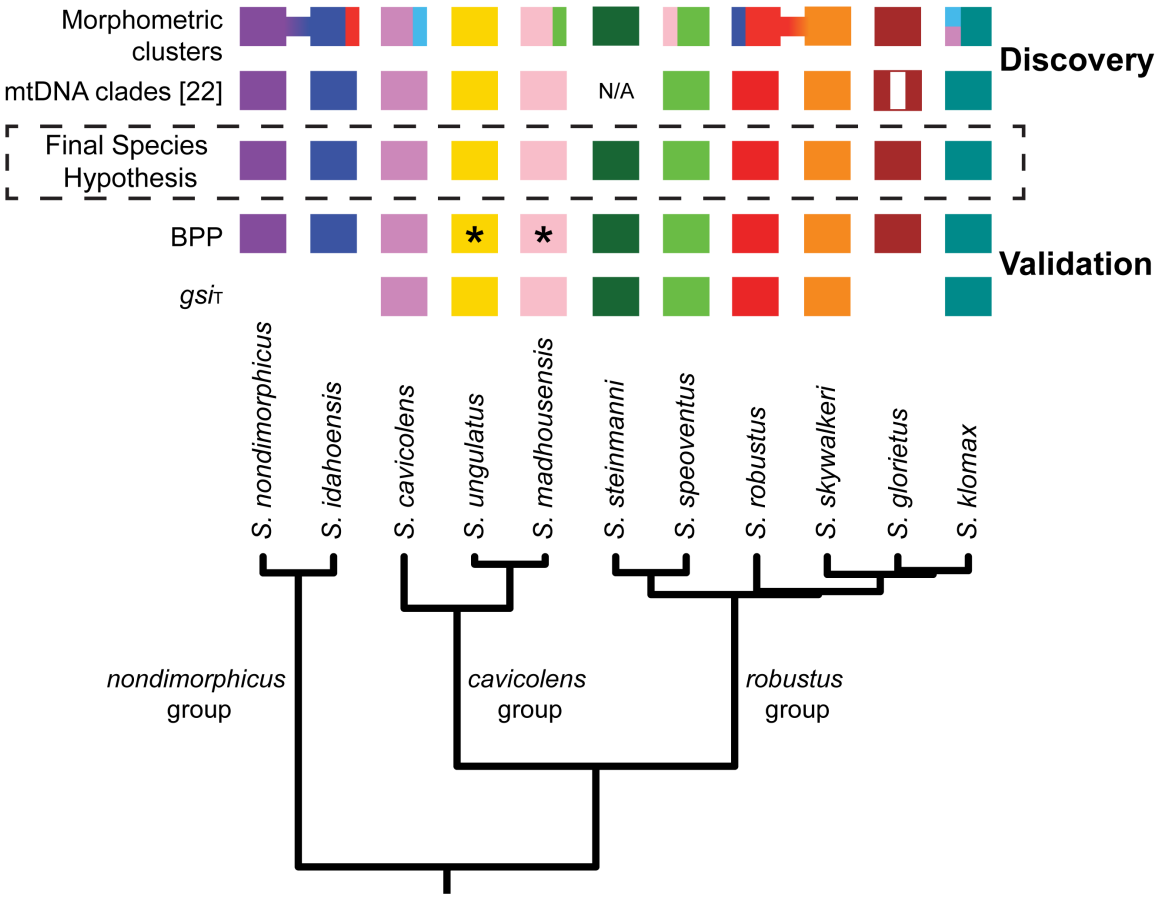

Figure 2.6. Results of integrative species delimitation. Solid color boxes indicate successful identification or delimitation of a species for the particular approach. For the morphometric clustering method, connected boxes indicate clusters including specimens from multiple species within the same species group. Clusters including specimens from multiple species from different species groups are indicated with multicolor boxes. For the mtDNA analyses [22], the vertically striped box for *S. glorietus* indicates paraphyly. For *S. steinmanni*, only one specimen was sequenced, so mitochondrial monophyly could not be assessed. For BPP analyses, asterisks indicate that *S. ungulatus* and *S. madhousensis* were not supported in analyses with certain prior combinations (see Results). Only species with gsi_T values greater than 0.8 are indicated.

Species Limits Testing	-lnL	BF
GlorCan + TSVsurf; TSVtrog; glorS	-19481.2477	2.3138
GlorCan + glorS; TSVtrog + TSVsurf	-19480.0908	0
GlorCan + glorS; TSVtrog; TSVsurf	-19481.2280	2.2744
GlorCan + TSVtrog + TSVsurf; glorS	-19481.753	3.3244

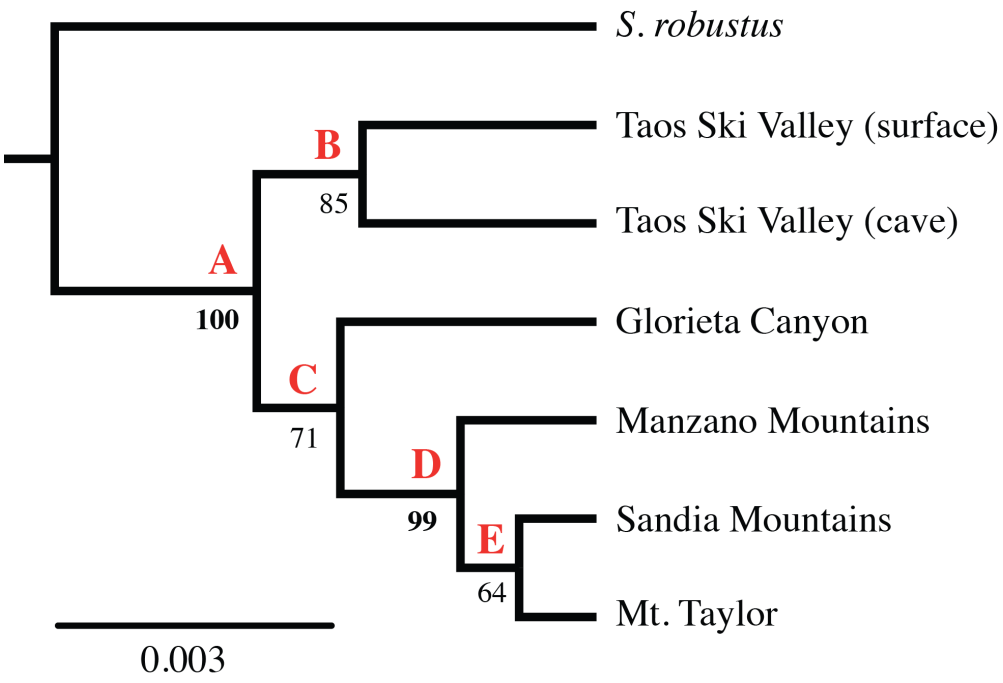

BP&P	A	B	C	D	E
$\theta \sim \Gamma(2,10), \tau \sim \Gamma(2,10)$	1	1	0.99	0.86	0.32
$\theta \sim \Gamma(2,10), \tau \sim \Gamma(2,1000)$	1	1	0.99	0.85	0.32
$\theta \sim \Gamma(2,1000), \tau \sim \Gamma(2,10)$	1	1	1	1	0.99
$\theta \sim \Gamma(2,1000), \tau \sim \Gamma(2,1000)$	1	1	1	1	0.99

Figure 2.7. Species delimitation in S. glorietus complex. Top: Results of the species limits testing using BFD. GlorCan = Glorieta Canyon. TSV surf = Taos Ski Valley surface population. TSVtrog = *S. klomax*. glorS = *S. skywalkeri*. Bottom: Species tree and BPP results from analyses in which all populations of the *glorietus* complex are each treated as putative species.

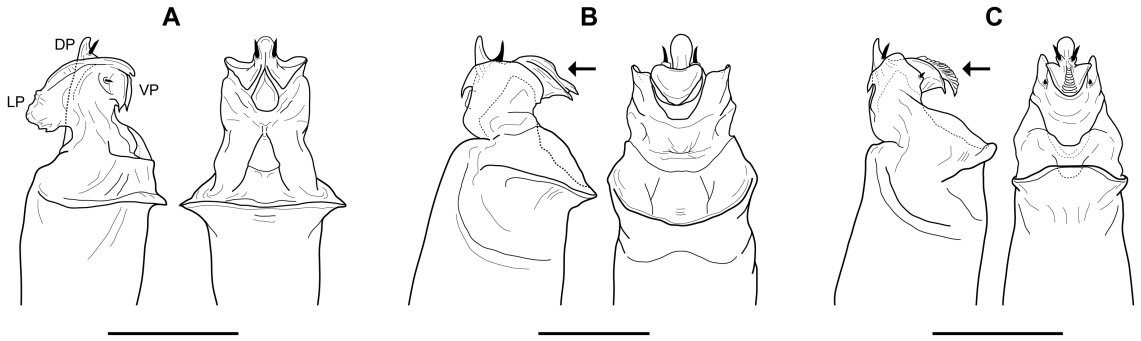

Figure 2.8. Comparative penis morphology for *Sclerobunus* species groups. A) *cavicolens* group - lateral and ventral views, *S. ungulatus* (Model Cave, NV). B) *nondimorphicus* group - lateral and ventral views, *S. idahoensis* (Meadow Creek, ID), arrow indicates smooth dorsal surface of the ventral plate. C) *robustus* group - lateral and ventral views, *S. robustus* (Chiricahua Mountains, AZ), arrow indicates dorsal surface of the ventral plate with many folds. DP = dorsal plate, LP = lateral plates, VP = ventral plate. Scale bars = 0.25 mm.

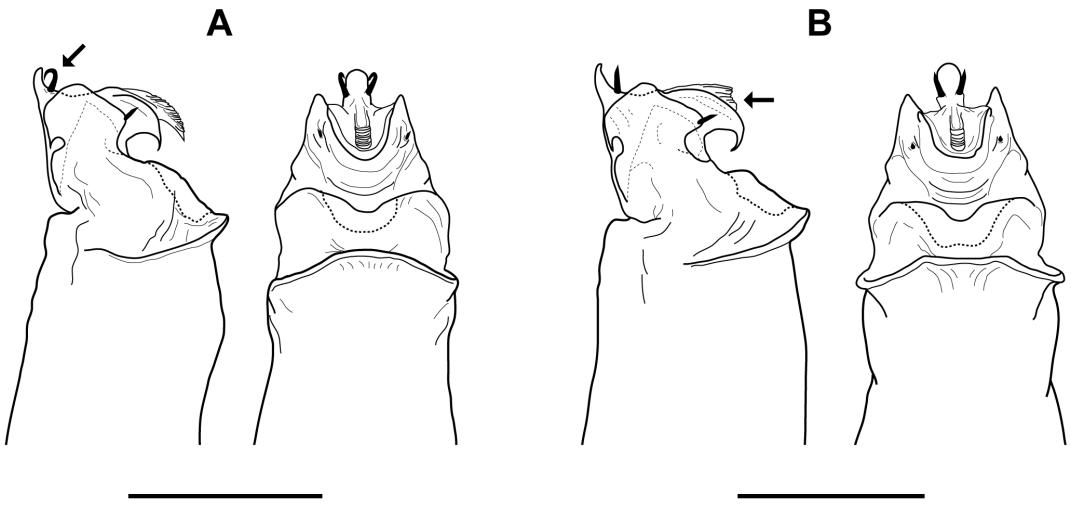

Figure 2.9. Comparative penis morphology for *S. speoventus* and *S. steinmanni*. A) lateral and ventral views, *S. speoventus*, paratype (Cave of the Winds, CO), arrow indicates curved subapical spines. B) lateral and ventral views, *S. steinmanni*, holotype (Mallory Cave, CO), arrow indicates dorsoventrally compressed ventral plate. Scale bars = 0.25 mm.

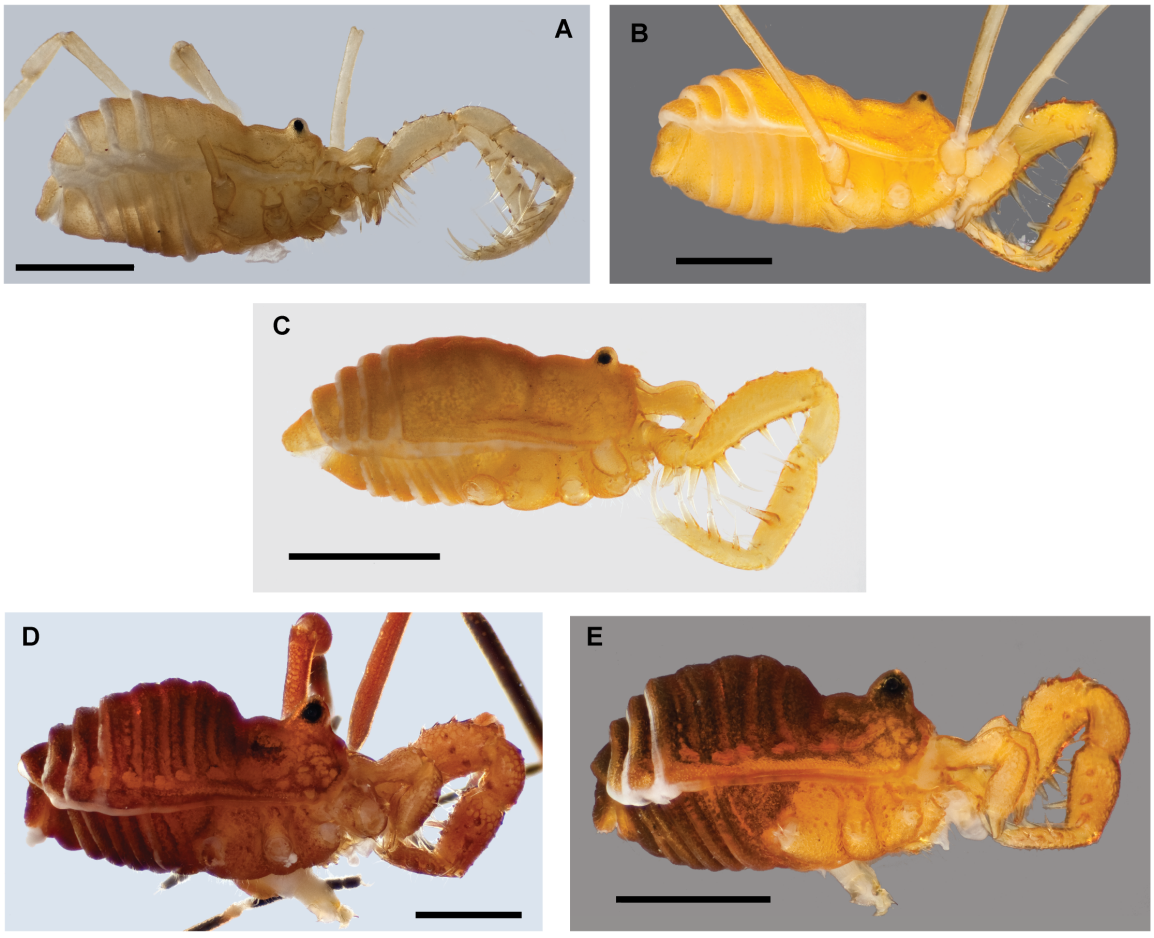

Figure 2.10. Habitus morphology of the *nondimorphicus* and *cavicolens* groups. A) *S. cavicolens*, male, image horizontally reflected (Lewis and Clark Caverns, MT) [835849]. B) *S. ungulatus*, male (Model Cave, NV) [835874]. C) *S. madhousensis*, male (North Madhouse Cave, UT) [835858]. D) *S. nondimorphicus*, male, image horizontally reflected (Iron Creek, WA) [835861]. E) *S. idahoensis*, male (Hobo Cedar Grove, ID) [835854]. Scale bars = 1 mm. Morphbank numbers indicated in brackets.

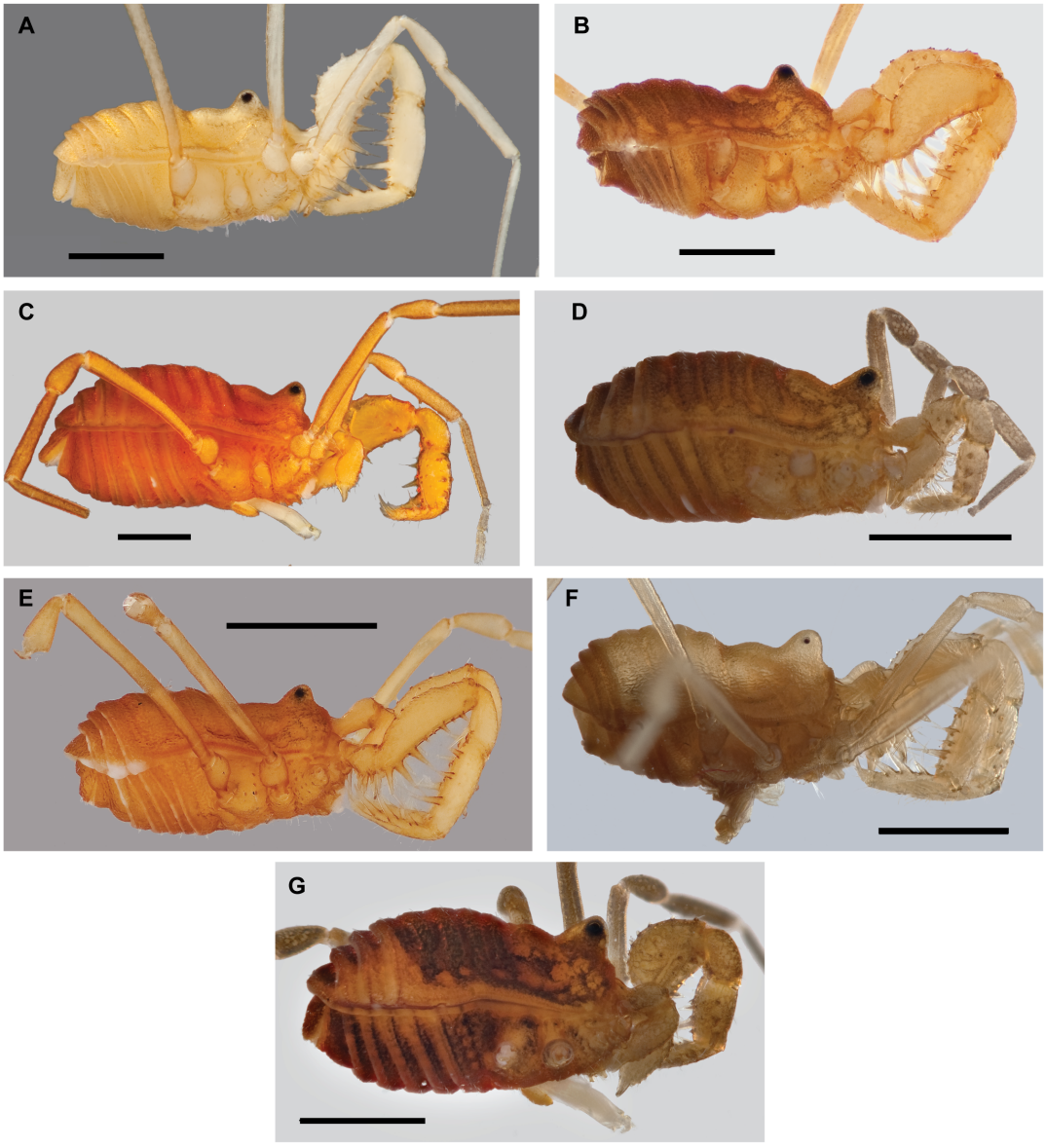

Figure 2.11. Habitus morphology of the *robustus* group. A) *S. speoventus*, paratype male (Cave of the Winds, CO) [835868]. B) *S. steinmanni*, holotype male (Mallory Cave, CO) [835871]. C) *S. robustus* male (Apex Valley, CO) [835865]. D) *S. glorietus,* male (Glorieta Canyon, NM) [835850]. E) *S. klomax*, holotype female (Taos Ski Valley, NM) [835857]. F) *S. jemez*, holotype male (Terrero Cave, NM) [835856]. G) *S. skywalkeri*, paratype male, image horizontally reflected (Manzano Mountains, NM) [835867]. Scale bars = 1 mm. Morphbank numbers indicated in brackets.

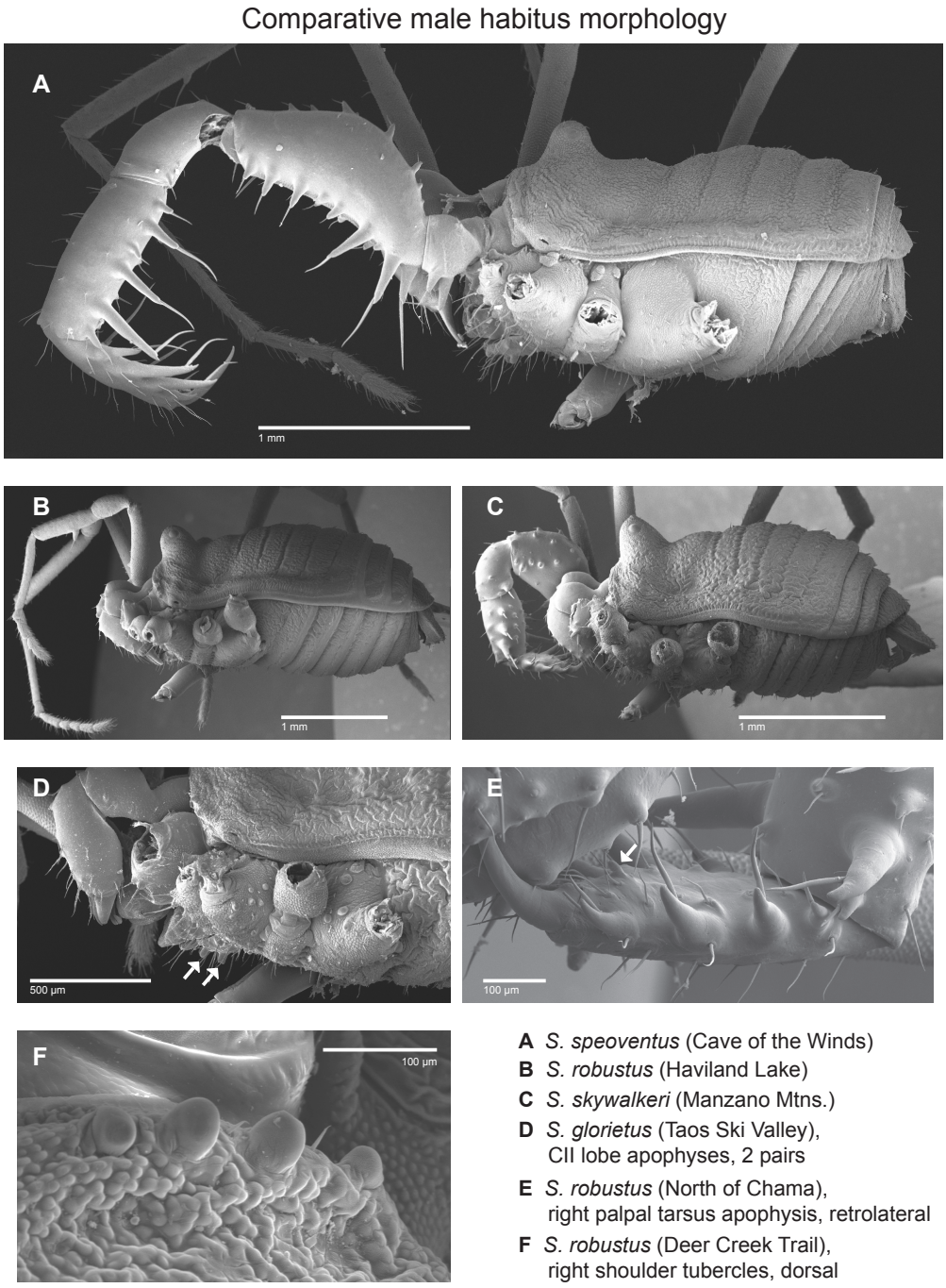

Figure 2.12. Comparative male habitus and ocularium morphology. In D and E, arrows indicate sexually dimorphic structures.

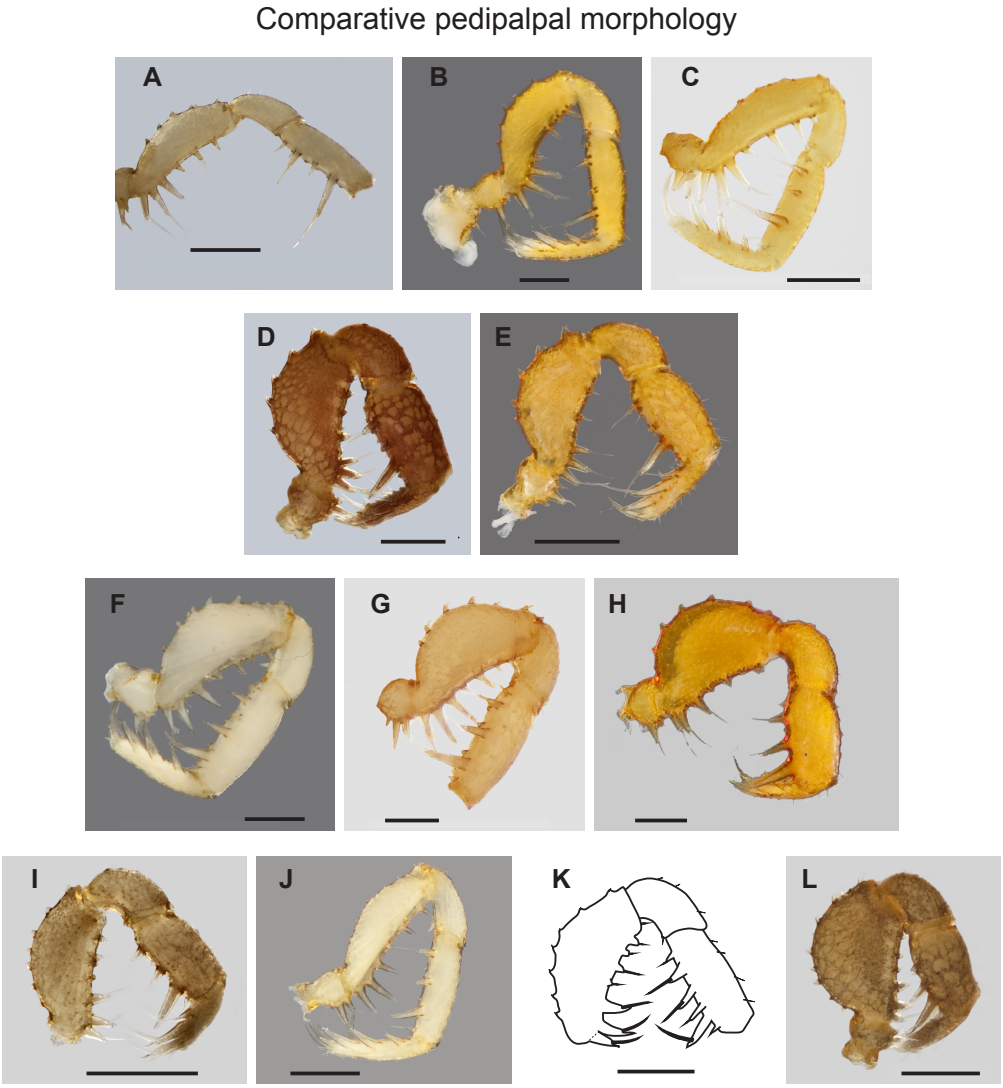

A *S. cavicolens* (Lewis and Clark Caverns)
B *S. ungulatus* (Model Cave)
C *S. madhousensis* (North Madhouse Cave)
D *S. nondimorphicus* (Iron Creek)
E *S. idahoensis* (Hobo Cedar Grove)
F *S. speoventus* (Cave of the Winds)
G *S. steinmanni*, holotype (Mallory Cave)
H *S. robustus* (Apex Valley)
I *S. glorietus* (Glorieta Canyon)
J *S. klomax*, paratype female (Taos Ski Valley)
K *S. jemez*, holotype (Terrero Cave)
L *S. skywalkeri*, paratype (Manzano Mtns.)

Images reflected horizontally: A,D,K
Scale bars = 0.5 mm

Figure 2.13. Comparative pedipalpal morphology.

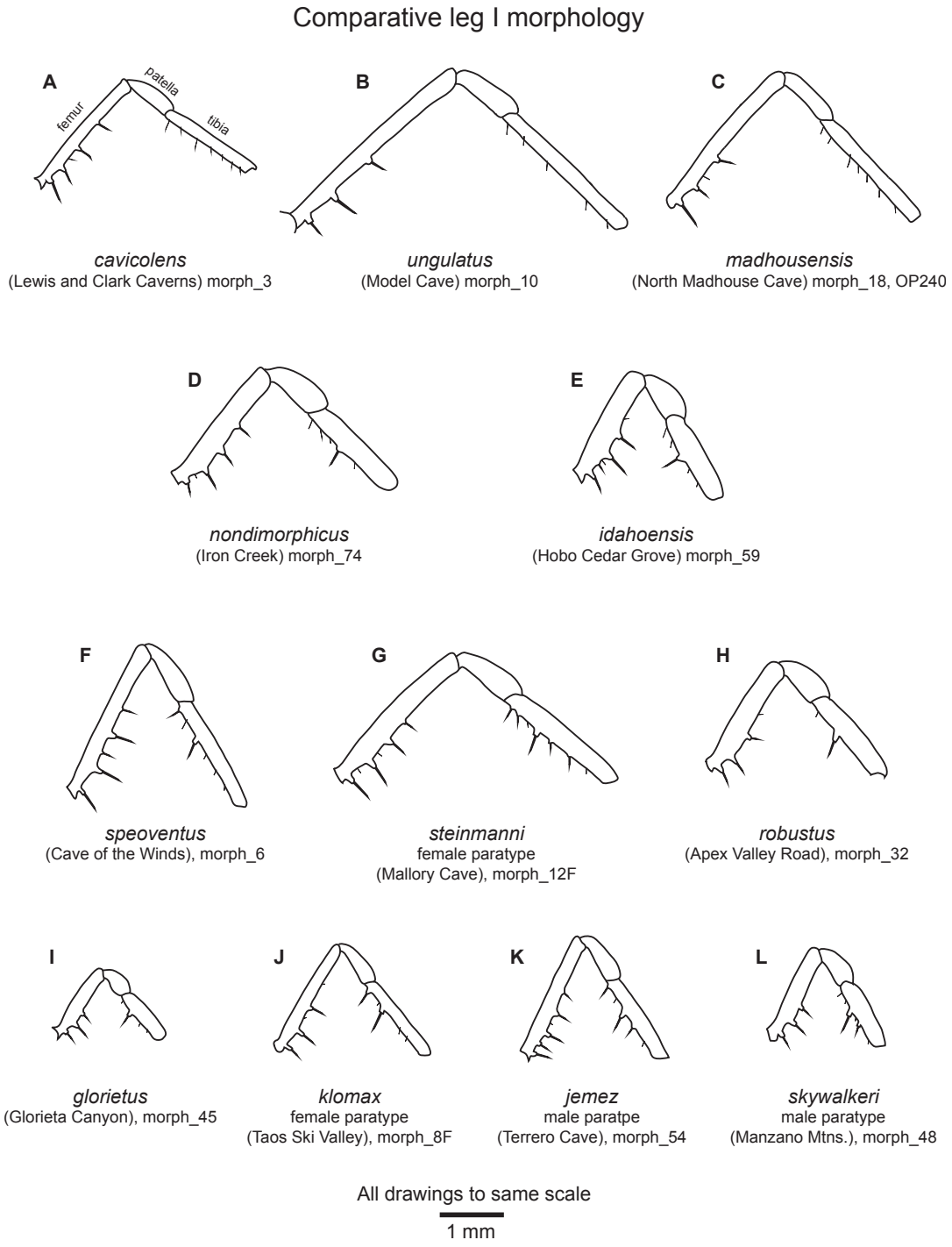

Figure 2.14. Comparative leg I morphology. "Morph" numbers correspond to those in Appendices B.3 and B.4.

Table 2.1. Nuclear gene data alignment and diversity statistics.

Locus	Type	n	Length	VS	PIS	s	N	H	θ (site)	θ (seq)	R	Taj D	BIC
TPR	Exon	68	917 (784)	153	135	153	50	0.988	0.0407	31.946	0.6	0.211	HKY+G
CHP1	Exon	52	901 (752)	120	103	120	36	0.983	0.0353	26.556	3.8	0.480	TrN+G
CHP2	Exon	52	708 (673)	96	85	96	40	0.988	0.0316	21.245	1.4	0.078	K80+G
nrm	3'UTR	49 (56)	978 (591)	91	76	91	31	0.974	0.0345	20.409	1	-0.096	HKY+G
DNO	Exon	59	645 (560)	92	81	92	44	0.989	0.0354	19.801	3.7	-0.218	HKY+G
SKI	Exon	68	701 (684)	142	124	142	57	0.993	0.0434	29.649	0.7	-0.108	GTR+I+G
ADARB2	Exon	54	839 (784)	97	90	97	35	0.978	0.0272	21.286	0.6	0.411	K80+G
PGM	3'UTR	41 (49)	591 (313)	120	105	120	22	0.968	0.0896	28.047	6.6	-0.045	HKY+G

Notes: Locus abbreviations in File S2. n, number of phased sequences (for UTRs, number of total sequences); length, length of alignment (length with any missing sites removed); VS, variable sites; PIS, parsimony informative sites; s, segregating sites; N, number of haplotypes; H, haplotype diversity; θ (site), theta per site; θ (seq), theta per sequence; R, recombination value; Taj D, Tajima's D (no significant values); BIC, model chosen with PartitionFinder.

Table 2.2. Results of *gsi* analyses.

	TPR	**CHP1**	**CHP2**	**nrm**	**DNO**	**SKI**	**ADAR**	**PGM**	gsi_T
S. cavicolens	1	1	1	1	1	1	1	1	1
S. madhousensis	1	1	1	1	1	1	1	1	1
S. ungulatus	1	1	1	1	1	1	0.5765	1	0.8221
S. nondimorphicus	0.4516	0.6232	0.5357	0.6562	0.5874	0.5203	0.6851	0.5814	0.5801
S. idahoensis	0.8607	0.6839	0.5357	0.3774	0.6878	0.8201	0.395	0.4783	0.6048
S. robustus	0.8712	0.9088	0.7041	1	0.8561	1	0.8421	1	0.8978
S. glorietus	0.4426	0.4694	0.5755	0.6405	0.5403	0.6344	0.64	0.6811	0.578
S. klomax	0.4925	1	1	1	1	0.4022	1	1	0.8618
S. skywalkeri	1	1	1	1	0.5786	0.5446	0.3769	1	0.8125
S. speoventus	1	1	1	1	1	1	1	1	1
S. steinmanni	1	1	1	1	1	1	1	1	1

Notes: Values for individual genes are from individual *gsi* analyses. All values are significant (p-value <0.05).

CHAPTER 3

Population genomic evidence for multiple Pliocene refugia in a montane-restricted harvestman (Arachnida, Opiliones, *Sclerobunus robustus*) from the southwestern United States

The integration of ecological niche modeling into phylogeographic analyses has allowed for the identification and testing of potential refugia under a hypothesis-based framework, where the expected patterns of higher genetic diversity in refugial populations and evidence of range expansion of non refugial populations are corroborated with empirical data. In this study we focus on a montane-restricted cryophilic harvestman, *Sclerobunus robustus*, distributed throughout the heterogeneous Southern Rocky Mountains and Intermontane Plateau (SRMIP) of southwestern North America. We identified hypothetical refugia using ecological niche models (ENMs) across three time periods, corroborated these refugia with population genetic methods using double-digest RAD-seq data, and conducted population level phylogenetic and divergence dating analyses. ENMs identify two large temporally persistent regions in the mid-latitude highlands. Genetic patterns support these two hypothesized refugia with higher genetic diversity within refugial populations and evidence for range expansion in populations found outside of hypothesized refugia. Phylogenetic analyses identify five to six genetically divergent, geographically cohesive clades of *S. robustus*. Divergence dating analyses suggest that these separate refugia date to the Pliocene and that divergence between clades predates the late Pleistocene glacial cycles, while diversification within

clades was likely driven by these cycles. Population genetic analyses reveal effects of both isolation by distance (IBD) and isolation by environment (IBE), with IBD more important in the continuous mountainous portion of the distribution, while IBE was stronger in the populations inhabiting the isolated sky islands of the south. Using model-based coalescent approaches, we find support for post-divergence migration between clades from separate refugia.

I. INTRODUCTION

The field of phylogeography has evolved considerably since the original pioneering work of Avise et al. (1987). Improvements in sequence data collection techniques and analytical methods (McCormack et al. 2013; Garrick et al. 2015; Edwards et al. 2015), and the quantitative integration of geological, ecological, and climatic data, for example, have all served to elevate phylogeography as a multidisciplinary science (Avise 2009; Hickerson et al. 2010). One such improvement has been the incorporation of environmental and bioclimatic data, in the form of ecological niche models (ENMs), into phylogeographic and population genetic analyses (Carstens & Richards 2007; Kozak et al. 2008; Chan *et al*. 2011). Not only do ENMs allow researchers to reconstruct the full potential geographic distribution of a species, but also, with the use of reconstructed past bioclimatic conditions, the ostensible distribution of that species through time (Graham et al. 2010). The ability to identify persistent and stable habitats has allowed researchers to adopt a hypothesis-based approach, where persistent regions are interpreted as

hypothesized refugia that produce predictable patterns of genetic diversity (Carnaval et al. 2009). Hypotheses can be generated regarding the expected genetic patterns of a species, which are then tested using empirical molecular data (e.g., Devitt et al. 2013).

Phylogeographic studies have confirmed several predictable genetic patterns regarding populations that have persisted in refugia and those that have expanded out of refugia into previously uninhabitable regions. Populations that have persisted in refugia will tend to show more diversity relative to populations outside of hypothesized refugia (e.g., Carnaval et al. 2009; Boyer et al. 2016). Conversely, populations inhabiting regions not predicted to be persistent will show evidence of range expansion, where there is a pattern of decreasing genetic diversity as geographic distance from the refugia increases (e.g., Gomez et al. 2005; Vandewoestijne & Van Dyck 2010; Jezkova et al. 2015). Here, populations at the expanding front show lower levels of diversity due to successive founder events by populations moving into previously uninhabited areas (Hewitt 2000; Hewitt 2004). In temperate taxa of the northern hemisphere this is typically manifested as a latitudinal gradient due to post-glacial northward expansion, where genetic diversity decreases with increasing latitude as taxa moved northward following the retreat of glaciers. The timing of diversification should be contemporaneous with the age of hypothetical refugia, and in the case of multiple hypothesized refugia, phylogeographic structure should additionally reflect the separate histories of distinct refugia (e.g., Hugall et al. 2002; Martínez-Solano et al. 2006; Devitt et al. 2013). Taken together, the detection of these genetic patterns can corroborate the presence of refugia and elucidate the

phylogeographic history of taxa and of focal regions, and are particularly evident in dispersal-limited taxa.

The southwestern United States provides an excellent region for phylogeographic and landscape genetic studies due to its highly heterogeneous topography with stretches of habitat of varying continuity. Here, we refer to the mountains of Arizona (AZ), Colorado (CO), New Mexico (NM), and Utah (UT) as the Southern Rocky Mountains and Intermontane Plateau (SRMIP). Studies focusing on taxa distributed across all mountainous regions of the SRMIP are relatively few. The vast majority of phylogeographic and population genetic studies of southwestern taxa analyze genetic differentiation and population structure focusing only on small portions of the SRMIP, mainly the Madrean sky islands of southern AZ and NM (e.g., Barber 1999; Masta 2000; Downie 2004; Smith & Farrell 2005; Tennessen & Zamudio 2008; McCormack et al. 2008; Ober et al. 2011; Bryson et al. 2013; Mitchell & Ober 2013; Ober & Connolly 2015; Hendrixson et al. 2015; Manthey & Moyle 2015), or the southern Rocky Mountains (e.g., DeChaine & Martin 2005a; Knowles et al. 2007; Massatti & Knowles 2014). Only a single phylogeographic study of *Sciurus aberti* (Lamb et al. 1997) spans the entire mountainous SRMIP region. Studies in this region attribute the depth of differentiation between sky island populations to the late Pleistocene glacial cycles occurring <1.6 MA. A subset of these studies have explicitly conducted divergence dating analyses and concluded that isolated sky island populations are older than expected given the favorable conditions for gene flow present during the last glacial maximum (LGM) ~20 KA. Studies in other taxa have also generally challenged the

importance of late Pleistocene glaciations (e.g., Klicka & Zink 1997). In addition, the arthropods of the southwestern Madrean sky islands are recently receiving much attention with sustained research focusing on various aspects of their biology and systematics (Moore et al. 2013; Meyer et al. 2015).

Opiliones (more commonly called harvestmen) are arachnid taxa typically characterized by low vagility and high ecological constraints. These biological characteristics make them ideal candidates for phylogeographic and biogeographic studies (e.g., Boyer et al. 2007; Thomas & Hedin 2008; Giribet et al. 2010; Hedin et al. 2012; Schönhofer et al. 2013; Schönhofer et al. 2015; Boyer et al. 2016; DiDomenico & Hedin 2016; Emata & Hedin 2016; Starrett et al. 2016). One such candidate is the genus *Sclerobunus* Banks 1893, with 12 species distributed throughout western North America. The widespread species *Sclerobunus robustus* (Packard 1877), first described from Colorado, was later redescribed and recorded with a very broad distribution throughout the American southwest and Rocky Mountains (Briggs 1971). Following taxonomic changes proposed in a generic revision (Derkarabetian and Hedin 2014), this species is distributed throughout the mountainous habitat of the SRMIP region. In the southern portion of this region, suitable habitat is found on the extremely discontinuous Madrean sky islands, isolated mountains surrounded by uninhabitable, low-lying desert and scrub-grassland, while further north the southern Rocky Mountains are much more continuous with higher connectivity between suitable habitat. *Sclerobunus robustus* is a cryophilic microhabitat specialist, typically found underneath rotting logs and rocks (and sometimes

in caves) in moist, high elevation conifer and aspen forests (Briggs 1971; Derkarabetian et al. 2010).

A previous phylogeographic analysis of *S. robustus* (Derkarabetian et al. 2011) demonstrated that, despite homogeneity in both somatic and genitalic morphology, the species is split into eastern and western lineages and includes six deeply genetically divergent, geographically cohesive mitochondrial phylogroups (Figure 3.1). Divergence dating analyses based on mitochondrial cytochrome oxidase I (COI) sequence data using biogeographic and geologic calibrations of outgroup taxa show that diversification between these phylogroups occurred during the Pliocene (~3.8 - 5.5 MA), while diversification within the clades occurred during the Pleistocene. Additionally, based on population genetic statistics and gene tree topologies, Derkarabetian et al. (2011) suggested that the mid-latitude highlands of southern Utah/Colorado and northern New Mexico may have acted as refugia during unfavorable warmer conditions. However, the previous study of *S. robustus* was limited in that it relied almost entirely on COI data and included no quantitative assessments of refugia. In order to establish a more accurate estimate of genealogical relationships and divergence dates of *S. robustus*, and to gain a better understanding of the geologic and climatic processes contributing to population structure, a multi-locus dataset is needed. In particular, analyzing datasets consisting of 100s - 1000s of SNPs can lead to better estimates of population genetic statistics even when low numbers of samples are included per population (Willing et al. 2012).

The present study employs the recently developed ddRAD-seq protocol (Peterson et al. 2012) to obtain hundreds of loci, and associated single nucleotide polymorphisms

(SNPs), which are then used in phylogeographic and landscape genomic analyses to explore the phylogeographic history of the *S. robustus* complex. Our objectives are to identify potential refugia, reconstruct a population level phylogeny, estimate diversification dates, and explore how geography and environment have shaped patterns of genetic diversity in *S. robustus*. Specifically, we use ENM reconstructions to identify regions of habitat that potentially served as refugia and examine whether genetic patterns support the presence and location of these hypothesized refugia. Based on previous phylogeographic studies integrating niche modeling and genetic analyses (e.g., Carnaval et al. 2009; Devitt et al. 2013), we expect to see higher levels of genetic diversity for populations found within hypothesized refugia, evidence of range expansion for populations found outside of hypothesized refugia, and high measures of phylogeographic structure between refugia. The broad distribution of *S. robustus* across the SRMIP allows a comparison of genetic patterns in differing geographic backdrops, in this case, the isolated Madrean sky islands of southern Arizona and New Mexico versus the more contiguous regions of the Southern Rocky Mountains.

II. MATERIALS AND METHODS

(1) Taxon sampling

We collected surface-dwelling *S. robustus* from 39 localities throughout its distribution (Figure 3.1, Appendix C.1). In this paper study we use the term "population" as an equivalent to all specimens/samples from a single collecting locality (i.e., 39

populations). Specimens were preserved in 100% EtOH. For genetic analyses, 1-2 specimens of *S. robustus* were selected per population, depending on available sample size, with the exception of San Francisco Mountains, AZ where 3 samples were chosen (Figure 3.1), for a total of 65 specimens. Additionally, a single sample each of *S. nondimorphicus* and *S. idahoensis* were included as outgroup taxa. All cave populations of *S. robustus* were excluded from this study as these cave populations are found at lower elevation and outside of habitat deemed suitable compared to surface dwelling populations. The bioclimatic variables representative of these cave localities will not reflect the actual habitat requirements of surface *Sclerobunus*. Additionally, those cave populations that have been included in phylogenetic analyses are extremely recent derivations and not genetically distinct from geographically proximate surface populations. Cave populations, and their genetic affinities with surface populations, are more thoroughly discussed in Derkarabetian et al. (2010) and Derkarabetian et al. (2011).

(2) Identification of putative refugia

To identify regions of habitat that most likely served as refugia we operated under the premise that potential refugia will be regions where climate reconstructions support suitable habitat that are persistent through time and variable climatic conditions (Kozak et al. 2008). This general framework has been utilized numerous times to identify potential refugia (e.g., Knowles et al. 2007; Carnaval et al. 2009; Graham et al. 2010; Chan *et al*. 2011). For example, Devitt et al. (2013) used bioclimatic data to reconstruct niche models for three time periods (current, Holocene, LGM datasets), which were then combined to

identify regions of suitable habitat shared across time. In addition to reconstructing ENMs across these time periods, we conducted separate ENM analyses on localities split into eastern and western lineages, which are both well-supported clades (Derkarabetian et al. 2011). Given their similar geographic distributions, we treat the eastern and western lineages as "latitudinal replicates" and assume that habitats predicted as suitable to both lineages across time would more likely represent refugia.

ENMs were reconstructed in Maxent version 3.3.3k (Phillips et al. 2006) using 30 arc-seconds resolution datasets of altitude and 19 bioclimatic variables (WorldClim v1.4; Hijimans et al. 2005). While *S. robustus* likely selects suitable microhabitat (i.e., niche) on a fine scale preferring the underside of fallen bark, rotting logs, and rocks, these preferred microhabitats are restricted to moist high elevation forests, which are more directly influenced by the coarse bioclimatic variables used in ENM reconstructions. As such, we believe that the standard bioclimatic variables have utility in this system, and other taxa with similar microhabitat specificities (e.g., Rissler & Apodaca 2007; Bond & Stockman 2008; Bond 2012; DiDomenico & Hedin 2016). In total we used 77 presence records (25% of which were used as test points), including 43 records from recent fieldwork, plus 34 unique museum records that either had GPS information associated with the specimens or could be unequivocally georeferenced based on provided locality information: 19 records from the American Museum of Natural History, nine from the Museum of Comparative Zoology, and six from the Museum of Southwestern Biology. These records were accessed through Symbiota Collections of Arthropods Network database (SCAN; http://symbiota4.acis.ufl.edu/scan/portal). All Maxent settings were left

at default values. To extract bioclimatic information for each collection locality, all 19 bioclimatic variables were added as layers to ArcMap implemented through ArcGIS Desktop v 10.3 (ESRI), and values were extracted using the "Extract Values to Points" function. We used this dataset to reduce the number of bioclimatic variables included in the final model by implementing the method of Jezkova et al. (2011) in order to identify highly correlated variables. This method generates a simplified climatic model with largely independent variables, reducing over-parameterization. This resulted in variables 10 and 11 (mean temperature of warmest and coldest quarters) and 14, 16, and 18 (precipitation of driest, wettest, and warmest quarters) being removed. The final model included 14 bioclimatic variables, in addition to altitude. Additionally, the Community Climate System Model (CCSM4) datasets were used at a downscaled resolution of 2.5 arc-minutes to model distributions during the LGM (~22,000 years ago) and mid-Holocene (~6000 years ago) using only the 14 retained bioclimatic variables.

We combined the results of six separate ENM analyses where ecological niches were estimated for eastern and western clades across the three temporal datasets. All ASCII Maxent results were opened as raster files in ArcMap where they were converted to binary presence/absence maps using a threshold as determined by the 10% minimum training logistic threshold. To identify regions of overlap, binary maps were added together using the "Raster Calculator" in the Spatial Analyst toolbox.

(3) Molecular data collection and bioinformatics

Genomic DNA was extracted individually from whole specimens, with intestines removed, using a Qiagen DNeasy Blood and Tissue Kit (Qiagen, Valencia, CA) as per manufacturer's protocol. Libraries for ddRAD-seq were prepared using a modified version of Peterson et al.*'s* (2012) protocol. The adaptors and primers used here are derived from Peterson et al. (2012), and also listed in (Table 3.1). Briefly, ~500 ng of gDNA were digested in a 50 µl reaction with 10 units of the restriction enzyme *Sbf1* (5'-CCTGCAGG) and 100 units of *Msp1* (5'- CCGG; New England Biolabs, Ipswich, MA), and 1X CutSmart Buffer (New England Biolabs). Samples were digested at 37°C for 3 hours with fragmentation verified via gel electrophoresis. Samples were purified using Agencourt AMPure XP bead cleanup (Beckman Coulter, Inc., Brea, CA) and quantified via Qubit. Adaptors were ligated to digested DNA in a 40 µl reaction that consisted of 33 µl digested DNA, 1.05 µM *MspI* P2 adaptor, 0.54 µM *SbfI* P1 adaptor (8 different adaptors, 1 per row), 400 U T4 DNA-ligase, and 1X T4 DNA ligase reaction buffer (New England Biolabs). Ligation reactions were incubated at room temperature for 40 minutes, then heat killed at 65°C for 10 minutes and cooled to room temperature at a rate of 2°C per 90 seconds. Samples with different adaptors were pooled by column and then purified using AMPure XP. Pooled samples were then size selected with a Pippen Prep automated size-selection instrument (Sage Science, Beverly, MA) at a size range of 400-600 bps. Primers with Illumina indices were added to the pooled samples using PCR; 50 µl reactions consisted of 23 µl DNA template, 2 uM PCR Primer P1, 2 uM PCR primer P2 (9 types for second-tier multipexing, 1 per pooled sample), and 1X Phusion High Fidelity

PCR Mastermix (New England Biolabs). Cycle conditions were 98°C for 30 seconds, 12 iterations of 98°C for 10 seconds and 72°C for 20 seconds (with a 16% ramp to slow cooling), and 72°C for 10 minutes. PCR products were purified via AMPure XP bead cleanup and quantified using a Bioanalyzer (Agilent Technologies, Santa Clara, CA). A pool consisting of an equimolar quantity of each library was sequenced as 100 bp SE reads on the Illumina HiSeq2500 platform at the University of California, Riverside IIGB Genomics Core Facility.

Raw read data were analyzed using the pyRAD version 3.0.5 software (Eaton 2014). This program assembles short read RAD-seq data using graph-based clustering algorithms that allow for indels and consists of seven steps: demultiplexing, quality filtering, within sample clustering, error rate and heterozygosity estimation, base calling and paralog detection, between sample clustering, and alignment across samples. Following extensive preliminary testing, the parameters used in all final analyses were as follows - maximum number of sites with quality score < 20 (NQual): 5, clustering threshold (Wclust): 0.95, minimum coverage for a cluster (Mindepth): 6, maximum individuals with a shared heterozygous site (MaxSH): 3. Multiple datasets were produced which varied in the minimum taxon coverage needed for a locus to be included (MinCov). MinCov values were 65, 48, 32, 16, and 4, although we only discuss the results of the 32 (~50% coverage) and 16 (~25% coverage) MinCov datasets (hereafter called the m32 and m16 datasets, respectively). All other parameters were kept at default values. pyRAD was run on the University of California, Riverside Institute for Integrative

Genome Biology (UCR-IIGB) Linux cluster. Unless indicated otherwise, all downstream analyses used matrices consisting of *S. robustus* samples only.

(4) Phylogenetics and divergence time estimation

Phylogenetic reconstruction and divergence dating were conducted with the BEAST version 2.2.1 package (Bouckaert et al. 2014) on concatenated matrices where assembled sequence reads were used as loci. We relied on a concatenation approach, as opposed to species tree methods, as this was required for estimating divergence times using BEAST. We suggest an alternative approach in the Discussion. PartitionFinder version 1.1.1 (Lanfear et al. 2012) was used to select the appropriate model of evolution for the entire concatenated matrix. Preliminary BEAST analyses were run aimed at testing strict versus relaxed clock models, and Yule versus coalescent tree models on the *S. robustus* concatenated dataset. These were run for 2 million generations sampling every 1000 with a 10% burn-in period. Multiple identical analyses each with four chains were conducted to confirm similarity of tree topology and posterior distributions of parameters between independent runs. These preliminary analyses produced identical topologies.

In order to provide a prior for the rate of evolution for the estimation of divergence dates with the ddRAD-seq dataset, the single samples of *S. nondimorphicus* and *S. idahoensis* were used in a separate analysis to calculate a "background *Sclerobunus* ddRAD-seq rate". The geographic disjunction between the Cascade Mountains of Oregon and Washington (*S. nondimorphicus*) and the northern Rocky

Mountains of Idaho (*S. idahoensis*) is a well-known break found in many other taxa (Brunsfeld et al. 2001; Shafer et al. 2010) and is dated at 2-5 MA, coinciding with the formation of the Columbia Plateau and subsequent rain shadow caused by the rising of the Cascade Mountains (Graham 1999). These two species are 7.6% divergent for COI (uncorrected distance, Derkarabetian et al. 2010) indicating a relatively older divergence that, coupled with estimated COI divergence rates of 3.54% per million years for arthropods (Papadopoulou et al. 2010) and 2.25% per million years for spiders (Bidegaray-Batista & Arnedo 2011), correspondingly dates to this geologic event. Although geologic evidence is not ideal for calibrating divergence analyses (Heads 2010), fossils are not known for this genus (or family). However, many studies of harvestmen taxa with similar biological characteristics (i.e., low vagility microhabitat specialists with high ecological constraints) indicate that they are ideally suited and highly informative for biogeographic studies across many time scales (e.g., Boyer et al. 2007; Boyer and Giribet 2009; Hedin et al. 2012; Schönhofer et al. 2013).

A pyRAD analysis using *S. nondimorphicus*, *S. idahoensis*, and three divergent *S. robustus* samples resulted in only 33 loci shared across the three species, and could not be used to estimate a rate across all three species directly. However, the *general characteristics* (e.g., average mutation rate, divergence) of ddRAD-seq loci across *Sclerobunus* species should be similar within *Sclerobunus* species. The level of genetic divergence for COI across *S. robustus* (~8.3%) is greater than the COI divergence between *S. nondimorphicus* and *S. idahoensis* (7.6%; Derkarabetian et al. 2011), indicating that *S. robustus* consists of deep species level divergences comparable to other

Sclerobunus species. The average rate of evolution across the *S. nondimorphicus* and *S. idahoensis* samples was calculated using a concatenated matrix of 945 RAD loci (89,008 bp) by calibrating the split as a normal distribution with mean of 3.5 and sigma value of 0.75.

Preliminary analyses using relaxed clock models failed to converge, and analyses using the coalescent model produced much older and largely unrealistic results, (e.g., the root of *S. robustus* at ~27 MA). The Yule model may be more appropriate as previous research (Derkarabetian et al. 2011) and ongoing studies with this dataset indicate that *S. robustus* is likely a cryptic species complex. Final divergence dating analyses used the strict clock, calibrated Yule, and a nucleotide substitution model chosen with PartitionFinder. Six independent analyses were run for 10 million generations each, logging every 1000 steps. All six runs were combined with LogCombiner with 10% burn-in, and the resulting clockRate parameter mean and variance were used as an a priori calibration for divergence analyses using the m32 and m16 *S. robustus* datasets. For the *S. robustus* divergence time analyses, the strict clock and Yule models were used along with the appropriate nucleotide model chosen by PartitionFinder. The clockRate prior was assigned a normal distribution (see results) matching that identified in the biogeographic calibration analysis and ran for 10 million generations, logging every 1000, with 10% burn-in. Tracer version 1.6 (Rambaut et al. 2014) was used to assess stationarity and check for ESS values above 200, and TreeAnnotator version 2 (Rambaut & Drummond 2014) was used to produce maximum clade credibility trees. The resulting topology of major clades is identical to exploratory analyses using loci shared between

ingroup samples and outgroups (*S. nondimorphicus* and *S. idahoensis*). Outgroup taxa were not included in these analyses because of very few shared loci with the ingroup (see above).

Additionally, we conducted Bayesian Skyline Plot analyses for all major lineages (Drummond et al. 2005), and constructed a lineage through time plot (LTT; Nee et al. 1992; Harvey et al. 1994) using the R package ape version 3.0-11 (Paradis et al. 2004). LTT plots were based on phylogenies including only one sample per population.

(5) Population genomic statistics and population structure

To maximize variability in the final dataset while simultaneously minimizing missing data for the calculation of population genetics statistics, all analyses used the m32 dataset. For all loci, we calculated several molecular diversity indices (gene diversity, number of differences, heterozygosity, polymorphic loci), and average F_{ST} for each collecting locality and clade with Arlequin version 3.5.2.2 (Excoffier & Lischer 2010). We conducted an AMOVA to analyze genetic structure between the six major clades. Using a single randomly sampled SNP from each variable locus (1265/1270 loci were variable), we explored population structure with a principal components analysis (PCA) using the dudi.pca and find.clusters functions in the R package adegenet (Jombart 2008; Jombart & Ahmed 2011). Additionally, to examine the correlation between genetic variation and geography, the first two principal components and geographic coordinate information for each collecting locality (Table S1) were used in a Procrustes analysis conducted in the R package vegan (Oksanen et al. 2015) assessing significance with 1000

permutations. Here, genetic variation in the form of the first two principal components is superimposed onto a geographic plot (e.g. latitude and longitude) and rotated to maximize similarity.

(6) Genetic, geographic, and environmental correlations

Geographic distance is commonly incorporated into explaining patterns of distribution and genetic differentiation in the form of isolation by distance (IBD; Wright 1943; Rousset 1997), where the degree of genetic differentiation between two populations is correlated with their geographic distance. Recently, the importance of environmental differences has been recognized, and described as isolation by environment (IBE; Wang & Summers 2010; Wang & Bradburd 2014). Many studies have shown the importance of incorporating environmental distances in some form when exploring patterns of genetic differentiation (e.g., Lee & Mitchell-Olds 2011; Wang et al. 2013; Manthey & Moyle 2015). We evaluated evidence for IBE with an environmental distance matrix created by first extracting data for each bioclimatic variable from each collecting locality (as for ENM analyses). This dataset was then subject to PCA using the dudi.pca function in the ade4 R package (Dray & Dufour 2007). The first two principal components were then used as points to calculate a pairwise distance matrix for all populations, and IBE was assessed using IBDWS (Jensen et al. 2005). Additionally, we conducted a multiple regression analysis using the MMRR script (Multiple Matrix Regression and Randomization; Wang 2013). This method allows for tests of correlation between multiple distance matrices, assessing how a dependent variable, in this case

genetic distance, responds to multiple independent variables (e.g., geographic and environmental distance), and evaluates significance through random permutations. All other correlations and regressions presented in the results were calculated using Pearson's product-moment correlation coefficient (r) in R 3.0.2 (R Core Team 2013). Any correlations using within-population statistics were based only on populations in which more than one sample was successfully sequenced (i.e., singleton populations were excluded). To assess the relationship between geographic distance and genetic distance we conducted isolation by distance (IBD) analyses using IBDWS for all major clades and groupings (i.e., all *S. robustus*, east vs. east clades, mtDNA clades). Pairwise geographic distances were calculated using the Geographic Distance Matrix Generator v.1.2.3 (Ersts, American Museum of Natural History, Center for Biodiversity and Conservation, http://biodiversityinformatics.amnh.org/open_source/gdmg) where the genetic distance matrix consisted of pairwise F_{ST} values derived from Arlequin.

(7) Migration estimation

Demographic model testing has been incorporated into phylogeographic analyses such that explicit demographic parameters can be estimated and multiple alternative phylogeographic scenarios can be modeled and formally compared (e.g., Richards et al. 2007; Carstens et al. 2013; Barrow et al. 2015). To test for the possibility of migration between distinct refugia, we used the coalescent-based program fastsimcoal2 (Excoffier et al. 2013). This program uses the site frequency spectrum derived from SNP data to estimate parameters and test observed data against expected data that is estimated through

user-defined models. We tested two simple divergence models, one without post-divergence migration and a second including post-divergence migration. These models were tested on two pairs of sister clades that are hypothesized to have persisted in separate refugia: the NW - SW clades and the CE - SE clades). We used SNP data derived from rerunning step 7 of pyRAD with only samples from the focal clades for each set of analyses included. MinCov values were set to be equal to 50% of total samples. The observed SFS files were created using a custom script (github.com/jordansatler/SNPtoAFS). For all analyses, the divergence time (Tdiv) prior was also fixed to the mean divergence recovered from m32 analyses. We ran two sets of analyses, one in which the mutation rate was estimated, and another set where the mutation rate was fixed at 8.4E -9 mutations per generation based on estimates from *Drosophila melanogaster* (Haag-Liautard et al. 2007). Migration rates were given a relatively diffuse prior with log-uniform distribution (minimum of 1E -5, maximum 1E -2). All runs used the following options: -N 100,000 (maximum number of simulations to perform), -L 40 (maximum number of loops to perform), and -M 0.001 (stopping criterion, as minimum relative difference of parameters between iterations). Each analysis was repeated 20 times, and favored models were chosen with AIC calculations.

We also estimated migration rates between these two clade pairs using the program Migrate-n (Beerli & Felsenstein 2001; Beerli 2006; Beerli & Palczewski). Sequence data were used as input, created by rerunning pyRAD as in fastsimcoal2 analyses. Base frequencies were calculated from the data, mutation rates across loci were allowed to vary, and starting values for theta (θ) and migration (M) were calculated using

F_{ST}. Based on initial testing, we chose uniform priors for θ (min. = 0, max. = 0.01, delta = 0.001) and M (min. = 0, max. = 1000, delta = 100). Each model was run for 20,000 steps at in increment of 100, with 20,000 discarded as burnin. A static heating scheme was used with four chains using temperature values of 1.0, 1.5, 3.0, and 100,000. Stationarity was assessed with ESS values and manual inspection of the posterior distributions. The number of migrants per generation (Nm) was calculated by multiplying the mutation-scaled effective immigration rate by θ, then dividing by an inheritance scalar of four for nuclear loci.

III. RESULTS

(1) Identification of potential refugia

The layered binary ENMs identified two large regions that likely supported suitable and climatically stable habitat in the mid-latitude regions: the San Juan/Tusas Mountains along the western CO/NM border, and the southeastern edge of the Mogollon Rim along the AZ/NM border (Figure 3.2). Other studies have suggested that for a given species, more central populations house the highest degree of genetic diversity, demonstrating expansion out of refugia in these "mid-latitude" regions (e.g., Hoskin et al. 2011; An et al. 2015; Peterson & Graves 2015). The combined ENMs also identify several regions of persistent habitat: the Chuska and Zuni Mountains of NM/AZ and the mountains of southwestern UT. There are no known museum records for *Sclerobunus* from these areas, and specimens were not found during recent collecting attempts in the

Zuni Mountains, AZ and the mountains of southwestern Utah. Individual ENMs for eastern and western clades and across all populations for current and LGM models are presented in Appendix C.3.

(2) Molecular data

In total, 67 samples were extracted, consisting of 65 *S. robustus* from 39 collecting localities, one *S. nondimorphicus*, and one *S. idahoensis* (Appendix C.1). On average, for the 65 *S. robustus* samples, sequencing resulted in 906,109.6 reads per sample (range: 172,984 - 1,738,861), with 828,371.1 (91.4%) reads per sample (range: 155,453 - 1,596,212) passing quality control. Only 15 loci (15 unlinked SNPs) were shared across all 65 samples of *S. robustus*. For *S. nondimorphicus* and *S. idahoensis*, 259,524 (230,004 passing QC) and 156,163 (141,440 passing QC) reads were sequenced, respectively, resulting in 945 shared loci. Matrix statistics are shown in Table 3.2 and sample sequencing statistics are shown in Appendix C.2.

(3) Phylogenetics and divergence time estimation

Final matrix statistics are presented in Table 3.2. All analyses used the HKY + I + G substitution model chosen for the entire concatenated matrix of 1270 loci by PartitionFinder. BEAST produced highly supported, nearly identical phylogenies for each dataset of varying coverage. In the m32 and m16 phylogenies, support increased as the number of loci increased. Across these datasets, phylogenies were largely identical (Figure 3.3 and Appendix C.4), recovering the major mtDNA clades obtained in

Derkarabetian et al. (2011): northwest (NW), southwest (SW), central eastern (CE), southeastern (SE), and northeastern (NE). The mitochondrial clade (Haviland: HAV) is monophyletic with high support in the m16 phylogeny, while in the m32 phylogeny it is paraphyletic with respect to the NE clade. Relationships among major clades and within-clade assignments recovered with the nuclear data presented here are identical to the clades recovered in Derkarabetian et al. (2011) using COI, with the exception of the placement and monophyly of HAV in the m32 analysis.

Calibrated BEAST analyses using concatenated loci for *S. nondimorphicus* and *S. idahoensis* resulted in a mean clockRate value of 1.83323E -3 substitutions per site per million years (95% HPD interval 1.0418E -3, 2.8222E -3). Preliminary testing resulted in small (but significantly different from 0) ucld.stdev values (m32: mean 0.314, HPD 0.246-0.388), indicating that the data are evolving in almost clock-like pattern, and rate variation across lineages is minor. More importantly, mean divergence time and HPD estimates with strict and relaxed clock models were virtually identical.

Divergence time estimates within *S. robustus* using this value as a rate calibration (normal distribution with mean 1.83323E -3 and sigma 0.0004) are shown in Figure 3.3 and Table 3.3. In general, node ages increase with increasing number of loci. Mean ages for the root of *S. robustus* increased from 3.89 MA (95% HPD: 2.47 - 5.73 MA) in the m32 dataset to 4.27 MA (2.71 - 6.24 MA) in the m16 dataset. In the m32, the most recent mean divergence *between* any two major clades occurred at 2.72 MA (1.73 - 4.02 MA) for CE+SE clades, while in the m16, this divergence time increased to 2.98 MA (1.91 - 4.39 MA). If, in the m32 analysis, NE and HAV are considered separate clades, the

earliest between-clade divergence is 2.52 MA (1.57 - 3.69 MA). The mean age of divergence *within* the most recently differentiated clade (SW) is 1.44 MA (0.9 - 2.13 MA) in the m32, which increased to 1.58 MA (0.98 - 2.29 MA) in the m16.

Associated with an expansion out of refugia, it is expected that there would be increases in both the size of populations and number of lineages post-expansion. Across all *S. robustus*, Bayesian skyline plots show two major increases in population size, one at the Pleistocene-Pliocene boundary ~2.5 MA, and another ~1.0 MA (Figure 3.3 inset). Similarly, skyline plots for all major clades, except NE+HAV, show an increase in population size with a major increase ~1.0 MA (Figure 3.4.). Here, the expectation of population size increase is recovered where increases are seen following isolation in separate Pliocene refugia and during Pleistocene glacial cycles. While the LTT plot (Figure 3.3 inset) does shows slight increases in lineage numbers corresponding to these increases in population size, particularly at ~1.0 MA, these increases do not significantly deviate from the null expectation of a constant rate of lineage diversification (Figure 3.4).

(4) Genetic, geographic, and environmental correlations

Molecular diversity indices and pairwise F_{ST} estimates for each clade are presented in Tables 3.4 and 3.5. The first two principal components from PCA analyses of 1265 SNPs (Figure 3.5, Appendix C.4) show three major groups corresponding to three main clades recovered in phylogenetic analyses: western (NW+SW), CE+SE, and NE+HAV. BIC analyses using the find.clusters function retaining the first 65 components favored six clusters, which corresponded to the mtDNA clades of previous work. In the

m32 analysis (Figure 3.5), the NW and SW clades are distinct, while in the m16 analysis (Appendix C.4) the HAV samples are separate from the NE samples. Procrustes analyses on both the m32 (Figure 3.6) and m16 (Appendix C.4) recovered significant similarity scores (>0.77, p-values = 0.001) between a population's location in SNP principal component space and their geographic location. The mean pairwise geographic distance of populations in each clade (i.e., overall size of distribution of a clade) and the mean pairwise F_{ST} of those clades shows a strong and significant negative correlation (Figure 3.7A), indicating that the clades with the smallest geographic distributions are the most genetically differentiated. The AMOVA testing genetic structure of the six clades indicated that differences among these clades accounted for the majority of variation (55.9%; Table 3.6).

Results of all IBD and IBE, including MMRR, analyses are shown in Table 3.7. IBD analyses recovered small but significant correlations across all *S. robustus*, and within the western, CE+SE, NE+HAV, and NE clades. IBE correlations were significant for most clades, the exceptions being CE+SE clades and the individual NE and HAV clades. MMRR analyses showed that environmental distance is a significant independent predictor of genetic distance across all *S. robustus* and within the SW and eastern clades, while both environment and geography were significant and contributed nearly equally in the western clade. Within the eastern clade, geographic distances are the significant predictor of genetic distances for the CE+SE, NE+HAV, and NE clades. The correlation between geographic distance and environmental distance was small and not significant (r = 0.1097, p = 0.061, 1000 permutations). PCA of bioclimatic variables used in

constructing the environmental distance matrix largely differentiated the northern (NW, NE, HAV, CE) and the southern populations (SW, SE) along PCA 1 (Figure 3.8), mirroring the latitudinal break seen in the distribution of these clades. The northern-most southern population (population 10 SW clade, Figure 3.1) and the southern-most northern population (population 13 CE clade, Figure 3.1) are in close proximity in the PCA (Figure 3.8), reflecting their similar latitudes. Here, it is important to note that the mountainous regions of New Mexico in between the northern and southern *S. robustus* clades (i.e. southern Sangre de Cristo Mountains, Mt. Taylor, Sandia Mountains, Manzano Mountains) are exclusively inhabited by several other *Sclerobunus* species (Figure 3.1; Derkarabetian & Hedin 2014).

Across all *S. robustus* populations, there is a latitude-genetic component showing a strong and significant negative latitudinal correlation with genetic diversity (Figure 3.7B). However, the only clades to show a significant correlation between latitude and genetic diversity are the eastern ($r = -0.9191$, $p < 0.0001$), the SE ($r = -0.9849$, $p = 0.0151$), and the SW ($r = -0.9449$, $p = 0.0045$) clades. Within the eastern clade, the three CE+SE populations largely drive this correlation, and although the NE clade shows a negative correlation, it is not significant ($r = -0.2878$, $p = 0.3643$). Within the NE+HAV clade, as latitude increases the divergence time of a population from its nearest relative decreases additionally suggesting a pattern of northward expansion (Figure 3.9). Conversely, for the SW clade, no significant correlation exists between divergence time of a population from nearest relative and latitude ($r = 0.3845$, $p = 0.347$). Correlations between genetic differentiation and latitude have been found in numerous studies (Sexton

et al. 2014), many of which either directly imply or explore this pattern in regards to post-glacial range expansion (e.g., Gomez et al. 2005; Vandewoestijne & Van Dyck 2010; Jezkova et al. 2015), where the expanding frontline populations show reduced genetic diversity relative to the stable ancestral populations (Hewitt 2000; Hewitt 2004).

(5) Migration estimation

For both clade pairs, fastsimcoal2 analyses using a fixed mutation rate favored the model that incorporated post-divergence migration between refugial clades (Figure 3.10A), with extremely low migration estimates. Conversely, fastsimcoal2 analyses that do not use a fixed mutation rate favored the model without post-divergence migration for the NW-SW pair only (Figure 3.10B). Migrate-n analyses show some degree of migration between clade pairs (Table 3.8). A potentially confounding factor for these coalescent model-based analyses in this taxon may be the high levels of population structure within clades, which may lead to erroneous inferences of population parameters (e.g., Chikhi et al. 2010; Heller et al. 2013). In this case, fastsimcoal2 may be inferring the presence of migration to account for the relatively high levels of variation seen within each clade. We interpret the actual estimates of migration from these analyses with caution, given the ultimate uncertainty in generation times and mutation rates. For these analyses, we assumed a generation time of one year. Generation and developmental times for *Sclerobunus* have not explicitly been examined, but available evidence from other related harvestmen suggest the adult stage can be reached in one year (Gnaspini 2007), although *S. robustus* is known to overwinter as adults (Cokendolpher et al. 1993).

IV. DISCUSSION

(1) Evidence for multiple refugia

The integration of ENMs and genetic data can be used to corroborate the presence of refugia, and can also reveal cases where multiple distinct refugia are identified, for example, as have been found recently in other arachnid taxa (Bidegaray-Batista et al. 2016; Wachter et al. 2016). Previously, Derkarabetian et al. (2011) suggested the presence of refugia in the mountains of the southern CO and northern NM border region. Our analyses suggest the presence of two large refugial regions for *S. robustus*: one in the San Juan Mountains near the western portion of the CO/NM border, and a second at the southeastern edge of the Mogollon Rim in southern AZ/NM. Additionally, it is clear that the remaining mountain ranges in CO were unlikely to serve as refugia, suggesting northward expansion of the NE clade. The nuclear data presented here corroborates the expansion of *S. robustus* out of multiple Pliocene refugia occurring in these mid-latitude highlands. The San Juan Mountains harbor a high amount of genetic diversity with representatives from 4/6 clades within ~150 km of each other. A recent study focusing on dispersal-limited mite harvestmen of Australia's wet tropics found similar patterns, where higher present day taxonomic diversity was statistically correlated with hypothesized climatically stable refugia (Boyer et al. 2016). Additionally, the three clades with the highest amount of internal genetic differentiation (HAV, CE, NW; Figure 3.7A) are found almost entirely within the San Juan Mountains. Additional support for this

hypothesis can be seen in the genetic patterns of the NE clade. The NE clade shows a strong phylogenetic pattern of northward expansion out of the San Juan refugium where divergence times of sister populations decrease with increasing latitude (Figure 3.9), with a corresponding negative (but not significant) correlation of latitude and genetic diversity. The previous COI analyses also showed a similar northward phylogenetic pattern for the NE clade, with lack of genealogical exclusivity only in some of the northern-most populations.

Southwestern *Sclerobunus* species are diverse within the mid-latitude highlands, specifically the southern Sangre de Cristo Mountains, which run parallel and are similar in latitude to the San Juan Mountains. In the Sangre de Cristo Mountains three other *Sclerobunus* species can be found (Derkarabetian & Hedin 2014). Similar spatial patterns in species diversity are seen in montane mammals where the northern sky islands of New Mexico hold a higher number of species relative to southern sky islands (Lomolino et al. 1989; Frey et al. 2007). In a study by Lomolino et al. (1989) examining 27 sky islands across the SRMIP, the Mogollon Mountains were recorded as having the highest number of species, while the other southern sky islands had a much lower species richness, adding support to the evidence found here that the Mogollon Mountains might have served as a southern refugium for montane restricted taxa.

Population genetic data for the southern clades (SW and SE) similarly suggest northward expansion, thus supporting the second Pliocene refugia identified at the eastern edge of the Mogollon Rim. Both SW and SE clades show a significant negative correlation between genetic diversity and latitude, although no clear phylogenetic pattern

of directionality is seen in either. However for the SW clade, genetic data show expansion out of a refugium that is further south than indicated by the ENMs. Early-Pleistocene expansion resulted in widespread but contiguous clades showing a typical pattern of decreasing genetic diversity with increasing latitude (much like that seen currently in the NE clade). Following this northward expansion, there was effectively simultaneous isolation of sky island populations that still retains a genetic footprint of northward expansion. Both LGM and mid-Holocene models predict some degree of connectivity between these populations (Appendix C.3), although the downscaled datasets may not have the resolution to pick up more fine scale corridors.

A potential weakness of using an ENM approach for identifying persistent regions as refugia in *S. robustus* is that all areas currently inhabited by *S. robustus* should be identified as persistent considering that, when divergence times are incorporated, all populations were likely present in their current distribution prior to the mid-Holocene and LGM. However, we argue that the use of downscaled LGM and Holocene data decreases sensitivity as downscaled data will not capture the smaller restricted patches of habitat that *S. robustus* likely persisted in during unfavorable conditions (e.g., within canyons and ravines), and will only capture larger persistent regions. These larger regions are more likely to have served as refugia during the warmer Pliocene, for which bioclimatic data do not exist.

Taken together, analyses from our study indicate the presence of two large refugia in the SRMIP: the San Juan Mountains near the western CO/NM border and the eastern end of the Mogollon Rim. Model-based analyses indicate the presence of some potential

migration between sister clades after initial separation in these distinct refugia. ENM predictions for the LGM indicate climatic conditions that likely supported connective habitat between these refugia, particularly for the eastern clades, while these refugia remain largely separate in current and mid-Holocene reconstructions (Appendix C.3). To our knowledge, no other studies specifically indicate presence of montane Pliocene refugia in either of these two regions. Phylogeographic studies identifying refugia in the southwest typically focused on relatively young taxa with any refugia dating to the Pleistocene (e.g., Mitten et al. 2000; Knowles et al. 2007; DeChaine & Martin 2005b). It is important to note, that while mean divergence dates between clades occur in the Pliocene, there is still some degree of uncertainty as the HPD values partially extend into the early Pleistocene. However, the divergence times recovered using ddRAD-seq data in this study are younger than, but still largely consistent with, previous work in *Sclerobunus* using traditional molecular markers (Derkarabetian et al. 2010; Derkarabetian et al. 2011). Additional phylogeographic studies of other codistributed montane taxa of similar age will be needed to corroborate the presence of these Pliocene refugia and whether they have shaped diversification patterns across taxa (e.g., Satler et al. 2016).

(2) Spatiotemporal patterns in *Sclerobunus robustus*

The initial separation of *S. robustus* into eastern and western lineages occurred ~3.89 MA (2.47 - 5.73 MA). As noted in Derkarabetian et al. (2011), the distributions and break between eastern and western clades largely coincides with that seen in the

tassel-eared squirrel *Sciurus aberti* found in mixed-conifer forests of the SRMIP (Lamb et al. 1997). Additionally, although currently restricted to the northern portion of the SRMIP, the montane grasshopper *Melanoplus marshalli* also shows a split into eastern and western clades (Knowles et al. 2007). Based on divergence dates and Bayesian skyline plots, two episodes of population expansion occurred within *S. robustus*. First, an expansion coinciding with the initial divergence of eastern and western lineages into subclades that occurred near the Pliocene-Pleistocene boundary 2.5 - 2.8 MA. The warmer climate during the Pliocene likely played a role in separating the widespread and contiguous *S. robustus* into multiple units restricted to individual refugia separated by dispersal barriers. Second, following isolation during warmer climate, each individual clade then expanded ~1.0 MA during the cooler climate of the late Pleistocene, where glacial cycles contributed to population-level divergence (e.g., Knowles 2001; DeChaine & Martin 2005b). In addition, niche models for the LGM suggest that the majority of the sampled populations and clades, particularly those in the southern sky islands, remained distinct despite availability of suitable connective habitat.

Despite uncertainty and regardless of the dataset used, the divergence dates *between* major clades within *S. robustus* are conservatively estimated to occur in the late Pliocene to early Pleistocene, indicating this species is relatively old. Conversely, divergences *within* major clades fall within the late Pleistocene suggesting a role of the glacial cycles in differentiation among populations within major lineages. Although divergence dates estimated here are younger than previous studies that used multiple calibration points and a multilocus dataset (Derkarabetian et al. 2010) or a COI-only

dataset (Derkarabetian et al. 2011), the general conclusions of pre-Pleistocene divergences between clades and Pleistocene divergences within clades are consistent across studies. Within the SW clade distributed throughout the Madrean sky islands, divergence dates between populations in the m32 analysis ranged from 750 KA - 1.4 MA. These dates largely coincide with other arthropod studies in this region. For example, the spider *Habronattus pugilis* (Masta 2000) and beetle *Moneilema appresum* (Smith & Farrell 2005), both restricted to higher elevation habitats in the Madrean sky islands, are relatively young species with population divergences occurring between 300 KA - 1.7 MA. Similarly, other studies have suggested much more recent, but still largely pre-LGM, divergence estimates of <100 KA for the beetle *Scaphinotus petersi* (Ober et al. 2011; Mitchell & Ober 2013).

ENMs show suitable habitat throughout the mountainous regions of southwestern UT. *Sclerobunus* are not known from these mountains, and recent collecting attempts were unsuccessful. In this case, the Colorado River likely acted as a barrier to westward dispersal for the western clades with its formation beginning 6 MA (Lucchitta 1989; McMillan et al. 2006). Additionally, current bioclimatic conditions indicate many unsampled sky islands with suitable habitat, several of which are known to have locally derived cave populations of *S. robustus* (Welbourn 1999), suggesting the past, and potentially present, suitability of habitat on these mountains. It is uncertain how far south the southern clades expanded; *S. robustus* are not known from Mexico, although ENMs do indicate suitable habitat in the northern Sierra Madre Occidental.

(3) Patterns of genetic differentiation

Across *S. robustus* clades, there is a pattern of decreasing genetic differentiation as overall range size increases (Figure 3.7A), where the most geographically restricted HAV and CE clades show the highest levels of internal genetic divergence. The distribution of the HAV clade is highly restricted showing the smallest distribution (mean pairwise distance of ~79 km) yet shows the highest levels of genetic differentiation with a mean pairwise F_{ST} of 0.96, the highest average number of differences, and the highest levels of gene diversity (Table 3.4). Conversely, the SW clade is the most widespread clade (~210 mean km pairwise distance) and shows a comparatively lower F_{ST} of 0.73. A similar case is seen in the harvestmen genus *Cryptomaster*, where the relatively widespread *C. leviathan* shows little intraspecific genetic divergence across multiple mountain ranges, while the much more geographically restricted sister species *C. behemoth* shows higher population genetic structure (Starrett et al. 2016). The limited distributions seen in *S. robustus* clades are typical of short-range endemic taxa (Harvey 2002; Harvey et al. 2011) with limited dispersal capabilities and distributions in discontinuous habitats, which can lead to extreme levels of population structure (e.g., Keith and Hedin 2012; Hedin et al. 2015). Many species of *Sclerobunus*, and many harvestmen in general, can be considered short-range endemics (e.g., Ubick & Briggs 1992; Ubick & Briggs 2008; Boyer & Giribet 2009; Richart & Hedin 2013; Derkarabetian & Hedin 2014; DiDomenico & Hedin 2016; Emata & Hedin 2016; Starrett et al. 2016). The negative correlation of range size and genetic differentiation is clear in

S. *robustus*, however, it will be interesting to explore this pattern in other short-range endemics.

In a recent meta-analysis, Sexton et al. (2014) found that the majority of studies implicate IBE as a significant factor in genetic differentiation either alone or in combination with IBD. Here, we show that IBD and IBE both play a role in shaping genetic patterns, although in different clades of *S. robustus*. Across all populations, geographic and environmental distances both contribute to genetic differentiation of *S. robustus*, although multiple regression analyses indicate that environmental distance is a better predictor of genetic differentiation (Table 3.7). However, within the major clades, the relative importance of these variables seems to depend on the landscape connectivity. The eastern subclades (CE+SE and NE+HAV) suggest geographic distance as a stronger determinant of genetic patterns, particularly evident in the NE+HAV clade where populations are less genetically differentiated and found in highly contiguous habitat. Conversely, in the western clade, environmental distance plays a more important role in shaping genetic differentiation where the vast majority of populations are found on isolated sky islands separated by uninhabitable low-lying desert and scrub-grassland. Several studies have shown a similar situation where patterns of genetic differentiation are dependent on the continuity of habitat (e.g., Keyghobadi et al. 2005; Alberto et al. 2010; D'Aloia et al. 2014). These findings highlight the importance of examining the full distribution of a species when exploring the effects of geography and environment on the genetic differentiation of a species.

The contrasting genetic patterns seen between the SW and NE clades show two different temporal snapshots of the continuous changes in distribution and elevation undergone by montane-restricted taxa as a result of the interplay of climatic changes (Hewitt 2000, 2004) and niche conservatism (Wiens 2004; Wiens & Graham 2005). While both clades are nearly the same age, the genetic patterns and connectivity of the contemporary NE clade may be reminiscent of a former more contiguously distributed SW clade when climate favored more widespread and lower elevation forests. This formerly widespread and continuous SW clade would likely have shown significant IBD, much like the current NE clade. However, the importance of IBD becomes insignificant after populations become isolated on sky islands and local environmental conditions become more variable across the clade, thus resulting in IBE. As our study sampled few specimens per population relative the number of loci, the inclusion of more individuals per population would allow more fine-scaled analyses of gene flow and migration in these clades using model-based methods (Knowles & Carstens 2007).

(4) Divergence dating with ddRAD-seq data

Despite the increasing popularity of ddRAD-seq and similar methods, there are very few studies using these data to estimate divergence times (Stervander et al. 2015; see also Gottscho 2015). In order to calculate divergence times we made the assumption that the estimated mutation rate between *S. idahoensis* and *S. nondimorphicus* based on a biogeographic calibration is equivalent to the mutation rate of *S. robustus*. Very few loci were shared between the interspecific *Sclerobunus* taxa and *S. robustus*, therefore the loci

from the two interspecific samples from which the mutation rate was based on may be intrinsically different (divergence levels, mutation rate) from the loci of the 65 intraspecific *S. robustus* samples. The divergence levels between the interspecific *Sclerobunus* are comparable to divergences levels within *S. robustus*, assuaging this discrepancy. A potential shortcoming in our method is our choice of concatenation of ddRAD-seq loci. Specifically, those loci that are added when producing an m16 dataset are likely be more divergent than those loci that are only found in the m48 dataset, since fewer individuals will have the "m16 loci" due to allelic dropout. We recover an interesting pattern where estimated divergence dates increased when the minimum taxon coverage value decreased (Table 3.3). When increasing the threshold for missing data (e.g., from m48 to m16), more divergent loci are included in the dataset. As demonstrated for ddRAD-seq in Arnold et al. (2013), more divergent loci that are sampled less will tend to show deeper divergence times, and therefore increase node depths across the phylogeny. Partitioning loci in such a way to account for variation in divergence level may reduce uncertainty in divergence dates across datasets. For example, loci could be partitioned according to which MinCov value adds them to the dataset (a partition of m32-only loci, a partition of the subset of only m48 loci, etc.). Despite these cautions, we reiterate the similarity of divergence dating estimates from ddRAD-seq loci with previous estimates using more traditional markers (Derkarabetian et al. 2010; Derkarabetian et al. 2011), all of which recover largely Pliocene divergences among major clades.

V. REFERENCES

Alberto F, Raimondi PT, Reed DC, Coelho NC, Leblois R, Whitmer A, Serrão EA (2010) Habitat continuity and geographic distance predict population genetic differentiation in giant kelp. *Ecology*, **91**, 49-56.

An B, Zhang L, Liu N, Wang Y (2015) Refugia Persistence of Qinghai-Tibetan Plateau by the Cold-Tolerant Bird *Tetraogallus tibetanus* (Galliformes: Phasianidae). *PloS ONE*, **10**, e0121118.

Arnold B, Corbett-Detig RB, Hartl D, Bomblies K (2013) RADseq underestimates diversity and introduces genealogical biases due to nonrandom haplotype sampling. *Molecular Ecology*, **22**, 3179-3190.

Avise JC, Arnold J, Ball RM, Bermingham E, Lamb, T, Neigel JE, Reeb CA, Saunders NC (1987) Intraspecific phylogeography: the mitochondrial DNA bridge between population genetics and systematics. *Annual Review of Ecology and Systematics*, 18, 489-522.

Avise JC (2009) Phylogeography: retrospect and prospect. *Journal of Biogeography*, **36**, 3-15.

Banks N (1893) The Phalangida Mecostethi of the United States. *Transactions of the American Entomological Society*, **20**, 149-152.

Barber PH (1999) Phylogeography of the canyon treefrog, *Hyla arenicolor* (Cope) based on mitochondrial DNA sequence data. *Molecular Ecology*, **8**, 547-562.

Barrow LN, Bigelow AT, Phillips CA, Lemmon EM (2015) Phylogeographic inference using Bayesian model comparison across a fragmented chorus frog species complex. *Molecular Ecology*, **24**, 4739-4758.

Beerli P (2006) Comparison of Bayesian and maximum-likelihood inference of population genetic parameters. *Bioinformatics*, **22**, 341-345.

Beerli P, Felsenstein J (2001) Maximum likelihood estimation of a migration matrix and effective population sizes in n subpopulations by using a coalescent approach. *Proceedings of the National Academy of Sciences*, **98**, 4563-4568.

Beerli P, Palczewski M (2010) Unified framework to evaluate panmixia and migration direction among multiple sampling locations. *Genetics*, **185**, 313-326.

Bidegaray-Batista L, Arnedo MA (2011) Gone with the plate: the opening of the Western Mediterranean basin drove the diversification of ground-dweller spiders. *BMC Evolutionary Biology*, **11**, 317.

Bidegaray-Batista L, Sánchez-Garcia A, Santulli G, Maiorano L, Guisan A, Vogler AP, Arnedo MA (2016) Imprints of multiple glacial refugia in the Pyrenees revealed by phylogeography and paleodistribution modelling of an endemic spider. *Molecular Ecology*, **25**, 2046-2064.

Bond JE (2012) Phylogenetic treatment and taxonomic revision of the trapdoor spider genus *Aptostichus* Simon (Araneae, Mygalomorphae, Euctenizidae). ZooKeys, **252**, 1–209.

Bond JE, Stockman AK (2008) An integrative method for delimiting cohesion species: finding the population-species interface in a group of Californian trapdoor spiders with extreme genetic divergence and geographic structuring. *Systematic Biology*, **57**, 628-646.

Bouckaert R, Heled J, Kühnert D, Vaughan T, Wu CH, Xie D, Suchard MA, Rambaut A, Drummond AJ (2014) BEAST 2: a software platform for Bayesian evolutionary analysis. *PLoS Computational Biology*, **10**, e1003537.

Boyer SL, Clouse RM, Benavides LR, Sharma P, Schwendinger PJ, Karunarathna I, Giribet G (2007) Biogeography of the world: a case study from cyphophthalmid Opiliones, a globally distributed group of arachnids. *Journal of Biogeography*, **34**, 2070-2085.

Boyer SL, Giribet G (2009) Welcome back New Zealand: regional biogeography and Gondwanan origin of three endemic genera of mite harvestmen (Arachnida, Opiliones, Cyphophthalmi). *Journal of Biogeography*, **36,** 1084-1099.

Boyer SL, Markle TM, Baker CM, Luxbacher AM, Kozak KH (2016) Historical refugia have shaped biogeographical patterns of species richness and phylogenetic diversity in mite harvestmen (Arachnida, Opiliones, Cyphophthalmi) endemic to the Australian Wet Tropics. *Journal of Biogeography*, DOI: 10.1111/jbi.12717.

Briggs T (1971) The harvestmen of the family Triaenonychidae in North America. *Occasional Papers of the California Academy of Sciences*, **90**, 1-43.

Brunsfeld SJ, Sullivan J, Soltis DE, Soltis PS (2001) Comparative phylogeography of northwestern North America: a synthesis. *Special Publication-British Ecological Society*, **14**, 319-340.

Bryson RW, Riddle BR, Graham MR, Smith BT, Prendini L (2013) As old as the hills: montane scorpions in southwestern North America reveal ancient associations between biotic diversification and landscape history. *PLoS ONE*, **8**, e52822.

Carnaval AC, Hickerson MJ, Haddad CF, Rodrigues MT, Moritz C (2009) Stability predicts genetic diversity in the Brazilian Atlantic forest hotspot. *Science*, **323**, 785-789.

Carstens BC, Richards CL (2007) Integrating coalescent and ecological niche modeling in comparative phylogeography. *Evolution*, **61**, 1439-1454.

Carstens BC, Brennan RS, Chua V, Duffie CV, Harvey MG, Koch RA, McMahan CD, Nelson BJ, Newman CE, Satler JD, Seeholzer G, Posbic K, Tank DC, Sullivan J (2013) Model selection as a tool for phylogeographic inference: an example from the willow *Salix melanopsis*. *Molecular Ecology*, **22**, 4014-4028.

Chan LM, Brown JL, Yoder AD (2011) Integrating statistical genetic and geospatial methods brings new power to phylogeography. *Molecular Phylogenetics and Evolution*, **59**, 523-537.

Chikhi L, Sousa VC, Luisi P, Goossens B, Beaumont MA (2010) The confounding effects of population structure, genetic diversity and the sampling scheme on the detection and quantification of population size changes. *Genetics*, **186**, 983-995.

Cokendolpher JC, MacKay WP, Muma MH (1993) Seasonal population phenology and habitat preferences of montane harvestmen (Arachnida: Opiliones) from Southwestern New Mexico. *The Southwestern Naturalist*, **38**, 236-240.

D'Aloia CC, Bogdanowicz SM, Harrison RG, Buston PM (2014) Seascape continuity plays an important role in determining patterns of spatial genetic structure in a coral reef fish. *Molecular ecology*, **23**, 2902-2913.

DeChaine EG, Martin AP (2005a) Marked genetic divergence among sky island populations of *Sedum lanceolatum* (Crassulaceae) in the Rocky Mountains. *American Journal of Botany*, **92**, 477-486.

DeChaine EG, Martin AP (2005b) Historical biogeography of two alpine butterflies in the Rocky Mountains: broad-scale concordance and local-scale discordance. *Journal of Biogeography*, **32**, 1943-1956.

Derkarabetian S, Steinmann DB, Hedin M (2010) Repeated and time-correlated morphological convergence in cave-dwelling harvestmen (Opiliones, Laniatores) from montane western North America. *PLoS ONE*, ***5***, e10388.

Derkarabetian S, Ledford J, Hedin M (2011) Genetic diversification without obvious genitalic morphological divergence in harvestmen (Opiliones, Laniatores, *Sclerobunus robustus*) from montane sky islands of western North America. *Molecular Phylogenetics and Evolution*, **61**, 844-853.

Derkarabetian S, Hedin M (2014) Integrative taxonomy and species delimitation in harvestmen: A revision of the western North American genus *Sclerobunus* (Opiliones: Laniatores: Travunioidea). *PLoS ONE*, **9**, e112001.

Devitt TJ, Devitt SEC, Hollingsworth BD, McGuire JA, Moritz C (2013) Montane refugia predict population genetic structure in the Large-blotched Ensatina salamander. *Molecular Ecology*, **22**, 1650-1665.

DiDomenico A, Hedin M (2016) New species in the *Sitalcina sura* species group (Opiliones, Laniatores, Phalangodidae), with evidence for a biogeographic link between California desert and Arizona sky islands. *ZooKeys*, **586**, 1-36.

Downie DA (2004) Phylogeography in a galling insect, grape phylloxera, *Daktulosphaira vitifoliae* (Phylloxeridae) in the fragmented habitat of the Southwest USA. *Journal of Biogeography*, **31**, 1759-1768.

Dray S, Dufour AB (2007) The ade4 package: implementing the duality diagram for ecologists. *Journal of statistical software*, **22**, 1-20.

Drummond AJ, Rambaut A, Shapiro B, Pybus OG (2005) Bayesian coalescent inference of past population dynamics from molecular sequences. *Molecular Biology and Evolution*, **22**, 1185-1192.

Eaton DA (2014) PyRAD: assembly of de novo RADseq loci for phylogenetic analyses. *Bioinformatics* **30**, 1844-1849.

Edwards SV, Shultz AJ, Campbell-Staton SC (2015) Next-generation sequencing and the expanding domain of phylogeography. *Folia Zoologica*, **64**, 187-206.

Emata KN, Hedin M (2016) From the mountains to the coast and back again: Ancient biogeography in a radiation of short-range endemic harvestmen from California. *Molecular Phylogenetics and Evolution*, **98**, 233-243.

Excoffier L, Lischer HE (2010) Arlequin suite ver 3.5: a new series of programs to perform population genetics analyses under Linux and Windows. *Molecular Ecology Resources*, **10**, 564-567.

Excoffier L, Dupanloup I, Huerta-Sánchez E, Sousa VC, Foll M (2013) Robust demographic inference from genomic and SNP data. *PLoS Genetics*, **9**, e1003905.

Frey JK, Bogan MA, Yates TL (2007) Mountaintop island age determines species richness of boreal mammals in the American Southwest. *Ecography*, **30**, 231-240.

Garrick RC, Bonatelli IA, Hyseni C, Morales A, Pelletier TA, Perez MF, Rice E, Satler JD, Symula RE, Thomé MTC, Carstens BC (2015) The evolution of phylogeographic data sets. *Molecular Ecology*, **24**, 1164-1171.

Gnaspini P (2007) Development. Pp. 455-472, In: *Harvestmen: The Biology of Opiliones* (eds. Pinto-da-Rocha R, Machado G, Giribet G). Harvard University Press, Cambridge, Massachusetts and London, England.

Gómez A, Vendramin GG, González-Martínez SC, Alía R (2005) Genetic diversity and differentiation of two Mediterranean pines (*Pinus halepensis* Mill. and *Pinus pinaster* Ait.) along a latitudinal cline using chloroplast microsatellite markers. *Diversity and Distributions*, **11**, 257-263.

Gottscho, AD (2015) Lineage diversification of lizards (Phrynosomatidae) in southwestern North America: integrating genomics and geology. Doctoral dissertation, University of California, Riverside.

Giribet G, Vogt L, Gonzalez AP, Sharma P, Kury AB (2010) A multilocus approach to harvestman (Arachnida: Opiliones) phylogeny with emphasis on biogeography and the systematics of Laniatores. *Cladistics*, **26**, 408-437.

Graham A (1999) *Late Cretaceous and Cenozoic history of North American vegetation, north of Mexico*. Oxford University Press, New York.

Graham CH, VanDerWal J, Phillips SJ, Moritz C, Williams SE (2010) Dynamic refugia and species persistence: tracking spatial shifts in habitat through time. *Ecography*, **33**, 1062-1069.

Haag-Liautard C, Dorris M, Maside X, Macaskill S, Halligan DL, Charlesworth B, Keightley PD (2007) Direct estimation of per nucleotide and genomic deleterious mutation rates in *Drosophila*. *Nature*, **445**, 82-85.

Harvey PH, May RM, Nee S (1994) Phylogenies without fossils. *Evolution*, **48**, 523-529.

Harvey MS (2002) Short-range endemism amongst the Australian fauna: some examples from non-marine environments. *Invertebrate Systematics*, **16**, 555-570.

Harvey MS, Rix MG, Framenau VW, Hamilton ZR, Johnson MS, Teale RJ, Humphreys G, Humphreys WF (2011) Protecting the innocent: studying short-range endemic taxa enhances conservation outcomes. *Invertebrate Systematics*, **25**, 1-10.

Heads M (2010) Old taxa on young islands: a critique of the use of island age to date island-endemic clades and calibrate phylogenies. *Systematic Biology*, **60**, 24-218.

Hedin M, Tsurusaki N, Macías-Ordóñez R, Shultz JW (2012) Molecular systematics of sclerosomatid harvestmen (Opiliones, Phalangioidea, Sclerosomatidae): geography is better than taxonomy in predicting phylogeny. *Molecular Phylogenetics and Evolution*, **62**, 224-236.

Hedin M, Carlson D, Coyle F (2015) Sky island diversification meets the multispecies coalescent-divergence in the spruce-fir moss spider (*Microhexura montivaga*, Araneae, Mygalomorphae) on the highest peaks of southern Appalachia. *Molecular Ecology*, **24**, 3467-3484.

Heller R, Chikhi L, Siegismund HR (2013) The confounding effect of population structure on Bayesian skyline plot inferences of demographic history. *PLoS One*, **8**, e62992.

Hendrixson BE, Guice AV, Bond JE (2015) Integrative species delimitation and conservation of tarantulas (Araneae, Mygalomorphae, Theraphosidae) from a North American biodiversity hotspot. *Insect Conservation and Diversity*, **8**, 120-131.

Hewitt G (2000) The genetic legacy of the Quaternary ice ages. *Nature*, **405**, 907-913.

Hewitt GM (2004) Genetic consequences of climatic oscillations in the Quaternary. *Philosophical Transactions of the Royal Society of London B: Biological Sciences*, **359**, 183-195.

Hickerson MJ, Carstens BC, Cavender-Bares J, Crandall KA, Graham CH, Johnson JB, Rissler L, Victoriano PF, Yoder AD (2010) Phylogeography's past, present, and future: 10 years after. *Molecular Phylogenetics and Evolution*, **54**, 291-301.

Hijmans RJ, Cameron SE, Parra JL, Jones PG, Jarvis A 2005 Very high resolution interpolated climate surfaces for global land areas. *International Journal of Climatology*, **25**, 1965-1978.

Hoskin CJ, Tonione M, Higgie M, MacKenzie JB, Williams SE, VanDerWal J, Moritz C (2011) Persistence in peripheral refugia promotes phenotypic divergence and speciation in a rainforest frog. *The American Naturalist*, **178**, 561-578.

Hugall A, Moritz C, Moussalli A, Stanisic J (2002) Reconciling paleodistribution models and comparative phylogeography in the Wet Tropics rainforest land snail *Gnarosophia bellendenkerensis* (Brazier 1875). *Proceedings of the National Academy of Sciences*, **99**, 6112-6117.

Jensen JL, Bohonak AJ, Kelley ST (2005) Isolation by distance, web service. *BMC Genetics*, **6**, 13.

Jezkova T, Olah-Hemmings V, Riddle BR (2011) Niche shifting in response to warming climate after the last glacial maximum: inference from genetic data and niche assessments in the chisel-toothed kangaroo rat (*Dipodomys microps*). *Global Change Biology*, **17**, 3486-3502.

Jezkova T, Riddle BR, Card DC, Schield DR, Eckstut ME, Castoe TA (2015) Genetic consequences of postglacial range expansion in two codistributed rodents (genus *Dipodomys*) depend on ecology and genetic locus. *Molecular Ecology*, **24**, 83-97.

Jombart T (2008) adegenet: a R package for the multivariate analysis of genetic markers. *Bioinformatics*, **24**, 1403-1405.

Jombart T, Ahmed I (2011) adegenet 1.3-1: new tools for the analysis of genome-wide SNP data. *Bioinformatics*, **27**, 3070-3071.

Keith R, Hedin M (2012) Extreme mitochondrial population subdivision in southern Appalachian paleoendemic spiders (Araneae: Hypochilidae: *Hypochilus*), with implications for species delimitation. *Journal of Arachnology*, **40**, 167-181.

Keyghobadi N, Roland J, Strobeck C (2005) Genetic differentiation and gene flow among populations of the alpine butterfly, *Parnassius smintheus*, vary with landscape connectivity. *Molecular Ecology*, **14**, 1897-1909.

Klicka J, Zink RM (1997) The importance of recent ice ages in speciation: a failed paradigm. *Science*, **277**, 1666-1669.

Knowles LL (2001) Did the Pleistocene glaciations promote divergence? Tests of explicit refugial models in montane grasshopprers. *Molecular Ecology*, **10**, 691-701.

Knowles LL, Carstens BC, Keat ML (2007) Coupling genetic and ecological-niche models to examine how past population distributions contribute to divergence. *Current Biology*, **17**, 940-946.

Kozak KH, Graham CH, Wiens JJ (2008) Integrating GIS-based environmental data into evolutionary biology. *Trends in Ecology and Evolution*, **23**, 141-148.

Lamb T, Jones TR, Wettstein PJ (1997) Evolutionary genetics and phylogeography of tassel-eared squirrels (*Sciurus aberti*). *Journal of Mammalogy*, **78**, 117-133.

Lanfear R, Calcott B, Ho SY, Guindon S (2012) PartitionFinder: combined selection of partitioning schemes and substitution models for phylogenetic analyses. *Molecular Biology and Evolution*, **29**, 1695-1701.

Lee CR, Mitchell-Olds T (2011) Quantifying effects of environmental and geographical factors on patterns of genetic differentiation. *Molecular Ecology*, **20**, 4631-4642.

Lomolino MV, Brown JH, Davis R (1989) Island biogeography of montane forest mammals in the American Southwest. *Ecology*, **70**, 180-194.

Lucchitta I (1989) History of the Grand Canyon and of the Colorado River in Arizona. *Geologic evolution of Arizona: Arizona Geological Society Digest*, **17**, 701-715.

Manthey JD, Moyle RG (2015) Isolation by environment in White-breasted Nuthatches (*Sitta carolinensis*) of the Madrean Archipelago sky islands: a landscape genomics approach. *Molecular Ecology*, **24**, 3628-3638.

Martínez-Solano I, Teixeira J, Buckley D, García-París M (2006) Mitochondrial DNA phylogeography of *Lissotriton boscai* (Caudata, Salamandridae): evidence for old, multiple refugia in an Iberian endemic. *Molecular Ecology*, **15**, 3375-3388.

Massatti R, Knowles LL (2014) Microhabitat differences impact phylogeographic concordance of codistributed species: genomic evidence in montane sedges (*Carex* L.) from the Rocky Mountains. *Evolution*, **68**, 2833-2846.

Masta SE (2000) Phylogeography of the jumping spider *Habronattus pugillis* (Araneae: Salticidae): recent vicariance of sky island populations? *Evolution*, **54**, 1699-1711.

McCormack JE, Bowen BS, Smith TB (2008) Integrating paleoecology and genetics of bird populations in two sky island archipelagos. *BMC Biology*, **6**, 28.

McCormack JE, Hird SM, Zellmer AJ, Carstens BC, Brumfield RT (2013) Applications of next-generation sequencing to phylogeography and phylogenetics. *Molecular Phylogenetics and Evolution*, **66**, 526-538.

McMillan ME, Heller PL, Wing SL (2006) History and causes of post-Laramide relief in the Rocky Mountain orogenic plateau. *Geological Society of America Bulletin*, **118**, 393-405.

Meyer III WM, Eble JA, Franklin K, McManus RB, Brantley SL, Henkel J, Marek PE, Hall WE, Olson CA, McInroy R, Loaiza EMB, Brusca RC, Moore, W (2015) Ground-Dwelling Arthropod Communities of a Sky Island Mountain Range in Southeastern Arizona, USA: Obtaining a Baseline for Assessing the Effects of Climate Change. *PloS ONE*, **10**, e0135210.

Mitchell SG, Ober KA (2013) Evolution of *Scaphinotus petersi* (Coleoptera: Carabidae) and the role of climate and geography in the Madrean sky islands of southeastern Arizona, USA. *Quaternary Research*, **79**, 274-283.

Mitton JB, Kreiser BR, Latta RG (2000) Glacial refugia of limber pine (*Pinus flexilis* James) inferred from the population structure of mitochondrial DNA. *Molecular Ecology*, **9**, 91-97.

Moore W, Meyer III WM, Eble JA, Franklin K, Wiens JF, Brusca RC (2013) Introduction to the Arizona Sky Island Arthropod Project (ASAP): Systematics, biogeography, ecology, and population genetics of arthropods of the Madrean Sky Islands. Pp. 140–164, In: *Merging Science and Management In A Rapidly Changing World: Biodiversity and Management of the Madrean Archipelago III* (ed. Gottfried GJ et. al). USDA (RMRS-P-67), Washington DC.

Nee S, Mooers AO, Harvey PH (1992) Tempo and mode of evolution revealed from molecular phylogenies. *Proceedings of the National Academy of Sciences*, **89**, 8322-8326.

Ober K, Matthews B, Ferrieri A, Kuhn S (2011). The evolution and age of populations of *Scaphinotus petersi* Roeschke on Arizona Sky Islands (Coleoptera, Carabidae, Cychrini). *ZooKeys*, **147**, 183.

Ober KA, Connolly CT (2015) Geometric morphometric and phylogenetic analyses of Arizona Sky Island populations of *Scaphinotus petersi* Roeschke (Coleoptera: Carabidae). *Zoological Journal of the Linnean Society*, **175**, 107-118.

Oksanen J, Blanchet FG, Kindt R, Legendre P, Minchin PR, O'Hara RB, Simpson GL, Solymos P, Stevens MHH, Wagner H (2015) Package 'vegan', Community ecology package. Version 2-2. Available at: https://cran.r-project.org/package=vegan

Packard AS (1877) On a new cave fauna in Utah. *Bulletin of the United States Geological Survey of the Territories*, **3**, 157–169.

Papadopoulou A, Anastasiou I, Vogler AP (2010) Revisiting the insect mitochondrial molecular clock: the mid-Aegean trench calibration. *Molecular Biology and Evolution*, **27**, 1659-1672.

Paradis E, Claude J, Strimmer K (2004) APE: analyses of phylogenetics and evolution in R language. *Bioinformatics*, **20**, 289-290.

Peterson BJ, Graves WR (2015) Chloroplast phylogeography of Dirca palustris L. indicates populations near the glacial boundary at the Last Glacial Maximum in eastern North America. *Journal of Biogeography*. DOI: 10.1111/jbi.12621.

Peterson BK, Weber JN, Kay EH, Fisher HS, Hoekstra HE (2012) Double digest RADseq: an inexpensive method for de novo SNP discovery and genotyping in model and non-model species. *PloS ONE*, **7**, e37135.

Phillips SJ, Anderson RP, Schapire RE (2006) Maximum entropy modeling of species geographic distributions. *Ecological Modelling*, **190**, 231-259.

R Core Team (2013) R: A language and environment for statistical computing. R Foundation for Statistical Computing, Vienna, Austria. http://www.R-project.org/.

Rambaut A, Drummond AJ (2014) TreeAnnotator v2. 1.2. *Edinburgh: University of Edinburgh, Institute of Evolutionary Biology*.

Rambaut A, Suchard MA, Xie D, Drummond AJ (2014) Tracer v1. 6. Computer program and documentation distributed by the author. Available at: http://beast.bio.ed.ac.uk/Tracer

Richards CL, Carstens BC, Knowles LL (2007) Distribution modelling and statistical phylogeography: an integrative framework for generating and testing alternative biogeographical hypotheses. *Journal of Biogeography*, **34**, 1833-1845.

Richart C, Hedin M (2013) Three new species in the harvestmen genus *Acuclavella* (Opiliones, Dyspnoi, Ischyropsalidoidea), including description of male *Acuclavella quattuor* Shear, 1986. *ZooKeys*, **311**, 19.

Rissler LJ, Apodaca JJ (2007) Adding more ecology into species delimitation: ecological niche models and phylogeography help define cryptic species in the black salamander (*Aneides flavipunctatus*). *Systematic Biology*, **56**, 924-942.

Rousset F (1997) Genetic differentiation and estimation of gene flow from F-statistics under isolation by distance. *Genetics*, **145**, 1219-1228.

Satler JD, Zellmer AJ, Carstens BC (2016) Biogeographic barriers drive co-diversification within associated eukaryotes of the *Sarracenia alata* pitcher plant system. *PeerJ*, **4,** e1576.

Sexton JP, Hangartner SB, Hoffmann AA (2014) Genetic isolation by environment or distance: which pattern of gene flow is most common? *Evolution*, **68**, 1-15.

Shafer A, Cullingham CI, Côté SD, Coltman DW (2010) Of glaciers and refugia: a decade of study sheds new light on the phylogeography of northwestern North America. *Molecular Ecology*, **19**, 4589-4621.

Schönhofer AL, McCormack M, Tsurusaki N, Martens J, Hedin M (2013) Molecular phylogeny of the harvestmen genus *Sabacon* (Arachnida: Opiliones: Dyspnoi) reveals multiple Eocene–Oligocene intercontinental dispersal events in the Holarctic. *Molecular Phylogenetics and Evolution*, **66**, 303-315.

Schönhofer AL, Vernesi C, Martens J, Hedin M (2015) Molecular phylogeny, biogeographic history, and evolution of cave-dwelling taxa in the European harvestman genus *Ischyropsalis* (Opiliones: Dyspnoi). *The Journal of Arachnology*, **43**, 40-53.

Smith CI, Farrell BD (2005) Phylogeography of the longhorn cactus beetle *Moneilema appressum* LeConte (Coleoptera: Cerambycidae): was the differentiation of the Madrean sky islands driven by Pleistocene climate changes? *Molecular Ecology*, **14**, 3049-3065.

Starrett J, Derkarabetian S, Richart CH, Cabrero A, Hedin M (2016) A new monster from southwest Oregon forests: *Cryptomaster behemoth* sp. nov. (Opiliones, Laniatores, Travunioidea). *Zookeys*, **555**, 11-35.

Stervander M, Illera JC, Kvist L, Barbosa P, Keehnen NP, Pruisscher P, Bensch S, Hansson B (2015) Disentangling the complex evolutionary history of the Western Palearctic blue tits (*Cyanistes* spp.)–phylogenomic analyses suggest radiation by multiple colonization events and subsequent isolation. *Molecular Ecology*, **24**, 2477-2494.

Tennessen JA, Zamudio KR (2008) Genetic differentiation among mountain island populations of the striped plateau lizard, *Sceloporus virgatus* (Squamata: Phrynosomatidae). *Copeia*, **2008**, 558-564.

Thomas SM, Hedin M (2008) Multigenic phylogeographic divergence in the paleoendemic southern Appalachian opilionid *Fumontana deprehendor* Shear (Opiliones, Laniatores, Triaenonychidae). *Molecular Phylogenetics and Evolution*, **46**, 645-658.

Ubick D, Briggs TS (1992) The harvestman family Phalangodidae. 3. Revision of *Texella* Goodnight and Goodnight (Opiliones: Laniatores). *Texas Memorial Museum, Speleological Monographs*, **3**, 155-240

Ubick D, Briggs TS, (2008) The Harvestman Family Phalangodidae. 6: Revision of the *Sitalcina* Complex (Opiliiones: Laniatores). *Proceedings of the California Academy of Sciences*, **59**, 1–108.

Vandewoestijne S, Van Dyck H (2010) Population genetic differences along a latitudinal cline between original and recently colonized habitat in a butterfly. *PLoS ONE*, **5**, e13810-e13810.

Wachter GA, Papadopoulou A, Muster C, Arthofer W, Knowles LL, Steiner FM, Schlick-Steiner BC (2016) Glacial refugia, recolonisation patterns, and diversification forces in Alpine-endemic *Megabunus* harvestmen. *Molecular Ecology*, **25**, 2904-2919.

Wang IJ (2013) Examining the full effects of landscape heterogeneity on spatial genetic variation: a multiple matrix regression approach for quantifying geographic and ecological isolation. *Evolution*, **67**, 3403-3411.

Wang IJ, Bradburd GS (2014) Isolation by environment. *Molecular Ecology*, **23**, 5649-5662.

Wang IJ, Summers K (2010) Genetic structure is correlated with phenotypic divergence rather than geographic isolation in the highly polymorphic strawberry poison-dart frog. *Molecular Ecology*, **19**, 447-458.

Wang IJ, Glor RE, Losos JB (2013) Quantifying the roles of ecology and geography in spatial genetic divergence. *Ecology Letters*, **16**, 175-182.

Welbourn WC (1999) Invertebrate cave fauna of Kartchner caverns, Kartchner caverns, Arizona. *Journal of Cave and Karst Studies*, **61**, 93-101.

Wiens JJ (2004) Speciation and ecology revisited: phylogenetic niche conservatism and the origin of species. *Evolution*, **58**, 193-197.

Wiens JJ, Graham CH (2005) Niche conservatism: integrating evolution, ecology, and conservation biology. *Annual Review of Ecology, Evolution, and Systematics*, **36**, 519-539.

Willing EM, Dreyer C, Van Oosterhout C (2012) Estimates of genetic differentiation measured by F ST do not necessarily require large sample sizes when using many SNP markers. *PLoS One*, **7**, e42649.

Wright S (1943) Isolation by distance. *Genetics*, **28**, 114.

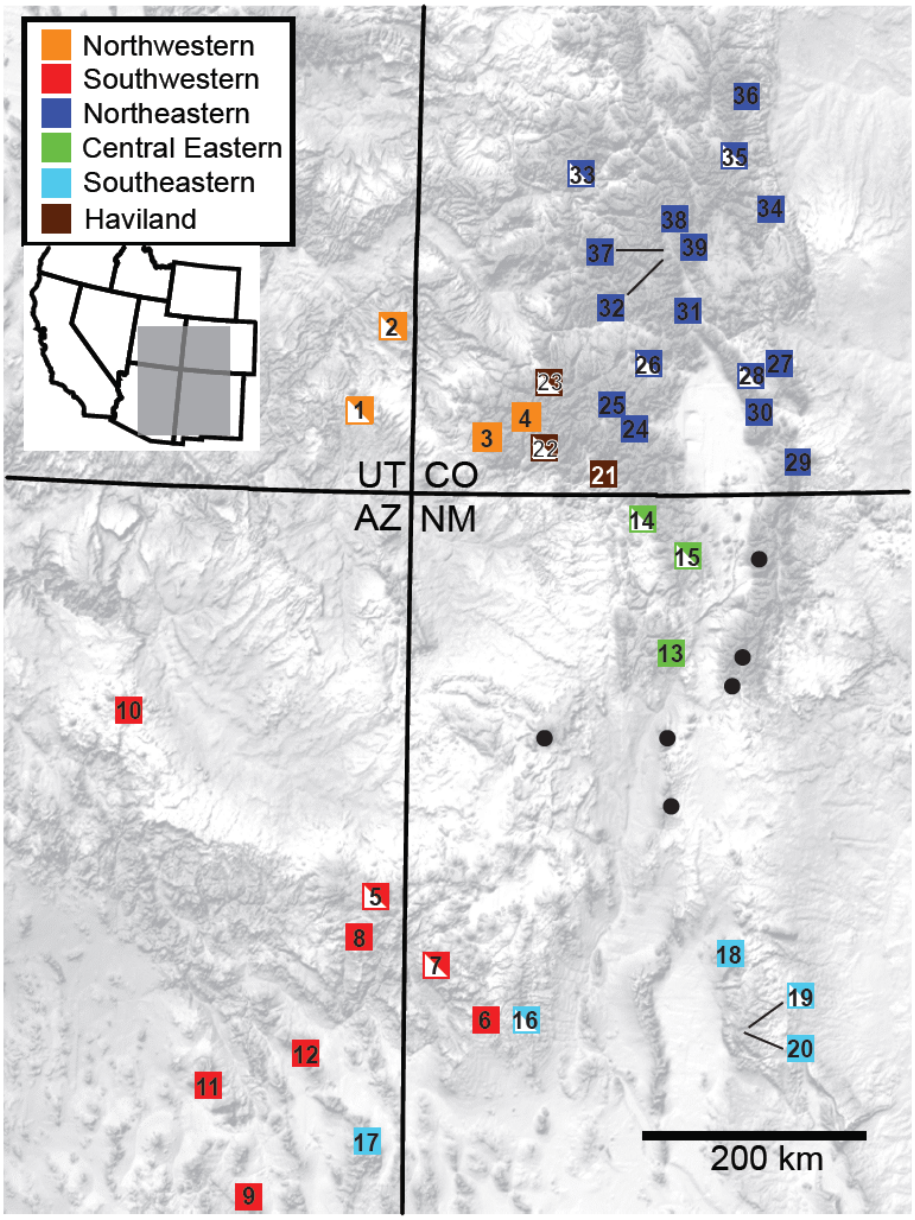

Figure 3.1. Geographic distribution and sampling localities of *S. robustus*, colored by clades recovered here (see Figure 3) and in Derkarabetian et al. (2011). Filled boxes indicate collecting localities where two samples were processed for ddRAD-seq. Half boxes indicate localities where a single sample was processed. Black circles indicate localities where other *Sclerobunus* species have been collected.

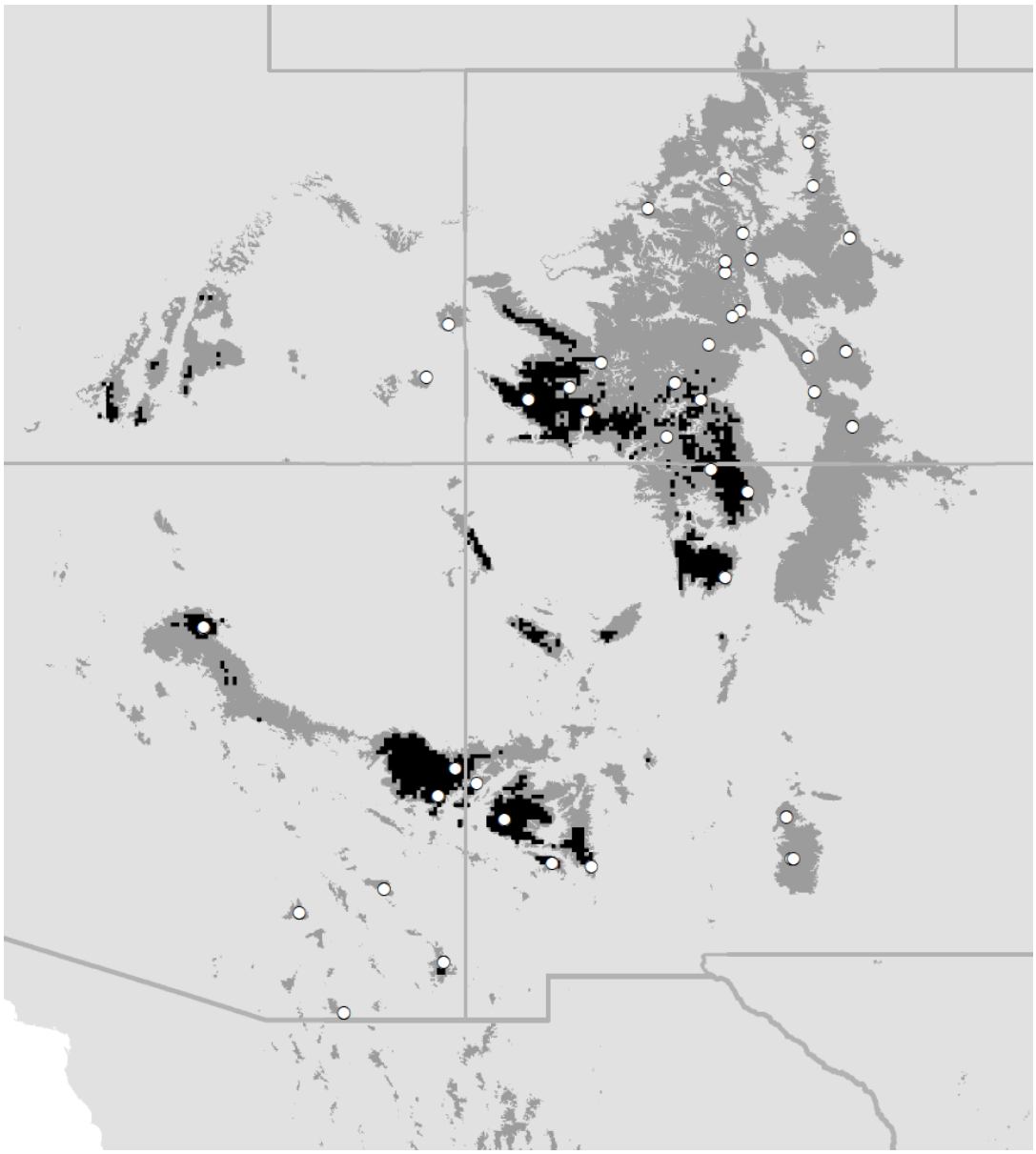

Figure 3.2. Binary ENMs for *S. robustus*. Grey regions denote ENM based on current bioclimatic conditions across all populations of *S. robustus*. Black regions indicate persistent habitat across eastern and western clades for current, mid-Holocene, and LGM niche models. White dots indicate *S. robustus* collecting localities used in constructing ENMs.

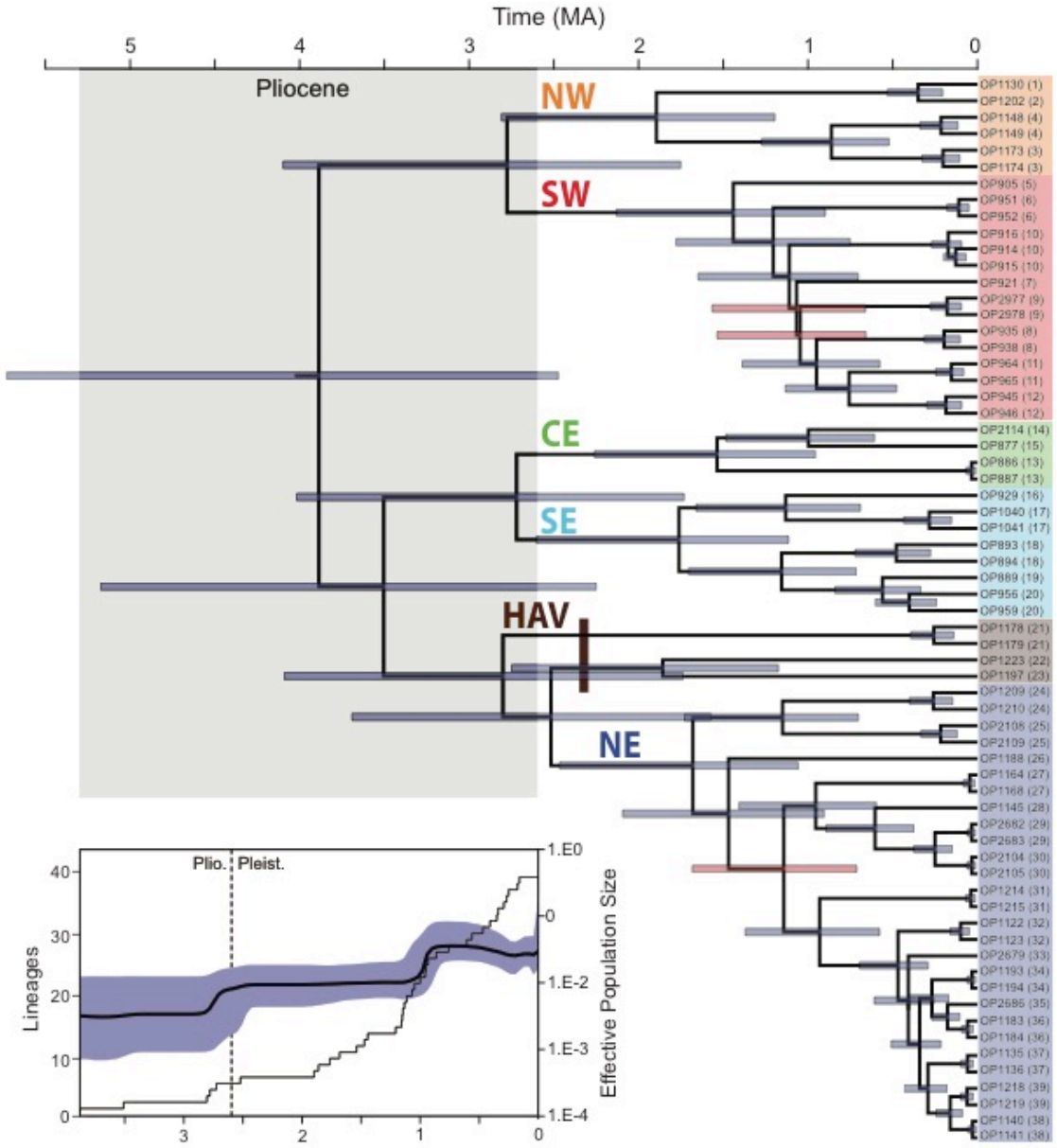

Figure 3.3. BEAST maximum clade credibility tree for the m32 dataset. Clade colors correspond to those in Figure 1. Node bars represent 95% HPD for divergence times. Blue HPD divergence bars indicate nodes with >0.95 posterior probability, red bars indicate <0.95. Inset: Bayesian Skyline for all *S. robustus*, and lineage through time plot for one sample per population.

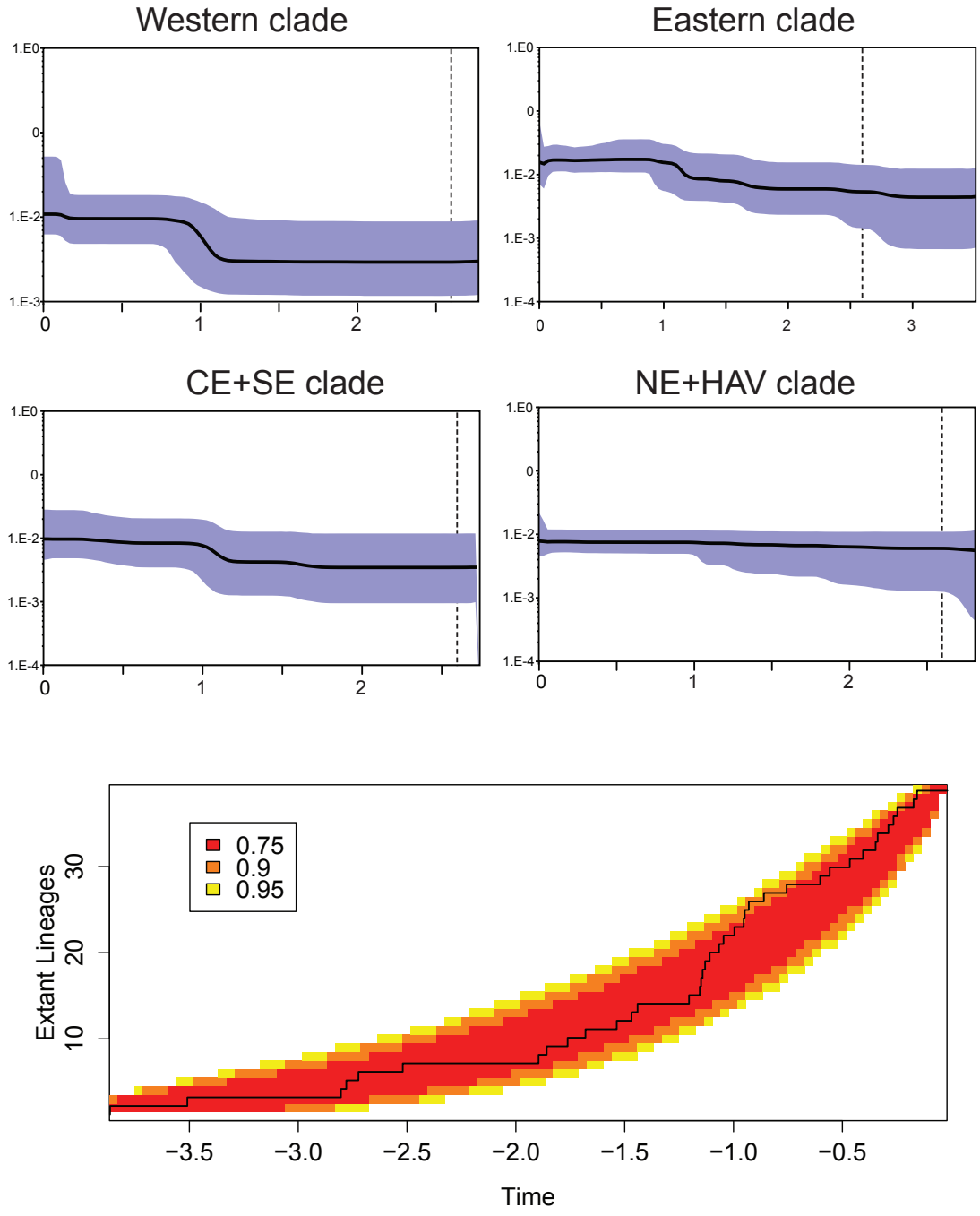

Figure 3.4. Bayesian skyline plots for major clade groupings. Vertical dashed line indicates Pleistocene-Pliocene boundary. LTT plot with null distribution created using the "rbdtree.n3.R" script (http://ib.berkeley.edu/courses/ib200b/labs/lab12/rbdtree.n3.R). Colored regions of the null distribution correspond to confidence intervals.

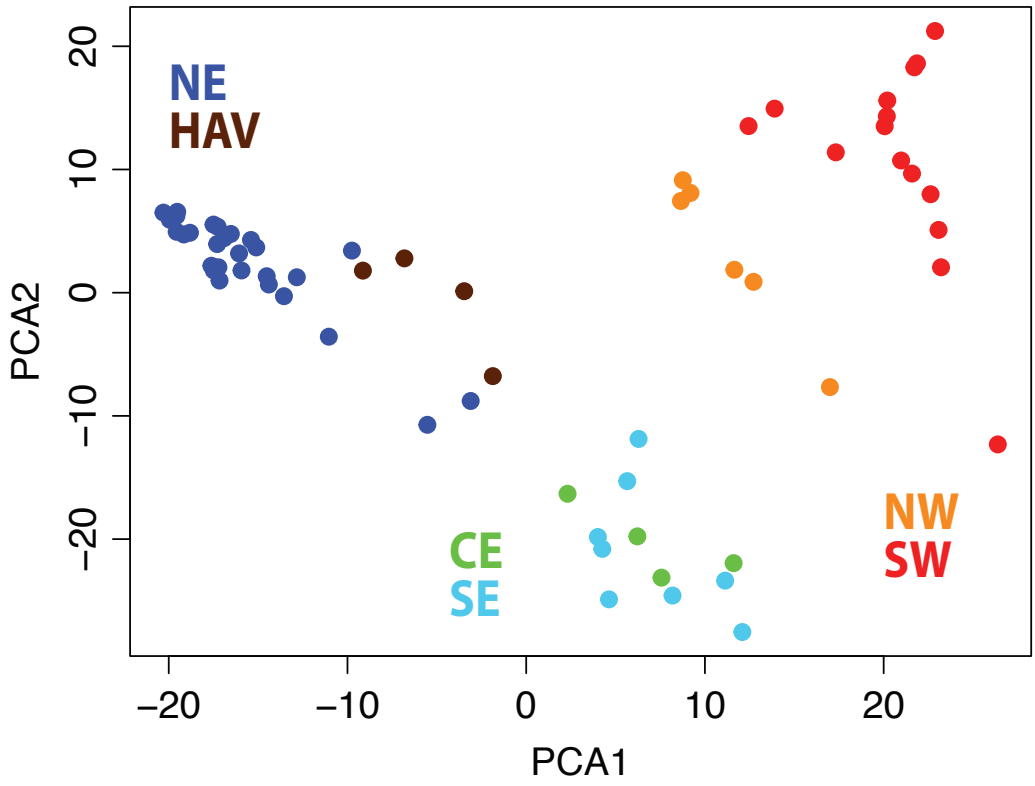

Figure 3.5. Results of principal components analysis for the m32 SNP dataset.

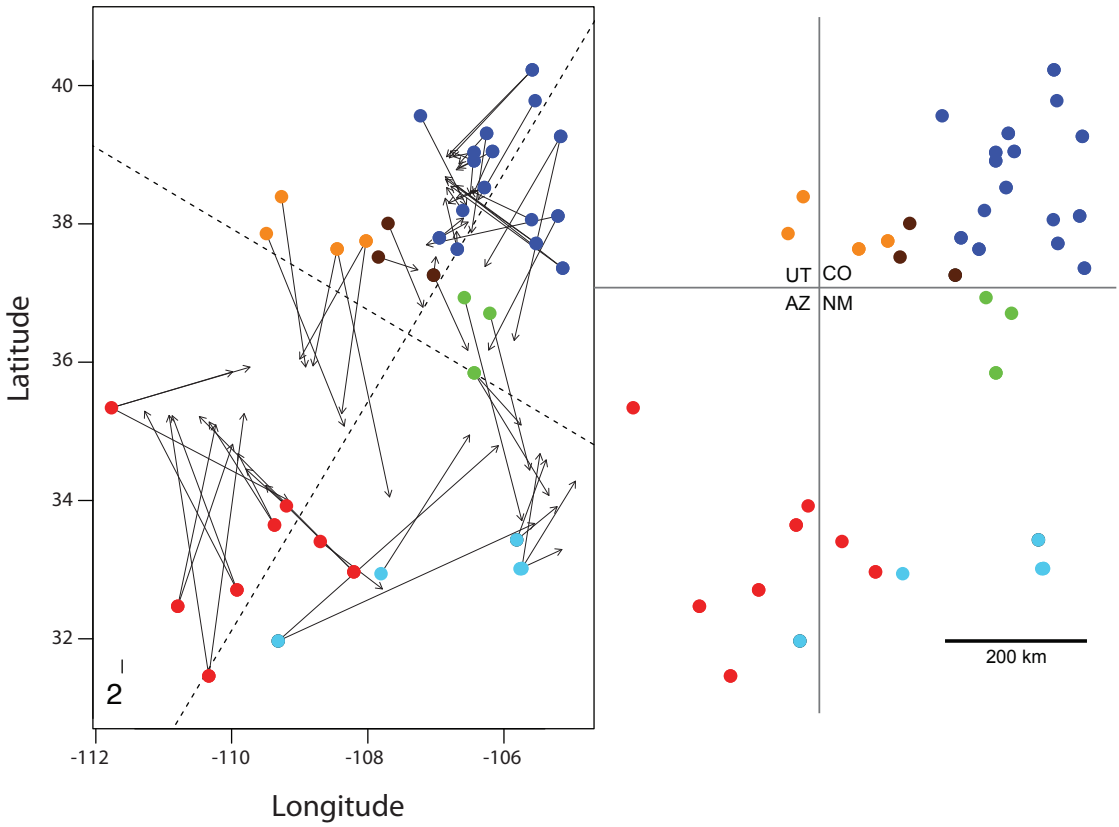

Figure 3.6. Results of Procrustes analysis for the m32 SNP dataset. Left pane: results of Procrustes plot, with arrows indicating direction and magnitude of movement of each point in SNP principal component space. Right pane: simplified geographic distribution of collecting localities. Procrustes plot was rotated 90° to correspond with placement in the geographic plot.

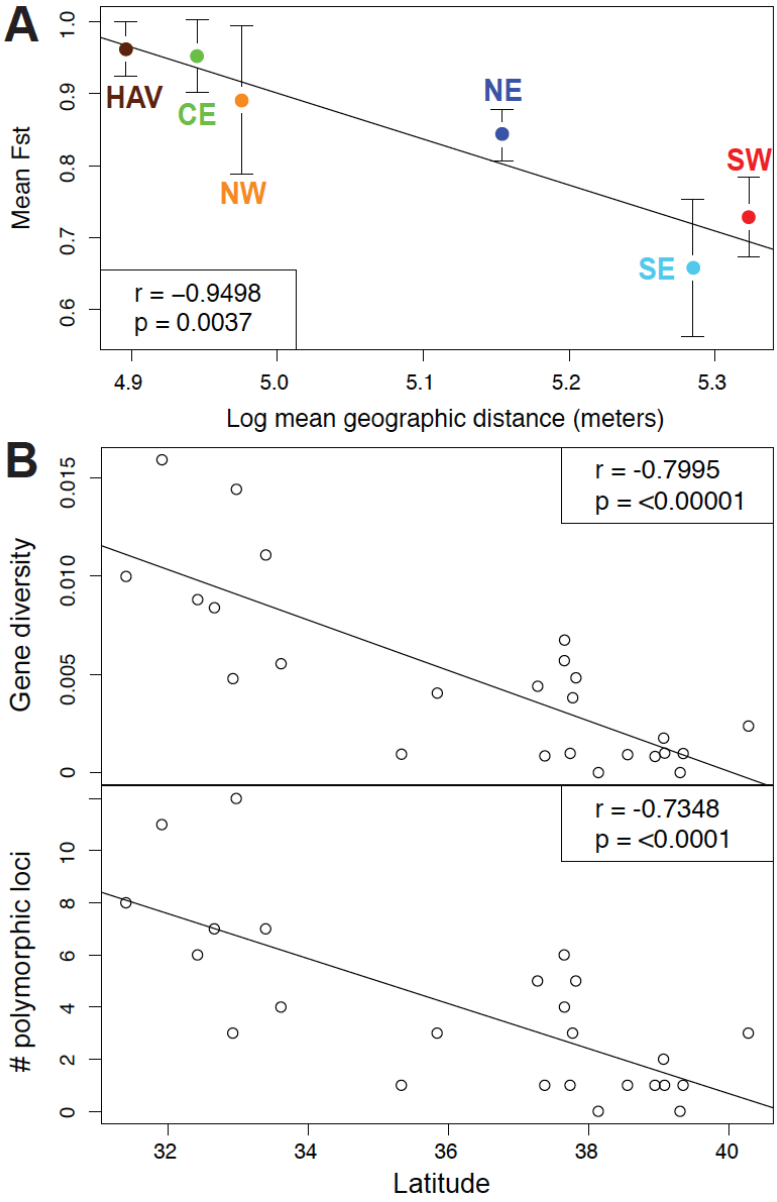

Figure 3.7. Genetic and geographic correlations. A) Correlation of mean pairwise geographic distance versus mean pairwise F_{ST} for each clade, with 95% confidence intervals. F_{ST} calculated in Arlequin with each population considered a separate sample. B) Latitude versus gene diversity and number of polymorphic loci of each population represented by more than one sequenced individual. Genetic statistics calculated using loci from the m32 dataset.

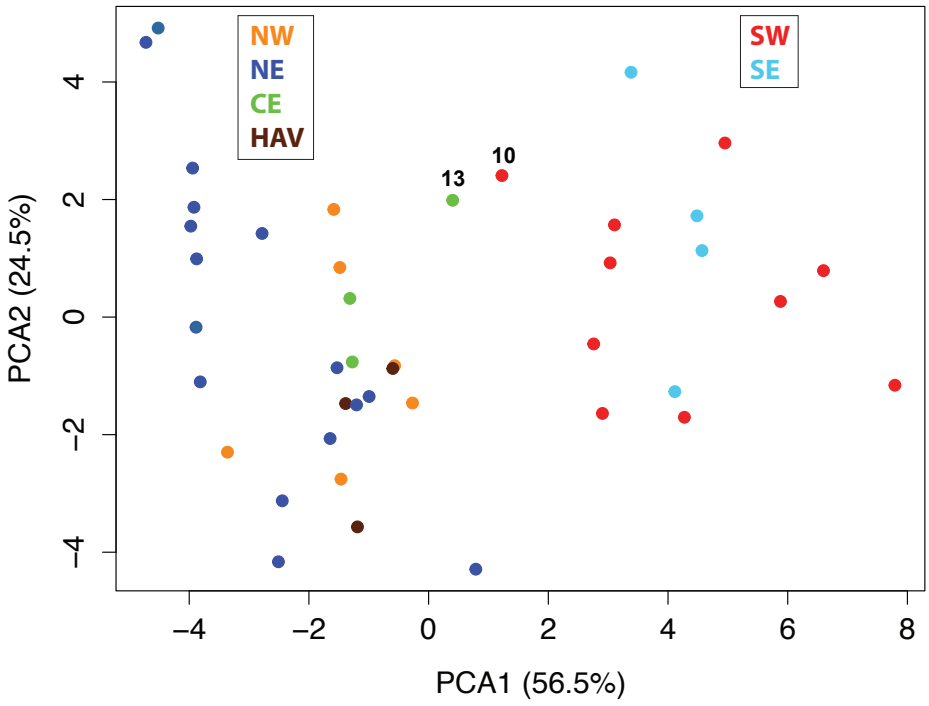

Figure 3.8. PCA plot of environmental variable extracted from occurrence records.

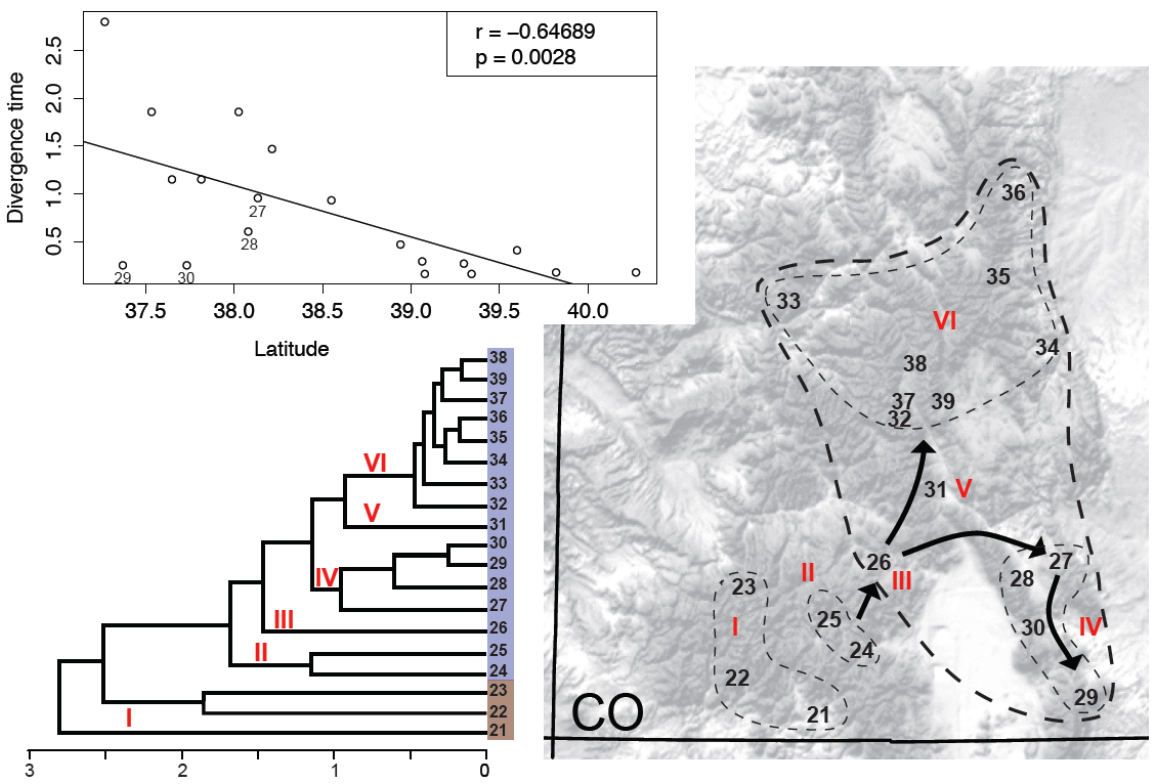

Figure 3.9. Phylogenetic and population genetic patterns for the NE clade. Top left: latitude versus divergence time of each population from its nearest relative. Bottom left: m32 phylogeny of the NE clade, indicating sublineages in red. Right: geographic distribution and expansion direction of the NE clade, with sublineages indicated.

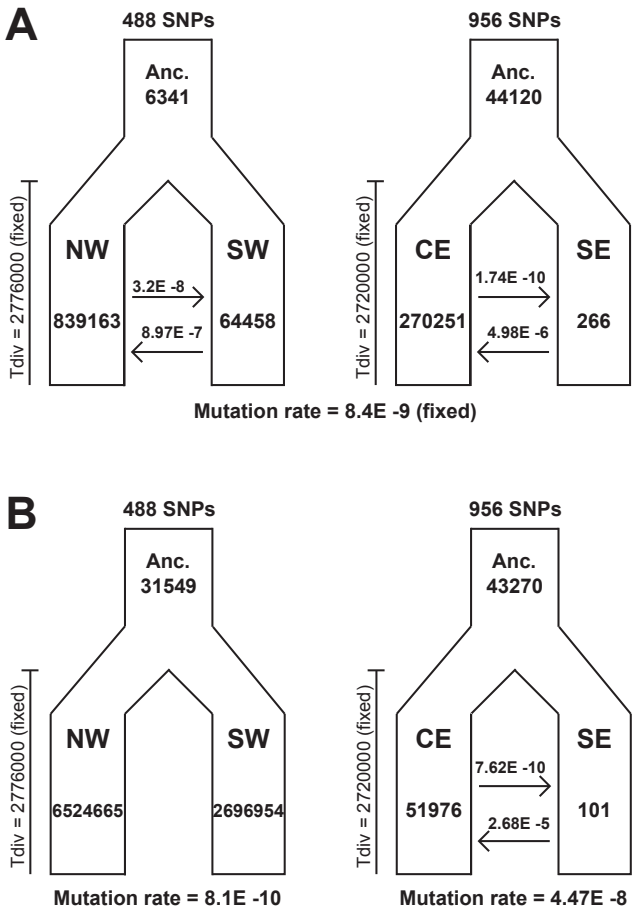

Figure 3.10. Models chosen with fastsimcoal2. A) Favored models with a fixed mutation rate. B) Favored models with mutation rate estimated. Point estimates of all parameters are included, which were taken from the iteration with the highest likelihood. The number of SNPs used in each analysis based on rerunning pyRAD is indicated above each model.

Table 3.1. Primers and barcodes used in ddRAD-Seq library preparation.

P1 Oligos	
GCATG_SbfI_P1.1.1	ACACTCTTTCCCTACACGACGCTCTTCCGATCTGCATGTGCA
AACCA_SbfI_P1.1.2	ACACTCTTTCCCTACACGACGCTCTTCCGATCTAACCATGCA
CGATC_SbfI_P1.1.3	ACACTCTTTCCCTACACGACGCTCTTCCGATCTCGATCTGCA
TCGAT_SbfI_P1.1.4	ACACTCTTTCCCTACACGACGCTCTTCCGATCTTCGATTGCA
TGCAT_SbfI_P1.1.5	ACACTCTTTCCCTACACGACGCTCTTCCGATCTTGCATTGCA
CAACC_SbfI_P1.1.6	ACACTCTTTCCCTACACGACGCTCTTCCGATCTCAACCTGCA
GGTTG_SbfI_P1.1.7	ACACTCTTTCCCTACACGACGCTCTTCCGATCTGGTTGTGCA
AAGGA_SbfI_P1.1.8	ACACTCTTTCCCTACACGACGCTCTTCCGATCTAAGGATGCA
GCATG_SbfI_P1.2.1	/5Phos/CATGCAGATCGGAAGAGCGTCGTGTAGGGAAAGAGTGT
AACCA_SbfI_P1.2.2	/5Phos/TGGTTAGATCGGAAGAGCGTCGTGTAGGGAAAGAGTGT
CGATC_SbfI_P1.2.3	/5Phos/GATCGAGATCGGAAGAGCGTCGTGTAGGGAAAGAGTGT
TCGAT_SbfI_P1.2.4	/5Phos/ATCGAAGATCGGAAGAGCGTCGTGTAGGGAAAGAGTGT
TGCAT_SbfI_P1.2.5	/5Phos/ATGCAAGATCGGAAGAGCGTCGTGTAGGGAAAGAGTGT
CAACC_SbfI_P1.2.6	/5Phos/GGTTGAGATCGGAAGAGCGTCGTGTAGGGAAAGAGTGT
GGTTG_SbfI_P1.2.7	/5Phos/CAACCAGATCGGAAGAGCGTCGTGTAGGGAAAGAGTGT
AAGGA_SbfI_P1.2.8	/5Phos/TCCTTAGATCGGAAGAGCGTCGTGTAGGGAAAGAGTGT
P2 Oligos	
MspI_P2.1	GTGACTGGAGTTCAGACGTGTGCTCTTCCGATCT
MspI_P2.2	/5Phos/CGAGATCGGAAGAGCGAGAACAA
PRIMERS	
PCR1`	AATGATACGGCGACCACCGAGATCTACACTCTTTCCCTACACGACG
PCR2_Idx_1_ATCACG	CAAGCAGAAGACGGCATACGAGATCGTGATGTGACTGGAGTTCAGACGTGTGC
PCR2_Idx_2_CGATGT	CAAGCAGAAGACGGCATACGAGATACATCGGTGACTGGAGTTCAGACGTGTGC
PCR2_Idx_3_TTAGGC	CAAGCAGAAGACGGCATACGAGATGCCTAAGTGACTGGAGTTCAGACGTGTGC
PCR2_Idx_4_TGACCA	CAAGCAGAAGACGGCATACGAGATTGGTCAGTGACTGGAGTTCAGACGTGTGC
PCR2_Idx_5_ACAGTG	CAAGCAGAAGACGGCATACGAGATCACTGTGTGACTGGAGTTCAGACGTGTGC
PCR2_Idx_6_GCCAAT	CAAGCAGAAGACGGCATACGAGATATTGGCGTGACTGGAGTTCAGACGTGTGC
PCR2_Idx_7_CAGATC	CAAGCAGAAGACGGCATACGAGATGATCTGGTGACTGGAGTTCAGACGTGTGC
PCR2_Idx_8_ACTTGA	CAAGCAGAAGACGGCATACGAGATTCAAGTGTGACTGGAGTTCAGACGTGTGC
PCR2_Idx_9_GATCAG	CAAGCAGAAGACGGCATACGAGATCTGATGGTGACTGGAGTTCAGACGTGTGC
PCR2_Idx_10_TAGCTT	CAAGCAGAAGACGGCATACGAGATAAGCTAGTGACTGGAGTTCAGACGTGTGC

Table 3.2. Matrix statistics. Matrix completeness was calculated by summing the number of loci across all samples and dividing by the total number of loci multiplied by 65 (Table S1). PIS = parsimony-informative sites.

	m48	**m32**	**m16**
Number of loci	498	1270	3303
Mean N loci	428	884	1579
Min	179	275	487
Max	489	1176	2417
Matrix completeness (%)	85.94	69.58	47.79
Total variable sites	4686	11431	24232
Total PIS	2277	5541	11453
Sampled unlinked SNPs	496	1265	3251
Sampled unlinked bi-allelic SNPs	285	617	1355
Concatenated matrix length	47061	120197	312584

Table 3.3. Mean estimated divergence dates for major clades and groupings, with 95% HPD in brackets.

	m48	**m32**	**m16**
S. robustus root	3.212 [2.003, 4.713]	3.886 [2.473, 5.727]	4.266 [2.709, 6.242]
Western clades	2.461 [1.543, 3.633]	2.776 [1.751, 4.098]	3.061 [1.928, 4.475]
NW	1.761 [1.106, 2.628]	1.895 [1.196, 2.809]	2.117 [1.332, 3.103]
SW	1.33 [0.822, 1.972]	1.441 [0.898, 2.129]	1.576 [0.979, 2.294]
Eastern clades	2.646 [1.683, 3.917]	3.504 [2.251, 5.172]	3.956 [2.506, 5.784]
CE+SE	2.081 [1.301, 3.078]	2.72 [1.731, 4.017]	2.982 [1.91, 4.386]
CE	1.273 [0.775, 1.88]	1.536 [0.957, 2.26]	1.677 [1.049, 2.444]
SE	1.355 [0.84, 1.997]	1.761 [1.115, 2.601]	2.003 [1.266, 2.938]
HAV+NE	2.128 [1.338, 3.146]	2.8 [1.739, 4.089]	3.157 [1.985, 4.602]
HAV	NA	NA	2.841 [1.791, 4.14]
NE	1.311 [0.807, 1.929]	1.68 [1.059, 2.466]	1.967 [1.247, 2.877]

Table 3.4. Genetic diversity statistics for clades based on the m32 loci. Standard deviations of statistics included in parentheses.

	N	**# haplotypes**	**Avg. # Diffs**	**Avg. gene diversity**	**# polymorphic loci**	**Expected heterozygosity**
NW	6	12	12.7878 (6.164517)	0.021067 (0.011423)	39	0.4501 (0.09533)
SW	15	30	9.35172 (4.40795)	0.015356 (0.008051)	69	0.26745 (0.13481)
CE	4	8	10 (5.071548)	0.020704 (0.011943)	27	0.53714 (0.08674)
SE	8	16	12.9 (6.106719)	0.023412 (0.01246)	58	0.37482 (0.1378)
HA V	4	8	24.14285 (11.78276)	0.034539 (0.019157)	61	0.51531 (0.06839)
NE	28	56	7.425974 (3.518801)	0.008429 (0.00443)	72	0.15894 (0.10663)

Table 3.5. Pairwise F_{ST} values for each clade. Diagonal shows average F_{ST} within clades. 95% confidence interval in parentheses.

	NW	SW	CE	SE	HAV	NE
NW	0.8914 (0.1029)					
SW	0.8931 (0.0213)	0.7286 (0.0557)				
CE	0.9689 (0.0138)	0.9339 (0.0173)	0.9526 (0.0511)			
SE	0.8867 (0.0312)	0.8220 (0.0399)	0.9040 (0.0375)	0.6583 (0.0956)		
HAV	0.9605 (0.0173)	0.9230 (0.0152)	0.9757 (0.0171)	0.8945 (0.0373)	0.9627 (0.0379)	
NE	0.9617 (0.0073)	0.9292 (0.0076)	0.9761 (0.0068)	0.8944 (0.016)	0.9612 (0.0104)	0.8428 (0.0355)

Table 3.6. AMOVA results across major clades.

Source of Variation	d.f.	Sum of squares	Variance components		Percentage of variation	Fixation indices		P-value
Among clades	5	683.356	6.40967	Va	55.92	0.55917	F_{CT}	<0.0001
Among populations within clades	33	483.357	4.14841	Vb	36.12	0.82095	F_{SC}	<0.0001
Within populations	91	82.333	0.90476	Vc	7.89	0.82095	F_{ST}	<0.0001
Total	129	1249.046	11.46284					

Table 3.7. Results of IBD, IBE, and MMRR analyses. Significant values are indicated in bold.

	IBD			IBE			MMRR							
	r	**R2**	**p-value**	**r**	**R2**	**p-value**	**R2**	**r - Geo**	**t-stat**	**t p-value**	**r - Env**	**t-stat**	**t p-value**	**Fstat**	**p-value**
All	**0.11**	**0.01**	**0.028**	**0.21**	**0.04**	**<0.001**	0.05	4.54 e-8	2.58	0.133	**0.18**	**5.49**	**0.009**	20.18	0.005
West	**0.41**	**0.17**	**0.003**	**0.40**	**0.16**	**0.023**	0.31	**2.48 e-4**	**3.59**	**0.003**	**0.44**	**3.53**	**0.019**	13.84	0.001
NW	0.59	0.35	0.09	**0.56**	**0.32**	**0.044**	0.35	1.49 e-6	0.40	0.839	0.21	0.17	0.87	0.82	0.425
SW	0.31	0.10	0.228	**0.57**	**0.33**	**0.034**	0.33	-3.95 e-8	-0.14	0.895	**0.76**	**2.90**	**0.023**	6.04	0.061
East	0.08	0.01	0.211	**0.22**	**0.05**	**0.001**	0.05	2.71 e-8	0.84	0.661	**0.22**	**4.02**	**0.021**	9.37	0.058
CE+SE	**0.38**	**0.14**	**0.027**	0.04	0.00	0.464	0.16	**4.00 e-7**	**2.21**	**0.032**	0.32	0.80	0.61	2.46	0.277
CE	-0.99	0.98	1	0.29	0.08	0.477	NA								
SE	0.28	0.08	0.228	0.26	0.07	0.203	0.18	3.97 e-7	0.99	0.323	0.56	0.94	0.418	0.77	0.582
HAV+NE	**0.29**	**0.09**	**0.003**	**0.21**	**0.05**	**0.032**	0.10	**5.83 e-7**	**3.16**	**0.032**	0.14	1.54	0.391	9.29	0.03
HAV	-0.95	0.90	1	0.06	0.00	0.348	NA								
NE	**0.26**	**0.07**	**0.02**	0.02	0.00	0.487	0.07	**7.67 e-7**	**2.92**	**0.031**	-0.09	-0.45	0.772	4.28	0.135

Table 3.8. Results of migrate-n analyses.

NW - SW				**CE - SE**			
Parameter	2.50%	Mode	97.50%	Parameter	2.50%	Mode	97.50%
Theta NW	0.00416	0.00458	0.00481	Theta CE	0.00407	0.0043	0.00451
Theta SW	0.00491	0.00516	0.00539	Theta SE	0.00456	0.00469	0.00484
Nm SW -> NW	0.4098	0.4766	0.5259	Nm SE-> CE	0.4388	0.4942	0.5457
Nm NW -> SW	0.4517	0.5085	0.5633	Nm CE -> SE	0.4856	0.5457	0.6112

CONCLUSIONS

The results presented in this dissertation extend beyond the focal taxonomic group. Chapter 1 required a collaborative effort in developing and testing a UCE probe set specifically designed for arachnids and their use in this study establishes the UCE approach as a valid and useful method for other harvestmen and arachnid researchers. These arachnid-specific UCEs have the potential to transform the field of arachnid systematics at all taxonomic levels, allowing efficient collection of 100s of loci from both freshly collected and museum-preserved specimens. In the context of integrative taxonomy, Chapter 2 resulted in a complete revision of the genus *Sclerobunus*, with description of five new species. The associated publication serves as a model taxonomic paper for harvestmen/arachnid researchers, bringing the current state of the fields of integrative taxonomy and species delimitation to a group in which taxonomic work is still largely based on traditional morphological approaches. Chapter 3 increased our understanding of how geology, geography, and climate affect patterns of genetic differentiation in the sky islands of southwestern North America, including insight into the genetic processes underlying the evolution of montane-restricted taxa.

A common theme from these chapters is how much there is still to be discovered and described in a taxonomic sense. Chapter 1 resulted in the description of a new family endemic to the Pacific Northwest of North America. While the genera were originally described in the 1970s, there unique and independent phylogenetic position is novel. Additionally, one of the species, *Cryptomaster behemoth* Starrett and Derkarabetian

2016, was described separately as a new species during the course of this research. The second chapter resulted in a complete revision of the genus *Sclerobunus*. Before my dissertation work, this genus only included two species; now there are 12, many of which are single-site endemics worthy of conservation attention. Since the completion and publication of this chapter several new undescribed *Sclerobunus* species have been uncovered, all of which were specimens unkown at the time of this research lying hidden in museum collections for decades. Finally, while no taxonomic work was done in Chapter 3, the phylogenetic results and and levels of genetic divergence suggest that *S. robustus* is likely made up of multiple cryptic species. Even in the relatively well-studied North America fauna, there is much waiting to be described.

APPENDIX A

Appendix A.1. Taxon sampling and sequencing statistics for Chapter 1. QC = quality control.

Voucher	Family	Species	Reads	Reads pass QC	Pass QC %	Contigs	UCE loci	total bp	mean length	50% loci	70% loci
OP4022	Occimastridae	*Cryptomaster behemoth*	5333005	4863561	91.2	262972	573	295712	516	346	105
OP3794	Occimastridae	*Cryptomaster leviathan*	6964535	6316217	90.7	272125	531	281317	530	314	126
OP1692	Occimastridae	*Speleomaster lexi*	5577654	4987279	89.4	305114	577	317649	551	321	140
OP1694	Occimastridae	*Speleomaster lexi*	3901723	3596856	92.2	196748	449	206219	459	251	134
OP2157	Paranonychidae	*Izunonychus ohruii*	6084646	5562118	91.4	377882	594	315464	531	315	135
OP2158	Paranonychidae	*Izunonychus ohruii*	5067606	4656703	91.9	366838	515	275653	535	307	134
OP3963	Paranonychidae	*Kainonychus akamai*	3348021	3015970	90.1	170561	395	195097	494	280	147
OP4222	Paranonychidae	*Kainonychus akamai*	5486832	4948427	90.2	243287	451	232499	516	285	131
OP4289	Paranonychidae	*Kaolinonychus coreanus*	17606592	16193452	92.0	892203	604	451061	747	261	127
OP4291	Paranonychidae	*Kaolinonychus coreanus*	17081213	15727941	92.1	907990	629	469174	746	280	117
OP4282	Paranonychidae	*Metanippononychus irei*	8914060	8112088	91.0	608550	669	426352	637	350	137
OP4076	Paranonychidae	*Metanippononychus tomishimai*	6360871	5805012	91.3	355938	543	282899	521	320	131
OP3704	Paranonychidae	*Metanonychus nigricans*	1313727	1227411	93.4	69908	502	357482	712	300	128
OP3744	Paranonychidae	*Metanonychus setulus*	7237544	6444996	89.0	414601	537	274115	510	310	129
OP4079	Paranonychidae	*Nippononychus japonicus*	7035917	6465594	91.9	515000	667	359653	539	359	103
OP4082	Paranonychidae	*Nippononychus japonicus*	6199509	5679562	91.6	457139	635	344151	542	351	145
OP3427	Paranonychidae	*Paranonychus brunneus*	8070407	7347599	91.0	195672	317	176460	557	224	110
OP3966	Paranonychidae	*Paranonychus fuscus*	4574849	4200897	91.8	188385	347	152175	439	251	128
OP3791	Paranonychidae	*Sclerobunus nondimorphicus*	6639823	5987156	90.2	385498	603	368963	612	315	98
OP1167	Paranonychidae	*Sclerobunus robustus*	4251886	3782834	89.0	250217	470	255093	543	278	130
OP3973	Paranonychidae	*Zuma acuta*	3357114	3103773	92.5	275565	541	290287	537	318	141
OP1047	Paranonychidae	*Zuma tioga*	2209747	1888919	85.5	153333	455	244588	538	314	139
OP3559	Travuniidae	*Briggsus bilobatus*	1148872	1093882	95.2	78959	556	416683	749	344	83
OP3625	Travuniidae	*Briggsus pacificus*	1355200	1267279	93.5	86176	530	380900	719	319	86

Voucher	Family	Species	Reads	Reads pass QC	Pass QC %	Contigs	UCE loci	total bp	mean length	50% loci	70% loci
OP1603	Travuniidae	*Erebomaster acanthinus*	5609996	5069444	90.4	262413	427	236718	554	275	147
OP3823	Travuniidae	*Erebomaster acanthinus*	4018325	3754740	93.4	248749	449	216410	482	303	111
OP2776	Travuniidae	*Holoscotolemon monzinii*	6482872	6045962	93.3	256859	488	210345	431	309	142
OP2771	Travuniidae	*Holoscotolemon unicolor*	4607886	4254043	92.3	220206	443	224217	506	290	133
OP3612	Travuniidae	*Isolachus spinosus*	9582977	8796083	91.8	609288	613	319025	520	356	129
OP3630	Travuniidae	*Isolachus spinosus*	6191985	5642668	91.1	338380	464	228898	493	305	149
OP2770	Travuniidae	*Peltonychia clavigera*	6818973	6310396	92.5	445330	660	374866	568	361	127
OP2768	Travuniidae	*Peltonychia lepreuri*	7215608	6587316	91.3	421655	682	417880	613	320	118
OP1679	Travuniidae	*Speleonychia sengeri*	10626874	9616265	90.5	735425	627	346954	553	350	142
OP1736	Travuniidae	*Speleonychia sengeri*	4596903	4201328	91.4	293407	473	231901	490	320	139
OP1610	Travuniidae	*Theromaster brunneus*	8281905	7562637	91.3	485101	559	310389	555	325	117
OP1626	Travuniidae	*Theromaster brunneus*	9743789	8934381	91.7	642496	579	323359	558	319	129
OP2508	*incertae sedis*	*Trojanella serbica*	7999346	7477528	93.5	403809	676	455308	674	340	119
OP4256	*incertae sedis*	*Yuria pulchra*	8182992	7378262	90.2	398045	498	270397	543	292	127
OP4263	*incertae sedis*	*Yuria pulchra*	7866796	6758709	85.9	519070	536	331186	618	302	117
OP4293	Synthetonychiidae	*Synthetonychia* sp.	9524832	8658412	90.9	629574	620	353527	570	342	148
OP4294	Synthetonychiidae	*Synthetonychia* sp.	2151926	1970199	91.6	104959	338	154602	457	239	148
OP4299	Triaenonychidae	*Americobunus ringueleti*	4759185	4361359	91.6	250286	332	147168	443	227	105
OP4300	Triaenonychidae	*Ankaratrix illota*	5717753	5303775	92.8	392990	422	201368	477	259	113
OP569	Triaenonychidae	*Bishopella laciniosa*	1486862	1385611	93.2	78555	434	283589	653	287	129
OP4296	Triaenonychidae	*Ceratomontia sp.*	6170833	5754767	93.3	279485	316	123612	391	218	140
OP4297	Triaenonychidae	*Chilenuncia donosoi*	1753649	1621015	92.4	27899	73	97413	1334	51	36
OP264	Triaenonychidae	*Fumontana deprehendor*	2246584	2044896	91.0	43425	338	175474	519	237	126
OP623	Triaenonychidae	*Fumontana deprehendor*	1265798	1174121	92.8	51466	465	304919	656	294	152
OP4295	Triaenonychidae	*Acumontia* sp.	3054430	2766040	90.6	196345	402	192148	478	254	112
OP4298	Triaenonychidae	*Nuncia* sp.	5932937	5503751	92.8	193532	190	75833	399	152	126
OP4301	Biantidae	*Hinzuanius* sp.	5854942	5389245	92.0	217649	265	111931	422	189	145

Voucher	Family	Species	Reads	Reads pass QC	Pass QC %	Contigs	UCE loci	total bp	mean length	50% loci	70% loci
OP3125	Cosmetidae	*Vonones* sp.	10553843	9729145	92.2	402414	262	99068	378	181	93
OP4292	Epedanidae	*Pseudobiantes japonica*	14974340	13684353	91.4	735172	527	266628	506	304	132
OP1089	Eupnoi	*Leiobunum calcar*	1315511	1242038	94.4	85406	378	260045	688	211	145
OP1518	Dyspnoi	*Sabacon cavicolens*	990843	907152	91.6	29863	321	206006	642	188	137
OP3383	Cyphophthalmi	*Siro* sp.	1260358	1179969	93.6	57803	508	352924	695	287	119
		Average Travunioidea	**6485861**	**5914495**	**91.2**	**366946**	**535**	**304295**	**563**	**310**	**126**
		Average all samples	**5927914**	**5416806**	**91.5**	**322995**	**483**	**272746**	**565**	**286**	**126**

APPENDIX B

Appendix B.1. Taxon sampling and voucher information for all samples included in genetic analyses.

Species	Locality	Date	Latitude/Longitude	SDSU Voucher	Collection
S. nondimorphicus	OR: Clackamas Co., FR 12 1.2 miles SE of jnct of SR 12/SR 20, nr. Rhododendron	11-May-11	45.3016, -121.8954	SDOP66	SD11_005
S. nondimorphicus	WA: King Co., Rattlesnake Lake, along Rattlesnake Ledge Trail, S of North Bend at I-90	30-Dec-02	47.4346, -121.7722	OP120	MCH02_208
S. nondimorphicus	OR: Clatsop Co., Ecola SP	10-Feb-07	45.9415, -123.9745	OP1056	MCH07-010
S. nondimorphicus	WA: Clallam Co., draw of creek draining Willoughby Lake, Willoughby Creek, near Shi Shi Beach, Olympic National Park.	21-Apr-07	48.2484, -124.6948	OP1638	CHR1638
S. idahoensis	ID: Shoshone Co., Hobo Cedar Grove Botonical Area, St Joe NF	25-Jul-11	47.0860, -116.1128	OP1649	SD11_018
S. idahoensis	ID: Idaho Co., Trib of Crooked Creek, FS 222 14.1 miles S of Red River Rd.	7-Jul-08	45.5791, -115.4431	OP2373	CHR2008_41
S. idahoensis	ID: Shoshone Co., Old River Rd, 16.7 miles NE of FS 9	29-Jul-08	47.6604, -116.1646	OP2413	CHR2008_91
S. idahoensis	MT: Mineral Co., Goose Creek, FS 282 9.7 miles S of Mullan Gulch Rd.	30-Jul-08	47.2279, -115.2464	OP2415	CHR2008_93
S. cavicolens	MT: Jefferson Co., Lewis and Clark Caverns State Park, Lewis and Clark Caverns, Paradise Room	4-Jul-08	45.8386, -111.8668	OP2143	SD08_027
S. cavicolens	MT: Jefferson Co., Lewis and Clark Caverns State Park, Lewis and Clark Caverns, Paradise Room	4-Jul-08	45.8386, -111.8668	OP2144	SD08_027
S. cavicolens	MT: Jefferson Co., Lewis and Clark Caverns State Park, Lewis and Clark Caverns, Paradise Room	4-Jul-08	45.8386, -111.8668	OP2145	SD08_027
S. ungulatus	NV: White Pine Co., GBNP, Model Cave	25-Jun-07	Withheld	OP1232	MCH 07_49
S. ungulatus	NV: White Pine Co., GBNP, Model Cave	25-Jun-07	Withheld	OP1233	MCH 07_49
S. madhousensis	UT: Utah Co., Professor Buss Cave	27-Apr-03	Withheld	OP239	M. Porter
S. madhousensis	UT: Utah Co., North Madhouse Cave	27-Apr-03	Withheld	OP240	M. Porter
S. steinmanni	CO: Boulder Co., Mallory Cave	29-Nov-08	Withheld	OP2568	DMNS 2008-75
S. steinmanni	CO: Boulder Co., Mallory Cave	15-Nov-12	Withheld	OP3108	DMNS2009-44.1

Species	Locality	Date	Latitude/Longitude	SDSU Voucher	Collection
S. steinmanni	CO: Boulder Co., Mallory Cave	15-Nov-12	Withheld	OP3109	DMNS2009-44.4
S. speoventus	CO: El Paso Co., Cave of the Winds, Manitou Springs	2-Jul-07	38.8704, -104.9216	OP1127	MCH 07_073
S. speoventus	CO: El Paso Co., Cave of the Winds, Manitou Springs	2-Jul-07	38.8704, -104.9216	OP1128	MCH 07_073
S. speoventus	CO: El Paso Co., Cave of the Winds, in Thieve's Canyon	12-Mar-09	38.8704, -104.9216	OP3110	DMNS2009-44.3
S. speoventus	CO: El Paso Co., Cave of the Winds, in Thieve's Canyon	12-Mar-09	38.8704, -104.9216	OP3111	DMNS2009-44.5
S. skywalkeri	NM: Cibola Co., Mt. Taylor, FR 193, 4.0 miles E of Hwy 547 in Lobo Canyon, NE of Grants	21-Jul-06	35.2318, -107.6388	OP903	MCH06_103
S. skywalkeri	NM: Torrance Co., Cibola NF, Manzano Mtns., road to Capillo Peak in Canon Huevo	19-Jul-06	34.6658, -106.3907	OP908	MCH06_096
S. skywalkeri	NM: Bernalillo Co., Sandia Mtns, 10.2 miles W of SR 14 along SR 536	3-Jun-08	35.2099, -106.4308	OP2101	SD08_015
S. glorietus	NM: Santa Fe Co., Glorieta Canyon, N of Gorieta Baptist Camp	20-Jul-06	35.6118, -105.7703	OP891	MCH06_099
S. glorietus	NM: Taos Co., Taos Ski Valley, 7.7 miles E of jnct. of Hwy 150E/Hwy 230 along Hwy 150E	20-Jul-06	36.5976, -105.4561	OP881	MCH06_100
S. glorietus	NM: Taos Co., Taos Ski Valley, 7.7 miles E of jnct. of Hwy 150E/Hwy 230 along Hwy 150E	20-Jul-06	36.5976, -105.4561	OP883	MCH06_100
S. glorietus	NM: Taos Co., Taos Ski Valley, 7.7 miles E of jnct. of Hwy 150E/Hwy 230 along Hwy 150E	3-Jul-07	36.5976, -105.4576	OP1169	MCH07_054
S. klomax	NM: Taos Co., vic. Taos Ski Valley, Hwy 150 NE of Arroyo Seco	20-Jul-06	36.5976, -105.4576	OP972	MCH06_100
S. klomax	NM: Taos Co., Taos Ski Valley, 7.7 miles E of jnct. of Hwy 150E/Hwy 230 along Hwy 150E	3-Jul-07	36.5976, -105.4576	OP1171	MCH07_054
S. robustus	CO: La Plata Co., vic. Haviland Lake CG, off Hwy 550, N of Durango	28-Jun-07	37.5329, -107.807	OP1224	MCH 07_057
S. robustus	CO: Archuleta Co., Pagosa Springs, Hwy 160, just E crossing San Juan River, hills south of highway	28-Jun-07	37.2682, -106.9992	OP1178	MCH 07_058

Species	Locality	Date	Latitude/Longitude	SDSU Voucher	Collection
S. robustus	UT: San Juan Co., Abajo Mtns., Manti La Sal NF, North Creek Road at crossing of North Creek, W of Monticello	27-Jun-07	37.8763, -109.4458	OP1131	MCH 07_052
S. robustus	CO: Dolores Co., Hwy 145, along Dolores River at FR 578	27-Jun-07	37.768, -107.9871	OP1148	MCH 07_055
S. robustus	AZ: Pima Co., Santa Catalina Mtns., vic. Sunset Trailhead	15-Jul-06	32.4265, -110.7424	OP965	MCH06_078
S. robustus	AZ: Cochise Co., Huachuca Mtns., upper Miller Canyon, Coronado NF	26-Mar-12	31.4066, -110.2874	OP2977	MCH12_011
S. robustus	NM: Sandoval Co., Hwy 4, Jemez Mtns., 3.9 miles W jnct. W Hwy 501 at Los Alamos	21-Jul-06	35.8384, -106.4044	OP887	MCH06_102
S. robustus	NM: Rio Arriba Co., N of Chama, along Hwy 17, 4.6 miles N jnct. of Hwy 17/US64	5-Jun-08	36.9394, -106.5493	OP2114	SD08_020
S. robustus	NM: Otero Co., HWY 244 SW of Silver Springs in Bradford Canyon, NE of Cloudcroft	19-Jul-06	32.978, -105.7087	OP959	MCH06_094
S. robustus	AZ: Cochise Co., Chiricahua Mtns., road to Barfoot Park, N of Buena Vista Peak	16-Jul-06	31.9179, -109.2725	OP1040	MCH06_082
S. robustus	CO: Mineral Co., S of Creede, along Deep Creek Rd. (Rd 550), 1.9 miles W Hwy 149	5-Jun-08	37.8140, -106.9147	OP2109	SD08_019
S. robustus	CO: Garfield Co., Hanging Lake Park, Hanging Lake Trail alond Dead Horse Creek	1-Aug-09	39.5985, -107.191	OP2680	SD09_002
S. nondimorphicus (transcriptome)	OR: Clackamas Co., FR 12 1.2 miles SE of jnct of SR 12/SR 20, nr. Rhododendron; Hedin et al., 2012	11-May-11	45.3016, -121.8954	OP2917	SD11_005
S. robustus (transcriptome)	AZ: Cochise Co., Huachuca Mtns., upper Miller Canyon, Coronado NF	26-Mar-12	31.4066, -110.2874	OP2981	MCH12_011
Theromaster brunneus (transcriptome)	NC: Buncombe Co., ~15 miles SW Asheville, Mt. Pisgah Hwy from Candler to Blue Ridge Pkw, 1.1 miles E Trillium Cove Lane	14-Jun-12	35.4497, -82.7226	OP3103	APP_11

Appendix B.2. Taxon sampling and voucher information for all samples included in morphometric analyses. Type column refers to type specimens used: H = holotype, P = paratype.

Species	Locality Info	Date	Latitude /Longitude	Collection	Sex	Voucher Information	Type
S. nondimorphicus	WA: Pacific Co., Ellsworth Creek Preserve, along Ellsworth Creek	2-Apr-08	46.4139 -123.8922	SD08_004	M	Morph_26	
S. nondimorphicus	WA: Lewis Co., Rainbow Falls State Park, 15.9 miles W of Chehalis River on SR 6	2-Apr-08	46.6302, -123.2318	SD08_002	M	Morph_30	
S. nondimorphicus	OR: Benton Co., Mary's Peak Campground, end of Mary's Peak Rd.	1-Oct-10	44.5091, -123.5605	SD10_005	M	Morph_71	
					F	Morph_42F	
S. nondimorphicus	WA: King Co., Rattlesnake Lake, along Rattlesnake Ledge Trail, S of North Bend at I-90	30-Dec-02	47.4346, -121.7722	MCH02_208	F	Morph_43F	
S. nondimorphicus	OR: Clackamas Co., Mermaloose Trail, 12.0 miles S of US 224 along FR 45	16-Aug-11	45.0986, -122.2219	SD11_028	M	Morph_72	
S. nondimorphicus	OR: Clackamas Co., FR 12 1.2 miles SE of jnct. of SR 12/SR 20, nr. Rhododendron	11-May-11	45.3016, -121.8954	SD11_005	F	SDOP67, Morph_44F	
S. nondimorphicus	OR: Clatsop Co., Lee Wooden Park, SR 202 4.3 miles N of SR 103	16-Jun-07	45.9576, -123.5815	CHR1695, 1996	M	CHR1695, Morph_73	
					F	CHR1696, Morph_45F	
S. nondimorphicus	WA: Lewis Co., Tributary of Iron Creek, NF 25 4.6 miles South of NF 300, Gifford Pinchot National Forest.	6-Aug-08	46.4033, -121.9902	CHR2483	M	CHR2483, Morph_74	
S. nondimorphicus	WA: Jefferson Co., Cedar Creek, E of US101, access from Ruby Beach.	4-Aug-08	47.7105, -124.4095	CHR1535	M	CHR1535, Morph_75	
S. idahoensis	ID: Idaho Co., Trib of Crooked Creek, FS 222 14.1 miles S of Red River Rd.	7-Jul-08	45.5791, -115.4431	CHR2008_41	M	Morph_28	
					M	Morph_29	
S. idahoensis	ID: Idaho Co., Grouse Creek, FS 1299 1.9 miles SW of Hungary Ridge Rd.	6-Jul-08	45.8120, -115.9530	CHR2008_37	M	Morph_55	
					F	Morph_30F	
S. idahoensis	ID: Idaho Co., FS 443 0.8 miles S of Selway River Rd.	6-Jul-08	46.0385, -115.2943	CHR2008_35	M	Morph_56	
					F	Morph_31F	
S. idahoensis	ID: Idaho Co., DeVoto Memorial Cedar Grove	5-Jul-08	46.5389,	CHR2008_31	M	Morph_57	

Species	Locality Info	Date	Latitude /Longitude	Collection	Sex	Voucher Information	Type
			-114.6762		F	Morph_32F	
S. idahoensis	ID: Kootenai Co., Rose Lake, 1.5 miles N of US 3 on S Rose Creek Rd.	23-Jul-11	47.5531, -116.4967	SD11_015	M	Morph_58	
					F	Morph_33F	
S. idahoensis	ID: Shoshone Co., Hobo Cedar Grove Botonical Area, St Joe NF	25-Jul-11	47.0860, -116.1128	SD11_018	M	Morph_59	
					F	Morph_34F	
S. idahoensis	ID: Clearwater Co., Rhodes Creek, FS 250 2.0 miles SE of SR 11	19-Jul-08	46.4767, -115.7809	CHR2008_65	M	Morph_60	
					F	Morph_35F	
S. idahoensis	ID: Shoshone Co., Placer Creek Rd. 4.6 miles SE of High St	29-Jul-08	47.4303, -115.8913	CHR2008_92	M	Morph_61	
					F	Morph_36F	
S. idahoensis	MT: Mineral Co., FS 320 9.3 miles S of Frontage Rd of I-90	10-Jul-12	47.1102, -115.0095	CHR2008_50	M	OP2378.1, Morph_65	
					M	OP2378.2, Morph_66	
S. idahoensis	MT: Mineral Co., Goose Creek, FS 282 9.7 miles S of Mullan Gulch Rd	30-Jul-08	47.2279, -115.2464	CHR2008_93	M	Morph_67	
					F	Morph_39F	
S. idahoensis	MT: Mineral Co., Deep Creek, Trout Creek Rd., 9.7 miles SW Diamond Match Rd.	30-Jul-08	47.0464, -114.9503	CHR2008_94	F	OP2416	
S. steinmanni	CO: Boulder Co., Mallory Cave	29-Nov-08	Withheld	DMNS2008-75	M	OP2658, DMNS 2008-75, Morph_31	H
S. steinmanni	CO: Boulder Co., Mallory Cave	15-Nov-12	Withheld	DMNS2009-44	M	OP3108, DMNS 2012-117.1, Morph_36	P
					F	DMNS 2012-117.2, Morph_12F	P
					F	DMNS 2012-117.3, Morph_13F	P
					F	OP3109,	P

Species	Locality Info	Date	Latitude /Longitude	Collection	Sex	Voucher Information	Type
						DMNS 2012-117.4, Morph_14F	
S. speoventus	CO: El Paso Co., Cave of the Winds, in Thieve's Canyon	12-Mar-09	38.8704, -104.9216	DMNS 2009-44	M	DMNS 2009-44.1, Morph_37	P
					M	DMNS 2009-44.2, Morph_38	P
					M	OP3110, DMNS 2009-44.3, Morph_39	P
					M	DMNS 2009-44.6, Morph_40	H
					M	OP3111, DMNS 2009-44.5, Morph_42	P
					F	DMNS 2009-44.4, Morph_16F	P
S. speoventus	CO: El Paso Co., Cave of the Winds, Manitou Springs	2-Jul-07	38.8704, -104.9216	MCH 07_073	M	OP1128, Morph_41	
					F	OP1127, Morph_17F	
					F	OP1129, Morph_18F	
S. speoventus	CO: El Paso Co., Cave of the Winds, Manitou Springs	2-Jul-07	38.8704, -104.9216	MCH 07_073	M	Morph_6	
S. speoventus	CO: El Paso Co., Cave of the Winds, Manitou Grand Caverns, Old Water Barrel	2-Feb-84	38.8704, -104.9216	CAS	F	CAS.1, Morph_15F	
S. speoventus	CO: El Paso Co., Cave of the Winds		38.8704, -104.9216	MCH 07_073	F	Morph_19F	

Species	Locality Info	Date	Latitude /Longitude	Collection	Sex	Voucher Information	Type
S. robustus	CO: Gilpin Co., Apex Valley Rd., jnct with HWY 119, 1.7 miles N of Black Hawk	31-Jul-09	39.8192, -105.5132	SD09_004	M	Morph_32	
					M	Morph_33	
					F	Morph_9F	
S. robustus	NM: Otero Co., HWY 244 SW of Silver Springs in Bradford Canyon, NE of Cloudcroft	19-Jul-06	32.978, -105.7087	MCH06_094	M	Morph_15	
					M	Morph_16	
S. robustus	CO: Rio Grande Co., Church Creek Trailhead, SW of South Fork, off Hwy 160	28-Jun-07	37.6481, -106.6520	MCH07_059	M	Morph_1	
					M	Morph_2	
S. robustus	CO: Garfield Co., Hanging Lake Park, Hanging Lake Trail alond Dead Horse Creek	1-Aug-09	39.5985, -107.191	SD09_005	M	Morph_34	
					M	Morph_35	
					F	OP2678, Morph_10F	
					F	OP2679, Morph_11F	
S. robustus	AZ: Pima Co., Santa Catalina Mtns., vic. Sunset Trailhead	15-Jul-06	32.4265, -110.7424	MCH06_078	M	Morph_12	
					M	Morph_13	
					M	Morph_14	
S. glorietus	NM: Taos Co., Taos Ski Valley, 7.7 miles E of jnct. of SR 150E/SR 230 alonf SR 150E	4-Jun-08	36.5976, -105.4561	SD08_017	M	Morph_9	
					F	Morph_2F	
S. glorietus	NM: Taos Co., Taos Ski Valley, 7.7 miles E of jnct. of SR 150E/SR 230 alonf SR 150E	20-Jul-06	36.5976, -105.4561	MCH06_100	M	OP882, Morph_19	
					M	OP883, Morph_20	
S. glorietus	NM: Taos Co., Taos Ski Valley, 7.7 miles E of jnct. of SR 150E/SR 230 alonf SR 150E	3-Jul-07	36.5976, -105.4576	MCH07_076	F	Morph 1F	
S. glorietus	NM: Santa Fe Co., Glorieta Canyon, N of Gorieta Baptist Camp	20-Jul-06	35.6118, -105.7703	MCH06_099	M	Morph_45	
					M	OP891, Morph_46	
					F	Morph_24F	
S. skywalkeri	NM: Torrance Co., Cibola NF, Manzano Mtns.,	19-Jul-06	34.6658, -	MCH06_096	M	Morph_47	H

Species	Locality Info	Date	Latitude /Longitude	Collection	Sex	Voucher Information	Type
	road to Capillo Peak in Canon Huevo		106.3907		M	Morph_48	P
					F	Morph_25F	P
S. skywalkeri	NM: Cibola Co., Mt. Taylor, FR 193, 4.0 miles E of Hwy 547 in Lobo Canyon, NE of Grants	21-Jul-06	35.2318, -107.6388	MCH06_103	M	Morph_49	P
					M	GBH2013.0005.1, Morph_50	
					F	Morph_26F	P
S. skywalkeri	NM: Cibola Co., Mt. Taylor	11-Aug-13	35.2412, -107.6082	GBH2013.0005	F	Morph_27F	P
S. skywalkeri	NM: Bernalillo Co., Sandia Mtns, 10.2 miles W of SR 14 along SR 536	3-Jun-08	35.2099, -106.4308	SD08_015	M	Morph_51	P
					M	Morph_52	P
S. klomax	NM: Taos Co., Taos Ski Valley, 7.7 miles E of jnct. of SR 150E/SR 230 alonf SR 150E	30-Jul-09	36.5973, -105.4564	SD09_001	F	Morph_8F	P
S. klomax	NM: Taos Co., vic. Taos Ski Valley, Hwy 150 NE of Arroyo Seco	20-Jul-06	36.5976, -105.4576	MCH06_100	F	OP972, Morph_3F	P
S. klomax	NM: Taos Co., Taos Ski Valley, 7.7 miles E of jnct. of SR 150E/SR 230 alonf SR 150E	3-Jul-07	36.5976, -105.4576	MCH 07_076	F	OP1171, Morph_4F	H
S. jemez	NM: Santa Fe Co., Terrero Cave	18-Jun-79	Withheld	CAS	M	CAS.1, Morph_53	H
					M	CAS.2, Morph_54	P
					F	CAS.3, Morph_28F	P
					F	CAS.4, Morph_29F	P
S. cavicolens	MT: Jefferson Co., Lewis and Clark Caverns State Park, Lewis and Clark Caverns, Paradise Room	4-Jul-08	45.8386, -111.8668	SD08_027	M	Morph_3	
					M	OP2145, Morph_24	
					F	OP2144, Morph_46F	
S. cavicolens	MT: Jefferson Co., Morrison Cave, Big Spring Room, 60 mi W Bozeman	22-Feb-41	45.8386, -111.8668	AMNH	M	AMNH.1, Morph_4	
S. ungulatus	NV: White Pine Co., GBNP, Model Cave	25-Jun-07	Withheld	MCH07_049	M	GBPA:427-8394,	

Species	Locality Info	Date	Latitude /Longitude	Collection	Sex	Voucher Information	Type
						Morph_10	
					M	GBPA:427-8395, Morph_11	
					M	OP1232, Morph_22	
S. madhousensis	UT: Utah Co., Professor Buss Cave	27-Apr-03	Withheld	M. Porter	M	OP239, Morph_17	
S. madhousensis	UT: Utah Co., North Madhouse Cave	27-Apr-03	Withheld	M. Porter	M	OP240, Morph_18	

Appendix B.3. Male morphometric dataset. Values highlighted in grey are missing values estimated via Multiple Imputation (see methods). ScuL = scute length, ScuWO = scute width at opisthosoma, ScuWA = scute width anteriorly, TH/W = tubercle height/width, GenOL/W = genital operculum length/width, PalFD = palpal femur depth, Che1/2W/L = cheliceral segment 1/2 length/width, LII = leg II, TrL = trochanter length, FeL = femur length, PaL = patella length, TiL = tibia length, ML = metatarsus length, TL = tarsus length.

Species	Voucher Number	Scu L	Scu WO	Scu WA	Eye TH	Eye TW	Gen OL	Gen OW	Pal FD	Che 1L	Che 1W	Che 2L	Che 2W	LII TrL	LII FeL	LII PaL	LII TiL	LII ML	LII TL
S. steinmanni	OP2658, DMNS 2008-75, Morph_31	2.38	2.64	1.74	0.13	0.31	0.42	0.42	0.68	0.54	0.30	0.97	0.32	0.53	2.94	1.03	2.64	3.00	2.30
S. steinmanni	OP3108, DMNS 2012-117.1, Morph_36	2.39	2.48	1.63	0.13	0.29	0.38	0.41	0.61	0.63	0.29	0.93	0.32	0.55	2.77	0.96	2.45	2.81	2.30
S. speoventus	DMNS 2009-44.1, Morph_37	1.98	2.13	1.38	0.11	0.26	0.34	0.39	0.51	0.49	0.26	0.90	0.30	0.44	2.43	0.83	2.14	2.46	2.06
S. speoventus	DMNS 2009-44.2, Morph_38	2.20	2.30	1.45	0.09	0.27	0.34	0.37	0.58	0.51	0.28	0.89	0.32	0.44	2.44	0.85	2.18	2.51	2.02
S. speoventus	OP3110, DMNS 2009-44.3, Morph_39	2.16	2.30	1.50	0.09	0.25	0.36	0.38	0.61	0.60	0.28	0.93	0.31	0.46	2.51	0.89	2.21	2.50	2.00
S. speoventus	DMNS 2009-44.6, Morph_40	1.94	2.10	1.35	0.09	0.24	0.32	0.37	0.49	0.53	0.25	0.83	0.28	0.42	2.50	0.80	2.26	2.59	2.25
S. speoventus	OP1128, Morph_41	1.96	2.15	1.40	0.11	0.28	0.36	0.36	0.52	0.63	0.26	0.87	0.30	0.47	2.66	0.83	2.34	2.74	2.30
S. speoventus	Morph_6	1.93	2.10	1.38	0.07	0.26	0.33	0.37	0.50	0.59	0.26	0.89	0.29	0.44	2.63	0.84	2.25	2.66	2.17
S. speoventus	OP3111, DMNS 2009-44.5, Morph_42	2.02	2.16	1.41	0.12	0.25	0.33	0.37	0.53	0.45	0.25	0.87	0.29	0.43	2.40	0.87	2.11	2.45	2.11
S. robustus	Morph_32	2.42	2.45	1.52	0.16	0.31	0.35	0.39	0.65	0.57	0.30	0.82	0.32	0.47	1.86	0.68	1.65	1.84	1.26
S. robustus	Morph_33	2.34	2.34	1.50	0.14	0.32	0.34	0.41	0.68	0.61	0.31	0.83	0.32	0.46	1.86	0.67	1.62	1.88	1.27
S. robustus	Morph_15	2.08	2.03	1.35	0.12	0.29	0.33	0.39	0.60	0.51	0.26	0.75	0.28	0.37	1.39	0.59	1.23	1.38	0.98
S. robustus	Morph_16	1.91	1.89	1.28	0.15	0.29	0.33	0.37	0.54	0.51	0.25	0.70	0.28	0.37	1.31	0.56	1.18	1.28	0.93
S. robustus	Morph_1	2.34	2.46	1.51	0.13	0.33	0.37	0.41	0.70	0.55	0.27	0.86	0.27	0.41	1.68	0.69	1.47	1.68	1.24
S. robustus	Morph_2	2.34	2.33	1.52	0.14	0.33	0.35	0.38	0.67	0.51	0.22	0.87	0.31	0.43	1.75	0.64	1.53	1.68	1.20
S. robustus	Morph_34	2.22	2.38	1.50	0.12	0.27	0.31	0.37	0.61	0.52	0.27	0.77	0.29	0.47	1.90	0.68	1.68	1.86	1.29
S. robustus	Morph_35	2.00	2.05	1.31	0.16	0.27	0.31	0.39	0.53	0.53	0.27	0.77	0.27	0.45	1.87	0.65	1.62	1.87	1.33
S. robustus	Morph_12	2.63	2.70	1.66	0.18	0.34	0.39	0.43	0.81	0.69	0.32	0.98	0.34	0.48	1.82	0.72	1.57	1.80	1.12
S. robustus	Morph_13	2.50	2.52	1.60	0.17	0.37	0.38	0.40	0.82	0.67	0.32	0.93	0.34	0.48	1.72	0.73	1.54	1.68	1.07

Species	Voucher Number	Scu L	Scu WO	Scu WA	Eye TH	Eye TW	Gen OL	Gen OW	Pal FD	Che 1L	Che 1W	Che 2L	Che 2W	LII TrL	LII FeL	LII PaL	LII TiL	LII ML	LII TL
S. robustus	Morph_14	2.59	2.72	1.66	0.14	0.33	0.36	0.43	0.80	0.64	0.31	0.92	0.35	0.52	1.77	0.75	1.57	1.78	1.12
S glorietus	Morph_9	1.69	1.80	1.09	0.09	0.24	0.28	0.36	0.37	0.34	0.21	0.63	0.23	0.31	1.08	0.47	0.96	0.99	0.89
S glorietus	OP882, Morph_19	1.81	1.79	1.15	0.09	0.26	0.30	0.38	0.38	0.40	0.22	0.65	0.24	0.33	1.21	0.50	1.03	1.12	0.93
S glorietus	OP883, Morph_20	1.71	1.72	1.06	0.11	0.22	0.27	0.33	0.37	0.38	0.21	0.60	0.23	0.31	1.09	0.47	0.96	1.03	0.91
S glorietus	Morph_45	1.73	1.69	1.08	0.11	0.24	0.28	0.34	0.43	0.36	0.21	0.61	0.24	0.32	1.11	0.47	0.98	1.02	0.78
S glorietus	OP891, Morph_46	1.83	1.82	1.09	0.13	0.27	0.27	0.33	0.40	0.44	0.21	0.64	0.24	0.34	1.13	0.49	1.06	1.09	0.93
S. skywalkeri	Morph_47	2.05	1.98	1.27	0.16	0.28	0.29	0.35	0.54	0.56	0.23	0.74	0.26	0.40	1.48	0.54	1.25	1.46	0.99
S. skywalkeri	Morph_48	2.00	1.96	1.32	0.16	0.29	0.30	0.38	0.54	0.51	0.25	0.73	0.26	0.41	1.43	0.57	1.22	1.42	1.02
S. skywalkeri	Morph_49	1.91	1.92	1.23	0.13	0.26	0.29	0.36	0.52	0.44	0.23	0.63	0.24	0.38	1.33	0.50	1.15	1.22	0.91
S. skywalkeri	GBH2013.0005.1, Morph_50	2.06	2.06	1.31	0.10	0.27	0.31	0.39	0.59	0.52	0.27	0.69	0.27	0.39	1.36	0.54	1.17	1.18	0.94
S. skywalkeri	Morph_51	2.11	2.10	1.30	0.16	0.28	0.30	0.37	0.53	0.50	0.24	0.71	0.27	0.39	1.44	0.57	1.28	1.33	0.93
S. skywalkeri	Morph_52	2.19	2.01	1.30	0.20	0.28	0.29	0.36	0.50	0.54	0.23	0.71	0.27	0.40	1.37	0.54	1.25	1.35	0.96
S. jemez	CAS.1, Morph_53	2.00	1.88	1.25	0.09	0.23	0.29	0.32	0.42	0.40	0.21	0.75	0.24	0.40	2.04	0.71	1.87	1.96	2.11
S. jemez	CAS.2, Morph_54	1.93	1.96	1.23	0.10	0.23	0.30	0.33	0.41	0.50	0.23	0.74	0.25	0.42	2.08	0.69	1.72	1.86	2.02
S. idahoensis	Morph_28	2.38	2.53	1.58	0.18	0.39	0.45	0.49	0.55	0.48	0.29	0.84	0.31	0.50	2.08	0.76	1.77	2.06	1.38
S. idahoensis	Morph_29	2.27	2.47	1.55	0.18	0.38	0.41	0.48	0.56	0.41	0.28	0.79	0.32	0.48	2.01	0.74	1.68	1.94	1.30
S. idahoensis	Morph_55	2.30	2.43	1.49	0.18	0.37	0.41	0.50	0.50	0.39	0.22	0.81	0.32	0.49	2.08	0.79	1.72	1.91	1.43
S. idahoensis	Morph_56	2.30	2.46	1.57	0.22	0.39	0.43	0.48	0.54	0.61	0.29	0.85	0.31	0.48	2.15	0.78	1.82	2.10	1.32
S. idahoensis	Morph_57	2.41	2.53	1.59	0.21	0.37	0.43	0.50	0.57	0.46	0.29	0.83	0.32	0.49	2.04	0.73	1.68	1.92	1.28
S. idahoensis	Morph_58	2.23	2.30	1.52	0.16	0.34	0.42	0.45	0.53	0.66	0.28	0.80	0.31	0.47	1.92	0.71	1.86	1.85	1.26
S. idahoensis	Morph_59	2.39	2.48	1.56	0.17	0.38	0.42	0.49	0.50	0.57	0.30	0.85	0.31	0.50	1.94	0.73	1.62	1.80	1.26
S. idahoensis	Morph_60	2.41	2.48	1.59	0.19	0.41	0.43	0.51	0.55	0.48	0.30	0.89	0.32	0.49	2.13	0.79	1.77	2.03	1.39
S. idahoensis	Morph_61	2.24	2.24	1.44	0.16	0.37	0.41	0.46	0.49	0.53	0.28	0.79	0.29	0.45	1.94	0.71	1.61	1.80	1.31
S. idahoensis	OP2378.1, Morph_65	2.26	2.42	1.45	0.14	0.36	0.44	0.51	0.49	0.46	0.27	0.83	0.31	0.47	1.98	0.73	1.68	1.86	1.38
S. idahoensis	OP2378.2, Morph_66	2.16	2.33	1.46	0.17	0.36	0.42	0.46	0.47	0.43	0.27	0.81	0.29	0.46	1.92	0.72	1.62	1.90	1.30
S. idahoensis	Morph_67	2.49	2.73	1.73	0.26	0.43	0.48	0.58	0.58	0.57	0.32	0.93	0.34	0.52	2.34	0.85	1.93	2.28	1.50

Species	Voucher Number	Scu L	Scu WO	Scu WA	Eye TH	Eye TW	Gen OL	Gen OW	Pal FD	Che 1L	Che 1W	Che 2L	Che 2W	LII TrL	LII FeL	LII PaL	LII TiL	LII ML	LII TL
S. nondimorphicus	Morph_26	2.33	2.31	1.59	0.19	0.39	0.44	0.47	0.55	0.51	0.29	0.91	0.31	0.47	2.43	0.83	1.96	2.14	1.59
S. nondimorphicus	Morph_30	2.34	2.48	1.58	0.19	0.39	0.45	0.51	0.53	0.54	0.29	0.89	0.31	0.49	2.36	0.82	2.03	2.18	1.60
S. nondimorphicus	Morph_71	2.44	2.52	1.60	0.17	0.41	0.42	0.52	0.52	0.57	0.30	0.87	0.32	0.52	2.24	0.79	1.93	2.18	1.49
S. nondimorphicus	Morph_72	2.43	2.59	1.68	0.23	0.38	0.47	0.52	0.54	0.57	0.31	0.91	0.32	0.54	2.38	0.79	2.03	2.38	1.45
S. nondimorphicus	CHR1695, Morph_73	2.33	2.35	1.59	0.19	0.38	0.47	0.49	0.53	0.57	0.30	0.88	0.31	0.50	2.36	0.76	1.90	2.25	1.50
S. nondimorphicus	CHR2483, Morph_74	2.50	2.56	1.63	0.19	0.40	0.46	0.51	0.60	0.58	0.30	0.90	0.34	0.52	2.43	0.81	2.00	2.35	1.46
S. nondimorphicus	CHR1535, Morph_75	2.28	2.45	1.58	0.19	0.38	0.43	0.51	0.53	0.56	0.28	0.90	0.32	0.51	2.28	0.78	2.00	2.32	1.58
S. cavicolens	Morph_3	1.68	1.65	1.06	0.08	0.23	0.32	0.38	0.31	0.46	0.21	0.70	0.15	0.34	2.10	0.63	1.82	1.88	2.11
S. cavicolens	AMNH.1, Morph_4	1.58	1.76	1.09	0.08	0.23	0.30	0.37	0.31	0.42	0.21	0.71	0.22	0.35	2.09	0.64	1.79	1.94	2.15
S. cavicolens	OP2145, Morph_24	1.64	1.66	1.06	0.08	0.22	0.30	0.36	0.30	0.42	0.21	0.67	0.21	0.35	2.08	0.64	1.36	1.91	1.95
S. ungulatus	GBPA:427-8394, Morph_10	2.17	2.18	1.54	0.09	0.27	0.39	0.41	0.41	0.53	0.28	0.94	0.23	0.52	3.48	0.94	3.03	3.20	3.08
S. ungulatus	GBPA:427-8395, Morph_11	2.17	2.15	1.51	0.08	0.29	0.36	0.44	0.43	0.52	0.28	0.94	0.23	0.54	3.52	0.94	3.06	3.29	3.13
S. ungulatus	OP1232, Morph_22	2.15	2.27	1.41	0.09	0.28	0.35	0.41	0.43	0.61	0.28	0.91	0.30	0.52	3.30	0.91	2.92	2.98	3.00
S. madhousensis	OP240, Morph_18	1.91	1.92	1.29	0.08	0.22	0.31	0.37	0.37	0.47	0.23	0.75	0.24	0.43	2.80	0.79	2.44	2.56	2.63
S. madhousensis	OP239, Morph_17	1.94	1.98	1.32	0.12	0.22	0.30	0.35	0.38	0.48	0.24	0.82	0.25	0.42	2.66	0.77	2.37	2.20	2.45

Appendix B.4. Female morphometric dataset. Values highlighted in grey are missing values estimated via Multiple Imputation (see methods). ScuL = scute length, ScuWO = scute width at opisthosoma, ScuWA = scute width anteriorly, TH/W = tubercle height/width, GenOL/W = genital operculum length/width, PalFD = palpal femur depth, Che1/2W/L = cheliceral segment 1/2 length/width, LII = leg II, TrL = trochanter length, FeL = femur length, PaL = patella length, TiL = tibia length, ML = metatarsus length, TL = tarsus length.

Species	Voucher Number	Scu L	Scu WO	Scu WA	Eye TH	Eye TW	Gen OL	Gen OW	Pal FD	Che 1L	Che 1W	Che 2L	Che 2W	LII TrL	LII FeL	LII PtL	LII TiL	LII ML	LII TL
S. steinmanni	DMNS 2012-117.2, Morph_12F	2.46	2.69	1.58	0.13	0.30	0.34	0.42	0.52	0.61	0.28	0.97	0.31	0.54	2.61	0.93	2.33	2.50	1.99
S. steinmanni	DMNS 2012-117.3, Morph_13F	2.40	2.64	1.59	0.13	0.31	0.35	0.43	0.49	0.58	0.28	0.93	0.29	0.54	2.59	0.88	2.30	2.41	1.94
S. steinmanni	OP3109, DMNS 2012-117.4, Morph_14F	2.33	2.58	1.59	0.12	0.30	0.38	0.44	0.49	0.61	0.26	0.97	0.29	0.55	2.45	0.88	2.18	2.40	1.96
S. speoventus	CAS.1, Morph_15F	2.06	1.88	1.27	0.08	0.25	0.30	0.38	0.38	0.51	0.24	0.88	0.27	0.38	2.40	0.77	2.09	2.39	2.08
S. speoventus	DMNS 2009-44.4, Morph_16F	2.10	2.38	1.40	0.13	0.26	0.32	0.36	0.43	0.49	0.27	0.89	0.29	0.43	2.24	0.82	2.15	2.20	1.93
S. speoventus	OP1127, Morph_17F	1.98	2.18	1.33	0.11	0.24	0.32	0.39	0.39	0.48	0.24	0.82	0.28	0.43	2.25	0.80	1.97	2.20	1.99
S. speoventus	OP1129, Morph_18F	1.96	2.16	1.35	0.11	0.21	0.30	0.34	0.41	0.57	0.26	0.89	0.29	0.46	2.35	0.78	2.05	2.28	1.97
S. speoventus	Morph_19F	1.97	2.19	1.29	0.12	0.25	0.33	0.36	0.43	0.57	0.44	0.88	0.28	0.46	2.33	0.74	1.96	2.21	1.99
S. robustus	Morph_9F	2.11	2.37	1.49	0.13	0.27	0.32	0.42	0.43	0.48	0.26	0.78	0.28	0.44	1.66	0.63	1.49	1.60	1.13
S. robustus	OP2678, Morph_10F	2.29	2.47	1.42	0.14	0.27	0.32	0.41	0.44	0.48	0.27	0.78	0.28	0.43	1.62	0.62	1.48	1.55	1.19
S. robustus	OP2679, Morph_11F	2.35	2.63	1.46	0.14	0.27	0.32	0.42	0.46	0.49	0.27	0.77	0.28	0.44	1.75	0.64	1.56	1.64	1.25
S. glorietus	Morph_1F	1.74	1.74	1.01	0.09	0.22	0.23	0.34	0.28	0.33	0.21	0.58	0.22	0.30	1.06	0.44	0.90	0.94	0.81
S. glorietus	Morph_2F	1.78	1.72	1.02	0.09	0.24	0.27	0.37	0.29	0.33	0.21	0.59	0.22	0.30	1.04	0.46	0.94	0.96	0.84
S. glorietus	Morph_24F	1.80	1.88	1.03	0.12	0.22	0.26	0.33	0.28	0.33	0.20	0.59	0.23	0.33	1.16	0.46	0.98	0.96	0.90
S. skywalkeri	Morph_25F	2.00	1.93	1.22	0.17	0.24	0.30	0.36	0.31	0.47	0.23	0.66	0.23	0.36	1.27	0.51	1.05	1.11	0.89
S. skywalkeri	Morph_26F	1.84	1.84	1.08	0.13	0.22	0.27	0.38	0.29	0.38	0.21	0.60	0.22	0.29	1.07	0.48	0.92	0.98	0.84
S. skywalkeri	Morph_27F	1.81	1.87	1.11	0.13	0.24	0.30	0.36	0.32	0.43	0.23	0.64	0.24	0.30	1.07	0.47	0.91	0.94	0.75

Species	Voucher Number	Scu L	Scu WO	Scu WA	Eye TH	Eye TW	Gen OL	Gen OW	Pal FD	Che 1L	Che 1W	Che 2L	Che 2W	LII TrL	LII FeL	LII PtL	LII TiL	LII ML	LII TL
S. klomax	Morph_8F	1.63	1.72	1.08	0.09	0.20	0.21	0.32	0.29	0.47	0.20	0.67	0.22	0.38	1.93	0.57	1.55	1.57	2.04
S. klomax	OP972, Morph_3F	1.82	1.95	1.16	0.10	0.20	0.26	0.34	0.32	0.37	0.21	0.70	0.22	0.41	2.06	0.63	1.77	1.67	2.09
S. klomax	OP1171, Morph_4F	1.85	1.94	1.17	0.08	0.19	0.29	0.36	0.33	0.39	0.22	0.72	0.23	0.41	2.09	0.67	1.84	1.93	1.96
S. jemez	CAS.3, Morph_28F	1.94	1.94	1.23	0.11	0.22	0.31	0.36	0.32	0.60	0.23	0.88	0.24	0.40	2.04	0.64	1.64	1.73	1.93
S. jemez	CAS.4, Morph_29F	1.97	1.94	1.23	0.09	0.21	0.31	0.38	0.33	0.42	0.22	0.71	0.24	0.42	1.96	0.62	1.62	1.67	1.79
S. idahoensis	Morph_30F	2.49	2.70	1.51	0.21	0.39	0.42	0.51	0.41	0.57	0.28	0.84	0.29	0.43	2.00	0.74	1.68	1.85	1.33
S. idahoensis	Morph_31F	2.30	2.40	1.46	0.19	0.37	0.41	0.47	0.41	0.41	0.28	0.81	0.28	0.46	2.05	0.74	1.76	1.98	1.26
S. idahoensis	Morph_32F	2.36	2.63	1.49	0.21	0.37	0.43	0.52	0.43	0.41	0.29	0.82	0.29	0.48	1.85	0.72	1.58	1.75	1.18
S. idahoensis	Morph_33F	2.30	2.40	1.46	0.18	0.36	0.41	0.46	0.39	0.36	0.26	0.80	0.28	0.43	1.72	0.69	1.48	1.64	1.12
S. idahoensis	Morph_34F	2.55	2.59	1.55	0.16	0.38	0.37	0.53	0.42	0.57	0.29	0.86	0.31	0.45	1.78	0.68	1.54	1.67	1.15
S. idahoensis	Morph_35F	2.44	2.59	1.49	0.20	0.38	0.41	0.46	0.42	0.56	0.28	0.84	0.30	0.47	1.99	0.78	1.70	1.88	1.31
S. idahoensis	Morph_36F	2.38	2.50	1.41	0.17	0.36	0.40	0.48	0.41	0.40	0.27	0.80	0.28	0.43	1.72	0.66	1.48	1.68	1.19
S. idahoensis	Morph_39F	2.69	2.83	1.69	0.23	0.41	0.46	0.53	0.43	0.53	0.32	0.91	0.32	0.47	2.06	0.80	1.64	2.00	1.27
S. idahoensis	OP2416, Morph_40F	2.40	2.67	1.52	0.17	0.39	0.46	0.51	0.41	0.49	0.28	0.83	0.29	0.47	1.92	0.72	1.59	1.79	1.25
S. nondimorphicus	Morph_42F	2.52	2.75	1.60	0.17	0.40	0.43	0.55	0.42	0.61	0.30	0.88	0.31	0.48	2.15	0.73	1.81	2.08	1.33
S. nondimorphicus	Morph_43F	2.36	2.66	1.54	0.18	0.39	0.42	0.55	0.41	0.62	0.28	0.86	0.30	0.57	2.03	0.70	1.64	1.92	1.40
S. nondimorphicus	Morph_44F	2.50	2.75	1.60	0.21	0.40	0.45	0.56	0.44	0.49	0.28	0.85	0.31	0.51	2.20	0.79	1.97	2.30	1.40
S. nondimorphicus	CHR1696, Morph_45F	2.53	2.66	1.62	0.22	0.37	0.47	0.56	0.43	0.68	0.28	0.88	0.31	0.51	2.15	0.79	1.86	2.15	1.38
S. cavicolens	OP2144, Morph_46F	1.67	1.78	1.07	0.09	0.23	0.29	0.39	0.26	0.38	0.21	0.64	0.22	0.41	1.94	0.68	1.66	1.76	1.93

Appendix B.5. Locus and primer information for the eight nuclear genes used.

Locus Name	Abbreviation	Region	Primer Name	Direction	Primer Sequence	ISCW vectorbase
Tetratricopeptide repeat protein	TPR	Exon	ScleroA1	Forward	CAACGAGAACCAATGCACATTGAAGGC	ISCW000183
			ScleroA2	Reverse	TTGATGTCTACCAATCTATGGAATGCG	
Conserved hypothetical protein	CHP1	Exon	ScleroA5	Forward	TGAATCGTCAAATGATTATTGGACCAGC	ISCW000678
			ScleroA6	Reverse	TTGTTGACTATCACGACCAGCTATYACC	
Conserved hypothetical protein	CHP2	Exon	ScleroB5	Forward	CGCTGGACGAATTGGAGTCATCGGAG	ISCW000678
			ScleroB6	Reverse	CATGCTTCTCGAATGCTTGATATATGC	
Neuromusculin	nrm	3' UTR	ScleroD7	Forward	CGATTTGTACGATGATGTGAAGACTGGC	ISCW006547
			ScleroD8	Reverse	GCATGTTACGCGAGAAGTGATAACAGTC	
1,4-dihydroxyl-2-napthoate octaprenyltransferase	DNO	Exon	ScleroE7	Forward	GCTGCCTTAGCSTACAAGTGTGCCCAAG	ISCW005714
			ScleroE8	Reverse	GTCTCGGAACCCTTTCTCCAAGTGGAAG	
Ski-interacting protein	SKI	Exon	ScleroF10	Forward	AACGTCTAGCAGCCGACGGCAGAGG	ISCW021146
			ScleroF11	Reverse	TYGGACGCTTGCTCGCCTTCTTAGC	
Double-stranded RNA-specific editase B2	ADARB2	Exon	ScleroG7	Forward	AATCGYAAGCGCCGTAGTGGAATGGATGG	ISCW018470
			ScleroG8	Reverse	GCAATCGTTAAGGGCAGCACCATTCATAC	

Locus Name	Abbreviation	Region	Primer Name	Direction	Primer Sequence	ISCW vectorbase
Phosphoglycerate mutase	PGM	3' UTR	ScleroH8	Forward	TCACAATGCMGCGCTGTGTGACGTGGC	ISCW020443
			ScleroH9	Reverse	ATACCTAACAATAGRAACTAGCCTGG	

Appendix B.6. Genetic sampling for this study. Voucher specimens in bold are those included in the 4-taxon panel (see methods). X = locus homozygous, s_het = locus with single heterozygous site, d_het = locus with two heterozygous sites, m_het = locus with multiple heterozygous sites. Shaded boxes denote unseccusful phasing of heterozygous loci.

Voucher	**Species**	**TPR (A1-A2)** Exon	**CHP1 (A5-A6)** Exon	**CHP2 (B5-B6)** Exon	**neu (D7-D8)** UTR	**DNO (E7-E8)** Exon	**SKI (F10-F11)** Exon	**ADARB2 (G7-G8)** Exon	**PGM (H8-H9)** UTR
SDOP66	***S. nondimorphicus***	X	X	X	s_het	X	X	X	X
OP1056	*S. nondimorphicus*	s_het	s_het	s_het	X	d_het	m_het	X	d_het
OP1638	*S. nondimorphicus*	X	X	failed	X	s_het	X	X	X
OP120	*S. nondimorphicus*	X	X	X	d_het	s_het	X	d_het	X
OP1649	*S. idahoensis*	m_het	X	X	X	s_het	s_het	X	X
OP2373	*S. idahoensis*	m_het	m_het	X	X	X	X	X	failed
OP2413	*S. idahoensis*	m_het	X	m_het	failed	m_het	m_het	X	X
OP2415	*S. idahoensis*	m_het	d_het	X	X	X	X	X	X
OP2143	*S. cavicolens*	X	X	X	X	X	X	X	X
OP2144	*S. cavicolens*	d_het	X	X	X	X	X	X	X
OP2145	*S. cavicolens*	X	X	X	s_het	X	s_het	X	X
OP1232	*S. ungulatus*	X	X	s_het	X	X	X	m_het	X
OP1233	*S. ungulatus*	failed	X	X	X	X	X	d_het	X
OP239	*S. madhousensis*	X	X	X	X	X	X	X	X
OP240	*S. madhousensis*	X	X	X	X	X	s_het	X	X
OP2568	*S. steinmanni*	s_het	X	X	X	X	X	X	failed
OP3108	*S. steinmanni*	failed	X	X	X	X	X	X	X
OP3109	*S. steinmanni*	X	X	failed	X	X	X	X	X
OP1127	*S. speoventus*	X	X	X	X	X	X	X	X
OP1128	*S. speoventus*	s_het	X	X	m_het	s_het	d_het	X	X
OP3110	*S. speoventus*	s_het	X	X	X	X	X	X	X
OP3111	*S. speoventus*	s_het	X	X	X	X	X	X	X
OP908	*S. skywalkeri*	d_het	X	d_het	s_het	s_het	d_het	X	s_het

Voucher	Species	TPR (A1-A2) Exon	CHP1 (A5-A6) Exon	CHP2 (B5-B6) Exon	neu (D7-D8) UTR	DNO (E7-E8) Exon	SKI (F10-F11) Exon	ADARB2 (G7-G8) Exon	PGM (H8-H9) UTR
OP2101	*S. skywalkeri*	X	X	s_het	X	X	s_het	X	s_het
OP903	*S. skywalkeri*	s_het	X	X	m_het	X	X	X	failed
OP891	*S. glorietus*	m_het	X	X	X	m_het	X	s_het	X
OP881	*S. glorietus*	m_het	X	X	X	X	X	X	s_het
OP883	***S. glorietus***	m_het	X	m_het	X	X	d_het	X	X
OP1169	*S. glorietus*	m_het	X	failed	X	X	s_het	X	d_het
OP972	*S. klomax*	X	s_het	X	X	X	m_het	X	s_het
OP1171	*S. klomax*	X	X	X	X	X	s_het	X	X
OP1224	***S. robustus***	X	m_het	X	m_het	m_het	m_het	X	m_het
OP1178	*S. robustus*	m_het	failed	X	s_het	X	m_het	d_het	m_het
OP1131	*S. robustus*	X	X	X	X	X	d_het	x	failed
OP1148	*S. robustus*	s_het	X	X	X	s_het	X	X	X
OP965	*S. robustus*	s_het	d_het	X	m_het	s_het	s_het	X	X
OP2977	***S. robustus***	X	X	m_het	m_het	X	s_het	X	X
OP887	*S. robustus*	X	X	X	s_het	X	X	X	X
OP2114	*S. robustus*	m_het	s_het	X	failed	X	m_het	s_het	X
OP959	*S. robustus*	s_het	failed	X	m_het	X	d_het	X	s_het
OP1040	*S. robustus*	d_het	X	d_het	d_het	s_het	d_het	s_het	m_het
OP2109	*S. robustus*	m_het	m_het	X	X	s_het	m_het	X	X
OP2680	*S. robustus*	X	X	X	s_het	s_het	s_het	X	failed

Appendix B.7. GenBank accession numbers. Specimens in bold are those included in the 4-taxon panel (see methods).

Voucher	**Species**	**TPR (A1-A2)** Exon	**CHP1 (A5-A6)** Exon	**CHP2 (B5-B6)** Exon	**neu (D7-D8)** UTR	**DNO (E7-E8)** Exon	**SKI (F10-F11)** Exon	**ADARB2 (G7-G8)** Exon	**PGM (H8-H9)** UTR
SDOP66	***S. nondimorphicus***	KJ585327	KJ585081	KJ585122	KJ585205	KJ585162	KJ585284	KJ585038	KJ585246
OP1056	*S. nondimorphicus*	KJ585328	KJ585082	KJ585123	KJ585206	KJ585163	KJ585285	KJ585039	KJ585247
OP1638	*S. nondimorphicus*	KJ585329	KJ585083		KJ585207	KJ585164	KJ585286	KJ585040	KJ585248
OP120	*S. nondimorphicus*	KJ585330	KJ585084	KJ585124	KJ585208	KJ585165	KJ585287	KJ585041	KJ585249
OP1649	*S. idahoensis*	KJ585331	KJ585085	KJ585125	KJ585209	KJ585166	KJ585288	KJ585042	KJ585250
OP2373	*S. idahoensis*	KJ585332	KJ585086	KJ585126	KJ585210	KJ585167	KJ585289	KJ585043	
OP2413	*S. idahoensis*	KJ585333	KJ585087	KJ585127		KJ585168	KJ585290	KJ585044	KJ585251
OP2415	*S. idahoensis*	KJ585334	KJ585088	KJ585128	KJ585211	KJ585169	KJ585291	KJ585045	KJ585252
OP2143	*S. cavicolens*	KJ585335	KJ585089	KJ585129	KJ585212	KJ585170	KJ585292	KJ585046	KJ585253
OP2144	*S. cavicolens*	KJ585336	KJ585090	KJ585130	KJ585213	KJ585171	KJ585293	KJ585047	KJ585254
OP2145	*S. cavicolens*	KJ585337	KJ585091	KJ585131	KJ585214	KJ585172	KJ585294	KJ585048	KJ585255
OP1232	*S. ungulatus*	KJ585338	KJ585092	KJ585132	KJ585215	KJ585173	KJ585295	KJ585049	KJ585256
OP1233	*S. ungulatus*		KJ585093	KJ585133	KJ585216	KJ585174	KJ585296	KJ585050	KJ585257
OP239	*S. madhousensis*	KJ585339	KJ585094	KJ585134	KJ585217	KJ585175	KJ585297	KJ585051	KJ585258
OP240	*S. madhousensis*	KJ585340	KJ585095	KJ585135	KJ585218	KJ585176	KJ585298	KJ585052	KJ585259
OP2568	*S. steinmanni*	KJ585341	KJ585096	KJ585136	KJ585219	KJ585177	KJ585299	KJ585053	
OP3108	*S. steinmanni*		KJ585097	KJ585137	KJ585220	KJ585178	KJ585300	KJ585054	KJ585260
OP3109	*S. steinmanni*	KJ585342	KJ585098		KJ585221	KJ585179	KJ585301	KJ585055	KJ585261
OP1127	*S. speoventus*	KJ585343	KJ585099	KJ585138	KJ585222	KJ585180	KJ585302	KJ585056	KJ585262
OP1128	*S. speoventus*	KJ585344	KJ585100	KJ585139	KJ585223	KJ585181	KJ585303	KJ585057	KJ585263
OP3110	*S. speoventus*	KJ585345	KJ585101	KJ585140	KJ585224	KJ585182	KJ585304	KJ585058	KJ585264
OP3111	*S. speoventus*	KJ585346	KJ585102	KJ585141	KJ585225	KJ585183	KJ585305	KJ585059	KJ585265
OP908	*S. skywalkeri*	KJ585348	KJ585104	KJ585143	KJ585227	KJ585185	KJ585307	KJ585061	KJ585267
OP2101	*S. skywalkeri*	KJ585349	KJ585105	KJ585144	KJ585228	KJ585186	KJ585308	KJ585062	KJ585268
OP903	*S. skywalkeri*	KJ585350	KJ585106	KJ585145	KJ585229	KJ585187	KJ585309	KJ585063	

Voucher	**Species**	**TPR (A1-A2)** Exon	**CHP1 (A5-A6)** Exon	**CHP2 (B5-B6)** Exon	**neu (D7-D8)** UTR	**DNO (E7-E8)** Exon	**SKI (F10-F11)** Exon	**ADARB2 (G7-G8)** Exon	**PGM (H8-H9)** UTR
OP891	*S. glorietus*	KJ585347	KJ585103	KJ585142	KJ585226	KJ585184	KJ585306	KJ585060	KJ585266
OP881	*S. glorietus*	KJ585351	KJ585107	KJ585146	KJ585230	KJ585188	KJ585310	KJ585064	KJ585269
OP883	***S. glorietus***	KJ585352	KJ585108	KJ585147	KJ585231	KJ585189	KJ585311	KJ585065	KJ585270
OP1169	*S. glorietus*	KJ585353	KJ585109		KJ585232	KJ585190	KJ585312	KJ585066	KJ585271
OP972	*S. klomax*	KJ585354	KJ585110	KJ585148	KJ585233	KJ585191	KJ585313	KJ585067	KJ585272
OP1171	*S. klomax*	KJ585355	KJ585111	KJ585149	KJ585234	KJ585192	KJ585314	KJ585068	KJ585273
OP1224	***S. robustus***	KJ585356	KJ585112	KJ585150	KJ585235	KJ585193	KJ585315	KJ585069	KJ585274
OP1178	*S. robustus*	KJ585357		KJ585151	KJ585236	KJ585194	KJ585316	KJ585070	KJ585275
OP1131	*S. robustus*	KJ585358	KJ585113	KJ585152	KJ585237	KJ585195	KJ585317	KJ585071	
OP1148	*S. robustus*	KJ585359	KJ585114	KJ585153	KJ585238	KJ585196	KJ585318	KJ585072	KJ585276
OP965	*S. robustus*	KJ585360	KJ585115	KJ585154	KJ585239	KJ585197	KJ585319	KJ585073	KJ585277
OP2977	***S. robustus***	KJ585361	KJ585116	KJ585155	KJ585240	KJ585198	KJ585320	KJ585074	KJ585278
OP887	*S. robustus*	KJ585362	KJ585117	KJ585156	KJ585241	KJ585199	KJ585321	KJ585075	KJ585279
OP2114	*S. robustus*	KJ585363	KJ585118	KJ585157		KJ585200	KJ585322	KJ585076	KJ585280
OP959	*S. robustus*	KJ585364		KJ585158	KJ585242	KJ585201	KJ585323	KJ585077	KJ585281
OP1040	*S. robustus*	KJ585365	KJ585119	KJ585159	KJ585243	KJ585202	KJ585324	KJ585078	KJ585282
OP2109	*S. robustus*	KJ585366	KJ585120	KJ585160	KJ585244	KJ585203	KJ585325	KJ585079	KJ585283
OP2680	*S. robustus*	KJ585367	KJ585121	KJ585161	KJ585245	KJ585204	KJ585326	KJ585080	
Transcript	*Theromaster brunneus*	KJ585385	KJ585371	KJ585374		KJ585377	KJ585382	KJ585368	
Transcript	*S. nondimorphicus*	KJ585386	KJ585372	KJ585375	KJ585388	KJ585378	KJ585383	KJ585369	KJ585380
Transcript	*S. robustus*	KJ585387	KJ585373	KJ585376	KJ585389	KJ585379	KJ585384	KJ585370	KJ585381

Appendix B.8. Statistical results of the Ezard et al. morphometric analyses for male and female datasets, including retained components, group assignments (clusters), outlier assignments (significant outliers highlighted), BIC model choice (model chosen is highlighted), squared eigenvalues (retained components are highlighted), and component loadings.

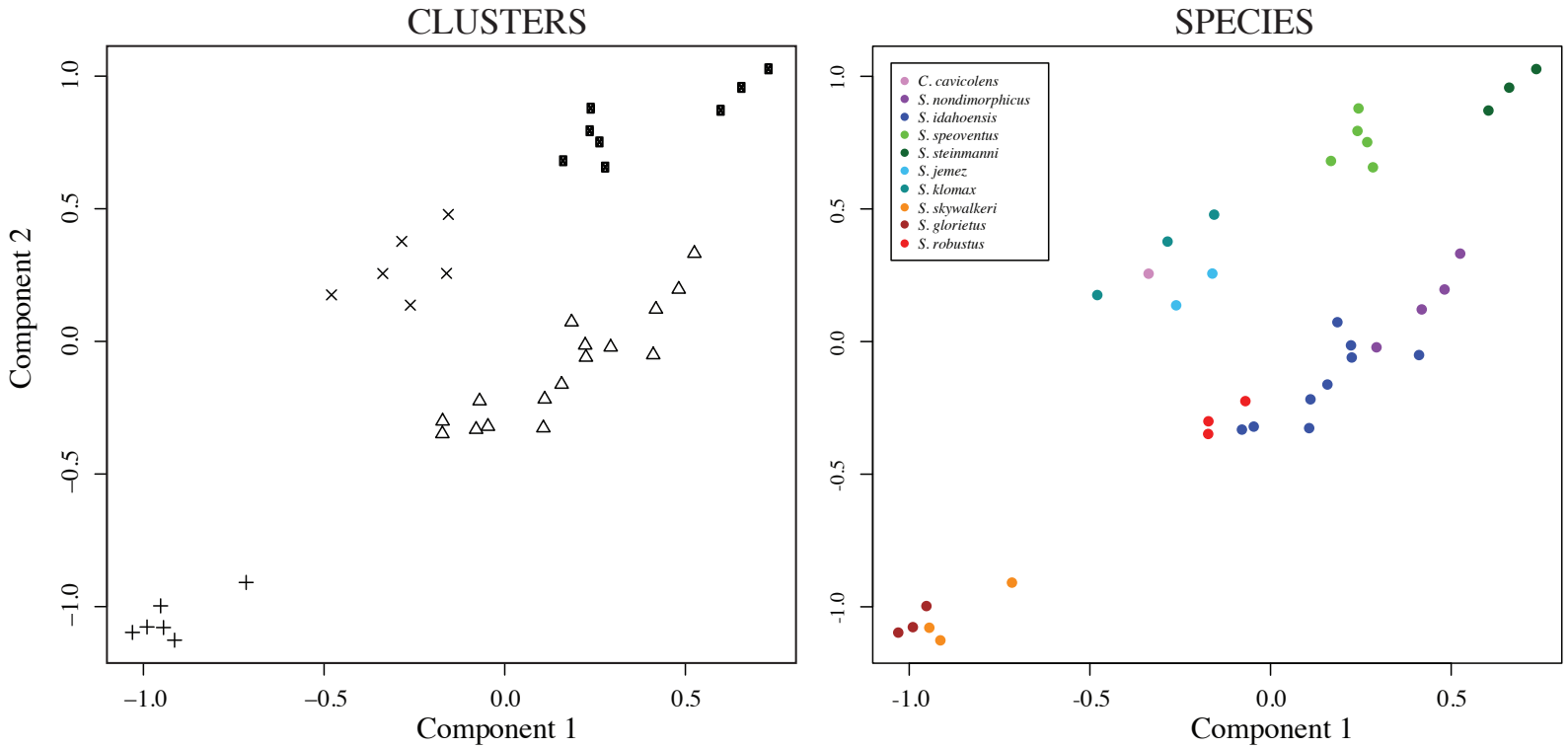

Appendix B.9. Maximum likelihood gene trees estimated using RAxML. Asterisks correspond to nodes recovered with a bootstrap value >80.

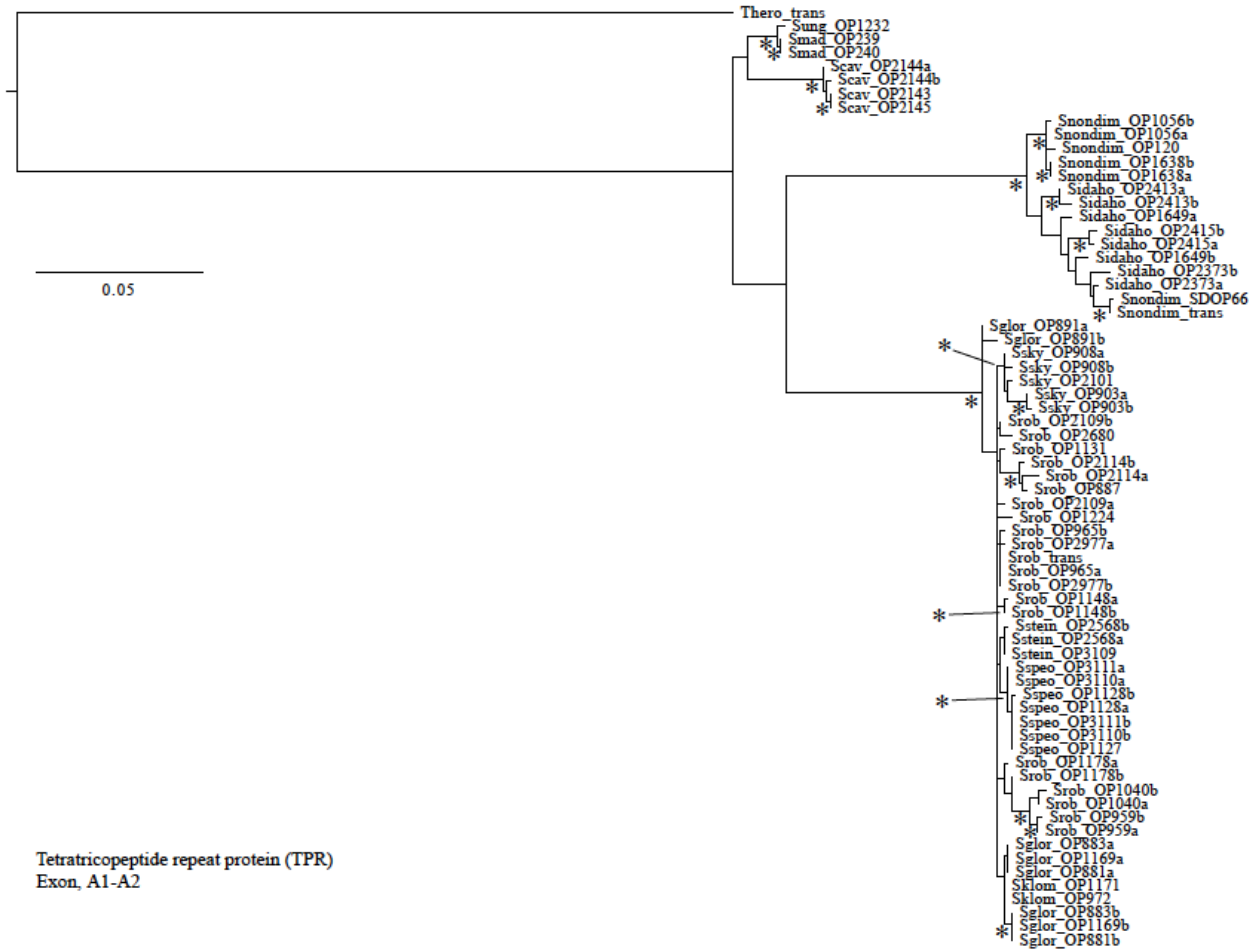

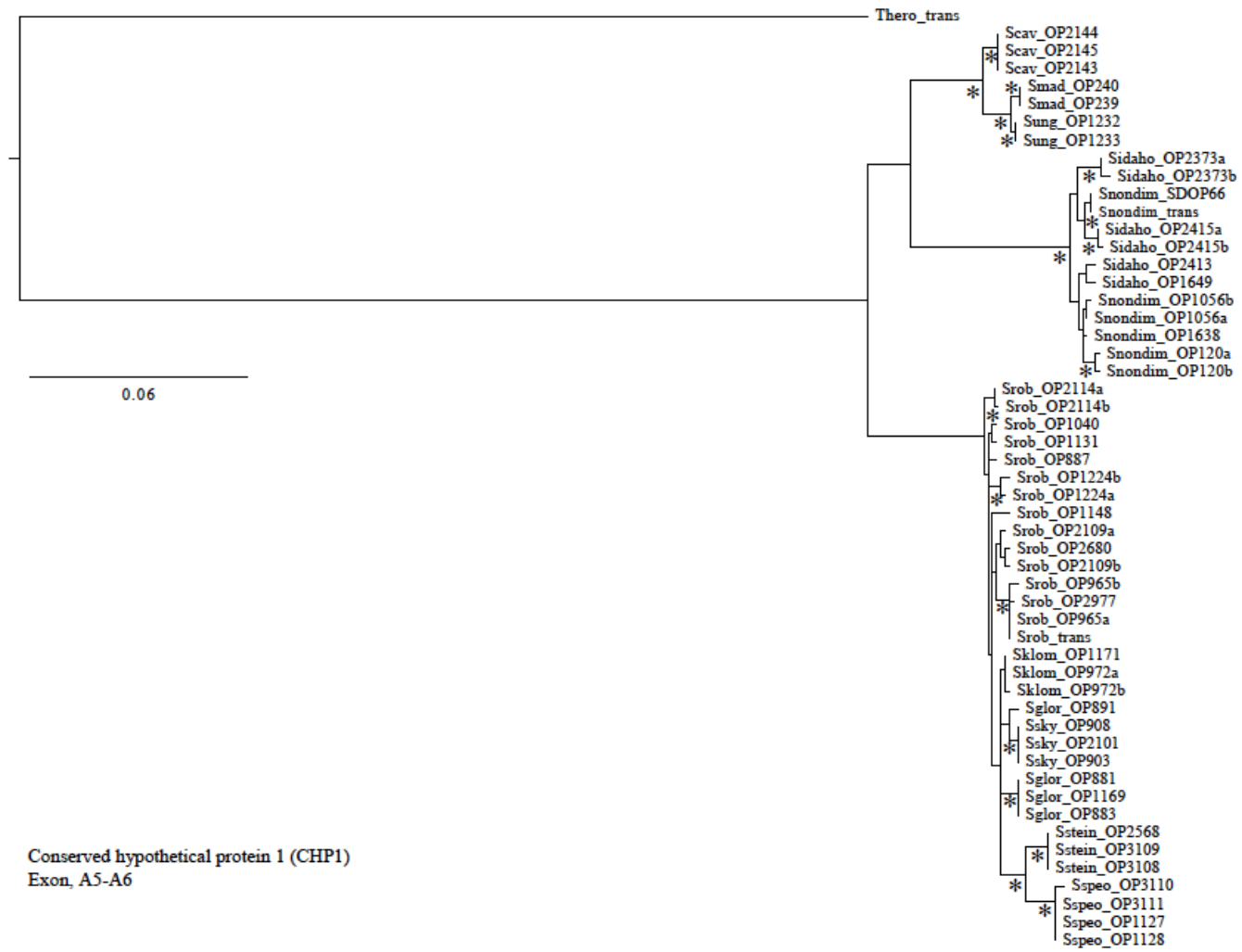

Conserved hypothetical protein 1 (CHP1)
Exon, A5-A6

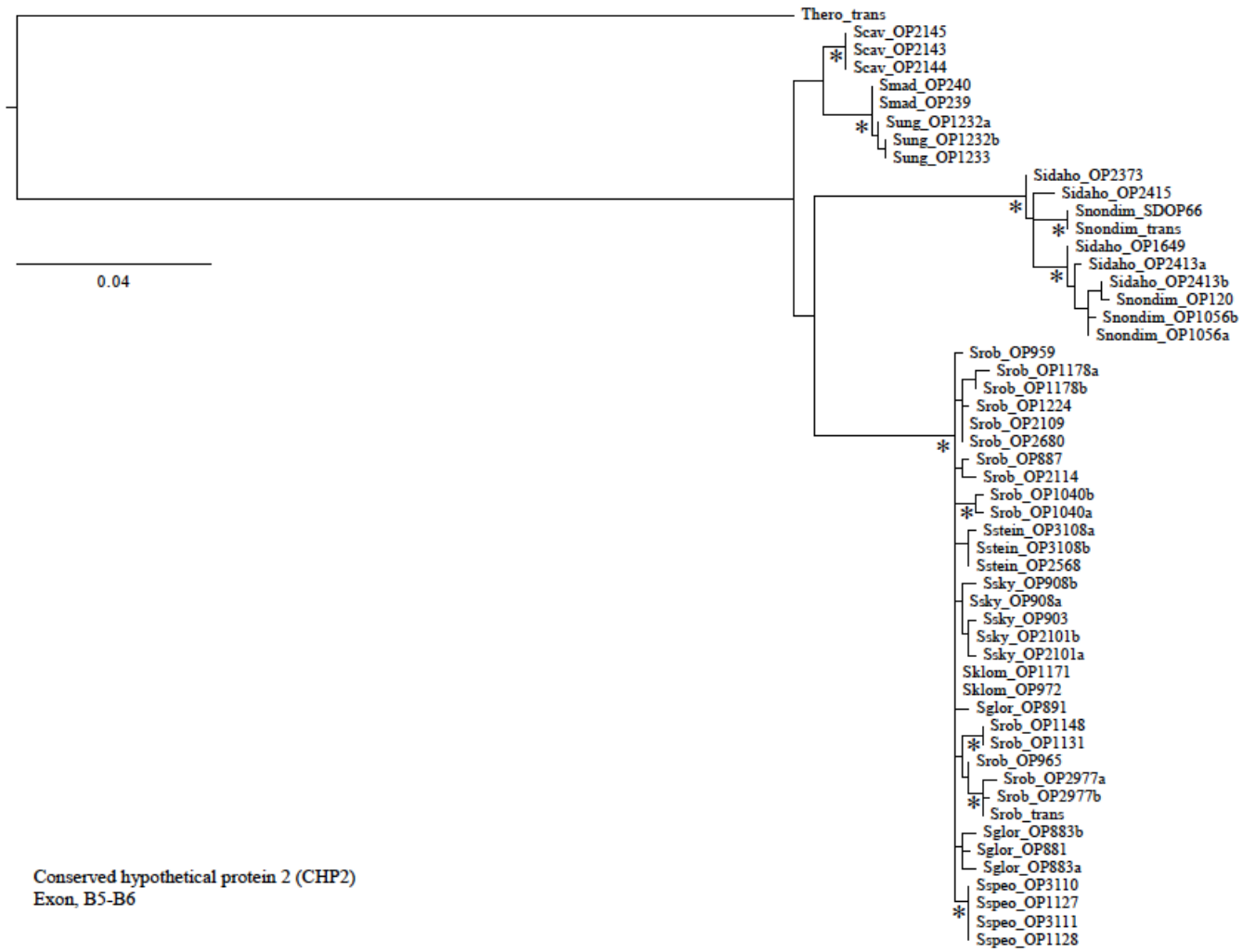

Conserved hypothetical protein 2 (CHP2)
Exon, B5-B6

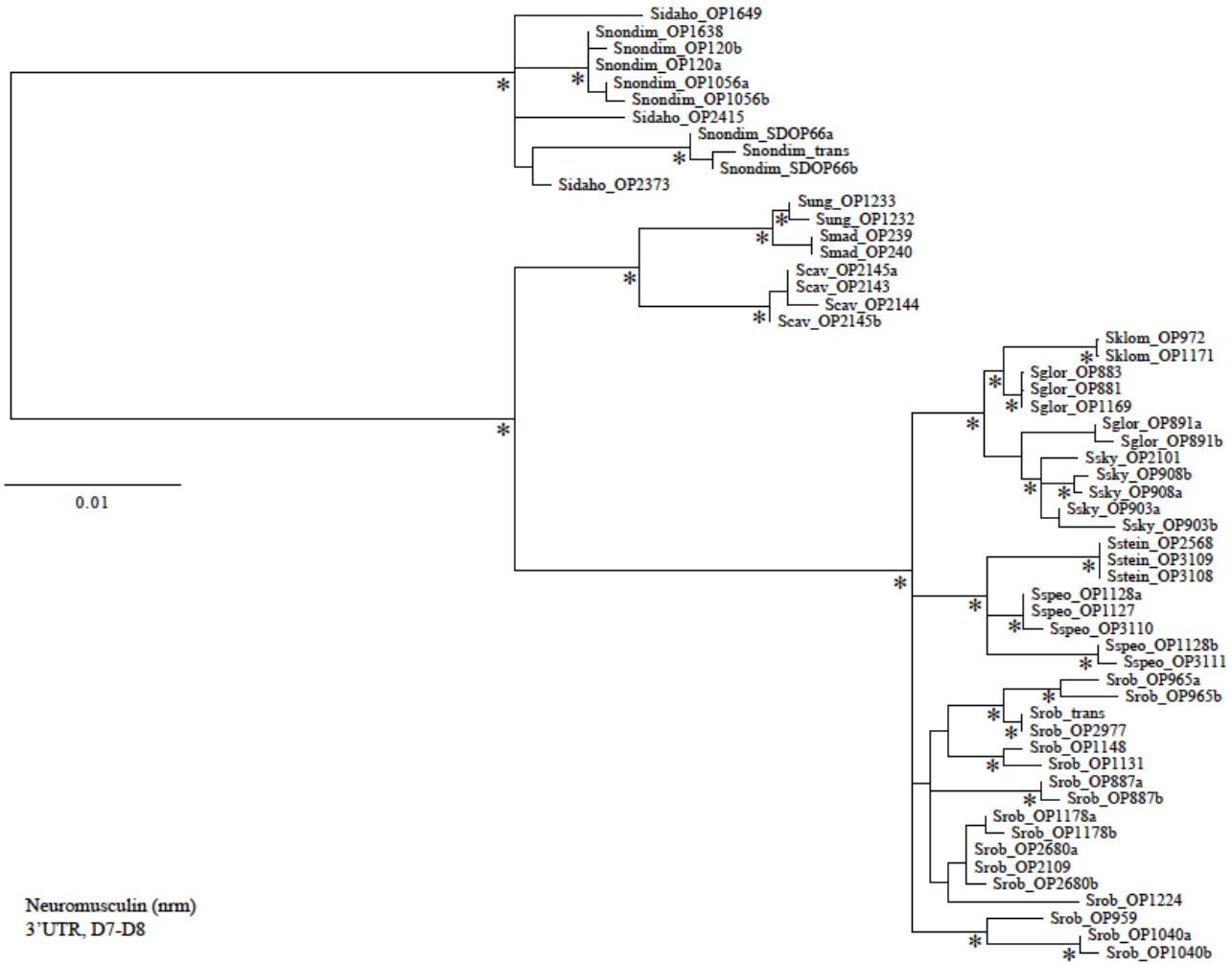
Sidaho_OP1649
Snondim_OP1638
Snondim_OP120b
Snondim_OP120a
Snondim_OP1056a
Snondim_OP1056b
Sidaho_OP2415
Snondim_SDOP66a
Snondim_trans
Snondim_SDOP66b
Sidaho_OP2373
Sung_OP1233
Sung_OP1232
Smad_OP239
Smad_OP240
Scav_OP2145a
Scav_OP2143
Scav_OP2144
Scav_OP2145b
Sklom_OP972
Sklom_OP1171
Sglor_OP883
Sglor_OP881
Sglor_OP1169
Sglor_OP891a
Sglor_OP891b
Ssky_OP2101
Ssky_OP908b
Ssky_OP908a
Ssky_OP903a
Ssky_OP903b
Sstein_OP2568
Sstein_OP3109
Sstein_OP3108
Sspeo_OP1128a
Sspeo_OP1127
Sspeo_OP3110
Sspeo_OP1128b
Sspeo_OP3111
Srob_OP965a
Srob_OP965b
Srob_trans
Srob_OP2977
Srob_OP1148
Srob_OP1131
Srob_OP887a
Srob_OP887b
Srob_OP1178a
Srob_OP1178b
Srob_OP2680a
Srob_OP2109
Srob_OP2680b
Srob_OP1224
Srob_OP959
Srob_OP1040a
Srob_OP1040b
0.01
Neuromusculin (nrm)
3'UTR, D7-D8

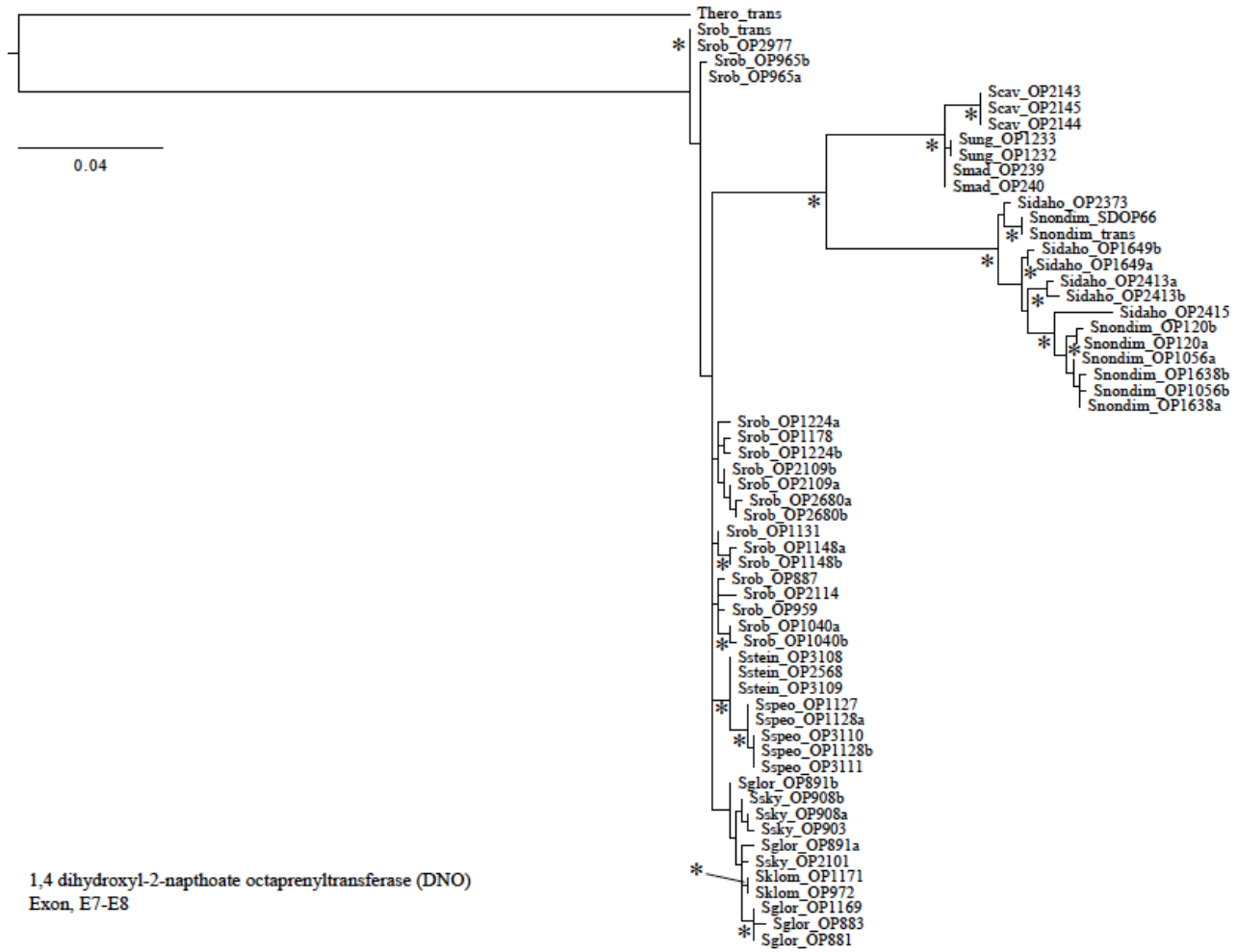

1,4 dihydroxyl-2-napthoate octaprenyltransferase (DNO)
Exon, E7-E8

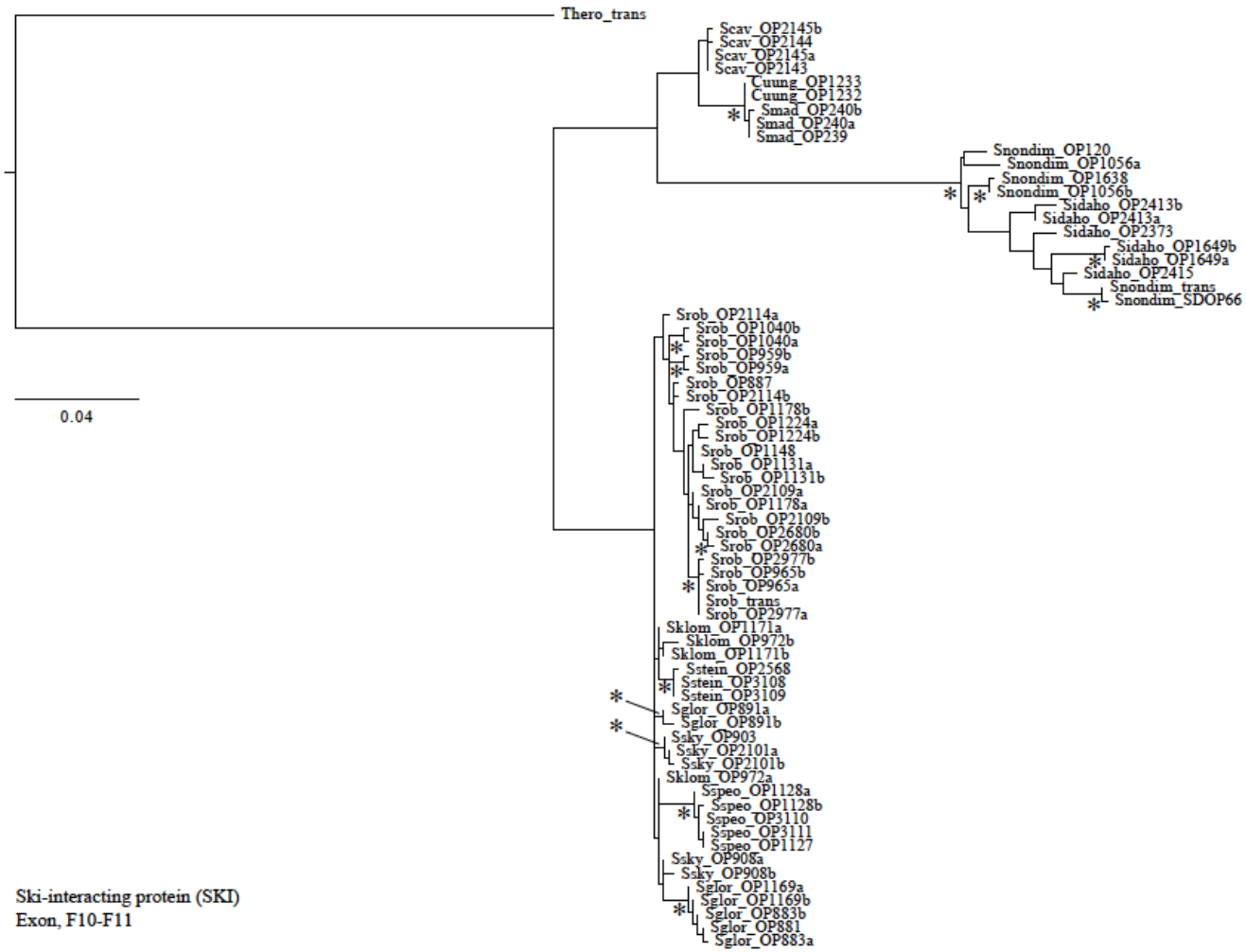

Ski-interacting protein (SKI)
Exon, F10-F11

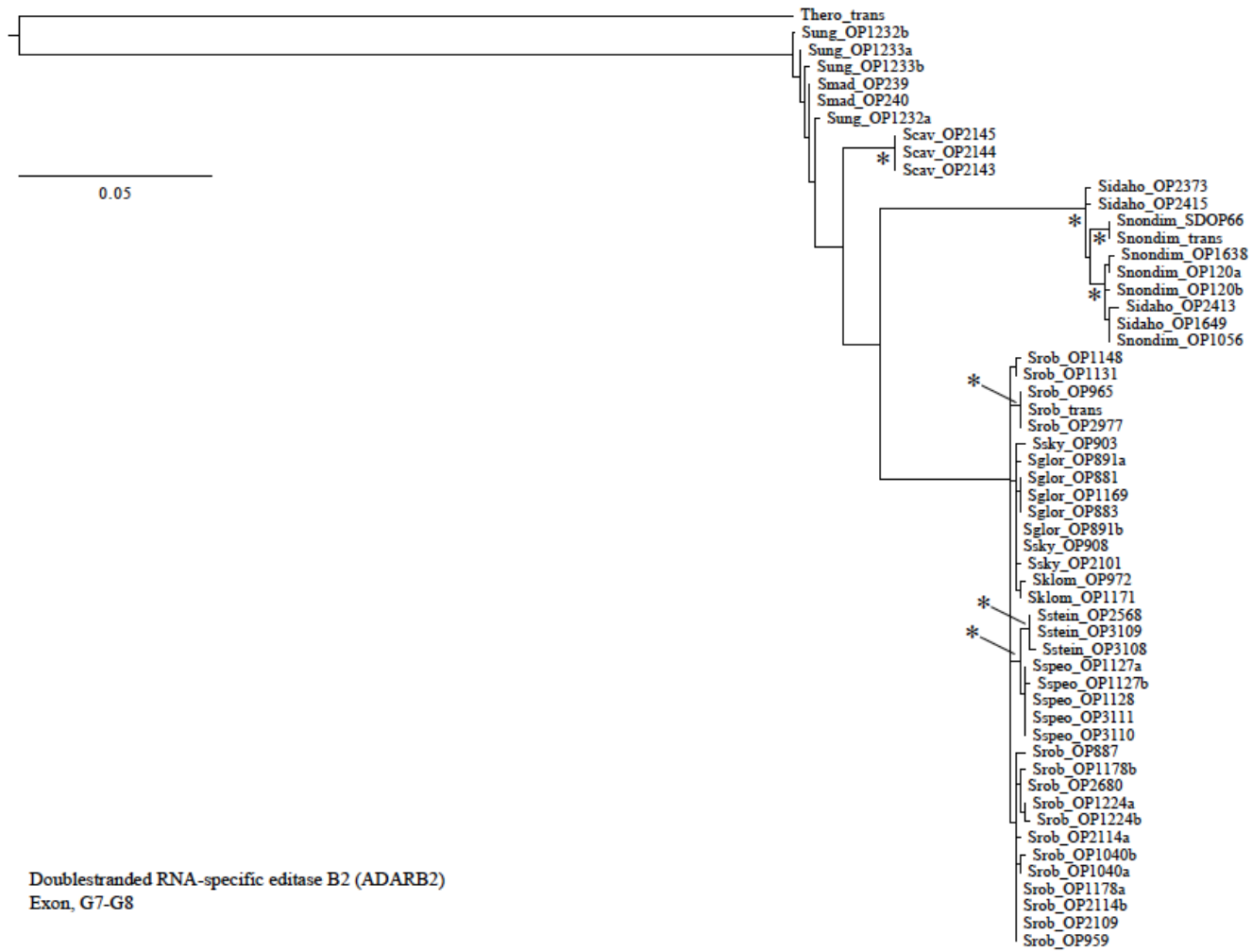

Doublestranded RNA-specific editase B2 (ADARB2)
Exon, G7-G8

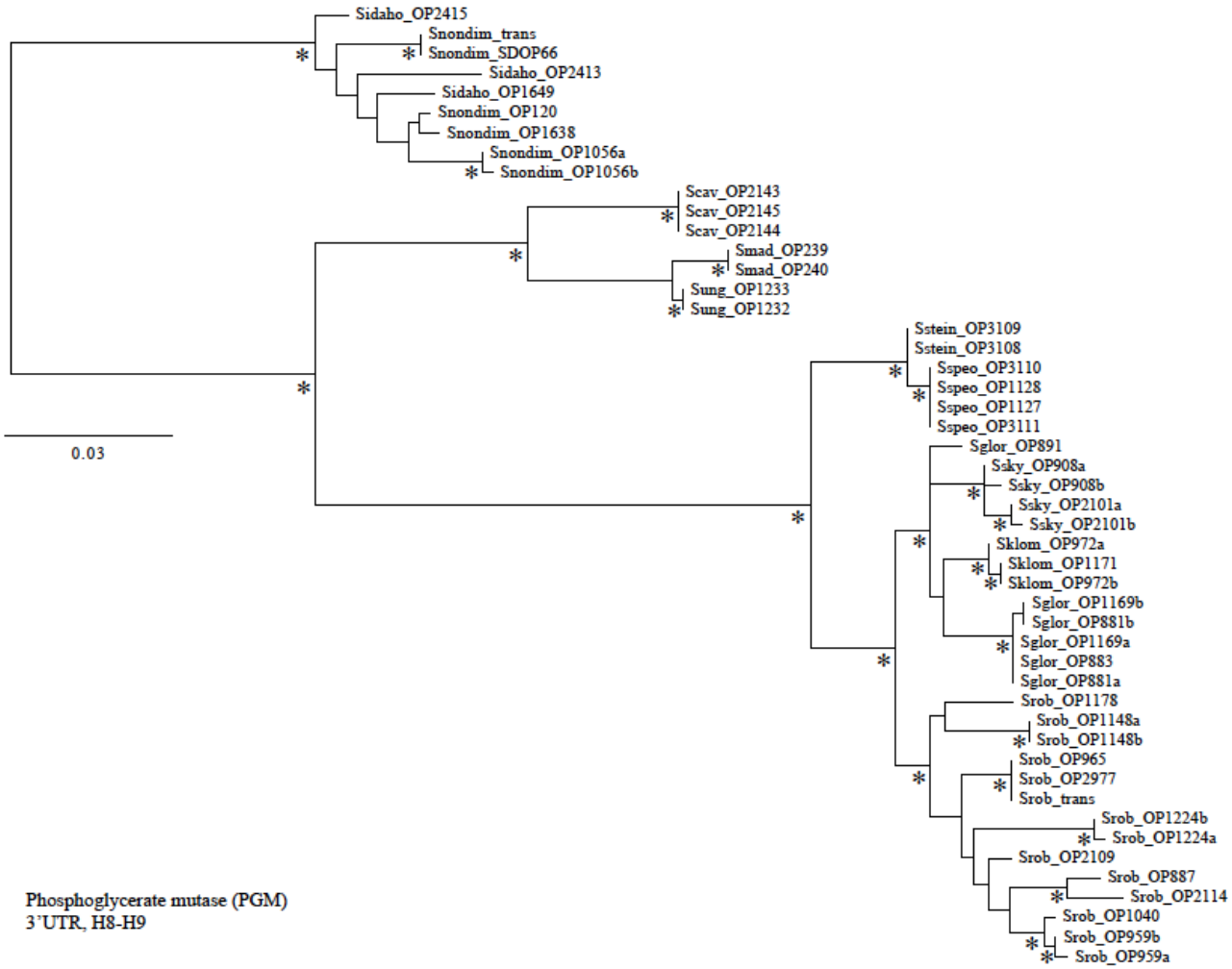

Phosphoglycerate mutase (PGM)
3'UTR, H8-H9

APPENDIX C

Appendix C.1. Taxon sampling, voucher number, and collecting information for all samples included

Voucher	Clade	Pop #	Locality	Lat/Long	Habitat	Elev (m)	Date	Field#
SDSU_OP877	CE	15	NM: Rio Arriba Co., HWY 64, E of Hopewell Lake CG turnoff, along Deer Trail Creek	36.7102 -106.1762	mixed aspen/spruce/pine forest above meadow	2740	20 July, 2006	MCH06_101
SDSU_OP886	CE	13	NM: Sandoval Co., Hwy 4, Jemez Mtns., 3.9 mi W jnct. W Hwy 501 at Los Alamos	35.8384 -106.4044	mixed aspen/spruce/pine flats	2740	21 July, 2006	MCH06_102
SDSU_OP887	CE	13	NM: Sandoval Co., Hwy 4, Jemez Mtns., 3.9 mi W jnct. W Hwy 501 at Los Alamos	35.8384 -106.4044	mixed aspen/spruce/pine flats	2740	21 July, 2006	MCH06_102
SDSU_OP889	SE	19	NM: Otero Co., HWY 244, 1.1 mi N jnct. w HWY 82 at Cloudcroft	32.9748 -105.7343	semi-disturbed conifer forest	2680	18 July, 2006	MCH06_093
SDSU_OP893	SE	18	NM: Lincoln Co., Hwy 532 (road to Ski Apache), ~11 mi W of Hwy 48	33.3969 -105.7826	dense spruce forest, steep N-facing slope	3040	19 July, 2006	MCH06_095
SDSU_OP894	SE	18	NM: Lincoln Co., Hwy 532 (road to Ski Apache), ~11 mi W of Hwy 48	33.3969 -105.7826	dense spruce forest, steep N-facing slope	3040	19 July, 2006	MCH06_095
SDSU_OP905	SW	5	AZ: Apache Co., Alpine Divide CG, off HWY 191, N of Alpine	33.8936 -109.1519	open mixed aspen, pine and spruce forest	2610	17 July, 2006	MCH06_086
SDSU_OP914	SW	10	AZ: Coconino Co., San Fransisco Mtns., vic. Arizona Snowbowl parking area, N of Flagstaff	35.3289 -111.7121	pine and spruce forest w large meadows	2800	22 July, 2006	MCH06_104
SDSU_OP915	SW	10	AZ: Coconino Co., San Fransisco Mtns., vic. Arizona Snowbowl parking area, N of Flagstaff	35.3289 -111.7121	pine and spruce forest w large meadows	2800	22 July, 2006	MCH06_104
SDSU_OP916	SW	10	AZ: Coconino Co., San Fransisco Mtns., vic. Arizona Snowbowl parking area, N of Flagstaff	35.3289 -111.7121	pine and spruce forest w large meadows	2800	22 July, 2006	MCH06_104
SDSU_OP921	SW	7	NM: Catron Co., Mogollon Mtns., ~11.2 mi E of Mogollon, E of Silver Creek Divide	33.3729 -108.6569	N-facing old growth doug-fir forest	2770	17 July, 2006	MCH06_087
SDSU_OP929	SE	16	NM: Sierra Co., Mimbres Mtns. Hwy 152, ~1 mi SE of Emory Pass	32.9021 -107.7682	pine forest, small N-facing ravine	2430	18 July, 2006	MCH06_090
SDSU_OP935	SW	8	AZ: Greenlee Co., HWY 191, ~1.4 mi S Hannagan Meadow	33.6139 -109.3268	dense aspen grove w occasional pine and spruce	2790	17 July, 2006	MCH06_085
SDSU_OP938	SW	8	AZ: Greenlee Co., HWY 191, ~1.4 mi S Hannagan Meadow	33.6139 -109.3268	dense aspen grove w occasional pine and spruce	2790	17 July, 2006	MCH06_085
SDSU_OP945	SW	12	AZ: Graham Co., Pinaleno Mtns. Hospital Flat, near Treasure Park	32.6651 -109.8758	doug-fir forest adjacent to meadow w aspen	2740	17 July, 2006	MCH06_083
SDSU_OP946	SW	12	AZ: Graham Co., Pinaleno Mtns. Hospital Flat, near Treasure Park	32.6651 -109.8758	doug-fir forest adjacent to meadow w aspen	2740	17 July, 2006	MCH06_083
SDSU_OP951	SW	6	NM: Grant Co., Pinos Altos Mtns. Bear Canyon road, 2.2 mi E Hwy 15	32.9287 -108.1662	pine forest, small N-facing ravine	2410	18 July, 2006	MCH06_089
SDSU_OP952	SW	6	NM: Grant Co., Pinos Altos Mtns. Bear Canyon road, 2.2 mi E Hwy 15	32.9287 -108.1662	pine forest, small N-facing ravine	2410	18 July, 2006	MCH06_089
SDSU_OP956	SE	20	NM: Otero Co., HWY 244 SW of Silver Springs in Bradford Canyon, NE of Cloudcroft	32.978 -105.7087	doug-fir/aspen forest in shallow N-facing slope	2650	19 July, 2006	MCH06_094
SDSU_OP959	SE	20	NM: Otero Co., HWY 244 SW of Silver Springs in Bradford Canyon, NE of Cloudcroft	32.978 -105.7087	doug-fir/aspen forest in shallow N-facing slope	2650	19 July, 2006	MCH06_094

Voucher	Clade	Pop #	Locality	Lat/Long	Habitat	Elev (m)	Date	Field#
SDSU_OP964	SW	11	AZ: Pima Co., Santa Catalina Mtns., vic. Sunset Trailhead	32.4265 -110.7424	mixed conifer forest, N-facing slope	2380	15 July, 2006	MCH06_078
SDSU_OP965	SW	11	AZ: Pima Co., Santa Catalina Mtns., vic. Sunset Trailhead	32.4265 -110.7424	mixed conifer forest, N-facing slope	2380	15 July, 2006	MCH06_078
SDSU_OP1040	SE	17	AZ: Cochise Co., Chiricahua Mtns., road to Barfoot Park, N of Buena Vista Peak	31.9179 -109.2725	old-growth coniferous forest, N-facing slope	2560	16 July, 2006	MCH06_082
SDSU_OP1041	SE	17	AZ: Cochise Co., Chiricahua Mtns., road to Barfoot Park, N of Buena Vista Peak	31.9179 -109.2725	old-growth coniferous forest, N-facing slope	2560	16 July, 2006	MCH06_082
SDSU_OP1122	NE	32	CO: Gunnison Co., S of Gothic, below Snodgrass Mtn	38.9397 -106.9808	aspen-dominated N-facing slope	2900	29 June, 2007	MCH07_061
SDSU_OP1123	NE	32	CO: Gunnison Co., S of Gothic, below Snodgrass Mtn	38.93967 -106.9808	aspen-dominated N-facing slope	2900	29 June, 2007	MCH07_061
SDSU_OP1130	NW	1	UT: San Juan Co., Abajo Mtns., Manti La Sal NF, North Creek Road at crossing of North Creek, W of Monticello	37.8763 -109.4458	N-facing conifer dominated forest, under logs	2620	27 June, 2007	MCH07_052
SDSU_OP1135	NE	37	CO: Lake Co., Hwy 82, W of Twin Lakes, along Lake Creek	39.0624 -106.4072	mixed aspen/conifer S of creek; rocks	2850	30 June, 2007	MCH07_066
SDSU_OP1136	NE	37	CO: Lake Co., Hwy 82, W of Twin Lakes, along Lake Creek	39.0624 -106.4072	mixed aspen/conifer S of creek; rocks	2850	30 June, 2007	MCH07_066
SDSU_OP1140	NE	38	CO: Lake Co., Hwy 91 NE of Leadville	39.3416 -106.223	gentle mixed aspen/conifer slope	3200	30 June, 2007	MCH07_067
SDSU_OP1141	NE	38	CO: Lake Co., Hwy 91 NE of Leadville	39.3416 -106.223	gentle mixed aspen/conifer slope	3200	30 June, 2007	MCH07_067
SDSU_OP1145	NE	28	CO: Custer Co., Sangre de Cristo Mtns., Alvarado CG, W of Hwy 69, SW of Westcliffe	38.0793 -105.5648	mostly conifer forest above CG	2740	02 July, 2007	MCH07_075
SDSU_OP1148	NW	4	CO: Dolores Co., Hwy 145, along Dolores River at FR 578	37.768 -107.9871	N-facing mixed conifer and aspen	2830	27 June, 2007	MCH07_055
SDSU_OP1149	NW	4	CO: Dolores Co., Hwy 145, along Dolores River at FR 578	37.768 -107.9871	N-facing mixed conifer and aspen	2830	27 June, 2007	MCH07_055
SDSU_OP1164	NE	27	CO: Custer Co., Hwy 165, S of McKenzie Jnct, Wet Mtns	38.1336 -105.1791	mixed apsen/conifer above small stream	2710	02 July, 2007	MCH07_074
SDSU_OP1168	NE	27	CO: Custer Co., Hwy 165, S of McKenzie Jnct, Wet Mtns	38.1336 -105.1791	mixed apsen/conifer above small stream	2710	02 July, 2007	MCH07_074
SDSU_OP1173	NW	3	CO: Dolores Co., along Beaver Creek, FR 525, off Hwy 526	37.6513 -108.4104	aspen dominated forest	2440	27 June, 2007	MCH07_054
SDSU_OP1174	NW	3	CO: Dolores Co., along Beaver Creek, FR 525, off Hwy 526	37.6513 -108.4104	aspen dominated forest	2440	27 June, 2007	MCH07_054
SDSU_OP1178	HAV	21	CO: Archuleta Co., Pagosa Springs, Hwy 160, just E crossing San Juan River, hills south of highway	37.2682 -106.9992	disturbed, mixed conifer forest	2160	28 June, 2007	MCH07_058
SDSU_OP1179	HAV	21	CO: Archuleta Co., Pagosa Springs, Hwy 160, just E crossing San Juan River, hills south of highway	37.2682 -106.9992	disturbed, mixed conifer forest	2160	28 June, 2007	MCH07_058
SDSU_OP1183	NE	36	CO: Larimer Co., vic. Longs Peak Trailhead, off Hwy 7	40.2705 -105.5549	mixed conifer near small stream	2820	01 July, 2007	MCH07_070

Voucher	Clade	Pop #	Locality	Lat/Long	Habitat	Elev (m)	Date	Field#
SDSU_OP1184	NE	36	CO: Larimer Co., vic. Longs Peak Trailhead, off Hwy 7	40.2705 -105.5549	mixed conifer near small stream	2820	01 July, 2007	MCH07_070
SDSU_OP1188	NE	26	CO: Saguache Co., Hwy 114 at North Pass, Cochetopa Hills	38.2138 -106.5724	N-facing aspen grove	3110	28 June, 2007	MCH07_060
SDSU_OP1193	NE	34	CO: Douglas Co., Road 67, along Sugar Creek, NE of Deckers	39.2978 -105.1398	conifer forest S of creek	2225	01 July, 2007	MCH07_072
SDSU_OP1194	NE	34	CO: Douglas Co., Road 67, along Sugar Creek, NE of Deckers	39.2978 -105.1398	conifer forest S of creek	2225	01 July, 2007	MCH07_072
SDSU_OP1197	HAV	23	CO: Ouray Co., Ouray at Cascade Falls	38.0249 -107.6654	N-facing conifer slope	2420	28 June, 2007	MCH07_056
SDSU_OP1202	NW	2	UT: San Juan Co., La Sal Mtns., La Sal Pass Road	38.4155 -109.2242	aspen grove	2900	27 June, 2007	MCH07_053
SDSU_OP1209	NE	24	CO: Rio Grande Co., Church Creek Trailhead, SW of South Fork, off Hwy 160	37.6481 -106.652	mixed aspen/conifer forest	2530	28 June, 2007	MCH07_059
SDSU_OP1210	NE	24	CO: Rio Grande Co., Church Creek Trailhead, SW of South Fork, off Hwy 160	37.6481 -106.652	mixed aspen/conifer forest	2530	28 June, 2007	MCH07_059
SDSU_OP1214	NE	31	CO: Chaffee Co., Hwy 50 along South Arkansas River, near Garfield	38.5494 -106.2557	mixed conifer/aspen S of river	2740	29 June, 2007	MCH07_063
SDSU_OP1215	NE	31	CO: Chaffee Co., Hwy 50 along South Arkansas River, near Garfield	38.5494 -106.2557	mixed conifer/aspen S of river	2740	29 June, 2007	MCH07_063
SDSU_OP1218	NE	39	CO: Park Co., above Weston Pass CG	39.0773 -106.1363	conifer forest above CG	3140	29 June, 2007	MCH07_064
SDSU_OP1219	NE	39	CO: Park Co., above Weston Pass CG	39.0773 -106.1363	conifer forest above CG	3140	29 June, 2007	MCH07_064
SDSU_OP1223	HAV	22	CO: La Plata Co., vic. Haviland Lake CG, off Hwy 550, N of Durango	37.5329 -107.807	mixed conifer N-facing hillside	2440	28 June, 2007	MCH07_057
SDSU_OP2104	NE	30	CO: Alamosa Co., Great Sand Dunes National Monument, Mosca Pass Trail	37.7319 -105.4982	pine forest, along creek, north facing slope	2630	4 June, 2008	SD08_018
SDSU_OP2105	NE	30	CO: Alamosa Co., Great Sand Dunes National Monument, Mosca Pass Trail	37.7319 -105.4982	pine forest, along creek, north facing slope	2630	4 June, 2008	SD08_018
SDSU_OP2108	NE	25	CO: Mineral Co., S of Creede along Tr 806, 1.9 mi from SR 149 along Deep Creek Rd	37.81397 -106.9147	mixed forest, north facing slope	2660	5 June, 2008	SD08_019
SDSU_OP2109	NE	25	CO: Mineral Co., S of Creede along Tr 806, 1.9 mi from SR 149 along Deep Creek Rd	37.81397 -106.9147	mixed forest, north facing slope	2660	5 June, 2008	SD08_019
SDSU_OP2114	CE	14	NM: Rio Arriba Co., N of Chama along SR 17, 4.6 mi from junction with HWY 64	36.9394 -106.5493	mixed forest, north facing slope in ravine	2490	5 June, 2008	SD08_020
SDSU_OP2679	NE	33	CO: Garfield Co., Hanging Lake Park, along Hanging Lake Trail	39.5985 -107.191	mixed forest/riparian habitat, along western slope	2120	1 August, 2009	SD09_005
SDSU_OP2682	NE	29	CO: Huerfano Co., Spring Creek Trailhead, 0.6 mi S of Cuchara on 12S	37.3702 -105.1095	mixed forest, north facing slope along trail	2670	30 July, 2009	SD09_002
SDSU_OP2683	NE	29	CO: Huerfano Co., Spring Creek Trailhead, 0.6 mi S of Cuchara on 12S	37.3702 -105.1095	mixed forest, north facing slope along trail	2670	30 July, 2009	SD09_002
SDSU_OP2686	NE	35	CO: Gilpin Co., Apex Valley Rd, 1.7 mi N of BlackHawk on 119	39.8192 -105.5132	pine forest, north facing slope	2580	31 July, 2009	SD09_004

Voucher	Clade	Pop #	Locality	Lat/Long	Habitat	Elev (m)	Date	Field#
SDSU_OP2977	SW	9	AZ: Cochise Co., Coronado NF, upper Miller Canyon, Huachuca Mtns	31.4066 -110.2874	Arbutus arizonica, Psedotsuga menziesii, Acer grandidentatum; under cobbles and boulders, deep moist soil, litter debris	1950	25 March, 2012	MCH12_014
SDSU_OP2978	SW	9	AZ: Cochise Co., Coronado NF, upper Miller Canyon, Huachuca Mtns	31.4066 -110.2874	Arbutus arizonica, Psedotsuga menziesii, Acer grandidentatum; under cobbles and boulders, deep moist soil, litter debris	1950	25 March, 2012	MCH12_014

Appendix C.2. pyRAD analysis statistics. QC = quality control, dpt.me = mean depth of clusters, H = heterozygosity, E = error rate, # poly = number of polymorphic sites, Poly = frequency of polymorphic sites. Last three cells in bottom row are matrix completeness.

	Step 2		Step 3		Step 4		Step 5				Total loci		
Voucher	**Reads**	**Pass QC**	**Clusters**	**dpt.me**	**H**	**E**	**# loci**	**# sites**	**# poly**	**Poly**	**m48**	**m32**	**m16**
OP877	972157	900374	32512	27.61	0.00320	0.00019	32512	363868	806	0.00222	387	775	1226
OP886	935889	871618	29646	29.25	0.00173	0.00014	29646	353407	367	0.00104	338	674	1116
OP887	868164	753269	39216	19.00	0.00310	0.00022	39216	458534	807	0.00176	420	904	1453
OP889	673819	623932	29756	20.71	0.00897	0.00022	29756	261101	1362	0.00522	308	532	760
OP893	845377	789516	31164	24.95	0.00716	0.00044	31164	386294	1776	0.00460	378	709	1102
OP894	1058917	966219	65569	14.31	0.00839	0.00044	65569	448363	1994	0.00445	405	773	1200
OP905	773672	710449	29910	23.39	0.00648	0.00051	29910	315340	1324	0.00420	399	634	1072
OP914	1002250	699167	60076	11.26	0.00579	0.00100	60076	457920	1223	0.00267	450	847	1501
OP915	770301	694940	27119	25.21	0.00368	0.00067	27119	370434	883	0.00238	449	862	1533
OP916	677386	614156	27602	22.08	0.00403	0.00026	27602	239105	459	0.00192	359	531	889
OP921	172984	155453	41270	3.73	0.00815	0.00229	41270	175724	874	0.00497	179	275	487
OP929	1738861	1596212	50852	29.54	0.00699	0.00042	50852	491225	1973	0.00402	440	858	1379
OP935	533095	487290	26034	18.39	0.00654	0.00019	26034	289822	1170	0.00404	431	691	1160
OP938	745922	684642	30969	21.55	0.00450	0.00027	30969	377204	1528	0.00405	455	769	1343
OP945	826136	754071	32579	22.75	0.00609	0.00043	32579	413934	1804	0.00436	458	805	1452
OP946	785693	716816	31652	22.32	0.00607	0.00031	31652	394298	1681	0.00426	453	785	1408
OP951	580942	511042	23822	20.06	0.00569	0.00102	23822	395572	1278	0.00323	440	764	1337
OP952	696077	642232	29493	21.50	0.00556	0.00041	29493	317676	1035	0.00326	364	594	1026
OP956	930065	849387	38676	21.57	0.01135	0.00039	38676	435072	2157	0.00496	439	865	1298
OP959	1134113	1041060	44161	23.24	0.00814	0.00045	44161	416239	1977	0.00475	426	829	1318
OP964	863036	773558	25680	28.17	0.00568	0.00048	25680	381308	1303	0.00342	394	655	1125
OP965	862054	772465	49764	14.98	0.00624	0.00041	49764	342784	1181	0.00345	427	727	1232
OP1040	766315	683373	31603	19.70	0.00541	0.00153	31603	402952	1959	0.00486	430	830	1261
OP1041	615356	571077	26253	20.39	0.00766	0.00051	26253	288669	1348	0.00467	384	674	941
OP1122	1066194	999751	28520	34.28	0.00275	0.00022	28520	368547	666	0.00181	478	1102	2191
OP1123	1169741	1093600	34754	30.84	0.00296	0.00016	34754	400165	744	0.00186	489	1162	2312
OP1130	904632	830573	32375	25.48	0.00380	0.00020	32375	316781	896	0.00283	404	758	1317
OP1135	1300978	1204633	68574	17.16	0.00410	0.00026	68574	391520	811	0.00207	463	1042	1990

	Step 2		Step 3		Step 4		Step 5				Total loci		
Voucher	**Reads**	**Pass QC**	**Clusters**	**dpt.me**	**H**	**E**	**# loci**	**# sites**	**# poly**	**Poly**	**m48**	**m32**	**m16**
OP1136	1524098	1402489	103616	13.31	0.00420	0.00028	103616	433471	910	0.00210	485	1153	2269
OP1140	956344	892406	39271	22.59	0.00243	0.00019	39271	408917	567	0.00139	483	1126	2156
OP1141	595177	552702	31731	17.23	0.00233	0.00019	31731	244996	307	0.00125	437	936	1628
OP1145	1140538	1057773	43499	24.21	0.00430	0.00022	43499	368798	906	0.00246	470	1088	2020
OP1148	580118	535016	30642	17.38	0.00414	0.00026	30642	278516	875	0.00314	405	730	1167
OP1149	988062	913563	32757	27.62	0.00378	0.00015	32757	398266	1143	0.00287	441	880	1561
OP1164	689546	637054	34789	18.27	0.00384	0.00028	34789	290336	679	0.00234	343	715	1288
OP1168	1001651	918539	33777	27.11	0.00328	0.00027	33777	331027	510	0.00154	415	932	1712
OP1173	758821	697923	31723	21.87	0.00540	0.00025	31723	256701	950	0.00370	317	548	890
OP1174	1024630	947892	32448	29.08	0.00469	0.00023	32448	383972	1257	0.00327	450	891	1485
OP1178	767391	713807	21742	32.55	0.00336	0.00019	21742	322067	799	0.00248	389	828	1399
OP1179	1213352	1121526	28337	39.48	0.00445	0.00022	28337	374475	1242	0.00332	452	1039	1796
OP1183	1320851	1208980	39961	29.97	0.00259	0.00034	39961	418079	742	0.00177	489	1176	2417
OP1184	946302	876209	28841	30.31	0.00184	0.00023	28841	398175	456	0.00115	481	1155	2349
OP1188	1410807	1294826	34534	37.29	0.00414	0.00027	34534	387558	1096	0.00283	476	1134	2111
OP1193	1324905	1216361	64540	18.73	0.00370	0.00035	64540	319572	620	0.00194	416	899	1704
OP1194	500712	460946	22741	20.23	0.00291	0.00024	22741	247950	491	0.00198	308	705	1363
OP1197	1160946	1075750	38179	28.12	0.00295	0.00021	38179	420217	857	0.00204	434	940	1684
OP1202	1181601	1050381	47408	20.56	0.00453	0.00039	47408	493926	1437	0.00291	463	932	1617
OP1209	744451	662880	38064	17.29	0.00482	0.00021	38064	497494	1625	0.00327	478	1126	2045
OP1210	804996	736820	28201	25.61	0.00414	0.00033	28201	367263	1079	0.00294	453	1025	1903
OP1214	695648	648197	24893	25.44	0.00253	0.00016	24893	304183	394	0.00130	471	1058	1911
OP1215	1056252	966888	55142	16.88	0.00351	0.00026	55142	395664	646	0.00163	468	1080	2100
OP1218	1062639	992713	36961	26.73	0.00382	0.00024	36961	382283	915	0.00239	455	1039	2013
OP1219	846362	788220	29220	26.68	0.00275	0.00026	29220	389300	650	0.00167	481	1120	2180
OP1223	816156	718312	29076	24.62	0.00316	0.00031	29076	491998	1104	0.00224	464	1046	1809
OP2104	964253	884218	52923	16.50	0.00292	0.00034	52923	379575	587	0.00155	473	1083	2043
OP2105	906743	838712	28298	29.52	0.00330	0.00021	28298	347011	782	0.00225	472	1101	2019
OP2108	879437	818138	22953	35.45	0.00363	0.00020	22953	339296	964	0.00284	463	1031	1824
OP2109	1025032	955679	29936	31.52	0.00363	0.00021	29936	362169	994	0.00274	469	1052	1879
OP2114	842129	773740	27167	28.30	0.00390	0.00017	27167	301083	929	0.00309	327	587	923

	Step 2		Step 3		Step 4		Step 5				Total loci		
Voucher	**Reads**	**Pass QC**	**Clusters**	**dpt.me**	**H**	**E**	**# loci**	**# sites**	**# poly**	**Poly**	**m48**	**m32**	**m16**
OP2679	662640	616391	25905	23.46	0.00291	0.00024	25905	283912	584	0.00206	455	1031	1852
OP2682	812588	752707	22659	32.73	0.00143	0.00020	22659	363648	267	0.00073	463	1087	2090
OP2683	1226382	1119835	73036	15.14	0.00293	0.00027	73036	410496	486	0.00118	469	1116	2189
OP2686	744190	696341	31505	21.99	0.00298	0.00028	31505	347607	621	0.00179	451	1001	1885
OP2977	635310	570184	26284	20.95	0.00556	0.00084	26284	363187	1297	0.00357	455	794	1371
OP2978	815937	739128	29308	24.57	0.00585	0.00038	29308	381044	1512	0.00397	451	826	1521
Average	**906110**	**828371**	**36487**	**23.58**	**0.00451**	**0.00037**	**36487**	**365201**	**1026**	**0.00282**	**0.859**	**0.696**	**0.478**

Appendix C.3. ENMs for all *S. robustus*, and the western and eastern clades for current, mid-Holocene, and LGM conditions.

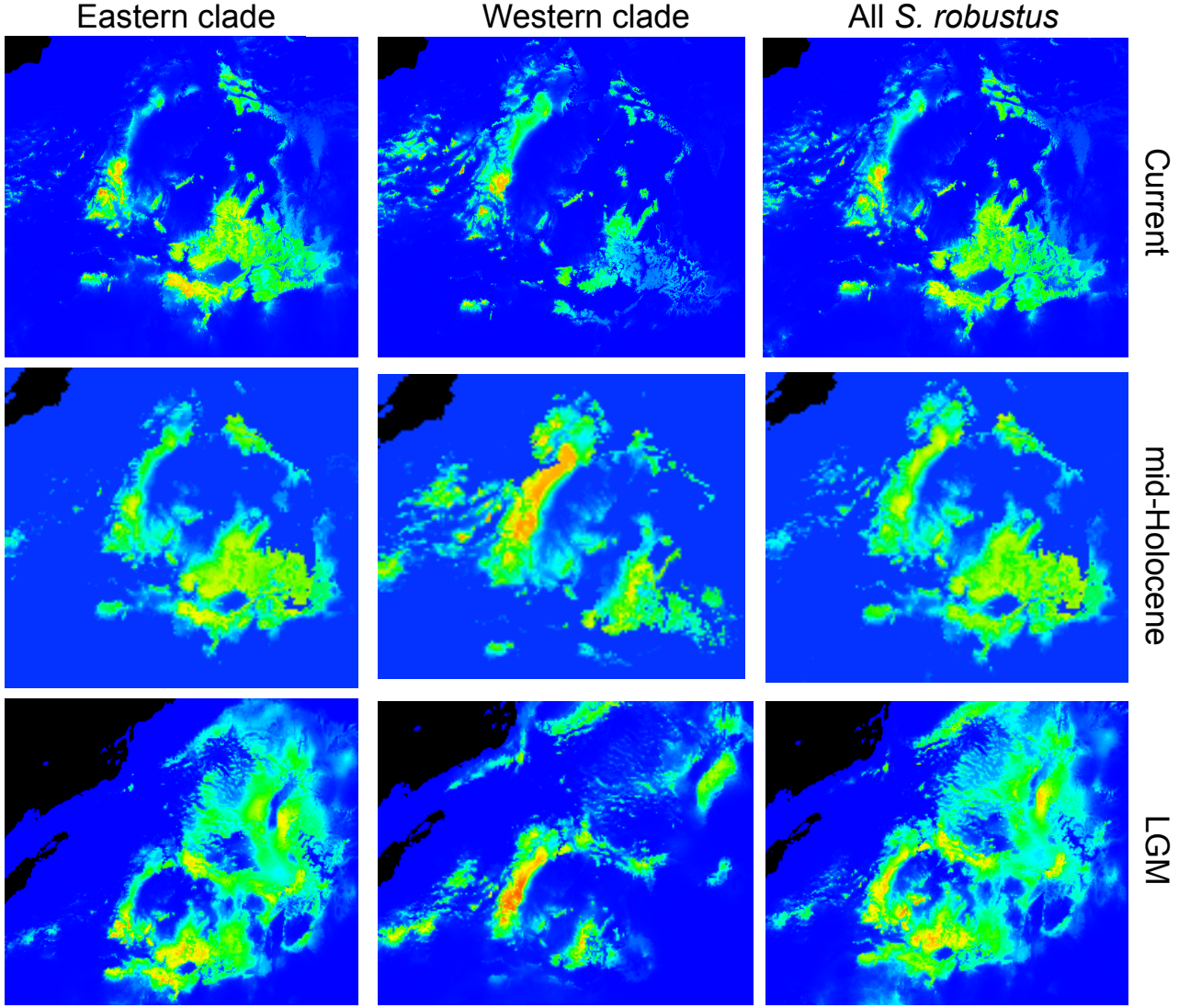

Appendix C.4. M16 results. BEAST phylogeny and divergence date estimates. Note all nodes are supported with posterior probabilities >99. SNP plots for the m16 dataset. Top: PCA plot. Bottom: Procrustes plot.